TARA DEEP ZINC-LEAD DEPOSIT IN NAVAN, CO. MEATH, IRELAND: ORE AND CARBONATE DEPOSITIONAL PROCESSES

DREW ALEXANDER DRUMMOND

Matriculation Number:

A Thesis Submitted For The Degree Of Doctor Of Philosophy

College of Science and Engineering, University of Glasgow.

Principal Academic Supervisor: Prof Adrian Boyce (SUERC)

Principal Industry Supervisors (Boliden Tara Mines): Dr John Ashton, Dr Robert Blakeman, Mr Ian Farrelly.

Submitted: August 2021.

Contents Page

Table of Figures

TABLES

Declaration of Originality

This study is a result of research carried out between October 2017 and August 2021, at the Scottish Universities Environmental Research Centre (SUERC), University of Glasgow, under the principal supervision of Professor Adrian Boyce with guidance from Dr Jonathan Cloutier (University of Tasmania). Alongside this I have had supervision from principal industry supervisors at Boliden Tara Mines DAC Exploration, Dr Robert Blakeman (Senior Exploration Geologist at Boliden Tara Mines Ltd), Dr John Ashton (Formally Chief Exploration Geologist at Boliden Tara Mines Ltd) and Mr Ian Farrelly (Head of Section, Exploration at Boliden Tara Mines Ltd).

I certify that the following work is my own work, and that significant academic debts and borrowings have been properly acknowledged and referenced. The copyright of this thesis rests with the author. No quotation form is permitted without full acknowledgment. I declare that the thesis does not include work forming part of a thesis presented successfully for another degree. I declare that the thesis has been produced in accordance with the University of Glasgow's Code of Good Practice in Research.

Signature:

Drew Alexander Drummond.

Acknowledgments

I have taken great pleasure in being able to see the progress of Tara Deep from the early stages of drilling, all the way through to the first stages of reaching the deposit via the access drift.

This research would not have been possible without the full financial support of Boliden Tara Mines Ltd. who are committed to funding researchers to develop their skills and help solve industrial problems. I would particularly like the thank Dr Robert Blakeman, Mr Ian Farrelly, Dr John Ashton, and everyone involved at the Tara Mines Exploration Department for their time and support throughout this PhD.

I would like to especially thank Prof Adrian Boyce for not only guiding me through these 4 years, but for having faith in me to pursue this PhD. I will forever be grateful for your guidance and support. I also want to thank Dr Jonathan Cloutier. At the University of St Andrews, Jonathan provided me with significant background knowledge in economic geology during my First-Class BSc (Hons) Geology degree and he has offered a vast amount of guidance and advice throughout the course of this PhD. I owe him a huge amount of thanks.

Several institutions and people have also been involved, and to these I will be forever grateful. I have had access to a considerable wealth of knowledge and experience both at the Scottish Universities Environmental Research Centre (SUERC) and Boliden Tara Mines Exploration Department. During my time spent at Boliden Tara Mines, I gained significant skills and experience in both the exploration industry and detailed economic geology research. I have met numerous helpful people, across many disciplines, that I will keep in contact with for many years to come. One of the biggest lessons I have learnt from my time in academia/industry so far is that you are only as good as the people around you. I have had the privilege to be surrounded by some fantastic industry and academic professionals, each of these have been further acknowledged at the end of each chapter.

Finally, and most importantly, a huge thank you to my family and friends who have been there for me through thick and thin.

Abstract

The Tara Deep Zn-Pb deposit (currently 26.2 Mt @ 8.4% Zn, 1.6% Pb) is the latest major discovery by Boliden Tara Mines (first announced in 2016) which significantly adds to the existing world-class Navan deposit. Located 2 km south of the Navan deposit in Co. Meath, Ireland, economic mineralization is hosted by upper Tournaisian carbonates (Pale Beds; 87% of the total economic resource), within a degraded footwall of a major south-dipping normal fault, and also within lower Viséan sedimentary breccias (S Fault Conglomerates; 13% of the total economic resource). Sphalerite and galena are the dominant sulfides, with massive, cavity fill and brecciated textures dominating. These textures attest complex, subsurface, episodic mineralization events that display considerable reworking, fracturing, dolomitization, open-space infill and selective replacement. Lower Viséan syn-rift sliding, erosion, and deposition of thick debrites and calc-turbidites at Tara Deep record basin margin processes near extensional faulting associated with formation of the Dublin Basin. These sedimentary breccias host detrital sulfide-rich clasts and offer unambiguous evidence that the onset of mineralization occurred during the upper Tournaisian.

Conventionally drilled $\delta^{34}S$ values of base metal sulfides have a bimodal distribution suggesting both bacteriogenic (-13.5 to -3.6 ‰) and hydrothermal sulfur sources (+3.4 to +16.2 ‰). Both textural and sulfur isotope data reveal the dynamic nature of mineralization at Tara Deep and infer fluid mixing. Conventional lead isotope analyses display remarkably homogenous $^{206}Pb/^{204}Pb$ of 18.23±0.006 (2σ, n=25), which is consistent with Pb isotope data across the Navan deposit. Subsequently, Tara Deep and Navan are isotopically similar, showing both a statistically identical Pb isotopic signature and a bimodal sulfide S isotopic distribution and homogeneous sulfate signature. In particular, the Pb isotopes and the hydrothermal S signature, correlate with Navan and agree that base metals were leached from the underlying Lower Palaeozoic basement, this suggests that similar deep, circulating metalliferous fluids were also involved at Tara Deep. However, despite these similarities, key differences can be recognized within the S isotope data; around 5‰ shifts to higher $\delta^{34}S$ in the surface-derived S isotope signatures

(both bacteriogenic sulfide and sulfate) indicate that Tara Deep's sulfur was sourced from a distinct seawater/connate fluid signature.

Floatation concentrate samples were obtained on representative drillholes from across the Tara Deep deposit by Boliden Tara Mines' laboratory to inform recovery data for future financial modelling. The concentrates produced were analysed for S and Pb isotopes. The samples reveal limited variation with mean $\delta^{34}S$ = -6 ± 5.9 ‰ (*n* = 38), and galena concentrate mean $^{206}Pb/^{204}Pb$=18.22 ± 0.004 (*n* = 19). Mass balance calculations suggest that ~90 percent of the Tara Deep sulfides were derived from bacteriogenic reduction of contemporaneous Lower Carboniferous seawater sulfate. In contrast, metals were acquired from a local, orogenic crustal source beneath the orebody. These concentrate isotopic signatures differ from those associated with the Main Navan Orebody, in particular the bacteriogenic mode, reiterating that Tara Deep should be considered as an isolated deposit in space, and potentially time, and not an allochthonous block of the Navan deposit. As was reported for the world-class Navan deposit, enhanced bacterial activity was fundamental to ore deposition at Tara Deep, providing significant reassurance for continuing exploration.

Tara Deep is located at depths of between 1.2-1.9 km within fault-controlled terraces on the degraded footwall of a major normal fault system. The system formed as a result of a rapidly subsiding basin margin during the upper Tournaisian extension. The region's long lived and dynamic evolution has resulted in a complex architecture of large normal and strike slip faults. The complexity of the Dublin Basin margin evolution at Navan can be divided into three distinct phases: pre-rift ramp sedimentation in the Lower Carboniferous (Mississippian), syn-rift abrupt detachment and destructive debris flows in the lower Viséan, and finally late-rift basin infill during the Viséan. Diagenetic processes include dolomitization, mineralization and extensive pressure solution, which complicate the lithofacies reconstruction by occluding pre-existing textures. Dolomitization occurs in four phases: D1 – D4. D1 predates mineralization and represents early replacement by non-ferroan euhedral dolomite (30 μm), this dolomite typically has cloudy cores (often associated with Mn), with clear ferrous rims. D2 represents interparticle infill by anhedral (50 μm) ferroan dolomite. D3 occurs as late, coarse, non-

ferroan saddle dolomite cement which occurs in vugs. D4 occurs as the last phase throughout the Tara Deep succession, is nanocrystalline, and is related to burial dolomitization witnessed by its close association with pressure solution seams. Pressure solution is extensive at Tara Deep and is partially responsible for the generation of common and distinct stylo-nodular textures in the Pale Beds, and can also lead to occlusion of the original host rock fabric in the Thin Bedded Unit. Oxygen and carbon isotopes are used to constrain these interpretations. Mineralization is also intimately linked to basin margin development and architecture and is recorded across early syn-rifting textures to late-rifting textures, highlighting the complexity and longevity of the mineralizing system within the Lower Carboniferous (Mississippian) carbonates.

Together these processes speak of a dynamic sedimentary, tectonic, and microbiological environment which has culminated in an exceptional accumulation and preservation of base metals during the Lower Carboniferous. Mineralization initiated during an early phase of the developing Dublin Basin (syn-diagenetically) and kept pace with rifting and subsequently an evolving basin. The Tara Deep deposit has many similarities with the neighbouring Navan deposit reflecting comparable controls on the mineralizing processes in terms of host rocks, Pb and S sources, and tectonic environment.

CHAPTER ONE: INTRODUCTION AND GEOLOGICAL CONTEXT

1.1 Overview

Ireland hosts the greatest concentration of zinc per square kilometre in the world (Fig. 1.1; Singer, 1995) and Irish-type Zn-Pb deposits are the mainstay of the Irish mining industry. Since the 1960s, five significant orebodies have been mined in Ireland (Tynagh, Silvermines, Navan, Galmoy and Lisheen) and over twenty prospects discovered (e.g., Kilbricken, Pallas Green). Following the closure of the Lisheen mine in 2015, the only operational mine in Ireland is Navan. The Navan deposit alone is the largest zinc producer in Europe and one of the largest underground zinc mines in the world. Tara Deep is the latest major Zn+Pb discovery (announced in 2016) by Boliden Tara Mines Exploration Department which sits 2 km SE of the Main Navan Mine's Southwest Extension. Hosted in Lower Carboniferous (Mississippian) carbonates at a depth of 1.2-1.9 km, this new discovery is providing a significant addition to the world-renowned Navan-cluster of deposits, resulting in a combined total production and *in situ* resources at end 2020 of over 151.7Mt (including Tara Deep) @ ~7.7% Zn and 1.8% Pb (Ashton, 2018).

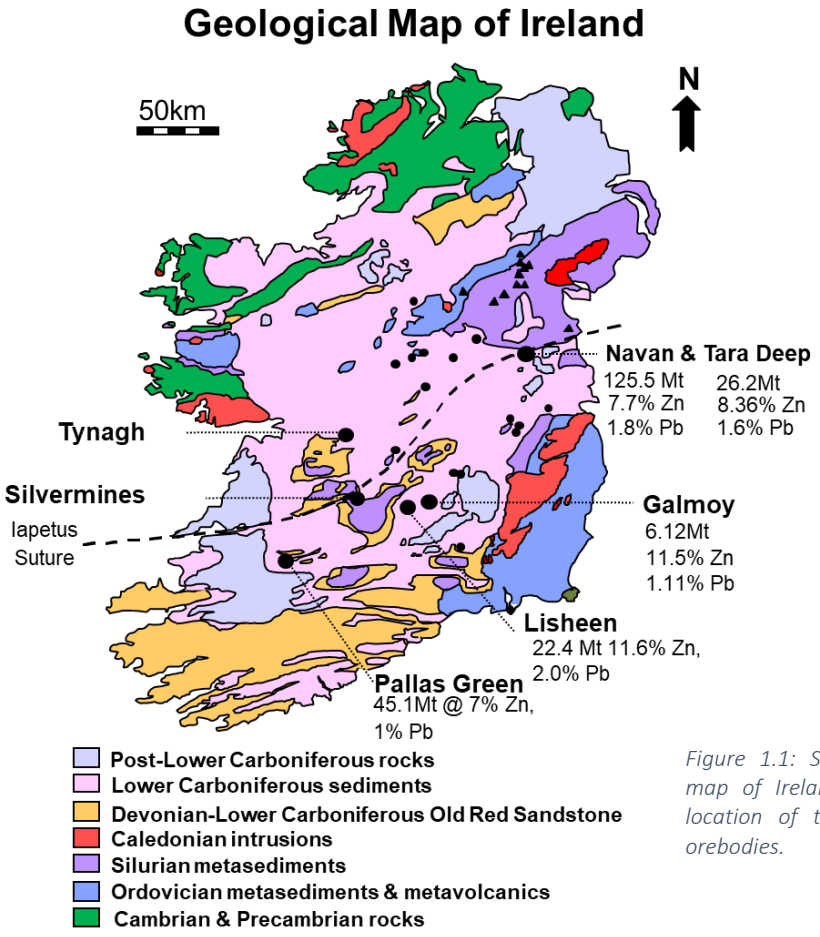

Figure 1.1: Simplified geological map of Ireland highlighting the location of the main Zn + Pb orebodies.

1.2 Thesis Aims and Objectives

The primary objective of this thesis is to answer the question- is the newly discovered Tara Deep deposit a deep-basin equivalent of the Navan Main Mine, having a similar genesis, context, and thus potential to host major high Zn-Pb resources?

More specifically, this study aims to understand, in detail, the depositional and tectonic processes that have led to the formation of Tara Deep. This will elucidate the genesis of the deposit, particularly ascertaining its tectonic, geological and genetic relationship to the adjacent giant Navan orebody. Whilst exploring these relationships, this study will outline the exploration potential for further ore discovery in the Dublin Basin, around and beyond this deposit. Relevant questions pertaining to the genesis, context, and potential of the Tara Deep deposit and its relationship to the neighbouring Navan deposit are addressed using the following techniques:

1) To study the variation in ore hosting stratigraphy across the deposit and to compare the relationship between the host rocks and mineralization. Analyses of the subsurface stratigraphy has been carried out through interrogation of drill-core intersections and by using extensive geochemical databases held by Boliden Tara Mines Exploration Department. Digital structural analyses has used Leapfrog Geo 3D modelling software, Leapfrog Geo 4.4, to explore the location, structure, and timing of mineralization relative to rifting, and to investigate stratigraphic differences and similarities between the development of Tara Deep and Navan deposit pre-, syn- and post-rift sequences, thus complementing current research. This has also facilitated understanding of the relationship between faulting and significant debris flow events to mineralization.

2) Carbonate textural analyses have been completed using standard petrographic techniques, cathodoluminescence and scanning electron microscopy, subsequently establishing paragenetic relationships to metallogenesis. Conventional oxygen and carbon isotopes have been used to back-up these interpretations. Focus has been paid to the complicated diagenetic processes in the Micrite Unit, Pale Beds and Thin Bedded Unit (TBU).

3) Petrographic and mineralogical analyses of base-metal sulfide textures have been carried out using standard transmitted and reflected light microscopy. This work also includes extensive and detailed logging of pertinent drill-cores. SEM imaging has been used to classify the various textures and determine the genetic model for the region.

4) In-depth S and Pb isotopic analyses of base-metal sulfides from Tara Deep, using conventional systems, has been used to inform ore genesis and to provide comparisons to the extensive database developed for the Navan deposit. In conjunction, drillhole concentrates have been assessed from across the entire Tara Deep deposit in order to determine the bulk source of sulfur and lead. Unlike many uneconomic prospects, the Main Navan Orebody – in common with all other economic "Irish-type" base-metal deposits - has a dual S source, characterised by a dominance of bacteriogenic sulfide (Anderson, 1990; Fallick et al., 2001). This has been combined with over 50 years of research into the Navan deposit and other regions of exploration within the Irish Orefield.

5) To assess the timing of rifting and differences in the stratigraphic succession between the Navan deposit and Tara Deep deposit cross-cutting relationships and key textures have been outlined. It is generally accepted that the Navan deposit formed across the regional syn-rift Chadian/lower Viséan time-slice (~345Ma; Ashton et al., 2015). Relative to the stratigraphy, Tara Deep appears to be of a similar age and thus exposed to the same tectonic events. However, the relative ages of rift-related activity at the two localities is currently unknown. Therefore, this study has looked at direct comparisons of pre- and syn-rift stratigraphy from Tara Deep. It has highlighted differences in the onset and diminution of rifting between Tara Deep and Navan.

6) Whilst exploring these relationships, the study has examined the prospectively of further ore discovery in the Dublin Basin and further afield.

1.3 Thesis Layout

This thesis is based upon a series of independent but interlinked manuscripts that have been/will be submitted to international geological journals (Chapters 2-4). The results, interpretations, and conclusions presented within these manuscripts are supplemented by introductory (Chapter 1) and conclusions and future research chapters (Chapter 5).

Each chapter contains its own respective manuscript and the references cited are included at the end of each chapter. Due to the very nature of a thesis by papers, repetition of some aspects of the thesis such as methods and much of the introduction is expected and unavoidable. Each manuscript has been included in the form in which it has or will be submitted. The content of each chapter is summarised below:

-Chapter 2 provides a detailed assessment of the ore depositional processes at Tara Deep, and for the first time constrains a detailed paragenetic sequence. This research assesses the dominant mineralization, textures and stable isotope geochemistry (S and Pb) at Tara Deep, and outlines whether these characteristics vary significantly to those observed at Navan- if different, are Boliden Tara Mines dealing with an isolated mineralization system? In some ways, this work can be considered a sister project to earlier research on the main Navan deposit by Anderson et al., (1998).

-Chapter 3 is a short express letter that looks at Tara Deep's drillhole (DH) concentrates in terms of their S and Pb isotopes. It provides the best bulk isotopic signature from across the entire deposit. This research assesses whether bacteriogenic sulfide was vital for ore deposition within the Tara Deep system, and whether Fallick et al., (2001) were correct- "without bacteria, there would be no giant ore systems".

-Chapter 4 assesses the carbonate depositional environments affiliated with Tara Deep. This research evaluates the significance of various textures recorded across the pre-rift, syn-rift and post-rift facies, in order to determine what these textures reveal in terms of the evolving depositional

environment. This research also assesses the dolomitization and mineralization processes which are intimately related to basin development.

-There are three appendices included in this thesis. Appendix 1 is a detailed outline of additional sample preparation and analytical methods. Appendix 2 outlines work in progress looking at the biogenicity of subsurface filamentous fabrics in the Pale Beds; the Covid-19 pandemic has restricted access to detailed chemistry and CT-scans on these textures. Finally, Appendix 3 outlines additional collaborative work, still in progress, looking at clumped isotope thermometry within the Tara Deep system. Unlike the rest of this research in this thesis, which is largely completed by myself, this has had significant guidance from Matthieu Clog. Appendix 4 states additional publications that have arisen throughout the course of this research.

1.4 Status of Manuscripts

At the time of submission, the status of the manuscripts collated in this thesis is as follows:

Chapter 2: Drummond, D. A., Blakeman, R. J., Ashton, J. H., Farrelly, I., Cloutier, J., Yesares, L., Boyce, A. J. Ore Depositional Processes at the Carbonate-Hosted Tara Deep Zn-Pb Deposit, Navan, Ireland. Economic Geology. Submitted July 2021.

Chapter 3: Drummond, D. A., Blakeman, R. J., Ashton, J. H., Farrelly, I., Cloutier, J., Boyce, A. J. Bacteriogenic Sulfide Dominance & Lead Isotopic Constraints At Tara Deep, Co. Meath, Ireland: Implications For Genesis, Context And Potential. Economic Geology. Pending submission as an Express Letter. This is not the manuscript that will be submitted but it is a mature version of it (Requires Acceptance of Chapter 2).

Chapter 4: Drummond, D. A., Hollis, C., Blakeman, R. J., Ashton, J. H., Farrelly, I., Cloutier, J., Boyce, A. J. Carbonate Depositional Processes At The Tara Deep Zn-Pb Deposit, Co. Meath, Ireland. New Insights For The Evolution Of The Dublin Basin Margin. Sedimentology/Basin Research. Pending submission; this is not the manuscript that will be submitted but it is a mature version of it.

1.5 Contribution of Co-authors to Manuscripts

The contribution of the listed co-authors to each manuscript is listed below:

Chapter 2:

Drew Drummond: principal investigator and author.

Adrian Boyce: S and Pb isotope assistance, discussion, manuscript review.

Ian Farrelly: funding acquisition, discussion, and manuscript review.

John Ashton: funding acquisition, Navan image templates and suggested cross section edits. Discussion and manuscript review.

Jonathan Cloutier: discussion and manuscript review.

Lola Yesares: discussion and manuscript review.

Robert Blakeman: discussion and manuscript review.

Chapter 3:

Drew Drummond: principal investigator and author.

Adrian Boyce: S and Pb isotope assistance, data validation, discussion, and manuscript review.

Ian Farrelly: discussion and manuscript review.

John Ashton: discussion and manuscript review.

Jonathan Cloutier: discussion and manuscript review.

Robert Blakeman: assistance organizing sample collection, discussion, and manuscript review.

Vanessa Pashley: Completed the analyses at the British Geological Survey in Keyworth during the Covid-19 pandemic.

Chapter 4:

Drew Drummond: principal investigator and author.

Adrian Boyce: discussion, C and O isotopes discussion and data validation, manuscript review.

Cathy Hollis: discussion on carbonate depositional processes and manuscript review.

Ian Farrelly: discussion and manuscript review.

John Ashton: discussion and manuscript review.

Jonathan Cloutier: discussion and manuscript review.

Robert Blakeman: discussion and manuscript review.

1.6 Brief Overview of Successful Discovery In the Navan Region.

Following-up on shallow soil geochemical anomalies in the late 1960s in Nevinstown, northwest of Navan, the first exploration drillhole was completed in December 1970 which intersected significant mineralization grading 12.7% Zn+Pb (Fig. 1.2; Ashton et al., 2015).

Figure 1.2: Murrogh O'Brien & Mike Robinson near the discovery site, early 70s (float location; Image Courtesy of John Ashton).

Development of the Navan mine began in 1974, with first production occurring in 1977. Located ~30 km NW of Dublin, this stratabound orebody was initially discovered by Tara Prospecting through drilling a shallow soil Zn-Pb anomaly (O'Brien and Romer, 1971), but now the mine is currently operated by Boliden Tara Mines Limited. In the 1990s, further exploration drilling resulted in the discovery of the Southwest Extension (SWEX; Fig. 1.3), adding 30 Mt to the resource base (Ashton et al., 2003). However, the action of a third party restricted the exploration of the Nevinstown discovery region (NE corner of the Main Orebody) until 2002 and the resource was purchased from the receiver Bula Ltd, and production commenced in 2004. A full review of the main phases of exploration can be viewed in Ashton et al., (2015). From 2000 to 2010, annual resource additions from underground and surface exploration and delineation drilling averaged 1.1 Mt. Despite these gains, mine depletion was occurring at 2.6 Mt per annum, inevitably leading to potential mine closure before 2020. Furthermore, drilling down dip from the SWEX had failed to intercept new resources, meaning that further ore discovery was vital to the survival of Boliden Tara Mines.

Following on from an Experts Meeting in 2010, two significant aims were developed; 1) it was hypothesised that the area to the south of the Navan deposit would contain an undiscovered major normal fault that likely controlled the development of extensional structures in the Navan area, and potentially provide a suitable conduit for metal-bearing fluids. 2) Seismic data acquisition had the potential to locate these structures. By late 2012, seven 2D seismic surveys (totalling 101 km), had been gathered, processed, and initially interpreted. Hosted in the footwall of a large south-dipping basin margin fault, Tara Deep was discovered (see Ashton et al., 2018).

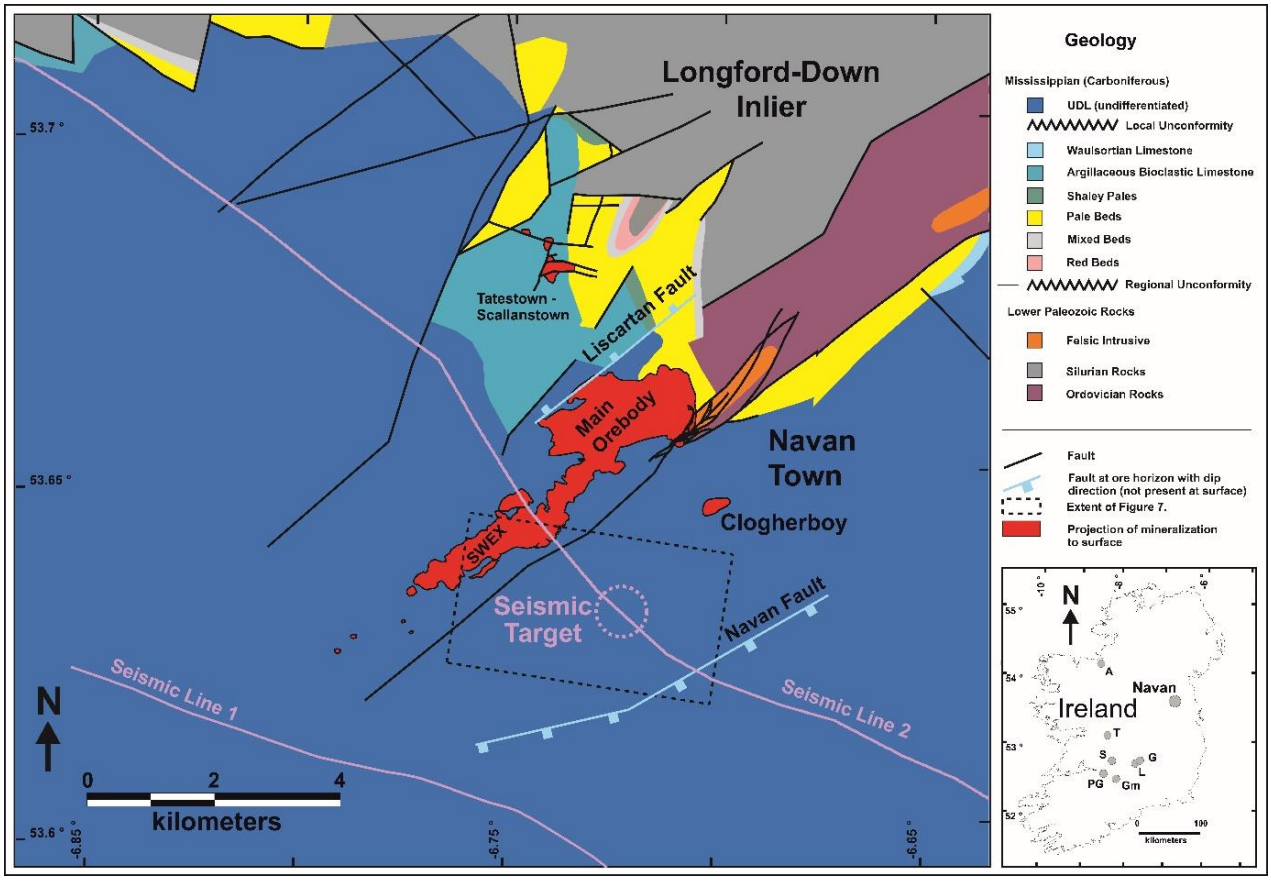

Figure 1.3: Geological map of the Navan deposit, just south of the Longford-Down Inlier, showing the location of the initial Tara Deep 'seismic target' extracted from Ashton et al., (2018).

1.7 Regional Geology and Tectonic Evolution of Central Ireland

Navan is located immediately south of the Longford-Down Lower Palaeozoic Inlier (Fig. 1.3), adjacent to a major NE-trending fault zone forming the southern margin to the inlier. During the Lower Carboniferous, the tectonostratigraphic position of the Irish Orefield was located on the southern margin of Laurussia, close to the equator, in a passive margin setting, separated from the approaching Gondwana supercontinent by the Rheic Ocean and eastern and western arms of the Theic and Paleo-Tethys oceans (Scotese, 2001). These were separated by the Armorican continental plate, which was bordered by opposite-facing subduction zones (Matte, 2001). At this time, the Laurussian continental margin was undergoing dextral transtensional strain because of oblique convergence, resulting in widespread intracontinental basin development throughout northern Europe.

The Irish Midlands Basin initiated in the upper Tournaisian as a broad area of subsidence on the Laurussian margin. It was bordered to the south by the deeper-water, extensional fault-controlled, Munster Basin. A diachronous, northward transgression across the Old Red Sandstone continent, locally termed Red Beds (Fig. 1.4), led to the establishment of a shallow marine ramp environment across most of south and central Ireland by the upper Tournaisian, and it was at this time that the carbonate host rocks for the ore deposits were laid down. A rift event at this time, linked to transtensional reactivation of Caledonian structures in the basement (approximately N–S extension), led to break-up of the Midlands into horst and graben domains, which controlled the rapid lateral facies variations that depict the remainder of the Carboniferous subsidence history (Russell, 1968; Strogen et al., 1990; Nolan, 1989; Hitzman et al., 1996). The late Westphalian–Stephanian (~305– 310 Ma) marked the cessation of subsidence, and alkaline volcanism, as Variscan compression (representing Gondwana colliding with the south Armorican margin) began to invert the earlier basins within the Irish Orefield (Wilkinson, 2014). Thus, in contrast to the thick basinal sequences that characterize the Proterozoic sedimentary exhalative (SEDEX) basins (e.g., Northern Australia), the Irish basins are relatively short lived (~50 My; Boyce et al., 1983).

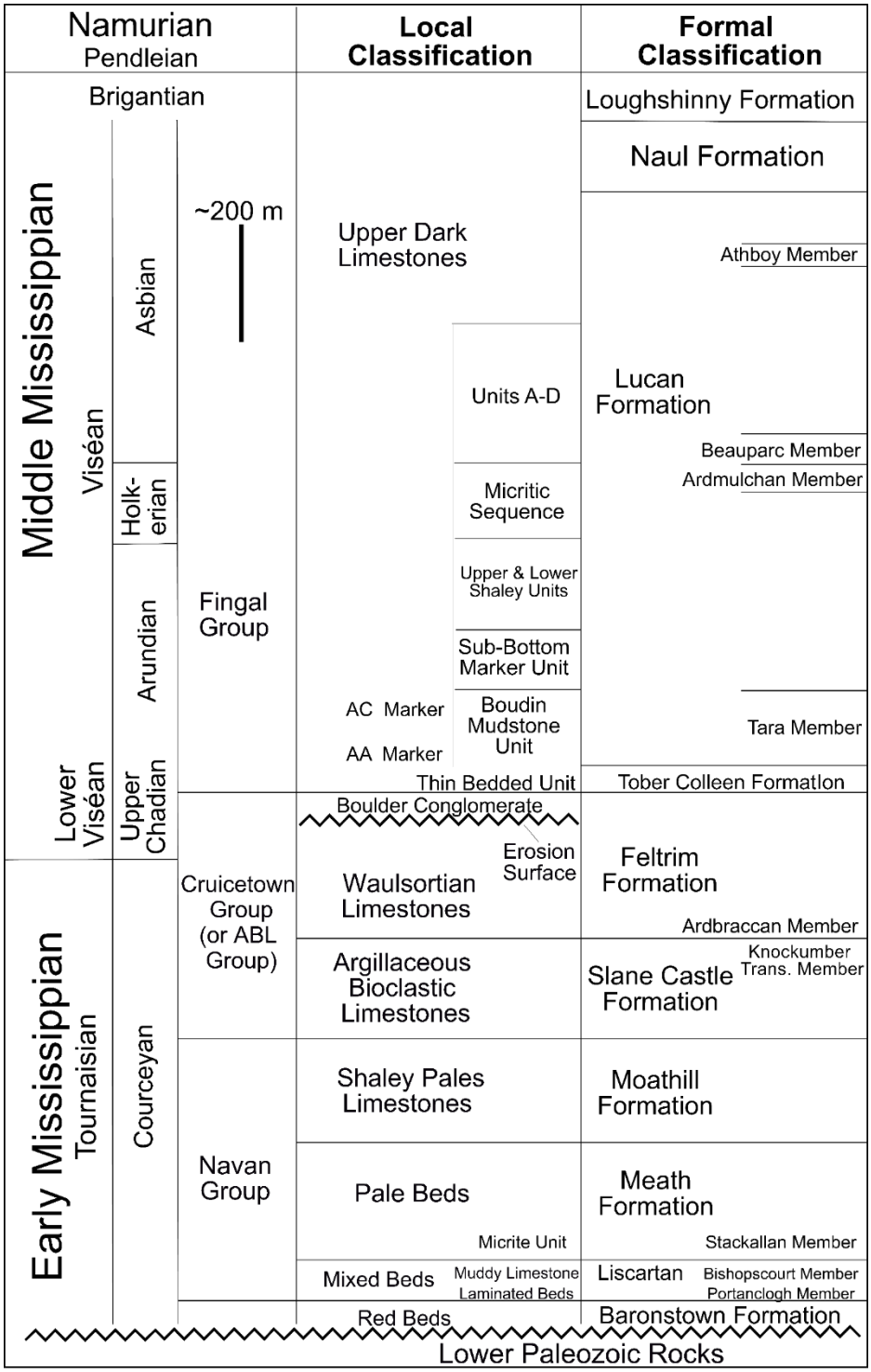

Figure 1.4 Formal and informal stratigraphy table of Mississippian (Lower Carboniferous) rocks in the Navan and Tara Deep area (after Philcox unpublished, 1984, 1989; Strogen et al., 1990 and Ashton et al., 2015)

1.8 Structure

The structures in the Navan area were created in three distinct tectonic events; 1) the collision of Laurentia and Avalonia and the associated basement suture. 2) The extensional rifting that developed the Dublin Basin (see Chapter 4), and 3) the inversion created by the Variscan orogeny.

It has long been recognised that various structures within Irish Zn+Pb deposits have an important role in controlling mineralization (Russell, 1968). At Navan and the SWEX (Fig. 1.5), the distribution of the mineralization reveals there is a clear NE to ENE-trending structural control on the distribution of mineralization, suggesting these major Lower Carboniferous faults created a special combination of stratigraphic, tectonic, hydrological and microbiological factors that cumulated to form extremely efficient metalliferous traps which formed the Navan and Tara Deep deposits (Ashton et al., 2015). Understanding these structural controls and thus metal distribution in Irish-type Zn-Pb deposits is of crucial economic importance in order to inform efficient exploration in the Irish Midlands (Fig. 1.6).

Navan's extensional faulting spans pre-rift, rift, and post-rift basin development. It transitions from northwest-dipping normal faults during upper Tournaisian- lower Viséan, to complex southeast-directed faulting and low-angle gravity slides that represent an extensional rifting episode on the northwest flank of the developing Dublin Basin during the lower Viséan (Ashton et al., 2015).

The Navan orebody is situated along an early east-northeast-trending, northwest dipping, extensional relay fault system within the horst-like footwall crest of a major tilt block (Ashton et al., 2015). This was emplaced by a large, southeast dipping extensional fault that developed during the early stages of the Dublin Basin (upper Tournaisian). Uplift of the footwall promoted gravitational instability of this structure, promoting further southeast-dipping faulting and low angle tectonic slides that eroded the crest of the tilted footwall block, including the pre-rift host rocks and earlier faults. The outcome of this event was the deposition of submarine debris-flows and fault talus deposits (Boyce et al., 1983).

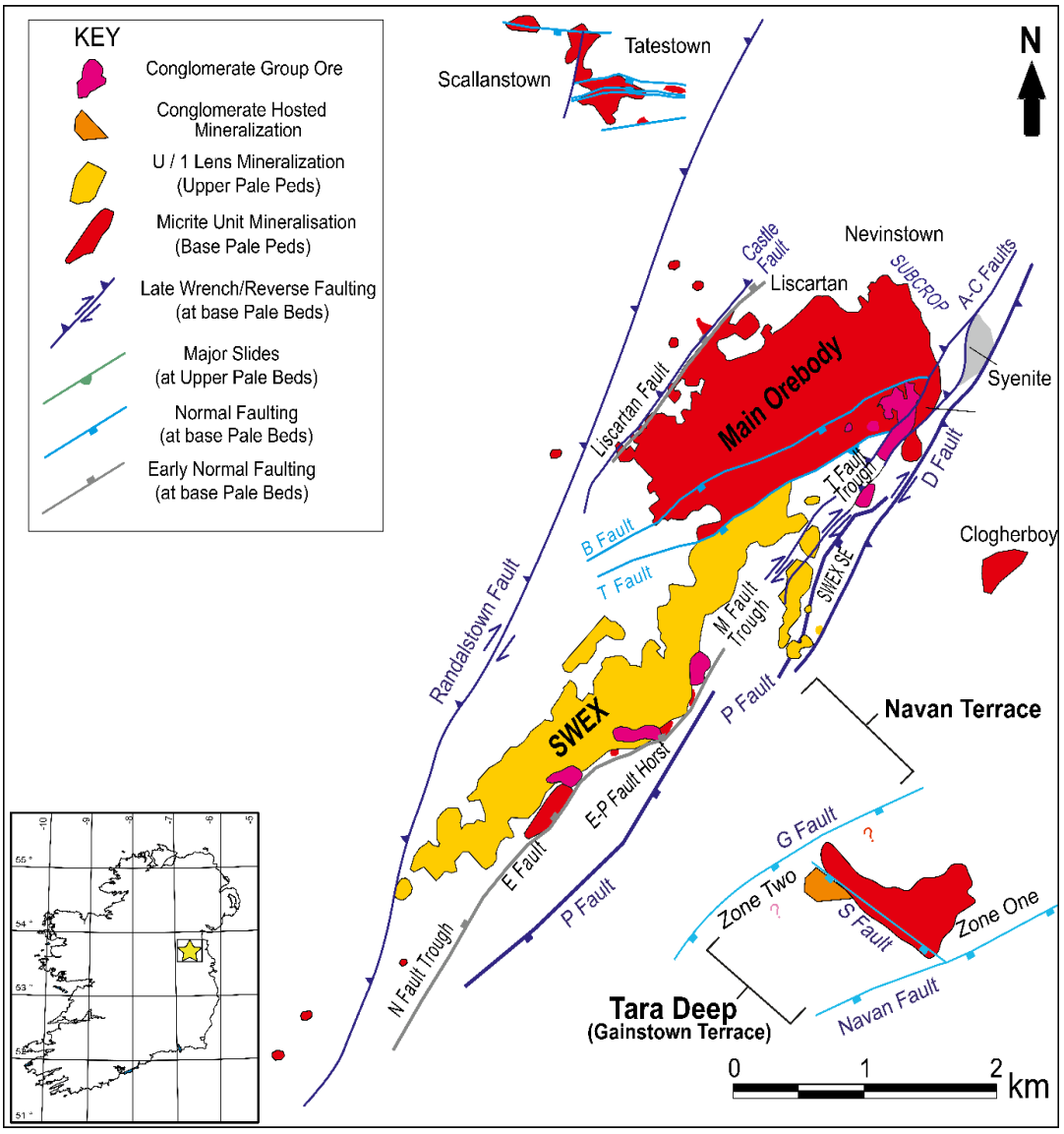

Figure 1.5 Structural plan showing the positioning of Tara Deep relative to the Navan Orebody, and the distribution of principal ore lenses and faults, modified from Ashton et al., (2015). Note the faults are shown as plan projections from their intersections with the ore lenses, not as outcrop positions. SWEX is an abbreviation of Southwest Extension.

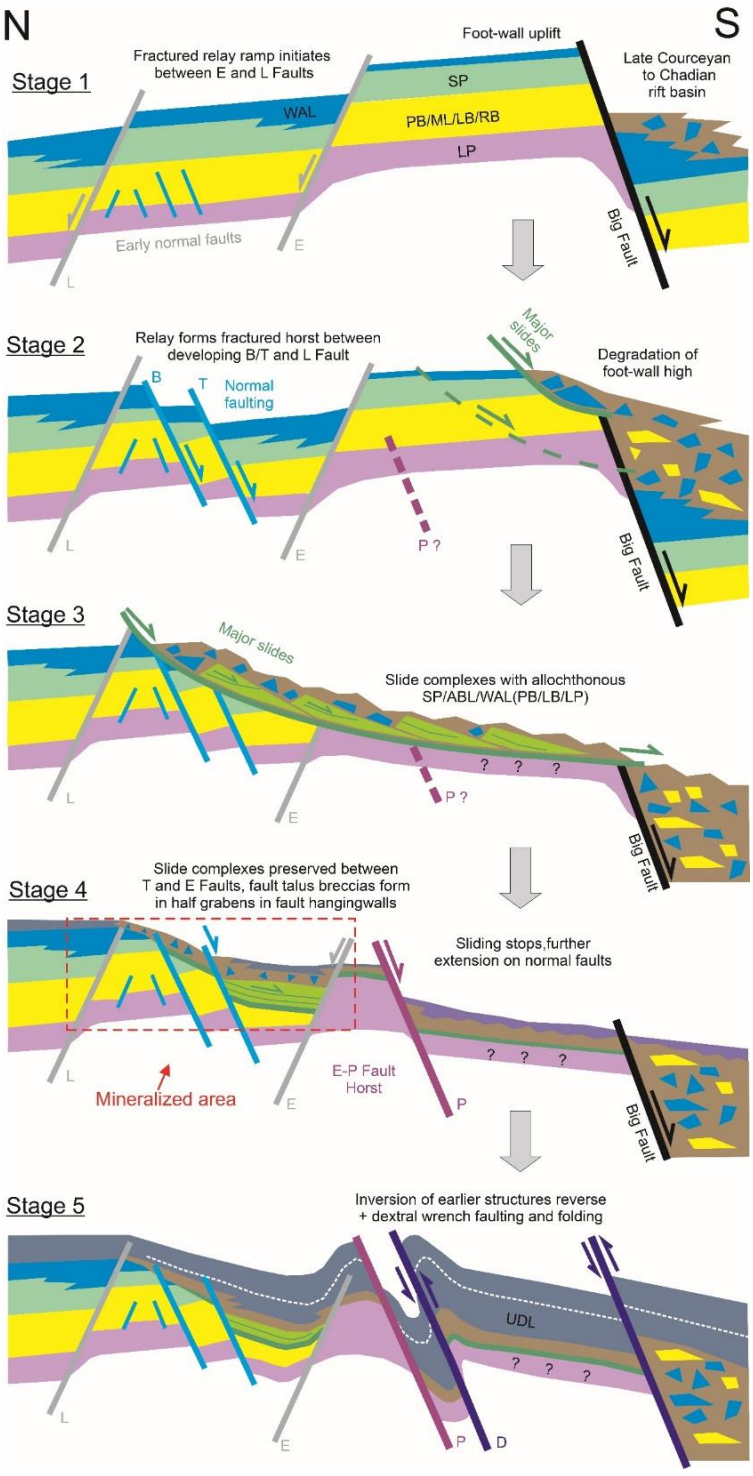

Figure 1.6 Idealized N-S sketch sections showing the progressive development of the extensional fault system at Navan and later inversion (extracted from Ashton et al., 2015). This schematic has been constructed from a combination of structural patterns and numerous sections prior to the discovery of Tara Deep. Stages 1 to 4 are arbitrary depictions of the progressive extensional faulting at Navan during the Lower Carboniferous, while Stage 5 depicts the final and much later Variscan inversion phase. The subset rectangle shown in Phase 4 approximates to the best mineralized area at the Navan Orebody, at roughly the end of the peak period of mineralization. Mineralization may well have commenced during Stages 1 to 3. Not scaled but sections are approximately 6km long.

1.9 Stratigraphy of the Navan Area

Philcox (1984) provided the earliest stratigraphical outline of the region from initial drill cores taken in the area, but since then subsurface exposure, geochemical analyses and over 20,000 drill cores have allowed for extensively detailed facies outlines of the region. Anderson et al., (1998) completed a meticulous review of the stratigraphical succession, which is still used within Boliden Tara Mines today. The most recent comprehensive review of the region is outlined in Ashton et al., (2015). The stratigraphical outline below will be in chronological order, from oldest to youngest. Throughout this study, informal local stratigraphic nomenclature (Fig. 1.7) is used due to its wide adoption within Irish-type deposits across Ireland, a comparison with formal classification can be seen in Figure 1.4.

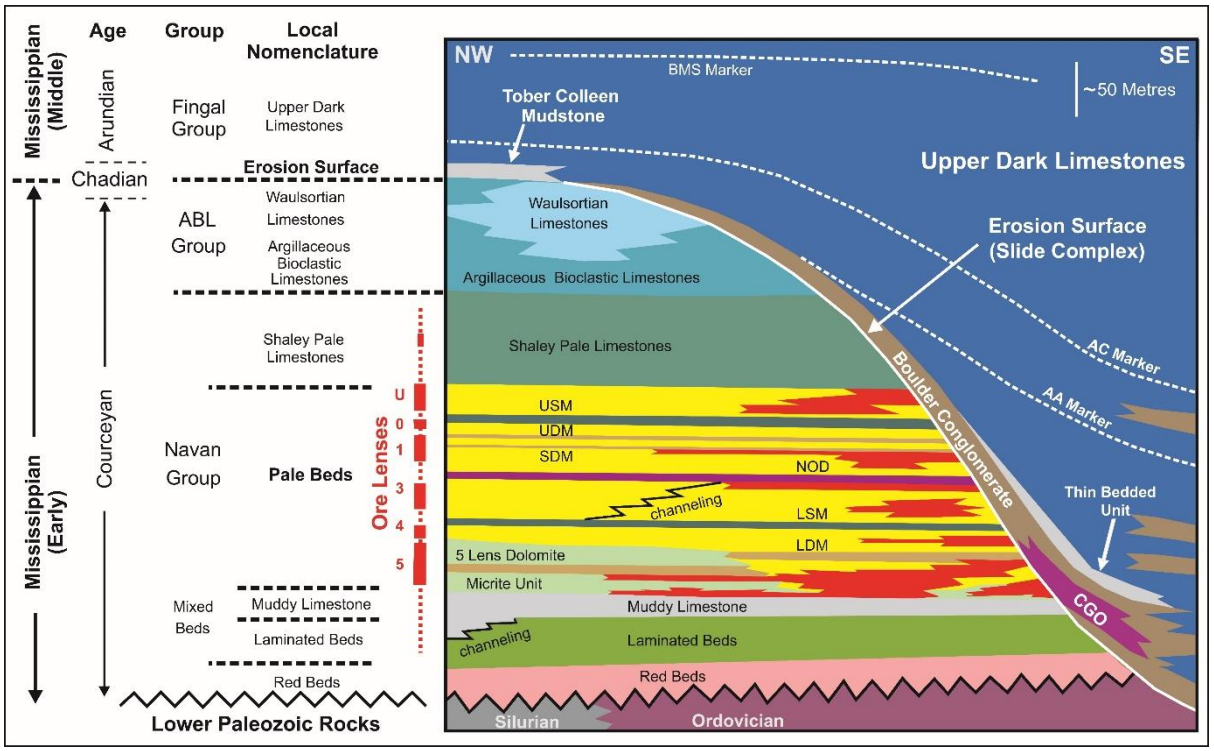

Figure 1.7. Stratigraphic table showing the main rock types in the Navan area (informal classification). Abbreviations of marker units are explained in the text. Extracted from Ashton et al., (2015) showing the main rock types in the Navan area (informal classification, see Figure 1.4 for formal stratigraphy). Abbreviations of marker units are Lower Dark Marker (LDM), Lower Sandy Marker (LSM), Nodular Marker (NOD), Sub Dark Marker SDM, Upper Dark Marker (UDM), Upper Sandstone Marker (USM).

1.10 Lower Palaeozoic Basement

The Lower Palaeozoic rocks stratigraphically below Navan, constitute a structurally complex, lithologically varied series of Ordovician and Silurian sedimentary, volcanic, and intrusive rocks (Everett

et al., 2003; Ashton et al., 2015). These underlying basement rocks were deformed in the late Silurian-Early Devonian by the Caledonian orogeny resulting in NE-SW structural fabrics which were subsequently reactivated and inherited by the overlying Carboniferous sequence (Russell, 1968; Strogen et al., 1996; Worthington and Walsh, 2011). In general, they display evidence of low-grade metamorphism, associated with anchimetamorphic to zeolite facies, with greenschist facies metamorphism in regions (Vaughan and Johnston, 1992).

There is considerable, faunal, structural, isotopic, and geophysical data to suggest that the Lower Palaeozoic rocks at Navan lie proximal to the Iapetus suture (Morris and Max, 1995). This suture zone is believed to represent closure of the Iapetus Ocean during the Caledonian Orogeny. It now comprises a corridor of complex faulting, running NE from the Shannon Estuary all the way to the east coast of Ireland and into northern England (Ashton et al., 2015). However, the understanding of this collision event is lacking, it is likely to have involved under thrusting of the southern East Avalonian plate below a northern Laurentian plate during the upper Silurian (Ashton et al., 2015). This event was accompanied and followed by transcurrent faulting and thrusting and the emplacement of syn- to post-orogenic granitic intrusions at c. 430 Ma, which includes the buried Kentstown Granite located ~5km southeast of Navan. As a consequence of this orogenic event, a strong broad northeast trending tectonic fabric on the Lower Palaeozoic rocks was developed, which later provides a template for structural activity including differential subsidence and basin development during the Lower Carboniferous.

Complex aeromagnetic anomalies attest the heterogeneous nature of the local Lower Palaeozoic basement, comprising highly fractured sediments, volcaniclastics, volcanics and intrusives. These rocks have a variably altered, chloritized or bleached appearance and contain mineralized fractures (Gillespie, 2013). There is insufficient drilling to assess the extent of alteration at depth, but sufficient fracture permeability existed to promote fluid flow and leaching in the basement (Everett et al., 1999).

The Navan deposit occurs in Tournaisian limestone immediately above the SW continuation of the Lower Palaeozoic Grangegeeth Terrane. This terrane is up to 5 km wide and trends in a NE direction and is encompassed in the NW and SE by Silurian sediments comprising greywacke, sandstone, siltstone and mudstone, which can be sub-divided into several distinct fault bounded terranes. Near this region, syenite intrusives of end-Silurian age outcrop over several square kilometres close to the major NE-trending faults in the region (Ashton et al., 2015). Although these syenite intrusions are proximal to the Navan deposit, it is not believed that they had any role in driving mineralization, and the intrusion did not extend below the Navan mineralization (Davidheiser-Kroll, 2014; Ashton et al., 2015).

Overall, the basement geology likely played a number of crucial roles by providing a source of metals for the Navan region, via leaching (see below Pb isotopic studies), whilst faulting and possibly lithological heterogeneities focused metalliferous fluids.

1.11 Lower Carboniferous (Mississippian) Pre-Rift Stratigraphy

Lower Carboniferous pre-rift stratigraphy unconformably overlies the Lower Palaeozoic basement. Basal Tournaisian fluviatile sediments, locally termed the Red Beds, infill the topography of the palaeo-surface and comprise impure red sandstones, caliche horizons, and polymict pebble conglomerates (Ashton et al., 2015). These Red Beds pass upwards into the Mixed Beds which host the locally termed Laminated Beds and the Muddy Limestone (Fig. 1.4). The Laminated Beds are a varied suite of thinly bedded, often bioturbated, dark argillaceous siltstone and mudstone with local paler siltstone, sandstone and calcarenite. The Laminated Beds formed in a variety of occasionally emergent, intertidal to shallow marine environments (Rizzi, 1992). The overlying Muddy Limestone hosts dark, well-bedded argillaceous and crinoidal limestone with prominent bioclastic horizons, and local in-situ coral colonies. The rocks are of shallow marine, lagoonal origin and in the northern part of the Navan deposit, are cut by a channel containing limestone conglomerates (see Anderson, 1990; Rizzi and Braithwaite, 1996).

Stratigraphically above the Muddy Limestone are the Pale Beds, these rocks are the main host rocks for the Navan Orebody and they comprise a varied sequence of pale to medium grey micrites,

oolitic and bioclastic grainstones, dolostones, calcareous sandstones, and minor argillaceous siltstone layers. The Pale Beds record change from generally quiescent deposition to a higher energy and variable shallow-shelf environment (Rizzi, 1992).

The lower Pale Beds consist of a distinctive fine-grained, pale grey, micritic, fenestral limestone, termed the Micrite Unit. Several pale dolomitic horizons occur within the Micritic unit. The most important, the 5 lens dolomite, forms a prominent marker horizon, which can reach 10 m thick in the western part of the deposit. This horizon is suggested to play an important control on ore localization (Anderson, 1990, Ashton et al., 2015). The sedimentary features of the Micrite Unit suggest a peritidal depositional environment.

Additional distinctive marker horizons have been defined within the remaining Pale Beds (Fig. 1.7), these can be used to subdivide the deposit into various ore lenses and guide structural interpretation of the orebody. These marker horizons are generally a few metres thick and characteristically exhibit greater sand, silt, or shale content than the enclosing limestone (Philcox, 1984). The nature of the marker horizons and associated Pale Beds varies significantly over the Navan area (Ashton et al., 2015). The middle Pale Beds are made up of a series of variable bioclastic and oolitic grainstone horizons, with significant limestone micro-conglomerate and thin silty and shaley calcarenites. Whereas the Upper Pale Beds constitute a heterogeneous package of locally dolomitised, sandy, bioclastic, oolitic, and silty calcarenite, displaying significant vertical and lateral lithological variations.

The overlying Shaley Pales (SP), consist of thinly bedded argillite and grainstone with local bryozoan-rich and thinly bedded calcareous sandstone, considered to represent a deeper water depositional environment than the Pale Beds (Philcox, 1984). They are divided into the lower, middle, and upper Shaley Pales, depending on the relative proportions of constituent lithologies.

The Argillaceous Bioclastic Limestone (ABL), overlies the Shaley Pales, and constitute well-bedded, dark, crinoidal argillaceous limestone. The ABL passes upwards and diachronously into the

Waulsortian (WAL) limestone (Ashton et al., 2015). The Waulsortian is irregularly developed in the Navan area, varying laterally between locally well-developed mudbank facies into crinoidal flank facies and transition facies into ABL. No significant mineralization is known in the ABL or the WAL at Navan, despite their importance as host rocks in other Irish Zn-Pb deposits (Wilkinson and Hitzman, 2014).

Within Irish geology, it is generally accepted that the main phase of extensional activity commenced around the time of Argillaceous Bioclastic Limestone and Waulsortian sedimentation and continued during the deposition of the Boulder Conglomerate and into the basal Upper Dark Limestone (Ashton et al., 1986).

1.12 The Erosion Surface and the Boulder Conglomerate (Syn-Rift)

Destructive submarine-sliding truncates the pre-rift stratigraphy at Navan, known locally as the Boulder Conglomerate (BC). The Boulder Conglomerate represents a major truncation feature, which is believed to be a consequence of extension and growth faulting in the Navan area during the upper Tournaisian/lower Viséan, followed by episodic, polymict, low angle gravity sliding (Boyce et al., 1983; Ford, 1996; Ashton et al., 2015). These complex debris flow events involve southwards directed mass movement, generally toward the developing Dublin Basin (Ford, 1996) and incorporate the pre-rift stratigraphy at Navan. Subsequently, they constitute polymict clasts of Waulsortian limestone, Shaley Pales, Argillaceous Bioclastic Limestones, Pale Beds, Mixed Beds and occasionally minor Lower Palaeozoics. The contact between the pre-rift stratigraphy and the Boulder Conglomerate is known as the Erosion Surface. The BC varies in thickness from less than one metre to greater than 50m, and the limestone-dominated clasts display considerable variation in size (2cm- >10m), shape and packaging (clast to matrix) and are often enclosed by a dark locally crinoid bearing argillaceous matrix. Rapid variations in thickness, texture and composition are interpreted to represent successive submarine debris-flows and fault-talus breccias (Boyce et al., 1983; Cook and Mullins, 1983; Ashton et al., 1992; Ford, 1996; Ashton et al. 2015). The Boulder Conglomerate can host mineralization, locally termed the Conglomerate Group Ore (CGO), and in general, tends to be more pyrite rich than the majority of the

Pale Beds-hosted ore (Anderson, 1990; Ashton et al., 1992; Ford, 1996). In areas where the Erosion Surface is absent, the Waulsortian passes up into dark mudstones which represent the Tober Colleen Formation and then into a thick sequence of calc-turbidites known as the Upper Dark Limestones, which represent the main infill of the Dublin Basin.

1.13 The Upper Dark Limestones (Late- to Post-Rift Stratigraphy)

The Boulder Conglomerate is overlain by a thick sequence of dark, well-bedded, turbiditic limestones and shales, representing several stratigraphic units of lower Viséan age, collectively called the Upper Dark Limestones (UDL; Strogen et al., 1990, Peace and Wallace, 2000; Ashton et al., 2015). They mostly comprise thin dark calcareous mudstones with well-bedded turbiditic grainstones, wackestones, and mudstones (Ashton et al. 2015). The depositional strike of the UDL succession is approximately parallel to the main NE fault trend. The lower part of the UDL, approximately up to the top of the Boudin Mudstone Unit (BMS), forms an onlapping sequence filling the topographic low left by the lower Viséan sliding and erosion. Although the BC commonly lies directly on the Erosion Surface, in some areas, particularly in the lower parts of the UDL, it occurs as multiple horizons, within calcareous mudstone of the Tober Colleen Formation (TCF), locally-termed the Thin Bedded Unit (TBU). This mudstone is typically unfossiliferous and includes subordinate interbeds of thin (10-15 cm) argillaceous micrite (Ashton et al., 2015). Upwards, it grades into thinly interbedded mudstones and fine calcarenites. This unit is preferentially developed where the Erosion Surface has cut deepest into the upper Tournaisian rocks and is poorly developed where down cutting is minor. Carbonaceous layers are present which have yielded plant fossils (Ford, 1996) and the unit frequently contains microcrystalline-framboidal pyrite laminations, with rare fine-grained laminations of sphalerite and galena. This unit will be discussed in detail within Chapter 4.

Overlying this, the Boudin Mudstone Unit consists mainly of coarse graded grainstones and unfossiliferous black calcarenites. This unit can contain conglomeratic regions and boulders (greater than 10 cm across) of upper Tournaisian units. These conglomerates grade upwards, and to the

southwest they thin and fine rapidly (Ashton et al., 2015). Interspersed in the unit are distinctive unfossiliferous mudstones with calcareous 'boudins', the origins of which are highly debated. Authors have considered them to represent diagenetic features modified by tectonic strain (Walker, 2004), whereas others believe they could represent an extensional feature associated with slope creep (Philcox, unpublished, 1984). However, in Chapter 4, this research outlines these textures as soft sediment deformation features, known as load casts.

Above the Boudin Mudstone, the lowest stratigraphic units in the UDL consist of fine graded beds with variations in proportions of grainstone, mudstone, chert and other lithologies. Thickness variations across the mine area are typically subtle and may reflect minor fault reactivation and/or differential compaction (Ashton et al., 2015). The succession is most easily sub-divided by distinctive thicker shale markers, termed the Lower and Upper Shaley units, overlain by the Micritic Sequence (see Philcox, 1984). This Micritic Sequence constitutes thin micrite beds gradationally interbedded with calcareous mudstone, that is locally intensely burrowed in the bottom part. Sections of this unit consists of thin graded calcarenites and shales with scattered small-scale slumps. Units A and D at the top of the UDL in the Main Orebody area, consist of very fine-grained graded limestone and shale, with differing proportions of chert and included shale clasts. Unit C is a distinctive, very thinly bedded micritic unit (Ashton et al., 2015).

1.14 Tertiary Magmatism

During the Cenozoic, several transgressive dolerite dykes were intruded, striking in a north-south direction and dipping westwards at angles from 20-65° (Ashton et al., 2015). Localised minor displacement of adjacent rocks and structures are evident, but there is no indication that these features follow earlier structures.

1.15 Inversion and Dislocation

After rifting, faulting has been variably, but in places strongly, inverted by post Lower Carboniferous compressive events of likely Variscan age. Reverse and dextral wrench-style fault movements have inverted mainly NE trending (Caledonide-derived) faults (the A, C, D and Randalstown faults), subsequently dislocating both the Navan orebody and earlier faulting. This phase of fault reactivation is locally accompanied by the development of intense folding within the Upper Dark Limestones. In the Main Navan Orebody, stratigraphic correlations either side of the A and C Faults (Fig. 1.5) have enabled measurement of large dextral and subsidiary reverse movements on these structures. On the SE flank of the orebody mineralization is cut by the P and D Faults. This region, known locally as the Navan Terrace (Fig. 1.5), is a complex structural corridor that may have contained now inverted extensional structures (Ashton et al., 2015). To the NW of the Navan Orebody, drilling information is sparse but points to similar dextral/reverse movements on the Randalstown Fault. Details of the structure of Variscan compression are given by Dolan (1983), Sanderson (1984), Cooper et al. (1984, 1986), Rothery (1988) and Coller (2005),

1.16 Mineralization

The Navan deposit (including the SWEX) forms an irregular northeast-trending ellipsoid, 1.5 km x 5 km in size. By considerable magnitude, the Navan Zn + Pb deposit is the largest of the Irish deposits and one of the largest Zn bodies discovered. The Main Navan Orebody (not including the SWEX) is developed between its surface sub-outcrop at Nevinstown (discovery site), dipping at 15°C to the southwest for ~2.5 km, reaching a depth of 700m. Mineralization dominantly consists of a series of stratabound lenses, hosted as subsurface infill and replacement of the Pale beds and Boulder Conglomerate (Anderson, 1990). These statabound ore lenses trend NE to ENE, approximately parallel to the B and T Faults. These lenses occur at various stratigraphic positions within the Pale Beds, with marker horizons existing between zones of mineralization. These marker horizons are used to divide the Pale Bed stratigraphy into mineralized lenses and are labelled from stratigraphically highest to

lowest from U followed by 0, 1, 2, 3, 4, and 5. A local mine nomenclature method is used to refer to each lens within the Main Orebody, based on location and position within the stratigraphic record. The method names a mineralised region by "zone-lens" (Ashton et al., 2015). For example, sulfide mineralization located in Zone 2 of lens 5, within the Pale Beds, would be referred to as the "2-5 Lens". Mineralization in the Main Navan Orebody and the surrounding cluster of deposits is most laterally persistent in the basal 5 Lens.

The mineralogy of the orebody is relatively simple with sphalerite and galena dominating in at a ratio >5:1 (Anderson et al., 1998; Ashton et al., 2015). The principal gangue minerals are pyrite, barite, calcite, and dolomite with regions hosting Sb- and Cu- sulfosalts e.g. bournonite ($PbCuSbS_3$), boulangerite ($Pb_5Sb_4S_{11}$) and semseyite ($Pb_9Sb_8S_{21}$) (Anderson, 1990; Blakeman et al., 2002; Steed, 1980; Ashton et al., 2015; Chapter 2). Freibergite and pyrargyrite are believed to be the principal host of silver. Pyrite and marcasite are present in subordinate amounts in the Pale Beds (~1-3% Fe), but increase in the upper lenses particularly below the erosional surface (e.g. 2-1 lens) and the Conglomerate Group Ore (typically ~20%; Ashton et al., 1992, 2015; Anderson et al., 1998; Davidheiser-Kroll, 2014).

A full review of each lens can be reviewed in Ashton et al., (2015). Focus here is on the 5 lens Micrite Unit (Fig. 1.8) and the Conglomerate Group Ore (Fig. 1.9), as they host the majority of the mineralization at Navan, and they appear equivalent to mineralization at Tara Deep; the other Pale Beds' lenses are currently not observed at Tara Deep.

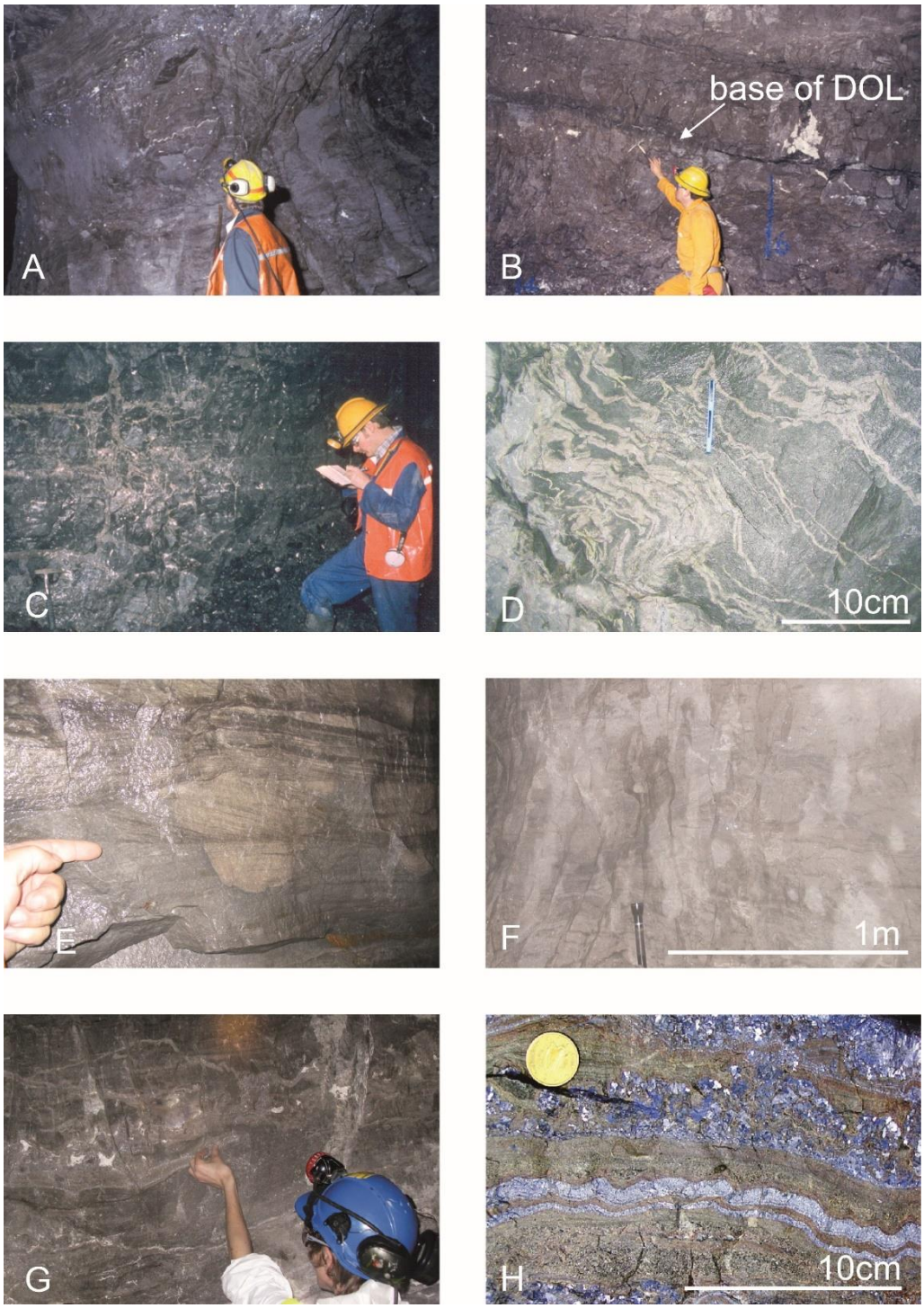

Figure 1.8 Photographs of underground mineralization at the Navan deposit. A. High grade Zn+Pb mineralization (extracted from Ashton et al., 2015) in 2-3 Lens (Zone 2 South). Calcarenites have been replaced by fine pale sphalerite over the entire face. In the upper part of the photograph extensive replacement has resulted in growth of much coarser galena mineralization. B. Dolomite in the 1-5 Lens (1-5 Lens West). Sphalerite-galena mineralization is localized below a prominent horizon of massive dolomitized sandy-oolites. C. Subvertical mineralized breccia zone 1-5 Lens (1-5 Lens Central). A northeast trending breccia zone has been cemented by sphalerite-galena mineralization, which also extends laterally into the host rocks as thin bedding-parallel bands. D. Contorted sulphide veins 3-5 Lens (south central SWEX). E. Disseminated sphalerite in 3-U lens. Selective replacement of sedimentary features in calcareous sandstones (central SWEX). F. Massive fine grained disseminated sphalerite causing almost total replacement of 3-U Lens calcarenites (central SWEX). G. Thin mineralized layer in the 3-1 Lens (north-central SWEX). Sphalerite-galena mineralization in bedding-parallel horizon shows geopetal fabrics and former voids infilled by barite and honeyblende sphalerite. Host-rock above and below the mineralized layer are irregularly veined with sulfides. H. Massive 3-1 Lens mineralization (south central SWEX). Alternating layers of sphalerite and coarser galena in a high-grade band.

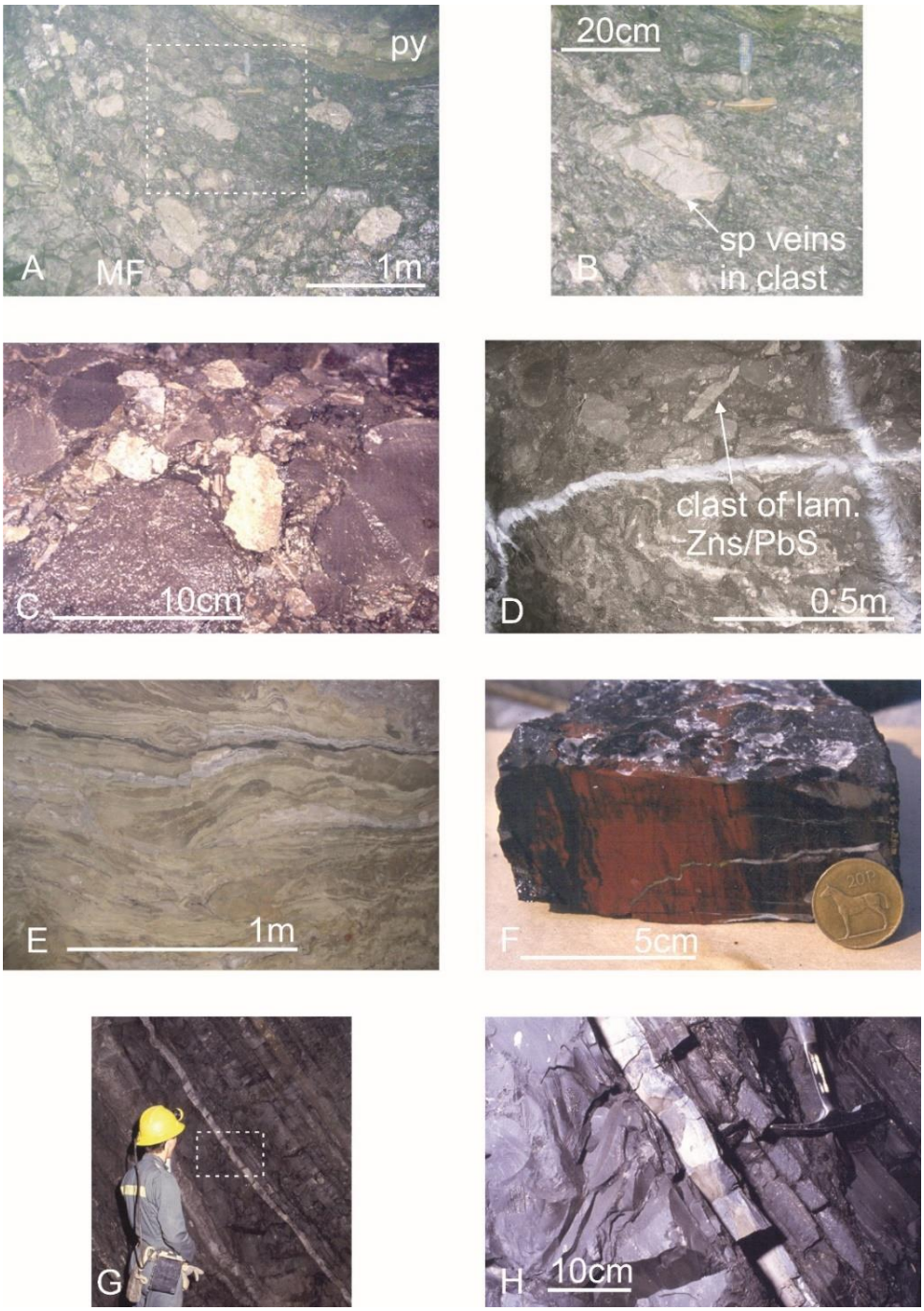

Figure 1.9. Images of the Boulder Conglomerate extracted from (Ashton et al., 2015) A. Boulder Conglomerate close to the M Fault (south central SWEX) containing mineralized clasts with layered pyrite in top right. B. Enlargement of clast from 1.9A showing veins of sphalerite in clast of 3-U Lens material truncated at clast margins. C. Clasts of sphalerite-galena mineralization in Boulder Conglomerate (Zone 2 South). D. Clast of layered sphalerite galena mineralization in Boulder Conglomerate (south central SWEX). E. Massive layered fine-grained pyrite with paler sphalerite and galena layers comprising Conglomerate Group Ore (south central SWEX). F. Silicified haematite in dark argillite near the Boulder Conglomerate – Upper Dark Limestone contact (Zone 3 southwest). G. Pale stratiform band of sphalerite-galena mineralization in the Thin Bedded Unit (basal UDL; Zone 3). H. Enlargement of stratiform sphalerite-galena layer from 1.9G.

Mineralization in the 5-lens is developed over the entire area of the Main Navan Orebody and forms the single most laterally continuous mineralized horizon, which represents ~90% of the total ore. It is highly complex, with intermixed lenses, sub-lenses, pods, mineralised breccias and veins that appear to have developed preferentially in the micrites, grainstones and dolomitized grainstones of the Lower Pale Beds (Anderson et al., 1998). Contacts between sulfides and micrites are generally sharp and indicate that the limestones were extensively corroded by the metalliferous hydrothermal fluids. At Navan, 5-Lens Micrite Unit mineralizations is dominantly stratabound. The ore is frequently disrupted and exhibits various breccia and soft sediment textures. Complex and varied textures are present across the Navan orebody. These textures are dominantly fine grained (<2 mm) subsurface textures, and there is strong evidence for tectonic disruption post ore deposition. A diversity of ore textures within the Pale Beds indicate that the majority of sulfide mineralization occurred by complex mineralization processes involving continual replacement, and open space infill (see Anderson, 1990 for a detailed review). Replacement textures range from delicate pseudomorphs of bioclasts to more destructive granular styles. Open space textures are common and include course grained galena, layered sphalerite, dendritic-skeletal galena, sulfide stalactites, internal sediment, and geopetal textures (Anderson et al., 1998). The diversity of textures alongside cross-cutting mineralization, highlight the longevity of the mineralization system.

The mineralization found within the Boulder Conglomerate, known as Conglomerate Group Ore (CGO; Fig 1.9), is characteristically distinct from the Pale Beds mineralization (Fig. 1.8; see Ford, 1996). The CGO tends to occur at topographic lows between fault structures. The CGO lenses make up a loosely northeast-trending pattern on the southeast side of the Navan deposit. The CGO accounts for 3% of the total Navan Mine resources, typically within pyritic lenses. It is often dislocated by faulting and slides, which have variable orientations, magnitude and age. Mineralization typically consists of irregular massive iron-sulfide-rich layers with local bedding-parallel morphologies and layering. The proportion of iron to zinc-lead sulfides are variable, as are grain size and textures. Iron sulfide textures include a) diagenetic laminae of fine-grained framboidal pyrite associated with dark argillites (Barker et

al., 2012), b) bands with a speckled appearance associated with medium-grained white calcite (Ford, 1996), and c) thicker layers of massive pyrite often accompanied by high-grade zinc-lead mineralization (Ashton et al., 1992; Ford 1996). Sphalerite and galena occur with the iron sulfides as massive bands, disseminations and in crosscutting veins. More importantly the CGO is temporally significant, sulfide clasts have been ripped up and incorporated within the Boulder Conglomerate formation, providing a crucial constraint on the timing of mineralization, these mineralized clasts are themselves encased by matrix replacement mineralization within the Boulder conglomerate, highlighting that at least part of the mineralization occurred after rifting and the associated formation of this erosional surface (Anderson, 1990; Ashton et al., 1992; Ford, 1996; Blakeman et al., 2002). Rare pods and nodules of red (rarely brown/green) hematitic silica (Fig. 1.9F) are also present in the Boulder Conglomerate and resemble similar, hydrothermal features reported from Silvermines, Tynagh, Crinkill and Lisheen (Andrew, 1986; Clifford et al., 1986; Hitzman et al., 1992, 1995; Cruise et al., 1999; Ashton et al., 2015). Finlay et al. (1984) noted the presence of anomalous values of manganese, arsenic, zinc and lead in these rocks (see also Walker, 2005; Walker, 2010).

1.17 Southwest Extension

In the southern region of the Main Orebody, at depths of around 450m, additional lenses are developed in the Upper Pale Beds and extend a further ~4 km to the southwest of the Main Navan Orebody, this region is known as the Southwest Extension (SWEX). Mineralised horizons within the SWEX extends to depths of 1 km (Ashton et al., 2015). Discovered in the 1990s, the SWEX hosts a total resource approaching 30 Mt (8% Zn+Pb). The SWEX lies immediately SW of the Main Orebody lying south of the T Fault (Fig. 1.5). Unlike the Main Navan Orebody, where the 5-lens mineralization is the most prolific, the SWEX mineralization is largely hosted within the 1 and U lenses (Ashton et al., 2015), with mineralization within the 5-Lens being very restricted and developed only between the E Fault and its associated branch. The northwest boundary to the SWEX is gradational and is characterised by an increase in irregularity, and a decrease in grade and thickness of the mineralization (Ashton et al., 2015).

The southeast boundary is sharper and defined by the Y, M and E Faults. Texturally the SWEX tends to take the form of irregular vein/stockwork mineralization with local areas of poddy, replacement mineralization (Ashton et al., 2015). Anastomosing sphalerite and minor galena veins are common, passing into sulfide pods that often contain angular clasts of host rock set in sulfide cement. Marcastite veins also occur in the Lower Pale Beds close to the E Fault in the footwall of the N Fault (Redmond, 1991, Ashton et al., 2015).

Three lenses of CGO are known in the SWEX. These occur in the immediate hanging walls of the M and N Faults. The mineralization is heterogeneous and varies from barren fine-grained pyrite occurring as bedding-parallel laminae and more massive beds, to areas of varying Zn/Fe ratios dominated by sphalerite and iron sulfide, with subordinate galena. In the eastern most area of the SWEX, the CGO occurs in the upper part of the Boulder Conglomerate. The lower BC contains large irregular blocks of 3-U lens-hosted massive sulfides comprising pale sandy dolomitic grainstones with extensive development of disseminated sphalerite, these are interpreted as slide blocks derived from a paleo-scarp on the M Fault and suggest that some mineralization was earlier and/or synchronous with the Boulder Conglomerate.

1.18 Dolomitization

Dolomitization is evident in nearly all of the carbonate-hosted Zn+Pb deposits in Ireland, however, relationships between dolomite formation and ore deposition are varied. It is important to consider that dolomitization likely occurred in stages in deposits such as Navan (Anderson, 1990), Silvermines (Andrew, 1986), and Tynagh (Boast et al. 1981), and formation of pre-ore dolomite may have been an important controlling factor in ore genesis, acting as seals for metalliferous fluids (Anderson, 1990). Although dolomite is closely associated with mineralization at Navan, sulfides are also commonly hosted by un-dolomitized limestones- this is unusual at other major Irish Zn-Pb deposits.

Anderson (1990) suggests that there are both pre- and post-ore dolomitization at Navan. Pre-ore dolomitization of bedding-parallel, silt-rich horizons were likely shallow burial, early diagenetic in

origin, whereas the pervasive dolomitization in the western region of the mine is believed to have been related to the mineralization event and late saddle dolomites have been noted (Anderson, 1990; Braithwaite and Rizzi, 1997).

Rizzi (1992) and Braithwaite and Rizzi (1997) studied the three dimensional distribution of pre-sulfide, early diagenetic, dolomite in the Pale Beds. Its morphology is suggested to form a plume shaped body trending in an east-northeast direction with "stratal fingers" extending outwards along sandy and silty grainstone lithologies. The plume was interpreted to be hydrothermal in origin based on limited fluid inclusion and isotopic analyses (Braithwaite and Rizzi, 1997; Anderson et al., 1998; Everett and Wilkinson, 2001).

Ford (1996) recorded clasts of replacive dolomitization within the Boulder Conglomerate which together with exotic sulfide clasts provides evidence that both mineralization and dolomitization initiated prior to the onset of the Boulder Conglomerate and continued during its formation. This suggested timing of hydrothermal activity correlates broadly with the onset of major southeast extensional faulting in the Navan area and an important correlation exists between the two events.

1.19 Fluid Inclusion Analysis and Fluid Mixing

Fluid inclusion analyses are useful in order to determine temperatures and compositional information for fluids involved in ore forming processes. The fluids are believed to represent those at the time of capture. Although significant fluid inclusion analyses have been conducted on coarse crystals of dolomite, calcite, sphalerite and barite at Navan (Peace, 1999; Braithwaite and Rizzi, 1997; Everett and Wilkinson, 2001; Peace et al., 2003; Wilkinson, 2010; Knight, 2012; Treloar, 2014) these inclusions are relatively rare, and hard to identify due to their small size, and the turbidity of inclusion-bearing phases. This has meant that due to the bulk of the ore at Navan being fine grained, unrepresentative analyses have been completed on coarse grained ore crystals and data needs to be interpreted with care.

The most detailed studies at Navan, obtained samples from pre-, syn- and post-ore dolomite, massive, vein- and breccia-hosted mineralization, and post-ore calcite veins (Barnicoat et al., 2004; Yardley et al., 2005; Wilkinson, 2010; Ashton et al., 2015). Fluid inclusions were only analysed in regions constrained to precise paragenetic stages and notes were taken where secondary inclusions overprinting such stages occurred. There have been two main categories of fluid inclusions at Navan. A) high temperature, low salinity fluid (100-140 °C, 5-10 wt.% eq NaCl) and B) low temperature, high salinity fluid (70-100 °C, 20-25% wt.% eq. NaCl). The low temperature, high salinity fluid, is believed to represent an evaporitic brine/connate fluid and is more prevalent in the late stages of paragenesis. The high temperature, low salinity, fluid is thought to represent the hydrothermal metal-bearing fluid. Intermediate values are thought to represent mixing of these two end members (Wilkinson, 2005a). The known characteristics of this low temp/high salinity fluid reflect source regions similar to modern day peritidal-environments. Current fluid inclusion analyses only reflects a limited sampling density of the length, breadth and textural complexity of the deposit. However, several general observations can be made. There appears to be a broad evolution from lower salinity, higher temperature fluids that were predominant during early dolomitization and mineralization towards a final, brine-dominant stage of permeability occlusion (Braithwaite and Rizzi 1997; Peace 1999; Ashton et al., 2015). The range in salinities and homogenization temperatures in both vein and non-vein ore samples are consistent with fluid mixing (Hitzman et al., 2002; Wilkinson et al., 2005a,c; Wilkinson, 2010).

The inverse relationship between homogenization temperature and salinity in fluid inclusion data at Navan, attributed to fluid mixing, is similar to patterns observed elsewhere in the Irish Orefield (Wilkinson, 2010). However, the higher temperature fluid end-member at Navan is cooler and mostly of lower salinity than the other Waulsortian hosted deposits, potentially reflecting a regional scale pattern (Wilkinson, 2010).

1.20 Timing of Mineralization

Textural relationships are critical when determining the timing of sulfide mineralization relative to deposition and diagenesis of the host rocks, but unequivocal relationships are rare in nature. At Navan, mineralization is believed to have occurred syn-diagenetically during the formation of the host rocks. In particular, the micrites, calcarenites and grainstones were semi-lithified during the time of sulfide mineralization, with the rheology of the host rocks having a controlling factor on the gross geometry and style of mineralization.

It is suggested that mineralization post-dated initial marine cementation and dolomitization of the host rocks. However, the interpretation of the timing of this varies, from near seafloor (Andrew and Ashton, 1985; Anderson et al., 1998; Everett and Wilkinson, 2001; Blakeman et al., 2002) to greater than 800 m burial depth and as late as the Holkerian (Peace and Wallace, 2000). Those that regard mineralization as epigenetic believe it has merely been superimposed on lithified rocks (Peace and Wallace, 2000). In contrast to other Irish-type deposits (e.g Silvermines), in-situ feeders regions have not been identified at Navan. However petrographic and geochemical analyses have revealed both textural relationships and metal distribution patterns that suggest fractures and faults acted as conduits at Navan (Boyce et al., 1983, Taylor, 1984; Blakeman et al., 2002; Davidheiser-Kroll, 2014).

It appears probable that the bulk of mineralization developed during early stages of rifting in the upper Tournaisian and that hydrothermal activity continued, probably episodically, into the lowermost Arundian, a timeframe of around 10 million years (Ashton et al., 2015). This is consistent with interpreted ages for other systems in the Irish Orefield (Wilkinson, 2003; Wilkinson et al., 2003; Schneider et al., 2007; McArdle, 1990).

Geochronological and paleomagnetic techniques have also been applied to the Navan system. Halliday and Mitchell (1983) published a single K-Ar age of 366±11 Ma from clay concentrates in the 2-1 Lens. Symons et al. (2002), based on comprehensive sampling and paleomagnetic studies, suggested an age of 334 Ma (Asbian) for mineralization and quoted “327±3 Ma as the youngest possible age for

the B ChRm" (i.e., the magnetization event). The paleomagnetic data from mineralized and unmineralized rocks at Navan give a consistent orientation, interpreted to reflect heating and recrystallization related to the hydrothermal event rather than by regional burial. It is unlikely that the paleomagnetic data are sufficiently precise to argue for an Asbian age for mineralization, especially in the absence of any other indicators for this timing (Wilkinson et al. 2017; Ashton et al., 2015). Nonetheless, there is clearly broad agreement between these studies that the mineralization is Lower Carboniferous in age and is not related to later events. Texturally, what is clear is that there is a correlation between extensional faulting and mineralization, the dislocated sulfides in the Boulder Conglomerate and lithogeochemical and petrographic work in the Upper Dark Limestones all reveal that mineralization took place over an extended time period. Finally, there is significant geologic evidence that ore at Lisheen (Carboni et al., 2003) and at Navan (Ashton et al., 1986) is cut by thrusts related to Variscan tectonic inversion, implying that mineralization had ceased prior to Variscan deformation at ~300 Ma (Wartho et al., 2006).

1.21 Metal Distribution

Metal distribution patterns in the Main Navan Orebody have been studied extensively (Andrew and Ashton 1985; Ashton et al. 1992; Blakeman, 2002, Blakeman et al. 2002; Barnicoat et al. 2004; Davidheiser-Kroll, 2014). In the Main Orebody, distinct elongate areas of high Zn+Pb are clearly parallel to northeast-southwest structural trends and are coincident with major faults or localized zones of minor extensional fracturing (Andrew and Ashton, 1985; Blakeman et al., 2002). There is a strong tendency for the Zn/Pb ratio to decrease westwards and for Fe to increase to the northeast. The highest Fe concentrations at the Navan Orebody occur in the pyritic, stratigraphically highest lens, the so-called Conglomerate Group Ore (Ashton et al., 1992). However, several distinct areas of Zn+Pb enrichment that do not display a similar linear relationship to the Main Orebody exist. The largest is in the central SWEX near the apex of the M, N and E Faults. Smaller isolated examples occur further southwest and in the NE SWEX. In terms of Zn/Pb ratios, the strong tendency for Pb enrichment in the western part of

the Main Orebody is not evident in the SWEX. Fe in the U lens shows no clear lateral trends apart from strong enrichment close to the CGO. The lenses of CGO over the Main Orebody and the SWEX tend to show distinct patterns with Zn+Pb highest adjacent to faults, widespread enrichment of Fe, and a tendency for the Zn/Pb ratio to decrease to the southeast.

In summary, at the Main Navan Orebody, metal distribution patterns reflect the strong structural control of the northeast and east-northeast trending faults and fractures. In the SWEX, the E Fault appears to be the principal controlling structure. The perceived lack of large lateral changes in Zn, Pb and Fe in the SWEX suggest a widespread mineralising system with fluids derived from the E Fault over a considerable strike length. However, the development of equant enriched regions in the Zn+Pb distribution plots indicates that several principal feeder areas along the E Fault were active and that fluids rose in steep conduits through these areas (Blakeman et al., 2002; Davidheiser-Kroll, 2014).

1.22 Lithogeochemical Halos

Lithogeochemical studies have defined irregular halos in the Pale Beds and Upper Dark Limestones characterized by enrichments of Zn, Pb, Fe, As, Mn, Sb, Cu, Tl, Ba and Mg (Finlay et al., 1984; Van Oyen and Viane, 1988; Walker, 2005; Walker, 2010). Due to the size of the orebody, the full extent of these halos is poorly understood (Marks et al., 2013).

In the Pale Beds to the northwest of the orebody there is a gradual but extremely irregular decrease in Zn and Pb values passing from ore into sub-economic mineralization, to weak mineralization, and finally into areas where there is little visual sign of alteration or trace element enrichment. Mineralization within the halo is extremely irregular, often related to faults and fractures and shows large variations in textural style and mineralogy.

Using 3D visualization software, Walker (2010) compiled all available data and noted the apparent large and irregular distribution of Zn, Pb, Fe, Sb, Cu, Tl, Ba and Mg in the Pale Beds surrounding the deposit and north of the Randalstown Fault. He concluded that the distribution of metals in the

Pale Beds halo was due to escape of metalliferous fluids into various minor and localized structural "traps". In the Upper Dark Limestones above the SWEX, Walker (2005) identified distinct halos for at least 100 m overlying the orebody and noted the presence of abundant pyrite. He ascribed anomalous values of Zn, Pb, Fe, Sb, Cd, Cu, Co, Ni, As, Tl, Mn and P to the escape of hydrothermal fluids into basal UDL sediments near the seafloor and interpreted the impartially regular patterns to be evidence for essentially syngenetic metal deposition.

1.23 Sulfur Isotopic Analyses

An extensive stable isotope database already exists for Navan (Anderson, 1990; Ford, 1996; Anderson et al., 1998; Fallick et al., 2001; Blakeman et al., 2002; Altinok, 2005) and other Irish-type deposits (Boyce et al., 1983; Caulfield et al., 1986; Wilkinson et al., 2005a; Barrie et al., 2009; Wilkinson and Hitzman, 2014) but currently no work has been undertaken on Tara Deep. In general, these studies have outlined two dominant populations of δ^{34}S in ore sulfides, -26 to -4 ‰ and -4 to 16 ‰. The lowest δ^{34}S subgroup is interpreted as the product of bacterial sulphate reduction (BSR) of seawater sulphate during the Lower Carboniferous (Coomer and Robinson, 1976), whereas the higher values represent hydrothermal sulfide which enters the orebody with the metalliferous hydrothermal fluids, sourced dominantly from the Lower Palaeozoic basement (Anderson et al., 1998). Fallick et al. (2001) quantified the importance of BSR at Navan using the δ^{34}S of mine concentrates (Fig. 1.10), taken from the Main Orebody 5-lens (and representing up to 1Mt of ore per sample). These revealed a mean value of -13 ±2‰, indicating more than 90% of Navan sulfide was bacteriogenic. This dominance is reflected in other economic mines in Ireland. The message was clear: bacteriogenic sulfide dominance is a critical signature of economically viable deposits in Ireland.

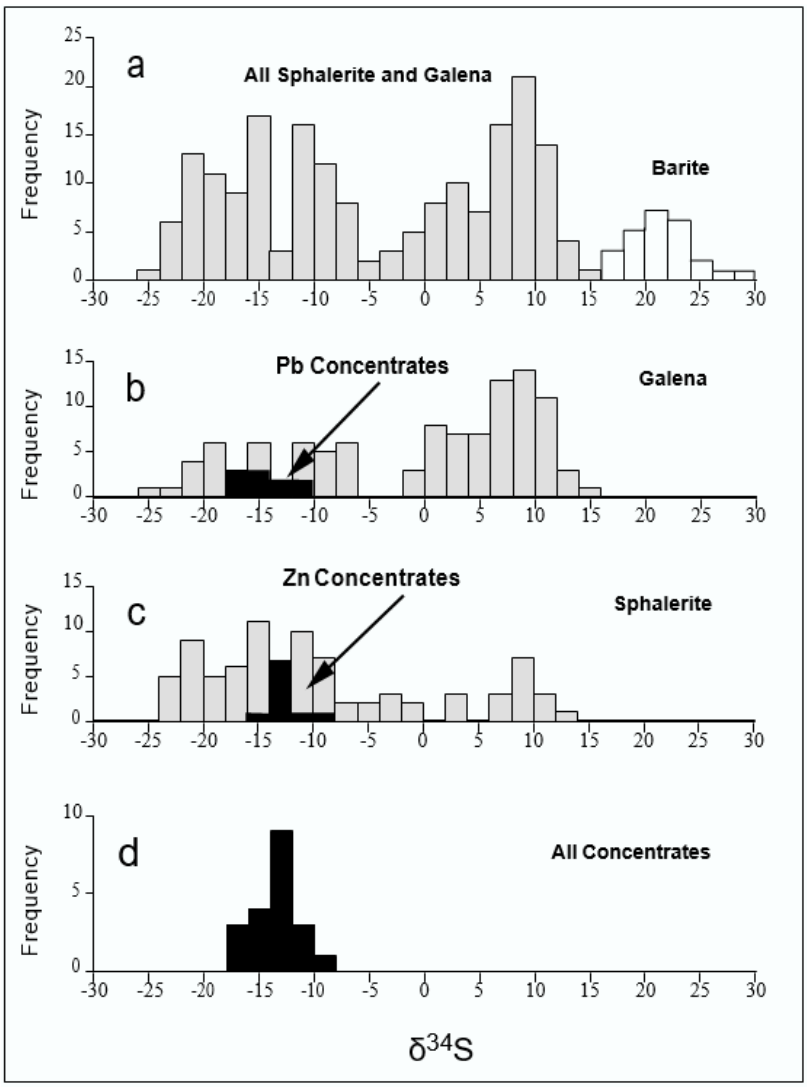

Figure 1.10 Histograms of published single mineral sulfur isotope data (Anderson et al., 1998), and sulfur isotope data from Zn and Pb concentrates from Fallick et al (2000). A) Published data from galena, sphalerite, and barite. B) Published data from galena and Pb concentrates data. C. Published data from sphalerite and Zn concentrates data. D) All Zn and Pb concentrates data combined.

1.24 Lead Isotope Analyses

Multiple lead isotope studies have been published in the Irish Midlands Orefield and these include data from Navan (Boast et al., 1981; Caulfield et al., 1986; O'Keeffe, 1986; LeHuray et al., 1987; Mills et al., 1987; Dixon et al., 1990; Fallick et al., 2001; Everett et al., 2003). These studies highlight that lead in galena and other ore sulfides from the Irish-type deposits reveal a homogeneous distribution across the deposits and possess a similar lead isotopic signature to sulfides in veins hosted by the underlying Lower Palaeozoic basement (Ashton et al., 2015). However, on a regional scale, a systematic variation in lead isotope ratios from northwest to southwest Ireland, crossing the Caledonide grain, is seen in

both Carboniferous-hosted and basement mineralization. These differing results across the Irish orebodies are interpreted to reflect mixing of lead in Ordovician and Silurian sediments during Caledonian accretion, derived from different crustal reservoirs north and south of the Iapetus suture (O'Keeffe, 1986; LeHuray et al., 1987; Dixon et al., 1990). A potential alternative source of lead from the Old Red Sandstone has been suggested but has been ruled out based on isotopic composition (Everett et al., 2003).

The first detailed analysis of lead isotopes at Navan by Mills et al., (1987) suggested that although the lead isotopic composition was relatively homogeneous in the lower lenses, it is increasingly less radiogenic in the upper two lenses. This has been interpreted as the result of extraction of Pb from the deepest, unradiogenic Lewisian basement stratigraphy. However, in more recent studies, this unradiogenic component has not been identified. Concentrate analyses conducted by Fallick et al., (2001) determined that Navan displayed a very limited range of lead isotope data ($^{206}Pb/^{204}Pb$=18.19±0.03, 2σ). These concentrates represent metallurgical bulk samples from the mine and they express the most statistically representative samples for the deposit. Although their results show that some of the $^{206}Pb/^{204}Pb$ clearly derives from Precambrian basement, their results outline that only a small fraction of the ore is derived from this deep source. Furthermore, analysis by Caulfield et al., (1986) reveal similar compositions at Tatestown (a satellite deposit to the NW of the Navan deposit; Fig. 1.5), revealing that there is no significant difference in metal sourcing.

1.25 Zn, Fe, Nd, Sr Isotopes

Nd-Sr studies on gangue minerals spanning the Navan paragenetic sequence, and from Lower Palaeozoic rocks, suggest that limestone buffered brine mixed with hydrothermal fluids that had passed through sub-Carboniferous rocks (Walshaw et al., 2006). Similar to the Pb isotope analysis, the $^{143}Nd/^{144}Nd$ ratio of the inferred basement-derived component was interpreted to be too low to suggest leaching from the Old Red Sandstone, the authors agreed with similar interpretations made by Mills et al., (1987), and state that both Lower Palaeozoic and Pre-Cambrian metal sources were involved. There

is also evidence of the earliest dolomite phase having Sr derived from Lower Carboniferous seawater or the host limestone, and having the most Lower Carboniferous marine-like Nd (Walshaw et al., 2006).

Zn isotope compositions of high-grade ore at Navan and elsewhere in the orefield are consistent with efficient leaching of metals from the putative Lower Palaeozoic source (Wilkinson et al., 2005B). Mobility of Zn and Pb is mainly sensitive to pH, temperature and fO2 changes, with Zn generally being more mobile than Pb (Anderson 1990; Cooke et al. 2000). Mirco-drilled colloform sphalerite textures at Navan, reveal a large variation in Zn, Fe and S compositions (Gagnevin et al., 2014). These display a positive correlation between δ^{66}Zn, δ^{56}Fe and δ^{34}S, interpreted to represent interplay between kinetic Zn and Fe isotope fractionation during sphalerite precipitation, and mixing of S between hydrothermal fluids and more locally sourced brines. The authors suggest that incoming pulses of metal-rich hydrothermal fluid triggered base metal sulfide mineralization, and that rapid precipitation of sphalerite and pyrite from hydrothermal fluids led to strong kinetic fractionation of Zn and Fe isotopes on very short time scales. Subsequently, restricting the use of Fe and Zn isotopes as exploration tools within deposits but revealing the possibility of detecting new deposits from isotopically heavy Zn-Fe geochemical halos. Barrie et al. (2009) agrees with this theory of metalliferous hydrothermal pulses triggering sulfide mineralization through the analysis of the micro-stratigraphy of sphalerite within colloform textures from Galmoy.

1.26 Helium Isotope Analyses

Current $^{3}He/^{4}He$ analogues reveal that mantle melting, and high $^{3}He/^{4}He$ values, are prevalent in extensional settings, but there is no existence of them in topographically-loaded basins or regions of compressional tectonics (Oxburgh, et al., 1986). Through analysis of $^{3}He/^{4}He$ trapped in fluid inclusions at Navan, and through obtaining an atmospheric-free supra-crustal value, Davidheiser-Kroll (2014) was able to show that at least a portion of mantle melting occurred during ore genesis. The quantity of trapped mantle ^{3}He varies within each deposit and between deposits across the Irish Orefield, Navan actually displays the smallest component. Thus, Davidheiser-Kroll (2014) strongly suggests that

enhanced mantle heat flow is ultimately responsible for driving fluid convection at Navan, and other Irish-ore deposits, rather than topographic flow as a consequence of compressional tectonics.

1.27 Carbonate Petrography at Navan

Extensive petrographic studies of the Navan host rocks have been completed involving drill core logging, thin section petrography, cathodoluminescence (CL), fluid inclusion and isotopic analyses (Anderson, 1990; Redmond, 1991; Rizzi, 1992; Farrelly, 1993; Braithwaite and Rizzi, 1997; Rizzi and Braithwaite, 1996, 1997; Anderson et al., 1998; Everett and Wilkinson, 2001; Thorpe, 2001; Peace, 1999; Peace et al. 2003; Knight, 2012). Anderson (1990) and Peace et al. (2003) outlined that mineralization commenced before the complete occlusion of porosity in the Pale Beds. This porosity likely provided a pathway for hydrothermal fluids, which themselves were corroded due to acidic metalliferous fluids flowing through an alkaline host rock.

Other textures have been described across the literature. Many of these authors have described early marine carbonate deposition and cementation involving micrite and radiaxial fibrous calcite (RFC) followed by dog-tooth and sparry calcite cements. Rizzi (1992) and Rizzi and Braithwaite (1996) noted that the Lower Pale Beds contained evidence of emersion and hard-grounds in numerous sedimentary cycles and described meteoric stalactitic cements from these cycles as evidence of subaerial exposure. They regarded this cementation as being early, complex, and not representing a single petrogenesis. A similar shallow burial origin for most of the calcite cements was inferred by Everett and Wilkinson (2001) based on the occurrence of vadose zone “dripstone” textures and parallels with the cementation history of the Waulsortian limestone (Lees and Miller, 1995; Wilkinson et al, 2003).

1.28 Oxygen and Carbon Isotopes

Oxygen and carbon isotopic analyses have been carried out on Navan carbonates (limestone and gangue; Rizzi, 1992; Braithwaite and Rizzi, 1997; and Peace, 1999). The 5 Lens dolomite unit ($\delta^{18}O_{V\text{-}SMOW}$

= 20.2 ‰ to 24.1 ‰; $\delta^{13}C_{V\text{-}PDB}$ = 1.3 ‰ to 2.9 ‰) has a similar compositional range to the 'stratal dolomites' that occur within the dolomite plume in the north-western part of the Main Orebody. Massive dolomite from within the core of the plume have lower $\delta^{13}C$ values but similar $\delta^{18}O$. Combining this with the morphology of the dolomite body and fluid inclusion data, the dolomite was proposed to have formed by upward flow of buoyant hydrothermal fluids derived from seawater (~60°C). Agreement exists through analysis of the 5-Lens dolomite by Peace (1999).

Overall, the carbon and oxygen data can be interpreted as reflecting exchange between elevated temperature hydrothermal fluids, depleted in ^{13}C and ^{18}O, with the host rocks and/or in situ pore waters. Model curves suggest that an initial negative shift in $\delta^{18}O$ occurred, followed by an increasingly negative shift in $\delta^{13}C$, which can be explained by isotope exchange between a hydrothermal fluid of constant input composition and temperature as a function of variable water/rock ratio (Ashton et al., 2015).

1.29 Maturation

Maturation studies indicate that the Navan host-rocks should have passed through the oil-window. Despite this, small amounts of crude oil are minorly distributed within vugs and carbonate veins in the Boulder Conglomerate, Waulsortian, and Upper Dark Limestones, suggesting that maturation was lower in the Navan area than thermal indicators suggest. Survival of low homogenisation temperatures and monophase fluid inclusions in weak minerals like calcite and barite at Navan, are unlikely to have been preserved if a Variscan heating event exceeded ~150°C (Wilkinson et al., 2003; Wilkinson, 2010).

1.30 Summary: Irish-Type Genetic Model

World-class orebodies, such as Navan, are major geochemical anomalies within the Earth's crust whose existence reflects an unusual convergence of numerous geological conditions. It is important to understand that genetic models of a deposit are used to constrain the most likely location of high-grade mineralization, alongside elucidating the deposit's size, morphology and whether any potential satellite

deposits exist. However, every model has its weaknesses and should only be used as a guide to outline a system, there is no one model fits all for each mineralization system, every deposit is unique and has its own dynamic geological processes ongoing.

The classification of Irish-type deposits has long been a debated concept in economic geology. In general, these deposits are mostly developed on the margins of kilometre-scale basins/sub-basins controlled by synsedimentary faults. Originally these Irish-type orebodies were not regarded as their own single entity, they were considered hybrids between sedimentary exhalative (SEDEX) and Mississippi Valley Type (MVT) deposits due to their similar geological characteristics and genetic models (see Anderson, 1990; Blakeman, 2002, Wilkinson and Hitzman, 2014), in particular their strong association with carbonate stratigraphy (limestone/dolostone). These Irish-Type deposits have features in common with both SEDEX and MVT deposits, such as MacArthur River, Red Dog, the Alpine-type deposits and deposits in the Selwyn Basin (Wilkinson, 2014). This cross-over between the two styles, characterises the deposits as a distinct species– as it does not conform to one model. This has also led to controversies in their genetic understanding (Peace and Wallace, 2000).

The primary characteristics of these Irish-type deposits (Fig. 1.11) are typically–calcite/dolomite-hosted, with sphalerite and galena dominating. Variable but locally major pyrite, marcasite, barite and anhydrite, with minor sulfosalts and local Cu-sulfides occur (e.g., Anderson et al., 1998; Ashton et al., 1986; Boast et al., 1981; Fusciardi et al. 2003). Their morphology are broadly stratiform–stratabound and occur as single or multiple lenses hosted by permeable and/or reactive horizons within the host rocks. Mineralization typically formed from carbonate subsurface replacement of Lower Carboniferous marine carbonate transgressive sequences within the Irish Midlands. In southern and central Ireland this is primarily the Waulsortian limestone formation. Whereas, in north and central Ireland this is dominantly the Navan Group (Anderson, 1990; Hitzman and Beaty, 1996; Philcox, 1984; Wilkinson and Hitzman, 2014; Ashton et al., 2015). Regionally, Zn–Pb mineralization is hosted by Lower Carboniferous (Mississippian) rocks, within both the Waulsortian limestone formation

and the Navan Group (Phillips and Sevastopulo, 1986). The host rocks underwent early diagenesis, including extensive calcite cementation and dolomitization (Gregg et al., 2001; Lee and Wilkinson, 2002; Lees and Miller, 1995; Peace et al., 2003; Reed and Wallace, 2001; Wilkinson, 2003). Mineralization within these units occurred through mixing of two fluids – one, a deep, metal-bearing hydrothermal fluid of moderate salinity with temperatures reaching at least 250°C; the other, a highly saline groundwater, or subsurface brine, derived from evaporation of Lower Carboniferous seawater (Banks et al., 2002, Wilkinson, 2010; Ashton et al., 2015). Major Caledonian fault systems, reactivated during Carboniferous extension, likely related to crustal thinning (Russell, 1978, 1986; Davidheiser-Kroll, 2014), exerted key structural controls on focusing fluid flow (Wilkinson and Hitzman, 2014). Pb isotopic evidence indicates that metals were sourced from the underlying basement, particularly the Lower Palaeozoic package of sediments and volcanic rocks, rather than regional fluid flow through the Red Beds (LeHuray et al., 1987; Everett et al., 2003; Walshaw et al., 2006; Fallick et al., 2001). Lead isotope analyses have revealed that there is a systematic variation in the isotopic composition of galena across the region, that mimics the underlying Lower Palaeozoic geology (Caulfield et al., 1986; Dixon et al., 1990; LeHuray et al., 1987; O'Keeffe, 1986). The variation in the Lower Palaeozoic rocks is interpreted to be due to sedimentary mixing of Pb derived from weathering of the two continental blocks (Grenvillian and Avalonian) on either side of the Iapetus Ocean (Dixon et al., 1990). An interpretation, that Pb was sourced from the clastic Old Red Sandstone, has been discounted based on its overly radiogenic signature and geologic arguments that it is unlikely to have acted as a continuous regional aquifer (Everett et al., 2003). This interpretation is backed-up by the fact that strontium, carbon, and oxygen isotope data also point to sourcing of components from beneath the Lower Carboniferous basin. Several similarities have been observed between various Irish-type deposits; cavity fill sulfides have been observed in the Waulsortian limestones at Tynagh (Boast et al., 1981) and in the Navan deposit (Anderson *et al.*, 1998). Evidence for early textures is limited within Irish-type deposits, especially at Navan, but the genetic significance of such evidence is vital. Although, not yet discovered at Navan, feeder zones are present at Silvermines (Taylor and Andrew, 1978; Fallick *et al.*, 2001) and breccia-

hosted and cavity fill sulfides are described from Kildare (Emo, 1986). Sulfur isotope analyses of barite ($\delta^{34}S$ 14.1–22.6‰; Andrew and Ashton, 1985; Boyce et al., 1983; Caulfield et al., 1986; Wilkinson et al., 2005a) is indicative of the Lower Carboniferous seawater sulphate at the time and followed the secular variation in seawater sulphate, which declined from about 21‰ at the start of the Tournaisian to about 12‰ in the late Stephanian (Kampschulte et al., 2001). A dominance of bacteriogenic sulfur reduction (BSR) is also an essential ingredient of the economic Irish-type deposits (Fallick et al., 2001), a feature shared, for example, with Alpine-type deposits (Schroll and Rantisch, 2005). This dominance of sulfur derived from BSR, alongside the strong seawater input, strongly suggests that mineralization occurred at shallow burial depths within the subsurface.

Finally, there is good geologic evidence that ore at Lisheen (Carboni et al., 2003) and at Navan (Ashton et al., 1986) is cut by thrusts related to Variscan tectonic inversion. This implies that mineralization had ceased prior to Variscan deformation at ~300 Ma (Wartho et al., 2006), with the entire Irish Orefield being exposed to minor deformation and metamorphism since the upper Palaeozoic.

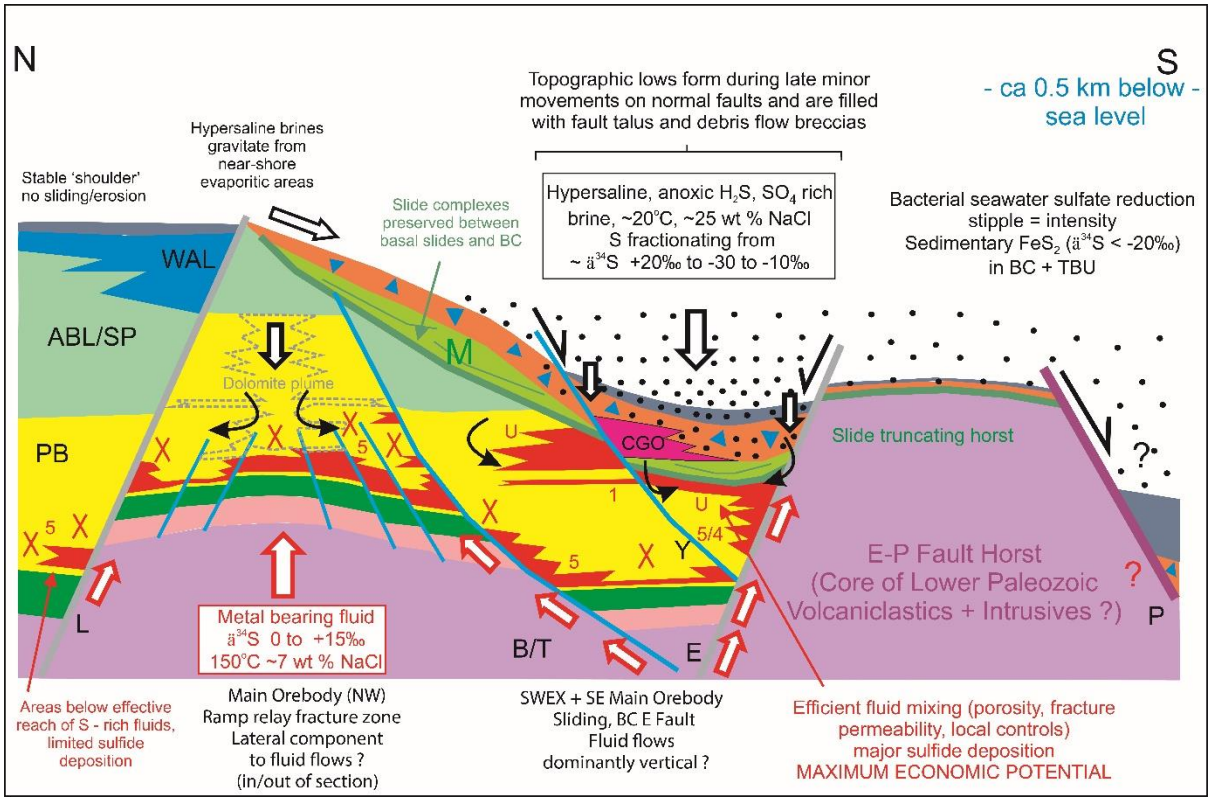

Figure 1.11. Cartoon N-S section illustrating the current model for fluid mixing and mineralization, especially in relation to main structures and the Boulder Conglomerate within the Navan Deposit (extracted from Ashton et al., 2015; highly diagrammatic and derived from a combination of mine sections). The cartoon refers to the period after cessation of major sliding, but during the formation of the Boulder Conglomerate, when it is envisaged that most mineralization had formed but was still in progress. Not scaled, section is approximately 3km long

1.31 References

Altinok, E., 2005, Zn-Pb-Fe Mineralization process, evolution of sea water oxidation state in a restricted basin, and diagenesis of deep water calcareous sediments: geochemical and geological study of the Navan Deposit, Dublin Basin, Ireland. Unpublished PhD thesis, Colorado School of Mines, p. 160

Anderson, I.K., Andrew, C.J., Ashton, J.H., Boyce, A.J., Caulfield, J.B.D., Fallick, A.E., and Russell, M.J., 1990, Preliminary sulphur isotope data of diagenetic and vein sulphides in the Lower Palaeozoic strata of Ireland and Southern Scotland: Implications for Zn + Pb + Ba mineralization: Journal of the Geological Society of London, v. 146, p. 715–720.

Anderson, I.K., Ashton, J.H., Boyce, A.J., Fallick, A.E. And Russell, M.J., 1998, Ore Depositional Processes In The Navan Zn-Pb Deposit, Ireland. Economic Geology v. 93, p. 535-563.

Andrew CJ (1986) The tectono-stratigraphic controls to mineralization in the Silvermines area, County Tipperary, Ireland. In: Andrew CJ, Crowe RWA, Finlay S, Pennell WM, and Pyne J (eds.) Geology and Genesis of Mineral Deposits in Ireland. Dublin: Irish Association for Economic Geology. p. 377–417.

Andrew, C.J., and Ashton, J.H., 1985. Regional setting, geology and metal distribution patterns of Navan orebody, Ireland: Trans. Inst. Min. Metall. (Sect.B: Appl. earth SCi.), v. 94, p. 66-93.

Ashton, J.H., Beach, A., Blakeman, R.J., Coller, D., Henry, P., Lee, R., Hitzman, M., Hope, C., Huleatt-James, S., O'donovan, B., Philcox, M.E., 2018. Discovery Of The Tara Deep Zn-Pb Mineralisation At The Boliden Tara Mine, Navan, Ireland: Success With Modern Seismic Surveys. In Seg Special Publications No 21, p. 365-381.

Ashton, J.H., Black, A., Geraghty, J., Holdstock, M. and Hyland, E., 1992, The geological setting and metal distribution patterns of Zn-Pb-Fe mineralization in the Navan Boulder Conglomerate. In: Bowden, A.A., Earls, G., O'Connor, P.G. and Pyne, J.F. (Eds). The Irish Minerals Industry 1980-1990. IAEG, Dublin, p. 171-210.

Ashton, J.H., Downing, D.T., and Finlay, S., 1986, The geology of the Navan Zn-Pb orebody, in Andrew, C.J. et al., eds., Geology and genesis of mineral deposits in Ireland: Irish Association for Economic Geology, Dublin, p. 243–280.

Ashton, J.H., Holdstock, M.P., Geraghty, J.F., O'Keeffe, W.G., Peace, W. and Philcox, M.E., 2003, The Navan Orebody - Discovery and Geology of the South West Extension. In: Kelly, J.G., Andrew, C.J., Ashton, J.H., Boland, M.B., Earls, G., Fusciardi, L., Stanley, G. (Eds). Europe's Major Base Metal Deposits. IAEG, Dublin, p. 405-430.

Ashton, J.H.; Blakeman, R.J.; Geraghty, J.F.; Beach, A.; Coller, D.; Philcox, M.E. 2015 The Giant Navan carbonate-hosted Zn–Pb deposit—A review. In Current Perspectives on Zinc Deposits;

Archibald, S.M.,Piercey, S.J., Eds.; Irish Association for Economic Geology: Dublin, Ireland, 2015; p. 85–122.

Banks, D.A., Boyce, A.J., and Samson, I.M., 2002, Constraints on the origins of fluids forming Irish Zn-Pb-Ba deposits: Evidence from the composition of fluid inclusions. Economic Geology, 97, p. 441-480.

Barker, G.J., Menuge, J.F., Boyce, A. J. and Barrie, C. D., 2012, Chemical and Isotopic Study of Sulphides from Conglomerate Group Ore, Navan, Ireland. Mineral Deposits Studies Group AGM, Cardiff, January, 2012.

Barnicoat, A.C., Wilkinson, J.C., Boyce, A.J., Yardley, B.W.D. and Graham, C.M., 2004, Multi-Scale Fluid Flow Path Analysis: Calibration and Modelling Using Mineralisation Systems. NERC Micro 2 Macro Project. Published on web at: www.bgs.ac.uk/micromacro/FinalMeeting/Yardley.pdf, p.34.

Barrie, C., Boyce, A., Boyle, A., Williams, P., Blake, K., Wilkinson, J., Lowther, M., Mcdermott, P. And Prior, D. (2009). On The Growth Of Colloform Textures: A Case Study Of Sphalerite From The Galmoy Ore Body, Ireland. Journal Of The Geological Society, 166(3), p.563-582.

Blakeman, R.J., 2002, The Compositions and routes of the fluids generating the Navan giant base-metal orebody. Unpublished PhD thesis, University of Glasgow, p. 207.

Blakeman, R.J., Ashton, J.H., Boyce, A.J., Fallick, A.E. and Russell, M.J., 2002, Timing of interplay between hydrothermal and surface fluids in the Navan Zn+Pb orebody, Ireland: Evidence from metal distribution trends, mineral textures and $\delta^{34}S$ analyses. Economic Geology, 97, p. 73-91.

Boast, A.M., Coleman, M.L., and Halls, C., 1981, Textural and stable isotopic evidence for the genesis of the Tynagh base metal deposit, Ireland: Economic Geology, v. 76, p. 27–55.

Boyce, A. J., Anderton, R. And Russell, M.J., 1983, Rapid Subsidence And Early Carboniferous Base-Metal Mineralization In Ireland. Trans. Instn Min. Metall. (Sect B: Appl. Earth Sci.), v. 92, p. 55-66.

Braithwaite, C.J.R. and Rizzi, G., 1997, The geometry and petrogenesis of hydrothermal dolomites at Navan, Ireland. Sedimentology, v. 44, p. 421-440.

Carboni, V., Walsh, J.J., Stewart, D.R.A., and Güven, J.F., 2003, Timing and geometry of normal faults and associated structures at the Lisheen Zn/Pb deposit, Ireland—investigating their role in the transport and trapping of: Society for Geology Applied to Mineral Deposits Meeting, 7th biennial, Athens, Greece, Proceedings, p. 665–668.

Caulfield, J.B., LeHuray, A.P. and Rye, D.M., 1986, A review of lead and sulphur isotope investigations of Irish sediment-hosted base metal deposits, with new data from the Keel, Ballinalack, Moyvoughly and Tatestown deposits, in Geology and genesis of mineral deposits in Ireland in Andrew, C.J., Crowe, R.W.A., Finlay, S., Pennell, W.M., and Pyne, J.F., eds., Dublin, Irish Association for Economic Geology, p. 591–615.

Clifford, J.A., Ryan, P. and Kucha, H., 1986, A review of the geological setting of the Tynagh orebody, Co., Galway. In: Geology and genesis of mineral deposits in Ireland. Andrew, C.J., Crowe, R.W.A., Finlay, S., Pennell, W. and Pyne, J.F. (Eds.) IAEG, Dublin, p. 419-439.

Coller, D., Beach, A., Ashton, J., Geraghty, J.,Holdstock, M., O'Keeffe W., Philcox, P. and Walker, N., 2005, Structural Geology and Tectonic Setting of the Navan Zn-Pb Orebody - Inversion of a Degraded Footwall-Uplift Fault Block. Presentation to Mineral Deposits Studies Group Annual Meeting, Belfast.

Cook, H.E. and Mullins, H.T., 1983, Basin margin environment. Chap. 11. 540-617. In: Scholle, P.A., Bebout, D.G. and Moore, C.H. (Eds). Carbonate depositional environments. Tulsa OK, AAPG, p. 708.

Cooke, D., Bull, S., Large, R. and McGoldrick, P., 2000. The Importance of Oxidized Brines for the Formation of Australian ProterozoicStratiform Sediment-Hosted Pb-Zn (Sedex) Deposits. Economic Geology, 95(1), p.1-18.

Coomer, P.G., and Robinson, B.W., 1976, Sulphur and sulphate-oxygen isotopes and the origin of the Silvermines deposits, Ireland: Mineralium Deposita, 11, p. 155-169.

Cooper, M.A., Collins, D.A., Ford, M., Murphy, F.X., Trayner, P.M., O'Sullivan, M.J., 1984. Structural style, shortening estimates and the thrust front of the Irish Variscides. In: Hutton, D.H.W., Sanderson, D.J. (Eds.), Variscan Tectonics of the North Atlantic Region Special Publication, 14. Geological Society of London, London, pp. 167–175.

Cooper, M.A., Collins, D.A., Ford, M., Murphy, F.X., Trayner, P.M., O'Sullivan, M.J., 1986. Structural evolution of the Irish Variscides. Journal of the Geological Society, London 143, p. 53–61.

Cruise, M.D., Boyce, A.J. and Fallick, A.E. 1999. Iron oxide alteration associated with the carbonatehosted Tynagh and Crinkill base-metal deposits, Ireland: evidence of the involvement of dissolved atmospheric oxygen. *In*: STANLEY, C.J. et al. (eds). Mineral deposits: Processes to Processing. Proceedings of the 5thBiennial SGA Meeting, Balkema, Rotterdam, London, United Kingdom, 2, p.833-836.

Davidheiser-Kroll, B. 2014. Understanding the fluid pathways that control the Navan ore body. PhD thesis, University of Glasgow.

Dixon, P.R., LeHuray, A.P., and Rye, D.M., 1990, Basement geology and tectonic evolution of Ireland as deduced from Pb isotopes. Journal of the Geological Society, London, 147, p. 121-132.

Dolan, J. M. 1983. A structural cross-section through the Carboniferous of northwest Kerry. *Irish Journal of Earth Sciences,* 6, p. 95-108.

Emo, G. T. 1986. Some considerations regarding the styles of mineralization at Harberton Bridge, Co. Kildare. In: Andrew, C. J., Crowe, R. W. A., Finlay, S., Pennell, W. M. & Pyne, J. (eds) Geology and Genesis of Mineral Deposits in Ireland. Irish Association for Economic Geology, Dublin, p. 461-470.

Everett, C. E. and Wilkinson, J., 2001, Fluid Evolution at the Navan Deposit: Preliminary fluid inclusion results. Unpublished Report. p. 14.

Everett, C. E., Rye, D.M. And Ellam, R.M., 2003, Source Or Sink? An Assessment Of The Role Of The Old Red Sandstone In The Genesis Of The Irish Zn-Pb Deposits. Economic Geology, 98, p. 31-50.

Everett, C. E., Wilkinson,J. J. Rye,D. M. 1999. Fracture-Controlled Fluid Flow In The Lower Palaeozoic Basement Rocks Of Ireland: Implications For The Genesis Of Irish-Type Zn-Pb Deposits. In: Mccaffrey,K. J. W., Lonergan,L. & Wilkinson,J. J. (Eds) Fractures, Fluid Flow And Mineralization. Geological Society, London, Special Publications, 155, p. 247-276.

Fallick, A.E., Ashton, J.H., Boyce, A.J., Ellam, R.M. and Russell, M.J., 2001, Bacteria were responsible for the magnitude of the world-class hydrothermal base metal sulfide orebody at Navan, Ireland. Economic Geology, 96, p. 885-890.

Farrelly, I., 1993, The relationships of mineralisation to faulting at Navan Mines, Co Meath, Ireland. Senior Sophistor Project. Trinity College Dublin, p. 60.

Finlay, S., Romer, D.M. and Cazalet, P.C.D., 1984, Lithogeochemical studies around the Navan Zinc-Lead orebody in County Meath, Ireland. In: Prospecting in areas of glaciated terrain, IMM, London, p. 35-36.

Ford, C.V., 1996, The integration of petrologic and isotopic data from the Boulder Conglomerate to determine the age of the Navan orebody, Ireland. Unpublished PhD Thesis, University of Glasgow, p.176.

Fusciardi, L.P., Guven, J.F., Stewart, D.R.A., Carboni, V., and Walshe, J.J., 2003, The geology and genesis of the Lisheen Zn-Pb deposit, Co. Tipper- ary, Ireland, in Kelly, J.G., Andrew, C.J., Ashton, J.H., Boland, M.B., Earls, G., Fusciardi, L., and Stanley, G., eds., Europe's major base metal deposits: Dublin, Irish Association for Economic Geology, p. 455–481.

Gagnevin, D. Menuge, J.F. Kronz, A. Barrie, C. Boyce, A.J. 2014, Minor Elements in Layered Sphalerite as a Record of Fluid Origin, Mixing, and Crystallization in the Navan Zn-Pb Ore Deposit, Ireland. Econ. Geol. v. 109, p. 1513-1528

Gillespie, A. 2013. A petrological and geochemical characterisation of lithologies and hydrothermal alteration in the basement to the Navan Ore Deposit, Ireland. Unpublished MSCi Thesis, University of Southampton, p. 253.

Gregg JM, Shelton KL, Johnson AW, Somerville ID, and Wright WR (2001) Dolomitization of the Waulsortian limestone (Lower Carboniferous) in the Irish Midlands. Sedimentology 48: p. 745–766.

Halliday, A.N., and Mitchell, J.G., 1983, K-Ar ages of clay concentrates from Irish orebodies and their bearing on the timing of mineralisation: Trans. Roy. Soc. of Ed., Earth Sciences, 74, p. 1-14.

Hitzman, M.W., and Beatty, D.W., 1996, The Irish Zn-Pb-(Ba) orefield, in Sangster, D.F., ed., Carbonate-hosted lead-zinc deposits: Society of Economic Geologists Special Publication, 4, p. 112–143.

Hitzman, M.W., Earls, G., Shearly, E., Kelly, J, Cruise, M. and Sevastopulo, G., 1995, Ironstones (iron oxide-silica) in the Irish Zn Pb deposits and regional iron oxide-(silica) alteration of the Waulsortian limestone in southern Ireland. In: Anderson, I.K., Ashton, J.H., Earls, G., Hitzman, M. And Tear, S., (Eds). Irish carbonate-hosted Zn-Pb deposits: Society of Economic Geologists GuidebookSeries, 21, p. 261-273

Hitzman, M.W., O'Connor, P., Shearley, E., Schaffalitzky, C., Beaty, D.W., Allan, J.R. and Thompson, T., 1992, Discovery and geology of the Lisheen Zn-Pb-Ag prospect, Rathdowney Trend, Ireland. In:

Bowden, A.A., Earls, G., O'Connor, P.G. and Pyne, J.F. (Eds). The Irish Minerals Industry 1980-1990. IAEG, Dublin, p. 227-246.

Hitzman, M.W., Redmond, P.B. and Beatty, D.W., 2002, The carbonate-hosted Lisheen Zn-Pb-Ag deposit, County Tipperary, Ireland. Economic Geology, 97, p. 1627-1655.

Kampschulte A, Bruckschen P, and Strauss H, 2001. The sulphur isotopic composition of trace sulphates in Carboniferous brachiopods: Implications for coeval seawater, correlation with other geochemical cycles and isotope stratigraphy. Chemical Geology 175: p. 149–173.

Knight, H., 2012, Seeking The deep fluid feeder zone of the Navan Zn-Pb deposit, Republic of Ireland. Unpublished MSc thesis, Imperial College, p. 44.

Lee, M.J. and Wilkinson, J.J., 2002, Cementation, hydrothermal alteration, and Zn-Pb mineralization of carbonate breccias in the Irish Midlands: textural evidence from the Cooleen Zone, near Silvermines, County Tipperary. Economic Geology, 97, p. 653-662.

Lees, A. And Miller, J., 1995, Waulsortian Banks. In Monty, C.L.V., Bosence, D.W.J., Bridges, P.H. And Pratt, B. R., (Eds). Carbonate Mud-Mounds. Int Assoc Sediment Spec Pub 23, Blackwell Science, Oxford, P.191-271.

LeHuray, A.P., Caulfield, J.B.D, Rye, D.M and Dixon, P.R., 1987, Controls on Sediment-Hosted Zn-Pb Deposits: A Pb Isotope Study of Carboniferous Mineralization in Central Ireland. Economic Geology, 82, p. 1695-1709.

Marks, F.R., Menuge, J.F., Boyce, A.J,. and Blakeman, R.J., 2013, Characterising a geochemical and isotopic halo of the Navan Zn-Pb Irish-type deposit. in MDSG Abstracts Volume 2013, Leicester, p. 71.

Matte P, 2001. The Variscan Collage And Orogeny (480_290 Ma) And The Tectonic Definition Of The Armorica Microplate: A Review. Terra Nova 13: p. 122–128.

McArdle, P., 1990, A review of carbonate hosted base metal - barite deposits in the Lower Carboniferous of Ireland. Chronique de la Miniere, Recherche, 500, p. 3-29.

Mills, H., Halliday, A.N., Ashton, J.H., Anderson, I.K., Russell, M.J., 1987, Origin of a giant orebody at Navan, Ireland. Nature, 327, p. 223-226.

Morris, P. & Max, M. D. 1995. Magnetic Crustal Character In Central Ireland. Geological Journal, 30, p. 49-67

Nolan, S.C., 1989, The style and timing of Dinantian synsedimentary tectonics in the eastern part of the Dublin Basin, Ireland. In: Arthurton, R.S., Gutteridge, P. and Nolan,S. C. (Eds). The role of tectonics in Devonian and Carboniferous sedimentation in the British Isles. Yorkshire Geological Society, Occasional Publication 6, p. 83-97.

O'Keeffe, W.G., 1986, Age and postulated source rocks for mineralization in central Ireland, as indicated by lead isotopes. In: Andrew, C.J., et al. (Eds). Geology and Genesis of Mineral Deposits in Ireland. IAEG, Dublin, p. 617–624.

OBrien, M.V. and Romer, D.M., 1971. Tara geologists describe Navan discovery: World Mining, 24, p. 38-39.

Oxburgh, E. R., O'nions, R. K. & Hill, R. I. 1986. Helium isotopes in sedimentary basins. Nature, 324, p. 632-635.

Peace, W. and Wallace, M., 2000. Timing of mineralization at the Navan Zn-Pb deposit: A post-Arundian age for Irish mineralization. Geology, 28(8), p.711.

Peace, W.M., 1999, Carbonate-hosted Zn-Pb mineralisation within the Upper Pale Beds at Navan, Ireland: Unpub. Ph.D. thesis, Univ. Melbourne, p. 284.

Peace, W.M., Wallace, W.M., Holdstock, M.P. and Ashton, J.H., 2003, Ore textures within the U lens of the Navan Zn-Pb deposit, Ireland. Mineralium Deposita. 38, p. 568–584.

Philcox ME, 1989. Lower Carboniferous lithostratigraphy of the Irish Midlands. IAEG, Dublin; 89.

Philcox, M.E. 1984. Lower Carboniferous Lithostratigraphy of the Irish Midlands; Irish Association for Economic Geology: Dublin, Ireland; p.89.

Phillips, W. E. A. & Sevastopulo, G. D. 1986. The Stratigraphic And Structural Setting Of Irish Mineral Deposits. In: Andrew, C. J., Growl, R. W. A., Finlay, S., Pennell, W. M. & Pyne, J. F. (Eds) Geology And Genesis Of Mineral Deposits In Ireland. Irish Association For Economic Geology, Dublin, 1-30.

Redmond, P.B., 1991. The production of a complete NW strike section across the Navan orebody with a study of the stratigraphy, mineralization and diagenetic history across the section, accompanied by a study of mineralization in underground exposure. Unpublished BSc Thesis, Trinity College Dublin, 111 p.

Reed, C.P., and Wallace, M.W., 2001, Diagenetic evidence for an epigenetic origin of the Courtbrown Zn-Pb deposit, Ireland. Mineralium Deposita, v. 36, p. 428-441.

Rizzi, G. and Braithwaite, C.J.R., 1996, Cyclic emersion surfaces and channels within Dinantian limestones hosting the giant Navan Zn-Pb deposit, Ireland. In: Strogen P., Somerville, I.D. & Jones, G.Ll. (eds), Recent Advances in Lower Carboniferous Geology, Geological Society Special Publication No. 107, p. 207-219.

Rizzi, G. And Braithwaite, C.J.R., 1997. Sedimentary cycles and selective dolomitization in limestones hosting the giant Navan zinc-lead ore deposit, Ireland. Exploration and Mining Geology, v. 6, p. 63-77.

Rizzi, G., 1992, The sedimentology and petrography of Lower Carboniferous limestones and dolomites; host rocks to the Navan zinc-lead deposit, Ireland. Unpublished PhD thesis, University of Glasgow, p. 369.

Rothery, E. 1988. En-Echelon Vein Array Development In Extension And Shear. Journal Of Structural Geology, 10, p. 63-71.

Russell, M. J. 1968. Structural controls of base metal mineralization in relation to continental drift. Transactions of the Institution for Mining and Metallurgy, 77B, p. 11-28.

Russell, M.J., 1978, Downward-excavating hydrothermal cells and Irish type ore deposits: Importance of an underlying thick Caledonian prism. Trans. Instn Min. Metall. (Sect B: Appl. Earth Sci.), 87, p. 168-171.

Russell, M.J., 1986, Extension and convection: a genetic model for the Irish Carboniferous base metal and barite deposits. In: Andrew, C.J., Crowe, R.W.A., Finlay, S., Pennell, W.M., Pyne, J.F., (Eds). Geology and Genesis of Mineral Deposits in Ireland. IAEG, Dublin, p 545-554.

Sanderson, O. J. 1984. Structural variation across the northern margin of the Variscides in NW Europe. In: Hutton, D. H. W. & Sanderson, D. J. (Eds) Variscan Tectonics Of The North Atlantic Region. Geological Society, London, Special Publication, 14, P. 149-166.

Schneider J, Von Quadt A, and Wilkinson JJ, 2007. Age of the Silvermines Irish-type Zn-Pb deposit from direct Rb-Sr dating of sphalerite. In: Andrew CJ, et al. (eds.) Digging Deeper: Proceedings of the 9th Biennial Meeting of the Society for Geology Applied to Mineral Deposits, Dublin, Ireland, 20–23 August 2007, p. 373–376. Dublin: Irish Association for Economic Geology.

Schroll, E., Rantitsch, G., 2005. Sulphur isotope patterns from the Bleiberg deposit (Eastern Alps) and their implications for genetically affiliated lead–zinc deposits. Mineralogy and Petrology. 84, p.1–18.

Scotese, C. R, Atlas of Earth History, Paleomap Project, Arlington, Texas, p.52.

Singer D, A., 1995. World-class base and precious metal deposits; a quantitative analysis. Economic Geology 90: 88–104.

Steed, G, M. 1980. Silver in the Tara Mines Mineral Deposit at Navan- With Particular Emphasis On The Ore To The West Of The Main Shaft Pillar. Boliden Tara Mines Internal Report.

Strogen, P., Somerville, I., Pickard, N., Jones, G. and Fleming, M., 1996. Controls on ramp, platform and basinal sedimentation in the Dinantian of the Dublin Basin and Shannon Trough, Ireland. Geological Society, London, Special Publications, 107(1), p.263-279.

Symons, D.T.A., Smethurst, M.T. and Ashton, J.H. 2002. Paleomagnetism of the Navan Zn-Pb deposit, Ireland. Economic Geology, v97, p.997-1012.

Taylor S (1984) Structural and paleotopographic controls of leadzinc mineralization in the Silvermines orebodies, Republic of Ireland. Econ Geol 79: p.529–548

Taylor, S and Andrew, C.J., 1978, Silvermines orebodies, Co. Tipperary, Ireland: Transactions of the Institution of Mining and Metallurgy, v. 87B, p. 111–124.

Thorpe, T.M., 2001, A Petrographic and Cathodoluminescence Study of Part of the Navan Zn-Pb Deposit, County Meath, Ireland. Unpublished MSci Research Project. Imperial College, p.73.

Treloar, M. 2014. The South West Extension - South (SWEXS) Mineralisation of the Giant Navan Zn-Pb Deposit; Genesis and Relation to the Main Orebody. Msci, Imperial College London

Van Oyen, P., and Viaene, W., 1988, Lithogeochemical investigations in the Navan area, Ireland., *in* Boissonnas J, Omenetto P., eds., Mineral deposits within the European Community, Special Publication The Society for Geology Applied to Mineral Deposits. v. 6, p. 378-390.

Vaughan, A. and Johnston, J. D., 1992, Structural constraints on closure geometr across the Iaepetus suture in eastern Ireland. Journal of the Geological Society of London, 149, p. 65-74

Walker M., 2010, Lithogeochemical Exploration Surrounding the Carbonate Hosted Zn-Pb Navan Orebody: A Historic Review, Analysis of Results and the Establishment of Future Exploration Programmes. MSc Thesis, University of Exeter, Cambourne School of Mines, p.140.

Walker, B., 2004. The Nature and Origin of the Carboniferous 'Boudin Shale' at Navan, County Meath. BSc Lab Project, Trinity College Dublin, p.27.

Walker, N., 2005, The Distribution Patterns of Pathfinder Elements in the Upper Dark Limestone Cover Sequence above the SWEX-B Mineralisation.MSc. thesis. National University of Ireland, Galway, p.150.

Walshaw R, Menuge J, Tyrrell S, 2006. Metal sources of the Navan carbonate-hosted base metal deposit, Ireland: Nd and Sr isotope evidence for deep hydrothermal convection. Minerium Deposita 41(8): p.803–819.

Wartho J-A, Quinn D, and Meere PA, 2006. The timing of Variscan deformation: UV laser 40Ar/39Ar dating of syn late-orogenic intrusions from SW Ireland. Geochimica et Cosmochimica Acta, 70(18), p. 690.

Wilkinson, J., Vowles, K., Muxworthy, A. and Mac Niocaill, C., 2017. Regional remagnetization of Irish Carboniferous carbonates dates Variscan orogenesis, not Zn-Pb mineralization. *Geology*.

Wilkinson, J.J., 2010, A Review of Fluid Inclusion Constraints on Mineralization in the Irish Orefield and Implications for the Genesis of Sediment-Hosted Zn-Pb deposits. Economic Geology, 105, p. 417-442.

Wilkinson, J.J., 2014, Sediment-Hosted Zinc–Lead Mineralization: Processes and Perspectives, In Treatise on Geochemistry (Second Edition), edited by Heinrich D. Holland and Karl K. Turekian, Elsevier, Oxford, p. 219-249.

Wilkinson, J.J., Boyce, A.J., Everett, C.E., Lee, M.J., 2003, Timing and depth of mineralization in the Irish Zn–Pb orefield. In: Kelly, J.G., Andrew, C.J., Ashton, J.H., Boland, M.B., Earls, G., Fusciardi, L., Stanley, G. (Eds.), Europe's Major Base Metal Deposits. Irish Assoc. Econ. Geol., Dublin, p. 483-497.

Wilkinson, J.J., Everett, C.E., Boyce, A.J., Gleeson, S.A. and Rye, D.M., 2005c, Intracratonic crustal seawater circulation and the genesis of sub-seafloor Zn-Pb mineralization in the Irish Orefield, Geology, 33, p. 805-808.

Wilkinson, J.J., Eyre, S.L. and Boyce, A.J., 2005a, Ore-forming processes in Irish-type carbonate-hosted Zn-Pb deposits: Evidence from mineralogy, chemistry and isotopic composition of sulfides at the Lisheen Mine. Economic Geology, 100, p. 63-86.

Wilkinson, J.J., Weiss, D.J., Mason, T.F.D. and Coles, B., 2005b, Zinc isotope variation in hydrothermal systems: Preliminary evidence from the Irish Midlands ore field. Economic Geology, 100, p. 583-590.

Wilkinson, J.J.; Hitzman, M.W. The Irish Zn–Pb Orefield: The View from 2014. In Current Perspectives on Zinc Deposits; Archibald, S.M., Piercey, S.J., Eds.; Irish Association for Economic Geology: Dublin, Ireland, 2015; p. 59–72.

Worthington, R. and Walsh, J., 2011. Structure of Lower Carboniferous basins of NW Ireland, and its implications for structural inheritance and Cenozoic faulting. *Journal of Structural Geology*, 33(8), p.1285-1299.

Yardley, B.W., Barnicoat, A.C., Freeman, S., Banks, D., Gleeson, S., Wilkinson, J.J., Boyce, A.J., Blakeman, R., Everett, K. and Ashton, J., 2005, Multi-scale fluid-flow path analysis: Calibration and modelling using mineralisation systems, in Shaw, R.P. (ed.) Understanding the micro to macro behaviour of rock-fluid systems: Geological Society of London Special Publications, 249, p. 148-149.

CHAPTER TWO: ORE DEPOSITIONAL PROCESSES AT THE CARBONATE-HOSTED TARA DEEP Zn-Pb DEPOSIT, NAVAN, IRELAND.

Drummond[1], D. A., Blakeman[2], R. J., Ashton[3], J. H., Farrelly, I[2]., Cloutier[4], J., Yesares[5], L., Boyce[1], A. J.

Corresponding Author's Email: drewdrummond59@gmail.com

[1]Scottish Universities Environmental Research Centre, Rankine Avenue, East Kilbride, Glasgow G75 0QF, United Kingdom.

[2]Boliden Tara Mines, Exploration Department, Navan, County Meath, Ireland.

[3]*Consultant Boliden Tara Mines.*

[4]Centre for Ore Deposit and Earth Sciences, University of Tasmania, Private Bag 79, Hobart, Tasmania, Australia

[5]Irish Centre for Research in Applied Geosciences, O'Brien Centre for Science (East), University College Dublin, Belfield Down, Dublin 4, Ireland.

Key words: Zn-Pb Mineralization, Tara Deep, Irish-Type, Navan, Petrogenesis, S Isotopes, Pb Isotopes.

2.1 Abstract

The Tara Deep Zn-Pb deposit (currently 26.2 Mt @ 8.4% Zn, 1.6% Pb) is the latest major discovery by Boliden Tara Mines (first announced in 2016) which significantly adds to the existing world-class Navan deposit. Located 2 km south of the Navan deposit in Co. Meath, Ireland, economic mineralization is hosted by upper Tournaisian carbonates (Pale Beds; 87% of the total economic resource), within a degraded footwall of a major south-dipping normal fault, and also within lower Viséan sedimentary breccias (S Fault Conglomerates; SFC). Sphalerite and galena are the dominant sulfides, with massive, cavity fill and brecciated textures dominating. These textures attest complex, subsurface, episodic mineralization events that display considerable reworking, fracturing, dolomitization, open-space infill and selective replacement. Lower Viséan syn-rift sliding, erosion, and deposition of thick debrites and calc-turbidites at Tara Deep record basin margin processes near extensional faulting associated with formation of the Dublin Basin. These debrites host detrital sulfide-rich clasts and offer unambiguous evidence that the onset of mineralization occurred during the upper Tournaisian. $\delta^{34}S$ values of base metal sulfides have a bimodal distribution suggesting both bacteriogenic (-13.5 to -3.6 ‰) and hydrothermal sulfur sources (+3.4 to +16.2 ‰). Both textural and sulfur isotope data reveal the dynamic nature of mineralization at Tara Deep and infer fluid mixing. Lead isotope analyses display remarkably homogeneous $^{206}Pb/^{204}Pb$ of 18.23 ±0.006 (2σ, n=25), which is coincident with Pb isotope data across the Navan deposit. Subsequently, Tara Deep and Navan are isotopically similar, showing both a statistically identical Pb isotopic signature and a bimodal sulfide S isotopic distribution and homogeneous sulfate signature. In particular, the Pb isotopes and the hydrothermal S signature, correlate with Navan and agree that base metals were leached from the underlying Lower Paleozoic basement, and suggesting that similar deep, circulating metalliferous fluids were also involved at Tara Deep. However, despite these similarities, key differences can be recognized within the S isotope data; around 5‰ shifts to higher $\delta^{34}S$ in the surface-derived S isotope signatures (both bacteriogenic sulfide and sulfate) indicate that Tara Deep's sulfur was sourced from a distinct seawater/connate fluid

signature. The Tara Deep deposit has many similarities with the neighbouring Navan deposit reflecting comparable controls on the mineralizing processes in terms of host rocks, Pb and S sources, and tectonic environment. Mineralization initiated during an early phase of the developing Dublin Basin (syn-diagenetically) and kept pace with rifting and subsequently an evolving basin.

2.2 Introduction

The Navan deposit is a world-class carbonate-hosted Zn–Pb orebody, hosted in upper Tournaisian carbonates, and mined by Boliden Tara Mines, with total production and remaining resources (excluding Tara Deep), exceeding 125Mt at end 2020. Following a seismic survey in late 2012, first drilling in the Tara Deep region, 2 km SE of the existing mine's Southwest Extension (SWEX, Fig. 2.1), intersected 32.5 m of mineralization at 11.1% Zn and 3.0% Pb at a depth of 1.6km (Ashton et al. 2018). Hosted in the footwall of a large south-dipping basin margin fault, Tara Deep occurs at depths of between 1.2 and 1.9 km. The current inferred resource at this new discovery is 26.2Mt @ 8.4% Zn and 1.6% Pb (Boliden Summary Report, 2020), and the deposit remains open to the south and west.

Navan is by far the largest Zn+Pb deposit yet discovered in the Irish Zn+Pb(±Ag±ba) orefield and has dominated European zinc production for over 40 years. It is a type example of an Irish-type carbonate-hosted base-metal deposit (Singer, 1995; Wilkinson, 2010; Wilkinson and Hitzman, 2014). These deposits are typically calcite/dolomite-hosted, with sphalerite dominating galena, typically by a ratio of 5:1 or greater. Variable but locally major pyrite, marcasite, barite and anhydrite occur, with minor sulfosalts and rare Cu-sulfides. They have features in common with both SEDEX and MVT deposits, such as MacArthur River, Red Dog, the Alpine-type deposits and deposits in the Selwyn Basin (Wilkinson, 2014). This cross-over between the two styles, characterises the deposits as a distinct species - Irish-type - and has also led to controversies in their genetic understanding (Peace and Wallace, 2000). What is agreed, are that these deposits have formed by mixing of two fluids –1) a deep, basement derived, metal-bearing hydrothermal fluid of moderate salinity with temperatures reaching

at least 250°C; 2) a highly saline groundwater, or subsurface brine, derived from evaporation of Mississippian seawater (Boast et al, 1981a; Samson and Russell, 1987; Banks and Russell, 1992; Banks et al., 2002, Wilkinson, 2010; Ashton et al., 2015). Major Caledonian fault systems, reactivated during Mississippian extension, likely related to crustal thinning (Russell, 1968; Boyce et al, 1983a; Davidheiser-Kroll et al, 2014), exerted key structural controls on focusing fluid flow (Russell, 1978, 1986; Wilkinson and Hitzman, 2014). Pb isotopic evidence indicates that metals were sourced from the underlying basement, particularly the Lower Paleozoic package of sediments and volcanic rocks, rather than regional or transcontinental fluid flow through the Tournaisian Red Beds of the Munster Basin or the Irish Midland Basin (LeHuray et al., 1987; Everett et al., 2003; Walshaw and Menuge, 2006; Fallick et al., 2001). A dominance of bacteriogenic sulfide is also an essential ingredient of the economic Irish-type deposits (Fallick et al., 2001), a feature shared, for example, with Alpine-type deposits (Schroll and Rantisch, 2005; Henjes-Kunst et al, 2017). An association with Mississippian volcanic diatremes and extrusive rocks at Pallas Green, Co. Limerick, has added a new element to the complex nature of these deposits (Elliot et al, 2019), although He isotopes had already identified a mantle contribution to the genetic system for all economic Irish-type deposits (Davidheiser-Kroll et al, 2014).

In this context, this research presents the first detailed examination of the new Tara Deep discovery with focus on the stratigraphy, mineralogy, textures, and S and Pb isotope geochemistry. The relationship to the Navan deposit (see Anderson et al., 1998, and Ashton et al., 2015) is explored to help constrain a genetic model and widen our understanding of Irish-type deposits. The Tara Deep deposit has many similarities with the existing Navan deposit, reflecting comparable controls on the mineralizing processes in terms of host rocks, Pb and S sources, and tectonic environment. Tara Deep thus offers exciting potential for future expansion of resources.

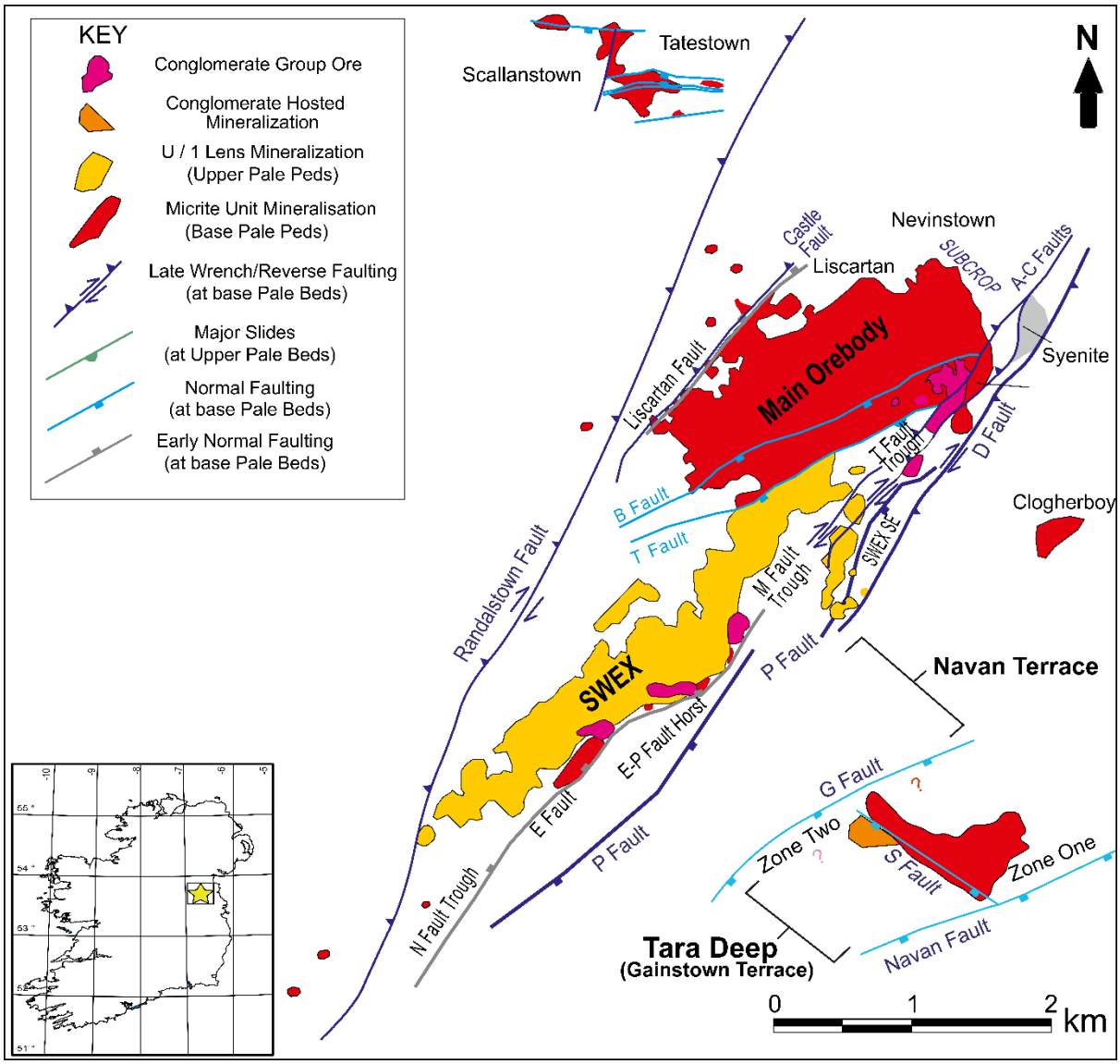

Figure 2.1 Structural plan showing the positioning of Tara Deep relative to the Navan Orebody, and the distribution of principal ore lenses and faults, adapted from Ashton et al., (2015). Note the faults are shown as plan projections from their intersections with the ore lenses, not as outcrop positions. SWEX is an abbreviation of Southwest Extension.

2.3 Geological Context

Regionally, Zn–Pb mineralization in the Irish Orefield is hosted by Mississippian (upper Tournaisian) rocks, within both the Waulsortian limestone Formation and the Navan Group (Hitzman and Beatty, 1996; Wilkinson and Hitzman, 2014; Phillips and Sevastopulo, 1986; Hitzman et al. 2002; Hitzman et al. 1995; Hitzman and Beatty, 1996; Lee and Wilkinson, 2002). The Navan deposit, including Tara Deep and some smaller deposits in the north eastern Irish Midlands e.g., Clogherboy and Tatestown, are hosted mainly by micrites of the basal Tournaisian limestone sequence (Pale Beds; see Strogen et al., 1996; Ashton et al., 2015). These rocks were deposited in tropical, typically photic to sub-photic seas and associated with sedimentary basin development during crustal extension (Boyce et al, 1983a; Philcox, 1989). Further south and west in the Irish Orefield, the Lisheen, Galmoy, Tynagh, Silvermines and Pallas Green deposits are hosted in dolomitized Waulsortian limestones (Hitzman and Beatty, 1996). Irish-type carbonate-hosted deposits are typically concentrated near normal, syn-sedimentary faults, which in the Navan area are associated with the northern margins of the Dublin Basin (Russell., 1986; Wilkinson and Hitzman, 2014; Ashton et al., 2015). The morphology of these orebodies are broadly stratabound and occur as single or multiple lenses hosted by permeable and/or reactive horizons within the host rocks (Ashton et al., 2015). There is significant evidence for syn-diagenetic deposition of some of these ores e.g. mineralized clasts in debris flow breccias (Boyce et al., 1983a; Ford, 1996; Anderson et al., 1998; Blakeman et al., 2002), hydrothermal vent phenomena (Boyce et al, 1983b, 2003; Banks and Russell, 1992), and for purely epigenetic subsurface replacement and open-space textures (Boyce et al, 1983a,1983b; Taylor, 1984; Blakeman et al, 2002; Anderson et al., 1998; Everett et al, 1999) intimately associated with dolomitization of the host sequence (e.g. Braithwaite and Rizzi, 1997; Gregg et al., 2001; Lee and Wilkinson, 2002). The bulk of the Zn-Pb mineralization appears to have been deposited epigenetically, but very early in the diagenetic history of the host rocks and basin evolution.

2.4 Navan Geology

Navan is located immediately south of the Longford Down Lower Paleozoic Inlier, within a major NE to ENE-trending structural corridor approximately coincident with the underlying Iapetus Suture (Vaughan & Johnston, 1992). To the south and west Mississippian platformal carbonates and calc-turbidites of the developing Dublin Basin sub-crop.

The Navan local stratigraphy records an overall marine transgression during the upper Tournaisian-lower Viséan and contains pre-, syn-, and post-rift elements. These rocks lie on a regional unconformity overlying Ordovician and Silurian volcano-sedimentary and igneous rocks, originally deposited on the Laurentian and Avalonian margins of the Iapetus Ocean (Romano, 1980; O'Keeffe, 1986, Murphy et al, 1991; Fritschle et al 2018). The Tournaisian Old Red Sandstone (ORS) of the Irish Midlands represents the oldest of the local Early Mississippian units and marks the start of the transition from subaerial to submarine deposition (locally termed Red Beds).

Stratigraphic and palaeogeographical settings of the Mississippian sequences are described in detail by Phillips and Sevastopulo (1986) and Philcox (1989). The Tournaisian/lower Viséan (pre-rift) stratigraphy at Navan records shallow water carbonate deposition within a developing peritidal environment (Ashton et al., 2015), followed by gradually deepening sea levels and the accumulation of ~200 m of micrites, bioclastic calcarenites, oolites, calcareous sandstones and siltstones. In local nomenclature, these 'Pale Beds' (Fig. 2.2) are the principal (but not the exclusive) host for mineralization, particularly within the Micrite Unit sub-group. This Micrite Unit is a fenestral limestone, exhibiting birds-eye features and representing deposition in a dominantly intertidal environment (Strogen et al., 1996; McNestry and Rees, 1992). Overlying this unit, the remaining Pale Beds at Navan comprise shallow marine oolitic grainstones and calcarenites with N-S trending channels recorded in the northern regions of the deposit (Rizzi, 1992; Anderson, 1990). Increasing water-depth led to the deposition of the Shaley Pales and Argillaceous Bioclastic Limestones (ABL), followed by the deep-water Waulsortian mudbank limestones, which unlike some other deposits across Ireland, are poorly

developed and unmineralized at Navan (Boyce et al., 1983a; Caulfield et al., 1986; Wilkinson et al., 2005; Barrie et al., 2009; Ashton et al., 2015; Wilkinson and Hitzman, 2014). Two-dimension seismic data, conducted in 2012, from the Navan area demonstrates that the rates of extension accelerated during the deposition of the ABL, such that marked changes in the thickness of this unit can be seen across extensional structures (Andrew, 1993; Ashton et al., 2018). In the Navan region, the timing of rifting is difficult to constrain, despite the preceding thickening of the ABL on the hanging wall of faults, the main phase of rifting has generally been accepted by the generation of the catastrophic Boulder Conglomerate (BC). The Boulder Conglomerate is a laterally extensive series of debrites, and a key expression of the main rift event in the lower Viséan (Ford, 1996), where rapid subsidence resulted in gravitational instability that has truncated much of the upper Tournaisian stratigraphy. Ultimately large collapse events led to the reworking and re-deposition of material as large allochthonous blocks and submarine sedimentary breccias (Fig. 2.2 & 2.3; Philcox, 1989; Andrew, 1993; Boyce et al., 1983a; Ford, 1996). These syn-rift deposits thicken markedly to the south, especially south of the large Navan fault (Fig. 2.1) especially with regards to the basal parts of the Upper Dark Limestone (locally termed the Thin Bedded Unit). Although the Boulder Conglomerate at Navan is a unit, it is likely composed of many individual sedimentary breccias related to multiple extension events (Ford, 1996). Thick accumulations of Arundian-Holkerian calc-turbidites and minor conglomerates formed the infill to the Dublin Basin, known locally as the Upper Dark Limestone (Nolan, 1989; Philcox, 1989; Ashton et al 2015). A detailed review of fault evolution at Navan is described within Ashton et al (2015). Finally, later Variscan compression led to inversion, and a local dip of 15-20^{o} SW was also probably imparted (Ashton *et al*. 2018).

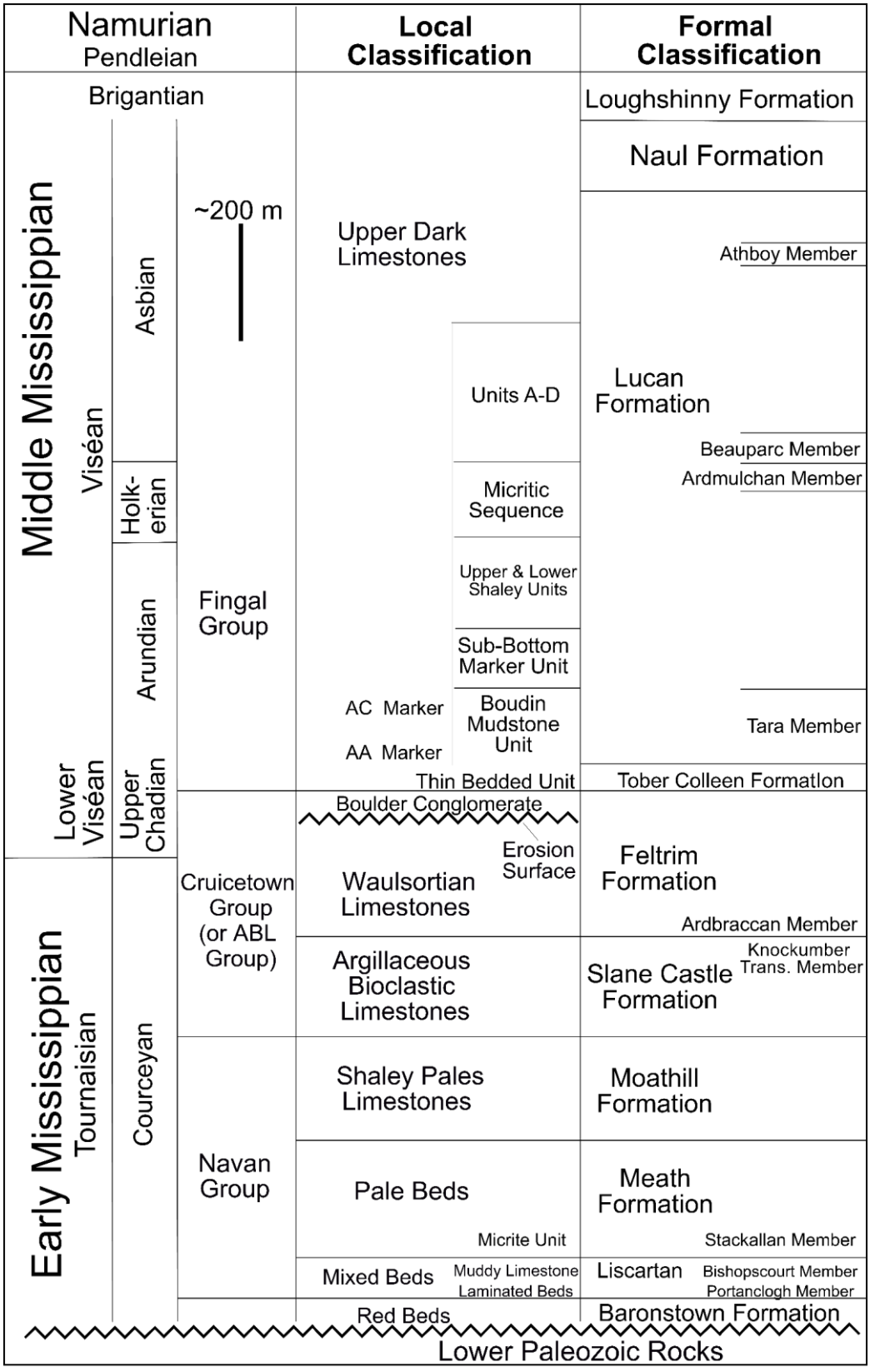

Figure 2.2 Formal and informal stratigraphy table of Mississippian rocks in the Navan and Tara Deep area (after Philcox, 1984, 1989; Strogen et al., 1990, 1996 and Ashton et al., 2015).

2.5 Methods

2.5.1 Drill Core Analyses and Sampling

Detailed logging of Tara Deep core was undertaken during the exploration drill core campaign. Representative samples were collected that outlined different stratigraphical units and mineralization styles and textures. One hundred seventy polished thin sections were created. Petrographic analyses were carried out using standard transmitted and reflected light microscopy at the Scottish Universities Environmental Research Centre (SUERC) and at the Grant Institute, University of Edinburgh. Detailed scanning electron microscopy (SEM) was completed at the University of Glasgow, using a Quanta 200F Environmental SEM with EDAX microanalysis.

2.5.2 S Isotope Analyses

Sulfides were prepared for conventional isotopic analyses by diamond micro-drilling techniques using samples collected from Tara Deep's mineralized units (n=163). Standard techniques for sulfides (Robinson and Kusakabe, 1975) and sulfates (Coleman and Moore, 1978) were used. Liberated SO_2 gases were analyzed on a VG Isotech SIRA II mass spectrometer, and standard corrections applied to raw $\delta^{66}SO_2$ values to produce true $\delta^{34}S$. Data are reported in $\delta^{34}S$ notation as per mil (‰) variations from the Vienna Cañon Diablo Troilite (V-CDT) standard. The standards employed were the international standards NBS-123 and IAEA-S-3, and the SUERC standard CP-1. Repeat analyses of these standards gave $\delta^{34}S$ values of +17.1‰, -32‰ and -4.6‰ respectively, with a standard error of reproducibility around ±0.3‰ during the processing of these samples.

2.5.3 Pb Isotope Analyses

Powdered samples of sulfides from mineralized drill core were dissolved using 1 ml 2% HNO_3 at the British Geological Survey in Nottingham. Dissolved samples were converted to bromide using 2 mls of concentrated HBr. Pb was separated using columns containing 100 microlitres of Dowex AG1x8 anion exchange resin using standard bromide separation methods. Prior to Pb isotope analyses each sample

was spiked with a thallium solution, which was added to allow for the correction of instrument-induced mass bias. Samples were then introduced into a Nu Plasma HR multicollector ICP-MS (inductively coupled plasma-mass spectrometer). For each sample, five ratios were simultaneously measured ($^{206}Pb/^{204}Pb$, $^{207}Pb/^{204}Pb$, $^{208}Pb/^{204}Pb$, $^{207}Pb/^{206}Pb$ and $^{208}Pb/^{206}Pb$). Each individual acquisition consisted of 75 sets of ratios, collected at 5-second integrations, following a 60 second de-focused baseline. The precision and accuracy of the method was assessed through repeat analyses of an NBS 981 Pb reference solution (also spiked with thallium). The average values obtained for each of the measured NBS 981 ratios were then compared to the known values for this reference material (Thirlwall, 2002). All sample data were subsequently normalised, according to the relative daily deviation of the measured reference value from the true, with the aim to cancel out the slight daily variations in instrumental accuracy. Internal uncertainties (the reproducibility of the measured ratio) were propagated relative to the external uncertainty.

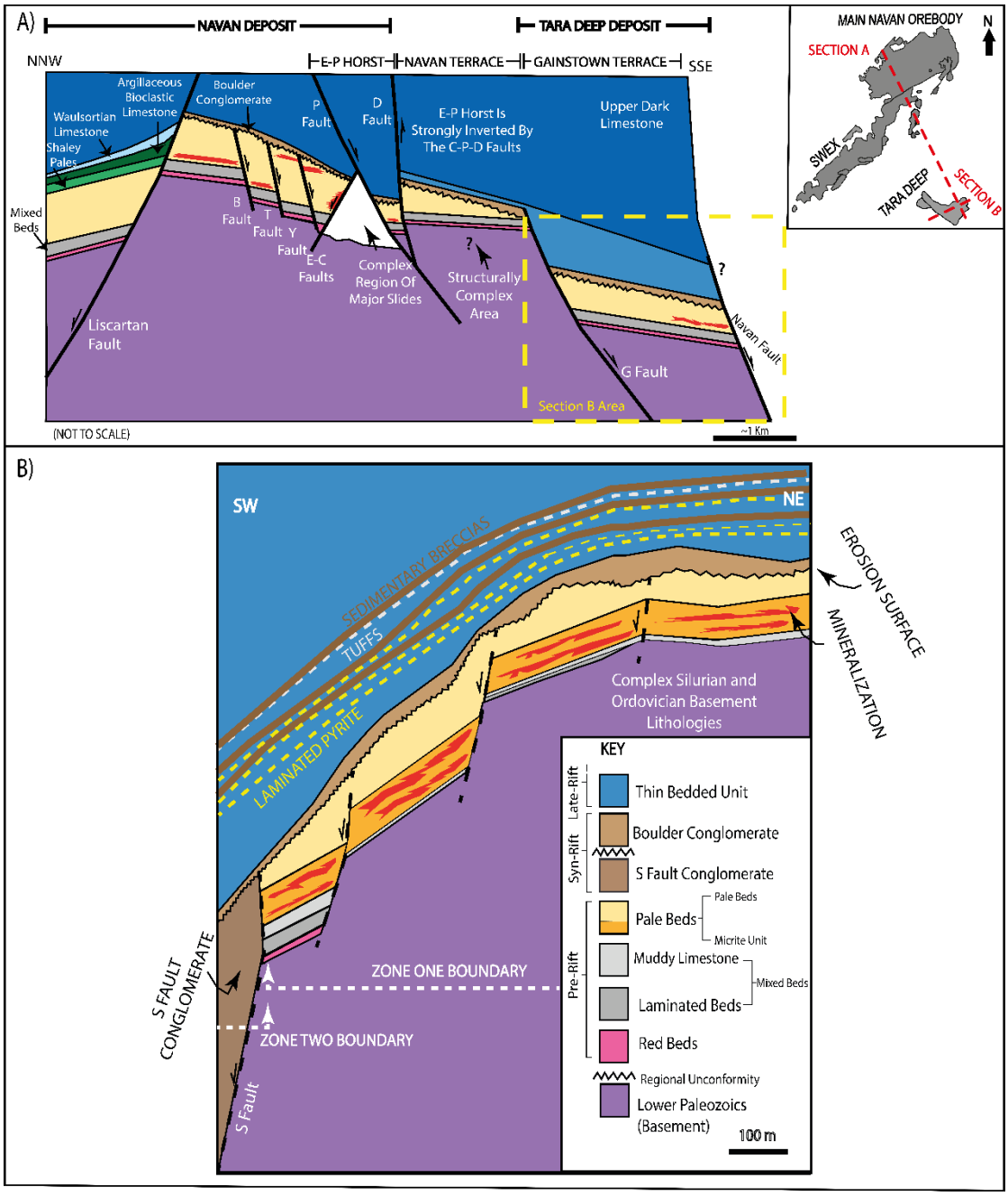

Figure 2.3 A) Highly schematic (NNW-SSE) post inversion cross section across the Navan to Tara Deep region, highlighting the principal controlling faults. A full review of the complex Navan structure can be found in Ashton et al., (2015). B) SW-NE schematic section highlighting the setting of the Tara Deep deposit (post-inversion) within the Gainstown Terrace (Fig. 2.1); a region consisting of a series of fault-controlled terraces, often faulting out much of the Mixed Beds and Red Beds. The S Fault divides the deposit into Zone One and Zone Two. The Micrite Unit is a subgroup of the Pale Beds, but a stronger demarcation is adopted here.

2.6 Results

2.6.1 Structure of the Tara Deep Deposit

Tara Deep is fault-bounded by structures that formed part of the northern margin of the Dublin Basin during the lower Viséan. Broadly N-S extension led to several major faults trending generally ENE and defining a series of fault bound terraces (Fig. 2.3). The southern margin of the Navan/SWEX deposit, is defined by a major horst bounded by the NW dipping E Fault (>500m normal throw) and the SE dipping P Fault (>800m apparent normal throw; see Ashton et al., 2018; Fig. 2.1). Southwards (~1.5 km), the SE dipping G Fault is developed (>500m normal throw) with the intervening area termed the 'Navan Terrace'. Both the E-P Horst and the Navan Terrace are poorly understood due to low resolution drilling and southwards-directed sliding and erosion (Ashton et al., 2015). The Navan Terrace is also strongly dislocated by a complex zone of later major SE dipping post-mineral faulting termed the D-Q Fault Zone. This complex zone of late inversion, like other late dextral-reverse faults at Navan, complicates the reconstruction of pre-inversion relationships between Navan and Tara Deep (a significant dextral offset is suspected).

Stepping down to Tara Deep (Fig. 2.3), a further ~1.5km south of the G Fault lies the SE dipping Navan Fault, which is the largest structure in the area and displays a normal displacement of at least 3km, as estimated from seismic data (Ashton et al., 2018). Tara Deep occurs in the Gainstown Terrace, lying between the G and Navan Faults, where strongly mineralized host rocks have been subject to several episodes of faulting (Fig. 2.3B). The terrace is dissected by several SW-dipping, low-angle listric normal faults with vertical displacements of <50m, striking broadly perpendicular to the G and Navan faults. Of most importance, in the western parts of the Tara Deep deposit, is a large complex zone of shearing cutting obliquely through the Gainstown Terrace, with the principal fault termed the S Fault, which trends NNW-SSE and dips steeply WSW with a normal throw of >600m. Preliminary structural interpretation suggests that this may be an inverted early slide fault. Seismic and drilling data indicate

that the G, Navan and S Faults (Fig. 2.1) do not significantly displace the lower Viséan debrites and basal units of the Upper Dark Limestone that overlie the truncated Pale Beds (Fig. 2.2 and Fig. 2.3).

The S Fault separates Tara Deep into Zone One (S Fault footwall) and Zone Two (S Fault hanging wall), which will be discussed separately. Zone One displays the Navan deposit's lower Pale Beds stratigraphy almost intact. However, to the west, Zone Two shows a complex series of sedimentary breccias and large rotated blocks of Tournaisian stratigraphy in the S Fault hanging-wall, where it gives rise to a complex, sheared and west-facing monoclinical geometry. The description of the Mississippian stratigraphy within both zones is separated into pre-, syn- and late-rift sections (Fig. 2.3B), with the Tournaisian units below the Boulder Conglomerate categorised as pre-rift, whereas the Boulder Conglomerate is categorized as syn-rift, and the Thin Bedded Unit of the Upper Dark Limestone is deemed late-rift.

2.6.2 Local Stratigraphy at Tara Deep Zone One: Pre- and Syn-Rift Statigraphy

Situated east of the S Fault and north of the Navan fault, Zone One hosts a similar upper Tournaisian sequence to that observed regionally at the Navan deposit. These upper Tournaisian sequences progressively steepen westward towards the S Fault from 15 to 40 degrees (Fig. 2.1 & 2.3B). The basal Early Mississippian Red Beds of terrestrial/fluvial origin are overlain by a shallow-water sequence of thinly laminated siltstones, sandstones, limestones and shales termed the Laminated Beds. A distinctive opaline quartz horizon, which is similar to that seen under the Navan deposit (Rizzi, 1992), being a diagenetic replacement of anhydrite, suggests at least localized peritidal conditions. As a result of the NNW trending low-angle faults that dissect Tara Deep (Fig. 2.3B), a complete intersection of this Tournaisian Mixed Beds package has not yet been made. The unit most affected by faulting is a succession of finely bedded sandstones (millimetre to cm scale), siltstones, minor carbonates and muds termed the Laminated Beds. Thus, there is likely structural contacts cutting the Tournaisian units (Fig. 2.3B).

The principal host for mineralization within this zone is the lower parts of the Pale Beds (~50 m in thickness; Fig. 2.1), locally termed the Micrite Unit in the Navan deposit. At Tara Deep this unit is characteristically fine-grained, organic-rich, navy/dark grey colour and fractured, showing no evidence of soft sediment deformation, suggesting it was fully lithified at the time of ore deposition. It also exhibits abundant birds-eye (fenestral) textures, which are typically associated with an intertidal depositional setting (Grover and Read, 1978). This package is a distinct manifestation of the same intertidal processes that developed the Micrite Unit in the Navan deposit (Rizzi, 1992, Anderson et al., 1998; Ashton et al., 2015). However, at Navan it consists of a sequence of heterogeneous and variably dolomitized micrites, oolites and calcarenites (including channels in the northern part of the mine; Anderson et al., 1998; Rizzi, 1992), whereas at Tara Deep this interval is far more consistent, with no current evidence for channelling. Oolitic grainstone horizons are often interbedded within the micrite (typically three), these are preferentially dolomitized, whereas the surrounding rock is variably dolomitized. An Upper and Lower Micrite can be distinguished on either side of a ~9m laterally continuous central dolomitized oolitic grainstone horizon across the entire Zone One. An equivalent dolomitised horizon is found in the Navan deposit, termed the 5-lens Dolomite. This, together with a consistency of thickness in the Micrite Unit (around 50m) across the Navan and Tara Deep deposits, suggests a strong similarity in depositional environment across the entire area.

Directly above the Micrite Unit, a succession of dominantly oolitic grainstones display a distinctive texture, locally-termed the 'Healed Conglomerates', which are succeeded by a series of emergent surfaces. Initial observations of this 'Healed Conglomerate' texture suggests it represents a diagenetic overprint of a nodular limestone, with pervasive pressure solution occurring through a partially lithified host rock, so called stylo-nodular textures or non-seam solution (see Wanless, 1979). Further research is being carried out to decipher its significance (Chapter 4). The key characteristics of this texture is typified by undolomitised 'ghost' nodules that have diffuse margins, sitting within a dolomitised stylo-cumulate matrix. Stylo-cumulate herein refers to insoluble residue accumulated along a pressure-solution surface. Subsequently, the matrix hosts numerous pressure solution seams

and dissolution has removed much of the pre-existing calcite, leaving behind heavy detrital mineral relics (albite, apatite, jadeite, lucite, quartz, zircons) and it is associated with burial dolomitization. Although the occurrence of the 'Healed Conglomerates' within the Navan deposit is unclear (Anderson, 1990; Rizzi, 1992), at Tara Deep the lithology is widespread (1.5km^2). Its true thickness is also unclear because it is superimposed by the Boulder Conglomerate. Mineralization in this lithology is patchy and typically uneconomic at Tara Deep.

Much of the pre-rift stratigraphy has been wholly or partly removed by a series of slides and debrites of lower Viséan age, termed collectively as the Boulder Conglomerate (BC), that cut through the succession from the north and north-east. The preserved debris flows are generally polymict and matrix supported, with clast sizes ranging from 1 cm to >10m. The matrix is a dark, almost black, highly fossiliferous argillite. The clasts in the lower sedimentary breccias are dominated by Waulsortian limestone but the abundance of Pale Beds increases in the upper breccias. In rare occurrences clasts of Lower Paleozoics are preserved. A major unconformity now exists between the BC and the underlying upper Tournaisian facies, and these debrites have superimposed early faulting (Fig. 2.3). This has been interpreted by several authors (Boyce et al., 1983a; Philcox, 1989; Cook and Mullins, 1983; Ashton et al. 1992; 2003; 2015; Ford, 1996) as the result of gravitational sliding, submarine debris flows and fault-talus breccia formation, representing syn-rifting brought about by major extension and growth faulting during the upper Tournaisian/lower Viséan. This erosion has resulted in the removal of >500m of pre-rift stratigraphy. On the footwall crest of the Navan Fault, the Boulder Conglomerate cuts down to the Lower Paleozoic basement. Subsequently, Tara Deep preserves a much more complex syn-rift sequence of events than the main Navan deposit and the SWEX deposit.

2.6.3 Zone Two: Pre- and Syn-Rift Stratigraphy

Zone Two occurs west of the S fault (Fig. 2.3), as a steeply dipping (>75°), structurally complex region of syn-rift origin that dissects the Gainstown Terrace (Fig. 2.1). Overlying the common hanging-wall of

the G and S faults, is a distinct sedimentary breccia, termed the S Fault Conglomerate (SFC), composed almost exclusively of Pale Beds clasts, with only very minor Waulsortian limestone towards the base. This unit also hosts clasts of detrital sulfide and rafts of displaced Micrite Unit mineralization. This mineralization is similar to that found at the base of the Boulder Conglomerate in the Navan Deposit in the hanging-wall of the T Fault (Ashton et al., 2015). The nature of these breccias again indicate a fault talus origin due to their polymict and angular nature. The SFC contains areas of very high Zn+Pb grades. Other distinctive minor sedimentary breccias occur in the S Fault hanging-wall, and these appear to pre-date the S Fault Conglomerate. Towards the south-eastern end of the S Fault hanging-wall, the S Fault Conglomerate gives way to an apparently extensive series of debrites of intermixed blocks of ABL and Shaley Pales that in places appears to overlie more orderly Middle and Lower Shaley Pales and in one area a raft of Pale Beds.

2.6.4 Zone One and Two: Late- to Post-Rift Stratigraphy

The Erosion Surface at the Tara Deep deposit is overlain by the basal unit of the Upper Dark Limestone (UDL) termed the Thin Bedded Unit (TBU; Fig. 2.3). The Thin Bedded Unit at the Navan deposit barely exceeds 20m in thickness. Seismic interpretation, drilling and detailed stratigraphic correlation studies indicate that the TBU at Tara Deep thickens dramatically across the P and G faults, reaching thicknesses of 120m in the east of Zone One and >600m in the west of Zone Two (Ashton et al., 2018). The TBU can be broken down into several sub-units, each of which host abundant iron sulfide laminations, separated by sedimentary breccias (see Yesares et al., in press). From oldest to youngest, they are termed the TBU-4, TBU-3, TBU-2 and TBU-1. The Thin Bedded Unit is also host to several tuff horizons of which the uppermost is the best preserved just beneath SB-1. These tuffs are missing at Navan, likely removed by later debris flow(s) during the formation of the Boulder Conglomerate. Overlying the TBU the Upper Dark Limestones comprise generally similar limestone turbidites to those elsewhere in the area (Philcox, 1989). Extensional activity in the area continued into the mid-Mississippian as polymict conglomerate

horizons occur sporadically throughout the Upper Dark Limestones (Ashton et al., 2015, Ashton et al., 2018).

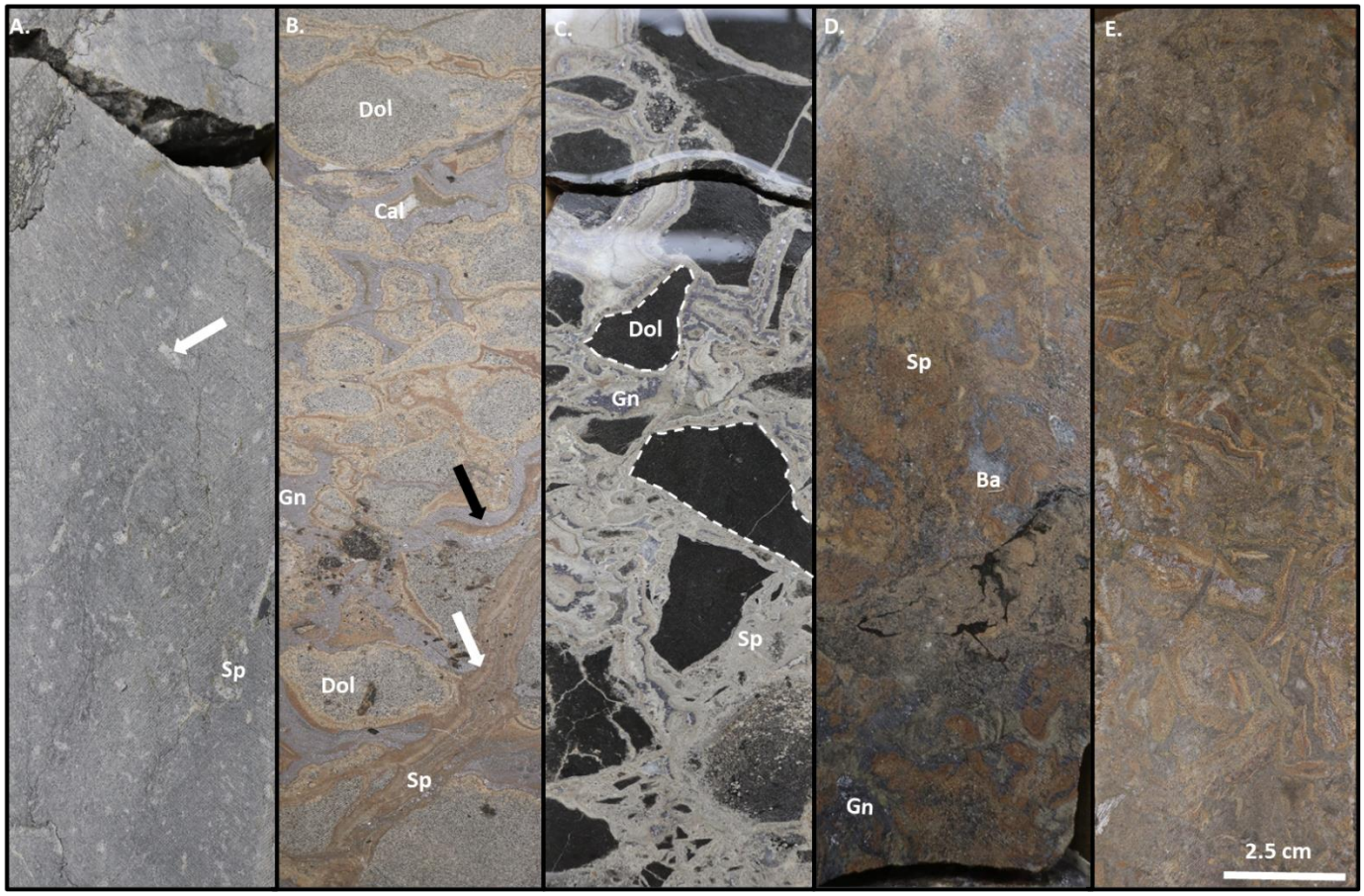

Figure 2.4: Drillcore (NQ) images outlining common mineralization textures within Zone One's Micrite Unit. A) Largely undolomitized Micrite Unit with characteristic birds-eye textures (fenestral; white arrow) with minor disseminated sphalerite (N02334/19; 1786.5 m) B) Coarse, intensely mineralized cavity fill within the Micrite Unit, consisting of classic colloform sphalerite (Sp; white arrow) nucleating on the cavity walls. These cavities have also been exploited by coarse galena (Gn; black arrow). Host rock has been replaced by dolomite (dol) prior subsurface mineralization, leading to a complete occlusion of the original fenestral fabric. Metalliferous fluids exploit and expand fractures in the Micrite Unit (N02499; 1786.2 m). (C) Brecciated mineralization with subrounded to angular clasts of dolomitized micrite (dashed lines) encased by high grade sphalerite mineralization, with subordinate coarse galena (N02334; 1815.3 m; wet). (D) Massive mineralization with a complete replacement of the host rock, and the original fabric, with dominantly sphalerite (Sp) mineralization with minor galena (Gn) and barite (Ba) (N02334; 1775.3 m; wet). E) Numerus disrupted cavity fill textures consisting of dominantly sphalerite with minor galena, with later barite infill between textures (N02445, 1780.05 m).

2.6.5 Mineralization

Mineralization at Tara Deep occurs primarily within three principal lithologies; A) the Pale Beds, in particular the Micrite Unit subgroup (Fig. 2.4A-E), B) S Fault Conglomerate (SFC; Fig. 2.5A-B), and C) microcrystalline (typically bedding parallel) pyrite-rich mineralization in the TBU (Fig. 2.5C). Based on the most recent estimation, the Pale Beds hosts 87% of the total economic resource, primarily within the Micrite Unit, whereas the SFC hosts 13% of the total resource. The TBU is sub-economic. The dominant ore minerals comprise sphalerite and galena, at a ratio of ~7:1. Other minerals in decreasing order of abundance include calcite, dolomite, pyrite, marcasite, barite, and much less commonly, anhydrite, chalcopyrite. A series of complicated sulfosalts also occur as inclusions with galena, dominantly bournonite and boulangerite. A variety of textures exist within each of these hosts, which are controlled by open-space infill, replacement, and dissolution within a subsurface environment.

A) Pale Beds (Zone One)

Pale Beds mineralization, almost entirely hosted in the Micrite Unit subgroup (Fig. 2.4A), dominates in Zone One, occurring in blocks bounded and displaced by low-angled listric faults that dip SW (Ashton et al., 2018). Mineralization within these blocks are typically stratabound, and gains in intensity as the footwall crest of the Navan Fault is approached. This interval is equivalent to the lowest lens - the 5-lens - of the Navan Deposit which hosts roughly 70% of the Main Orebody resource (Fig. 2.1 & 2.3; Ashton et al. 2015). The mineralization most frequently presents as massive, disrupted cavity fill, brecciated and massive mineralization textures, which are dominated by multistage infill and replacement mineralization processes. Late marcasite and barite are observed infilling and cross cutting many of these textures. Finally, late phase burial and associated pressure solution exploits these textures. Directly above the Micrite Unit, the remaining Pale Beds are typically poorly mineralized.

Mineralized textures found in the Pale Beds occur as follows, in order of relative abundance:

- *Cavity fill textures (Fig. 2.4B)* can occur on various scales (<0.5 cm-4cm) and is the most common texture associated with the Micrite Unit. They occur within both undolomitized and

dolomitized regions of the Micrite Unit. These mineralized textures consist of layered/colloform yellow-burgundy coloured sphalerite that nucleate on the cavity walls. Galena commonly forms isolated, dendritic or coarse crystals (0.5 cm-6 cm), nucleating within or on cavity walls. Colloform sphalerite can be accompanied by variable concentrations of minor trace elements (Fe, Mn, Cu, Ga, Ge, Ag, Cd, As and Hg). This is consistent with the Navan deposit (Gagnevin et al., 2014). Colloform regions can be observed nucleating around host calcarenites, or as disrupted, isolated textures. Weaknesses between individual colloform layers are often exploited by late phase barite and/or calcite.

- *Brecciated mineralization (Fig. 2.4C)* occurs as hydraulic fracturing and collapse brecciation within the Micrite Unit. Fracture fill and brecciated textures tend to dominate regions where complete dolomitization of the Micrite Unit has occurred. Ultimately, expansion of cavities through mineralization occurs over time, generating wider cavities and often allowing cavity bridging to take place. Sometimes when cavity collapse occurs, brecciated textures can develop. Thus, a continuum in processes likely exists, where convergence of cavity fill textures results in brecciated mineralization.
- *Massive mineralization (Fig. 2.4D)* occurs where replacement and infill mineralization has completely obliterated the original fabric of the intertidal carbonate mud, leaving behind only reworked dolomite and undissolved host rock components (e.g., jadeite, apatite, quartz, albite and mica). Examples exist where numerous cavity fill textures have been reworked, packed, and amalgamated together, creating regions of massive mineralization and highlighting the complexity and cyclicity of the mineralizing system (Fig. 2.4E).

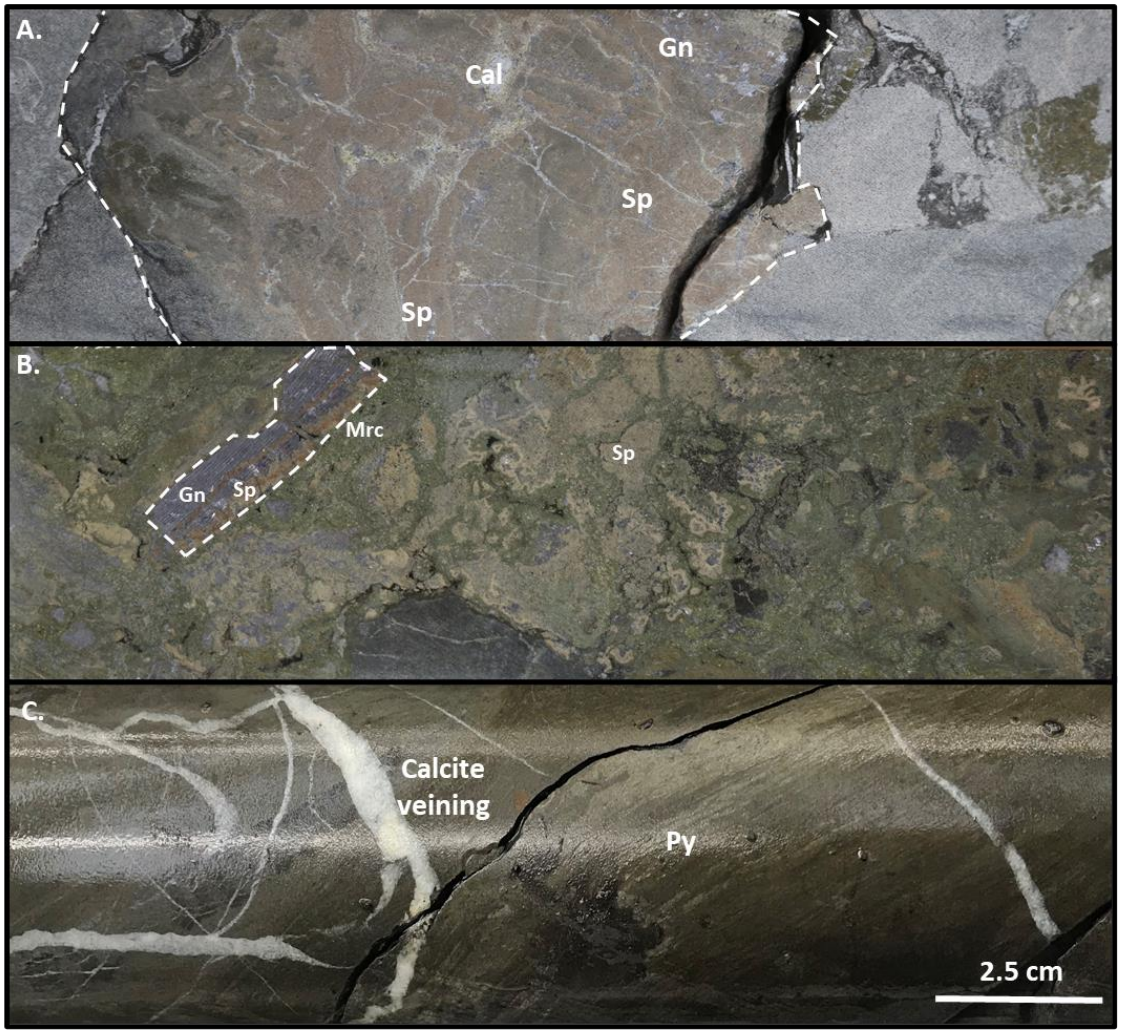

Figure 2.5 Drillcore (NQ) images outlining common mineralization textures within the S Fault Conglomerate (SFC). ***(A)*** *Allochthonous clasts of early sphalerite (Sp) mineralization, with minor coarse galena (Gn), hosted within the S Fault Conglomerate at Tara Deep (N02466; 1728.2m)* ***B)*** *Mineralized S Fault Conglomerate (SFC) with an allochthonous clast of cavity fill mineralization (indicative of the Micrite Unit) encased by later phase marcasite and sphalerite which replaces the debrite matrix (N02427; 1776.7 m)* ***C)*** *Massive microcrystalline pyrite within the TBU, overlying SFC mineralization, consisting of dominantly framboidal pyrite within an organic rich lutite (N02439; 1653.6 m).*

B) S FAULT CONGLOMERATE (SFC; Zone Two)

Mineralization in the SFC is concentrated near the hanging walls of the G and S Faults in Zone Two of Tara Deep. Mineralization in the SFC takes three forms: **1)** isolated allochthonous clasts of sulfide (> 1cm), similar to the Conglomerate Group Ore in the Main Navan Orebody, detrital clasts of mineralization are often embedded by late matrix replacement mineralization. The margins of these allochthonous clasts can be angular or sub-rounded, and range in size from <1 mm to 50 mm across (Fig. 2.5A). **2)** A raft of Micrite Unit mineralization (~50 m) hosted between complex sedimentary

breccias. This large raft of allochthonous Micrite Unit mineralization rest on the hanging wall of the S Fault (Fig. 2.3). **3)** As matrix replacement and infill, dominated by late phase marcasite and barite. Bioclast replacement is common within the high-grade SFC matrix (Fig. 2.5B). A zone of intense, replacive mineralization of up to 90m vertical thickness, with grades in excess of 50% Zn+Pb, can be found towards the top of the S Fault Conglomerate.

The SFC is characterized by bioclast replacement textures, which help to differentiate the SFC mineralization from allochthonous clasts of Pale Beds mineralization. At Tara Deep the abundance of iron sulfide within the SFC is typically 2-5%, whereas intersections of 30-40% iron sulfide can be made within the Conglomerate Group at the Navan Mine.

C) Laminated Iron Sulfides in the TBU

The overlying TBU comprises 0.5 cm to >3 m thick bedding-parallel layers of dominantly framboidal and microcrystalline pyrite hosted in a fine grained, organic-rich carbonate shale. This mineralization extends over a region of ~2 km^2. Minor remobilized sphalerite and galena are found within these laminae, again highlighting the multiphase nature to mineralization. The pyrite framboids are abundant and show a high degree of preservation, with recrystallization being poorly developed and constrained to regions that are more massive in texture. Regions of massive framboidal pyrite (~ 5m in thickness) can be intersected in the G Fault hanging wall, typically proximal to underlying normal faulting (Fig. 2.5C). Mineralization is often associated with hydrothermal chert and MnO staining in drill-core (Yesares et al. 2019; Yesares et al., in press). Rare, late phase barite veins crosscut the TBU Fe-sulfide laminations. Microscale textures in the TBU iron laminations at Tara Deep suggest they have been displaced by late compressional deformation, suggesting they predate Variscan compression. Similar iron sulfide laminated textures have also been recorded at Navan but they are less abundant (Ford, 1996; Anderson et al., 1998).

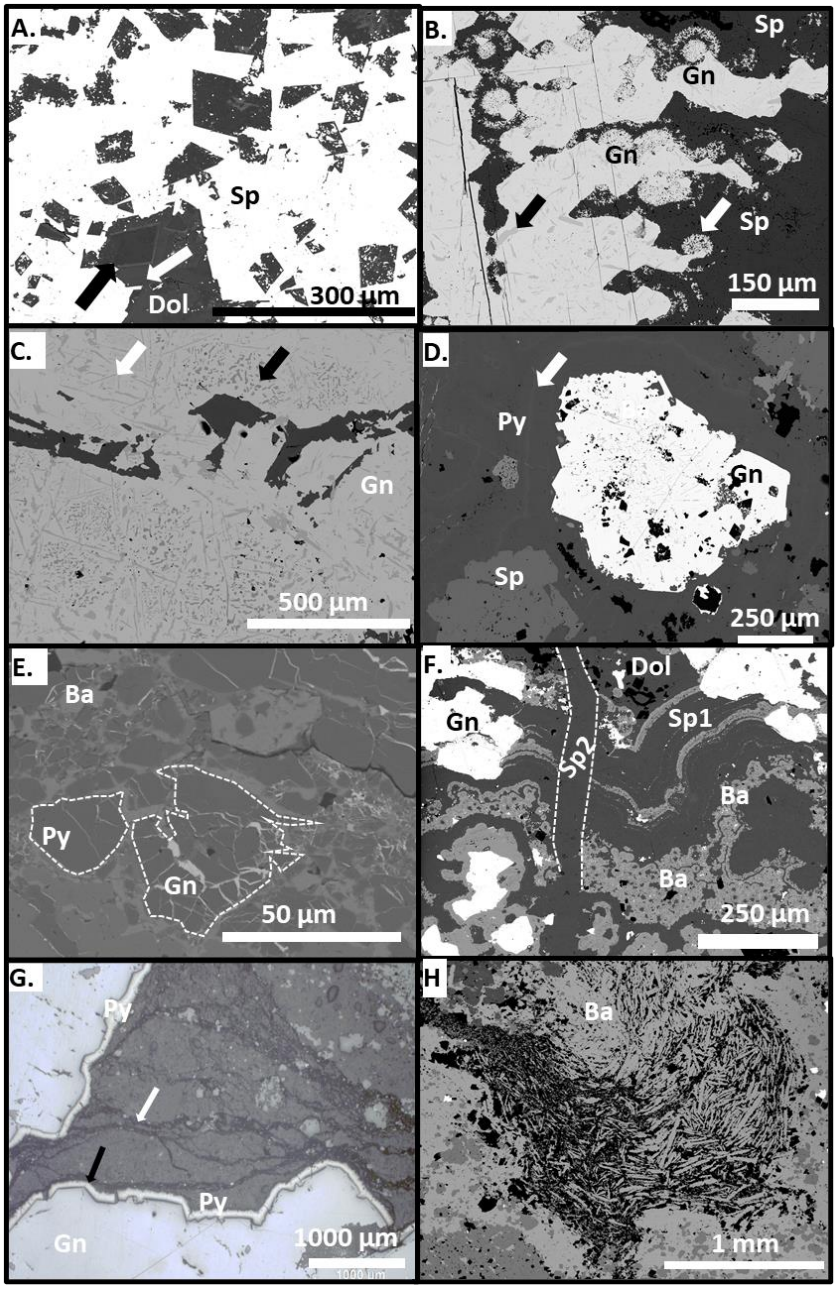

Figure 2.6 Standard petrology and backscattered electron (BSE) images from mineralized textures in the Micrite Unit. A) Dolomitization predates sphalerite mineralization. Note the corroded edges to the dolomite. Dolomitization consists an early Mn and Fe replacement phase with an iron rich coating (black arrow), with a later Fe-rich dolomite infill (white arrow; N02445; 1788.1 m) B) Dendritic galena with inclusions of Sb-sulfosalts (typically bournonite; black arrow). Sphalerite and galena precipitated at the same time highlighted by dendritic galena infilling microcrystalline sphalerite that encases it, generating zoned infill structures (white arrow; N02499; 1781.3 m). C) Globular Cu-sulfosalts (typically boulangerite; black arrow) and bladed Sb-sulfosalts (largely bournonite, white arrow) inclusions in hydrothermal galena (N02445;1788.1 m). (D) Coarse galena with Sb- and Cu-sulfosalts, encased by hydrothermal pyrite that displays faint arsenic zonations (white arrow; N02428;1473.6 m). (E) BSE image with galena crosscutting pyrite (dashed line) which is subsequently brecciated by barite (N02437/02; 1678.3) F) BSE image showing a complex relationship where colloform sphalerite (Sp1) has been infilled and exploited by late phase barite. A final phase of coarse honeyblende sphalerite (Sp2) crosscuts all of these textures (N02418/03; 1589.6 m) G) Pressure dissolution postdates mineralization, horsetail stylolites (white arrow) associated with abundant microcrystalline pyrite. Microcrystalline pyrite from pressure solution seams nucleates on the margins of pre-existing hydrothermal galena (black arrow; N02445; 1788.1 m) H) Laths of bladed barite are 'splintered' by pressure solution (N02334;1765.1 m). Mineral abbreviations; barite (Ba) boulangerite (Boul), bornonite (Bour), dolomite (Dol), galena (Gn), pyrite (Py) sphalerite (Sp).

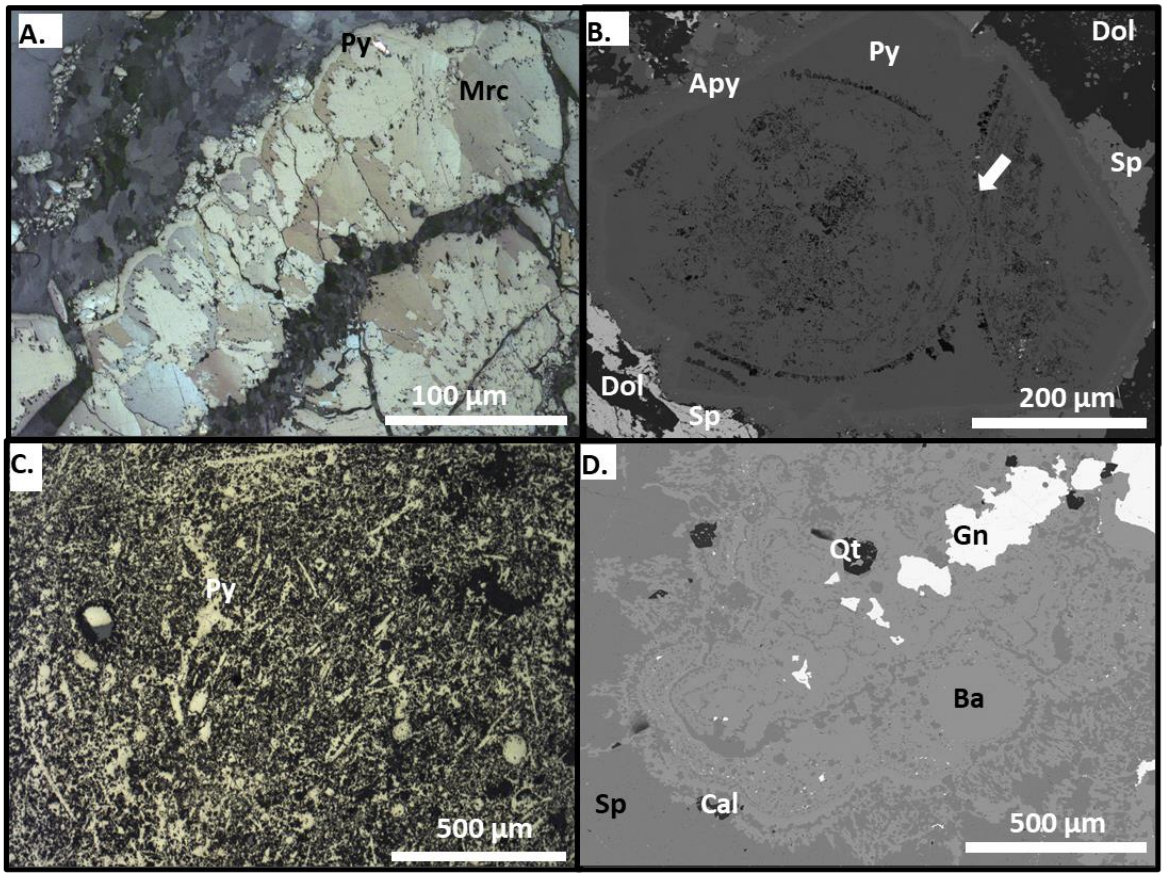

Figure 2.7 Reflected Light (RL) and Backscattered Electron (BSE) images of textures associated with the S Fault Conglomerate of Zone Two. Mineralization pre- and post-dates the formation of this submarine debrite, and the system becomes progressively more iron rich over time. ***A)*** *Cross- Polarized Reflected Light (XRL) image displaying marcasite replacing pyrite mineralization (N02439/06).* ***B)*** *BSE image shows pyrite replacing ooids. Ooids reveal evidence of compaction and still retain their isopachous marine cements (white arrow; N02477/01; 1748.6 m).* ***C)*** *Complete replacement, by dominantly pyrite, of a diverse variety of bioclasts (N02439/03; 1693.2 m).* ***D)*** *Layers within a colloform sphalerite are being exploited by late phase barite (N02427/04; 1792.5 m). Mineral abbreviations; arsenopyrite (Apy), barite (Ba), calcite (Cal), dolomite (Dol), galena (Gn), marcasite (Mrc), pyrite (Py) sphalerite (Sp), quartz (Qt).*

2.6.6 Paragenetic Sequence

The paragenetic sequence at Tara Deep is extremely complex, especially in high grade zones, and it is very likely that hydrothermal activity, tectonism, and burial have resulted in this complexity. The paragenetic sequence has been broken down into early-rift to late-rift phases which coincide with changing depositional environments and subsequently an evolving basin (Fig. 2.3B). All of these phases pre-date Variscan compression.

Early-rift phase mineralization: The majority of replacement dolomitization predates mineralization (Fig. 2.6A). Sphalerite and galena dominate the early phases of the paragenetic sequence and reveal a synchronous precipitation relationship. Dendritic galena and colloform/layered sphalerite textures are common within cavities of the Micrite Unit. These textures denote rapid, supersaturated precipitation, with sphalerite and galena precipitating at the same time. This is epitomized by dendritic galena infilling colloform sphalerite that encases it (Fig. 2.6B). Sphalerite also exists as zoned microcrystalline globules (~20 um). Abundant Sb- and occasional Cu- sulfosalts (bournonite and boulangerite, respectively) occur as micro-inclusions within galena (Fig. 2.6C-D).

Main-rift mineralization: Marcasite and barite are later phases that do not co-precipitate with early Zn-Pb textures. Marcasite replaces pre-existing textures, and often veins across pre-existing Micrite Unit textures. It is most abundant within the SFC where it replaces the matrix around earlier Zn+Pb clasts (Fig. 2.5B & 2.7A). The matrix of the SFC is dominated by bioclast replacement typically by pyrite and marcasite (Fig. 2.7B-C), these textures often encase early mineralized clasts (Fig. 2.5). Bladed, porous, barite postdates marcasite, and can be observed infilling interstitial space, veining and exploiting weaknesses between colloform sphalerite layers within the Micrite Unit (Fig. 2.6E) and SFC (Fig. 2.7D). Within the TBU, rare barite veins cross cuts microcrystalline pyrite laminations. Minor, late phase, coarse, honeyblende sphalerite postdates marcasite, but it is poorly understood, it is often synchronous with late calcite and barite (Fig. 2.6F).

Late-rift mineralization: The TBU is dominated by iron sulfides. Sphalerite, galena, marcasite and barite precipitation still occurs, but as minor typically disseminated and potentially remobilized phases (see Yesares et al., in press). Burial of the entire Tara Deep deposit has resulted in extensive pressure solution within every unit. Pressure dissolution subsequently postdates the Micrite Unit mineralization, with examples observed where stylolites cross-cut earlier base metal sulfides and barite (Fig 2.6 G-H). Each of these pressure solution seams are associated with framboidal and microcrystalline pyrite, which nucleate on pre-existing base metal sulfides.

In summary, crosscutting relationships reveal a dynamic and evolving paragenetic sequence (Fig. 2.8). Firstly, Zn-Pb dominates during the early phases of mineralization. Secondly, Ba+Fe ±Sp±Gn dominates during the main rifting event and the formation of the SFC. Finally, late in the paragenetic sequence, during the late phases of basin rifting, the system appears dominated by pyrite, with only minor Zn, Pb and Ba input, but overall the system is clearly waning. These observations are consistent across hundreds of complex samples but have been summarized (Fig. 2.9). The presence of barite and marcasite as an intermediate phase suggest a shift to metals being transported in reduced, acidic brines, which may have remobilised other base metal sulfides and facilitated the precipitation of honeyblende sphalerite (Cooke et al., 2000). Overall, the mineralizing system is dynamic and despite the evolving depositional and tectonic environment, mineralization is prolonged and responds to basin development.

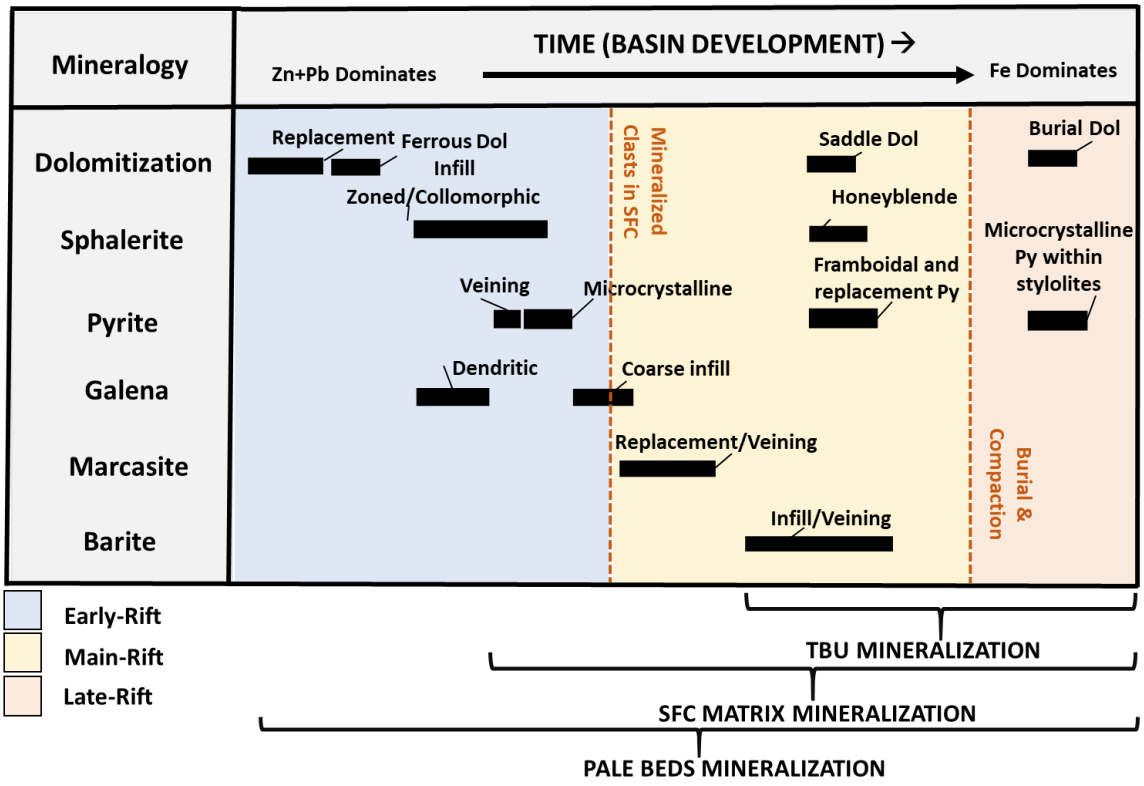

Figure 2.8 Paragenetic sequence for Tara Deep mineralization showing the general trend and the evolving mineral assemblages through time.

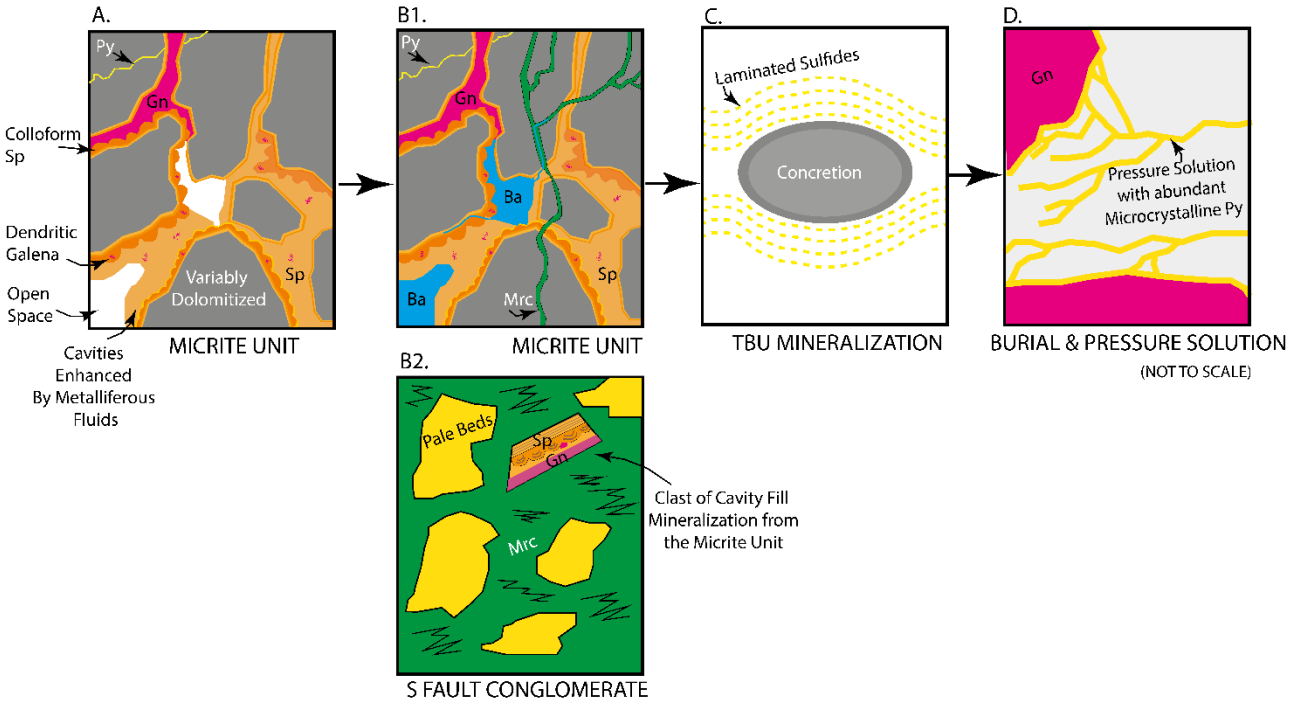

Figure 2.9 Schematic summary of the key textural relationships, which explore the timing of phases of mineralization within the Tara Deep deposit. It is worth noting that the ore is extremely complex and difficult to interpret, especially in high-grade zones, but these trends hold true across all samples and at various scales. A) Cavity fill mineralization in the dolomitized Micrite Unit (similar example see Fig. 2.4B), showing early colloform and dendritic textures (similar example in 2.6B). Metalliferous fluids enhance cavities and rapid precipitation textures are likely generated through fluid mixing. B1) Later phase Micrite Unit mineralization is exploited by marcasite veining and infilled by barite. Note the barite exploits weaknesses within colloform sphalerite (see Fig. 2.6E&F &2.7D) and crosscuts marcasite, it is often associated with coarse honeyblende sphalerite and late calcite veining. B2) Cavity fill textures from the Micrite Unit can be found encased by marcasite in the S Fault Conglomerate (SFC; see Fig. 2.5B). Clasts of Micrite Unit mineralization in the SFC offer unambiguous evidence that the onset of mineralization occurred prior to or during the upper Tournaisian. C) Laminated sulfide encases concretions within the Thin Bedded Unit, suggesting subsurface mineralization after a phase of early diagenesis. D) Pressure solution in the Micrite Unit and Thin Bedded Unit host abundant microcrystalline pyrite that nucleate on pre-existing textures (see Fig. 2.6G). Mineral abbreviations; barite (Ba), galena (Gn), marcasite (Mrc), pyrite (Py) sphalerite (Sp).

2.6.7 S Isotope Analyses

Cavity fill, brecciated and massive mineralization textures of the Pale Beds displays a dominant bimodal distribution of $\delta^{34}S$ in sphalerite and galena ranging between -13.5 to -3.6 ‰ (average= -8.5‰, σ= ±2.4) and +3.4 to +16.2 ‰ (average= 9.6‰, σ=± 2.9), suggesting two different S sources (Fig. 2.10A&B). The lowest values (-13.5 ‰ to -3.6‰) are interpreted as the product of bacterial reduction of seawater sulfate (BSR) during the Mississippian (Altinok, 2005, Anderson *et al.*, 1998; Anderson, 1990; Barrie et al., 2009; Blakeman *et al.*, 2002; Boyce et al. 1983b; Caulfield et al., 1986; Coomer and Robinson, 1976; Fallick *et al.*, 2001; Ford, 1996; Wilkinson and Hitzman, 2014; Wilkinson et al., 2005). The heavier values

(+3.4‰ to +16.2 ‰), are considered to represent hydrothermal sulfide which enters the orebody with the metalliferous hydrothermal fluids, sourced dominantly from the Lower Paleozoic basement (Anderson et al., 1998; Fallick et al., 2001).

Within the S Fault Conglomerate, a light signature dominates -16 to -5.9 ‰ in both allochthonous clasts and matrix replacement mineralization, with only two minor heavy hydrothermal S isotope signatures recorded (+7.7 to +8 ‰; Fig. 2.10B).

Barite and anhydrite from the Pale Beds have an average $\delta^{34}S$ of 26 ±1.7‰ (n= 17); one value from the SFC gives 29‰.

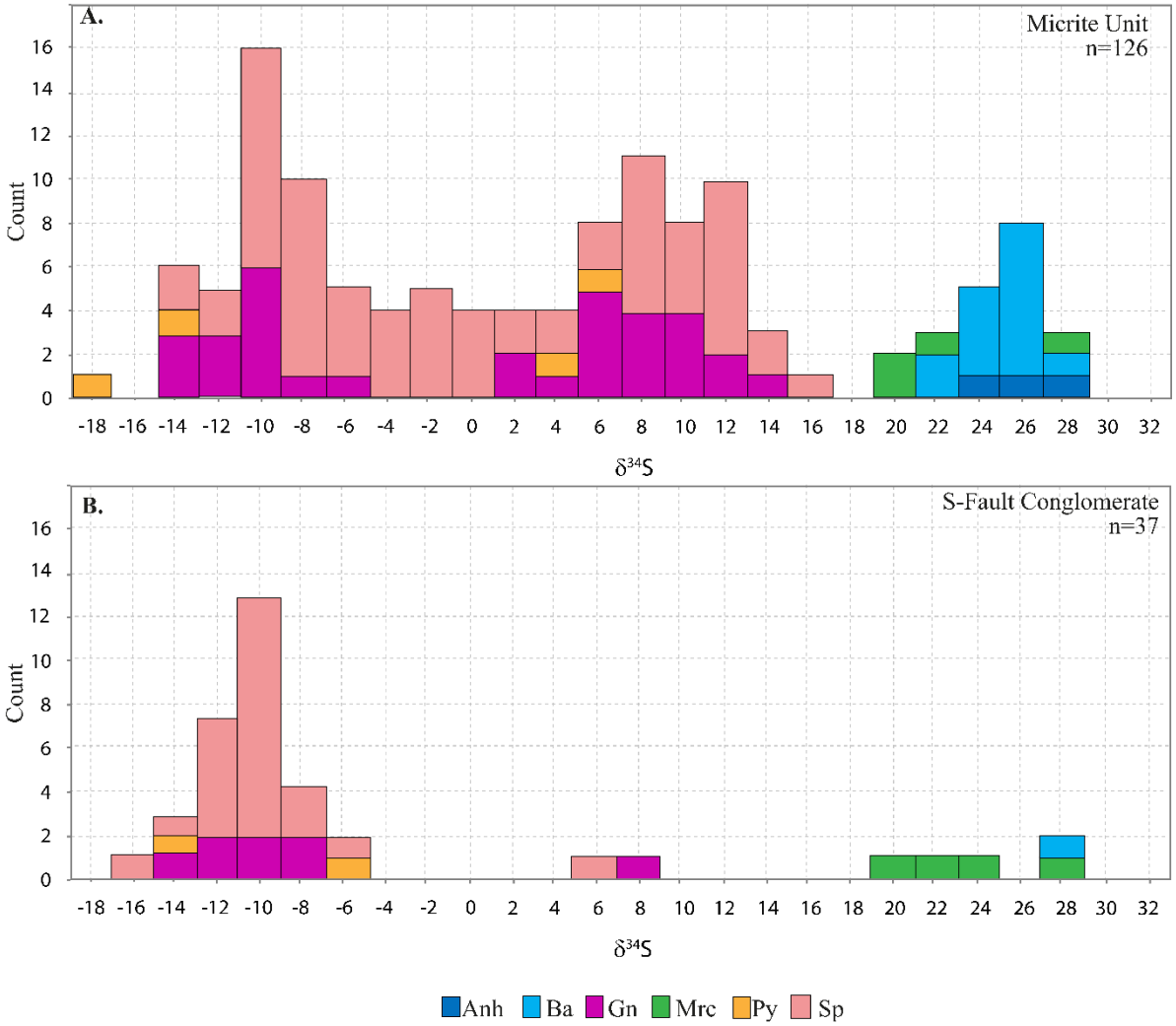

Figure 2.10 S isotope analyses of base metal sulfides from Tara Deep. A) Micrite Unit values outline a bimodal distribution bacteriogenic (-13.5 to -3.6 ‰) and hydrothermal sulfur source (+3.4 to +16.2 ‰) B) S-Fault Conglomerate (SFC) revealing a similar bacteriogenic involvement (-5.9 to -16‰) but with a minor hydrothermal component. Contemporaneous Mississippian seawater signature is recorded for barite and anhydrite in both regions (average=26.2‰).

2.6.8 Pb Isotopes

An extremely homogeneous lead isotope dataset exists for Tara Deep, with analyses completed on drilled out galena samples, ($^{206}Pb/^{204}Pb$=18.23±0.006, 2σ, n=26), revealing that lead (and by association, zinc) are sourced from the underlying Lower Paleozoic basement (Boast et al., 1981b; Caulfield et al., 1986; O'Keeffe, 1986; LeHuray et al., 1987; Mills et al., 1987; Dixon et al., 1990; Fallick et al., 2001; Everett et al., 2003).

2.7 Discussion

2.7.1 Controls on Ore Development

Certain factors including timing of mineralization and the location of fluid migration pathways are still highly debated within Irish-Type models (e.g., Hitzman and Beaty; 1996; Gleeson et al., 1999; Wilkinson et al., 2003; Wilkinson et al. 2005; Johnson et al. 2009; Torremans et al., 2018). There are no clear, single fault structures which can currently be identified as distinct feeder zones at Navan, as opposed to other Irish-type deposits such as Silvermines (Taylor, 1984). Instead, multiple faults of varying size, ranging down to minor fractures in the Navan Orebody, even those with very limited throws (<1m), were conduits for ore fluid movement (Blakeman et al, 2002). Yesares et al., (2019) argues that the high abundance of copper and antimony sulfosalts in galena from Tara Deep suggest a proximity to a feeder system. However, at this stage, determining that exact feeder is extremely ambiguous, especially considering the structural complexity, and because similar Cu-bearing sulfosalts have been recorded at the Navan deposit (Steed, 1980). However, at Tara Deep the predominance of massive lenses of iron sulfide overlying the S Fault hanging wall, highlights the important role of these early NNW-SSE faults.

The diversity of textures at Tara Deep reveal a dynamic mineralizing environment within the subsurface (Fig. 2.8). Most of these textures contain evidence of disruption and reworking of the original units. Within the Micrite Unit of the Pale Beds, mineralization is associated with replacement and open-space textures ultimately leading to the development of complex cavity fill, brecciated and

massive mineralization. A continuum exists between these textures with cavity fill textures amalgamating and forming brecciated mineralization, and in regions where complete replacement occurs, massive mineralization dominates. Open-space textures are epitomized by dendritic-skeletal galena and colloform sphalerite. Whereas matrix replacement textures are dominantly destructive and often leave behind little evidence of the pre-existing unit, however detailed petrographic examination can reveal delicately replaced bioclasts, partially replaced dolomites and detrital heavy mineral relics. Similar complex textures to those at Tara Deep have been outlined at other Irish-type deposits (see Anderson et al., 1998; Ashton et al., 1986; Boast et al., 1981a; Fusciardi et al. 2003, Doran et al., 2017).

The Micrite Unit was an effective trap for precipitation of sulfides due to its organic content, porosity (both fenestral textures and fractures), and finally its fully lithified nature. These factors have provided ideal conditions for fluid mixing, and a substrate for base metal sulfides to nucleate and replace. It was also an organic rich environment where sulfuretum thrived and replacement mineralization processes dominated (Fallick et al., 2001; Wilkinson et al., 2005). Within the SFC of Zone Two, allochthonous clasts of cavity fill textures (originally Pale Beds) are found engulfed by later matrix replacement mineralization (Fig. 2.6B). This indicates that ore deposition was prolonged, initiating during early phases of rifting and thus pre-Boulder Conglomerate. In addition, large rafts of allochthonous Pale Beds mineralization rest on the hanging wall of the S Fault, which are subsequently overlain by matrix replaced SFC mineralization; highlighting that rifting and footwall failure occurred pre-Boulder Conglomerate, and also providing time constraints for upper Tournaisian mineralization. Despite the regional debrites that occur, mineralization continues during the TBU deposition, with extensive deposition of laminated iron sulfides. Currently no significant evidence exists, apart from minor fractured and displaced laminated sulfides in the TBU, to highlight when mineralization ceased, however mineralization was still able to exploit pressure solution seams associated with burial (Fig. 2.6G-H). Regionally, there is significant geologic evidence that ore at Lisheen (Carboni et al., 2003) and at Navan (Ashton et al., 1986) are cut by thrusts related to Variscan tectonic inversion, implying that

mineralization had ceased prior to Variscan deformation at ~300 Ma (Johnston et al., 1996; Wartho et al., 2006).

The paragenetic sequence agrees with a period of prolonged mineralization (Fig. 2.8 & Fig. 2.9), which evolved with basin evolution. The Micrite Unit is the oldest host rock to be mineralized, and subsequently it has been exposed to all mineralizing events and records the entire paragenetic sequence for the Tara Deep system. Zn+Pb dominated during early phases of mineralization, with abundant dendritic galena and colloform sphalerite textures identified within cavities of the Micrite Unit; suggesting rapid, supersaturated conditions in an environment where there has been a sudden change in conditions brought about by fluid mixing (Fig.2.6B). Barite and marcasite are preserved as intermediate phases, particularly replacing the matrix of the SFC (Fig. 2.5B) and infilling any remaining porosity in the Micrite Unit. The preservation of late phase barite and marcasite suggests that during syn-rifting there was a shift to more acidic conditions, facilitating the transfer of barium in an ascending, reduced, fluids which subsequently mixed with a subsurface brine/connate fluid (see Cooke et al., 2000). This shift to more acidic conditions likely remobilised other base metal sulfides, in particular late coarse honeyblende sphalerite (Fig. 2.6F). The late timing of barite and marcasite within the paragenetic sequence is crucial as it highlights an evolving mineralization relationship, and despite the abundance of barite within mineralized regions, it did not coprecipitate with early base metal sulfides. It is also important to note that the size and morphology of barite crystals formed by different precipitation modes are distinct (see Paytan et al., 2002). Barite at Tara Deep often reveals a platy, highly porous fabric, with triangular pits, and internal crystal zonation (variations in concentrations of Sr). This crystal habit agrees with Ba-rich pore fluids being expelled and meeting sulphate-rich seas (diagenetic origin). Finally, pyrite dominates the last phases of the paragenetic sequence and subsequently late-rifting, it is highlighted by the abundance of laminated pyrite preserved in the TBU (Fig. 2.5C) and within pressure dissolution textures (Fig. 2.6G-H), suggesting the system is waning as it becomes Fe-rich and Zn+Pb deficient.

A broad statement is often made in Irish economic geology that mineralization occurs in the lowest, non-argillaceous, clean carbonate unit (Hitzman and Beaty, 1996), however this study stress extreme caution with this statement. Detailed petrography at Tara Deep reveals that mineralization exploits and precipitates in a range of carbonate depositional environments within the Micrite Unit, SFC and TBU. In each of these host rocks mineralization has exploited every available porosity; from fenestral textures, interparticle porosity, argillaceous matrix in debris flows, fractures, cavities and even pressure solution seams. This research proposes that fluid mixing was a greater control on the location of metalliferous fluids. Locations where seawater brines/connate fluids pooled within the subsurface ultimately provided traps for deep ascending metalliferous fluids. The heterogeneity brought about by emergent surfaces in the overlying Pale Beds (see Rizzi, 1992) likely facilitated brine percolation into the subsurface. Whereas dolomitized stratabound units within the Micrite Unit, possibly provided a suitable seal for these dense subsurface bacteriogenic rich brines/connate fluids, eventually interacting and mixing with hot, buoyant hydrothermal fluids, carrying metals from the basement when rifting commences.

2.7.2 Isotopic Constraints

Sulfur Isotopes

Existing Navan Data: An extensive S isotope database exists for Navan (Anderson, 1990; Ford, 1996; Anderson *et al*., 1998; Fallick *et al*., 2001; Blakeman *et al*., 2002; Altinok, 2005, Yesares et al., 2019) and other Irish-type deposits (Boyce et al., 1983b; Caulfield et al., 1986; Wilkinson et al., 2005; Barrie et al., 2009; Wilkinson and Hitzman, 2014), but comparatively little work has been undertaken on Tara Deep (Yesares et al., 2019). Studies in the Main Navan Orebody have outlined two principal populations of $\delta^{34}S$ in ore sulfides, -26 to -4 ‰ and -4 to 16 ‰. The lightest $\delta^{34}S$ subgroup is interpreted as the product of contemporaneous bacterial reduction of seawater sulfate (BSR) during the Mississippian (Coomer and Robinson, 1976), with an average bacteriogenic isotopic fractionation $\Delta^{34}S_{SO4\text{-}H2S}$ around 35‰ being

typical for ore sulfides. The higher sub-group likely represents hydrothermal sulfur which enters the orebody as metalliferous hydrothermal fluids, sourced dominantly from the Lower Paleozoic basement (Anderson et al., 1989; Boyce et al, 1993, 1994, O'Keeffe, 1986). Local sulfates (largely barite, and minor anhydrite) throughout the Navan deposit, have an average δ^{34}S of +21 ± 2‰ (n = 23; Andrew and Ashton, 1985; Boyce et al., 1983b; Caulfield et al., 1986) which is consistent with the range of δ^{34}S of Mississippian seawater sulfate (Claypool et al, 1980; Kampschulte et al., 2001).

Mixing of deep, basement-derived hydrothermal fluid, carrying metals and limited reduced sulfide, with a surface fluid containing bacteriogenic sulfide, was critical to the ore deposition at Navan, and in all other economic ore deposits in Ireland (Coomer and Robinson, 1976; Boyce et al. 1983b; Caulfield et al., 1986; Anderson *et al*., 1998; Anderson, 1990; Ford, 1996; Blakeman *et al*., 2002; Altinok, 2005, Wilkinson et al., 2005; Barrie et al., 2009; Wilkinson and Hitzman, 2014). This interpretation is also supported by fluid inclusion studies and radiogenic isotopes (Banks and Russell, 1992; Eyre, 1998; Everett et al, 1999; Samson and Russell, 1987 and see below). Fallick et al. (2001) quantified the importance of BSR at the Main Navan Orebody using the δ^{34}S of mine concentrates, taken from the Navan deposit's principal ore lens, the 5-lens (and representing up to 1Mt of ore per sample). Zn and Pb concentrates gave an isotopically homogeneous mean value of -13.6 ±2‰ (varying from -17.5 to -10‰), in contrast to the wide range (-25 to +15‰) obtained from laser and conventional S isotope techniques on individual ore sulfide samples (Anderson et al, 1998), indicating that more than 90% of Navan sulfide was bacteriogenic. This dominance is reflected in other mines in Ireland, creating a clear message: bacteriogenic sulfide dominance is a critical factor in development of economically viable mines in Ireland (Coomer and Robinson, 1976; Boast *et al*., 1981a; Thamdrup *et al*., 1993; Boyce *et al*., 1983b; Caulfield *et al*., 1986; Anderson, 1990; Ford, 1996; Anderson et al., 1998; Fallick et al., 2001; Banks *et al*., 2002; Blakeman, 2002, Blakeman et al., 2002; Weber and Jorgensen, 2002; Altinok, 2005, Wilkinson *et al*., 2005; Barrie *et al*., 2009; Anderson et al., 1998 and Yesares et al., 2019).

Tara Deep sulfates: Barite at Tara Deep is paragenetically distinct, and open-space infill and veining suggest that fluid mixing was occurring between a reduced, Ba-bearing fluid and an oxidised

seawater (Cooke et al., 2000). $\delta^{34}S$ of barite at Tara Deep have a mean value of 26.2 ± 1.8‰ (n=18; Fig. 2.10A & B), with a range of 22.7 to 29‰. These values are noticeably higher than the Irish Waulsortian-hosted deposits, which have a mean value of $\delta^{34}S$ of 18.2 ± 2 ‰ (n=48; data from Boast et al., 1981a; Boyce 1990; Wilkinson et al., 2005). Similarly, the values are 5‰ heavier, and distinct from, the mean $\delta^{34}S$ of the Navan deposit at 21 ± 2‰. Nonetheless, it is reasonably assumed that the homogeneous $\delta^{34}S$ from the barites are a close reflection of contemporaneous seawater sulfate in the dynamic environment of Tara Deep, which are thus distinct from the sulfate signal from the Navan deposit. The higher $\delta^{34}S$ in Navan deposits' sulfates, compared to other Irish ores, was suggested by Anderson et al (1998) to reflect a distinction in age and/or setting between the deposits. Indeed, the N-S transgression, and existing ages for the sequences in the Irish Orefield indicate that the Navan and Tara Deep deposits are likely younger than the Waulsortian-hosted deposits (Andrew, 1986, 1993; Schneider et al., 2007; Creaser et al., 2009, Symons et al., 2007). No matter the reason for this increased $\delta^{34}S$ at the Navan deposit, the mean values at Tara Deep differ and are clearly distinct. Thus, the mineralizing systems at Tara Deep and Navan were unlikely to be directly connected at the time of ore deposition, and it is implausible that Tara Deep represents an allochthonous slice of the Navan deposit.

Tara Deep sulfides: At Tara Deep, galena and sphalerite from Pale Beds-hosted mineralization reveal a dominant bimodal distribution of -13.5 ‰ to -3.6 ‰ and +3.4‰ to +16.2 ‰ (Fig. 2.10A), reflective of the Navan deposit's similar bimodal distribution. This bimodal pattern also occurs in the S Fault Conglomerate-hosted with BSR values of -16‰ to -5.9‰, but with a much-reduced minor hydrothermal component of +7.7‰ to +8‰ discovered to date (Fig. 2.10B). However, whilst this bimodal distribution is consistent with the same sources as interpreted for the Navan deposit, and other Irish-type deposits (BSR and hydrothermal sulfide) there is a clear distinction from the Navan deposit. At Tara Deep, the bacteriogenic sub-group distribution is shifted to less negative values, and their mean $\delta^{34}S$ is ~5‰ heavier than the Navan deposit (a mean of -13.6 ± 2‰ for 5-lens, Fallick et al., 2001; versus -8.5 ± 2.4‰ and -9.7 ± 2.1‰ for Tara Deep's Micrite Unit and SFC respectively). This resonates with the distinction in sulfate $\delta^{34}S$ as discussed above (with an overall mean of 26.2 ± 1.8‰). Taken as a whole,

the average extent of fractionation of bacteriogenic ore sulfide from the marine sulfate signal ($\Delta^{34}S_{SO4\text{-}H2S}$) is relatively constant at around 35‰ on average in both systems. This ~35‰ average extent of fractionation is also seen between contemporary marine sulfate and bacteriogenic ore sulfide at Lisheen, Silvermines and Tynagh (Wilkinson et al., 2005; Boyce et al., 2003; Boast et al., 1981a). In contrast, the hydrothermal end-member mean and distribution closely match that of the Navan deposit, averaging around 9‰ at Tara Deep.

Together, these data suggest that Tara Deep received a similar hydrothermal fluid input as the Main Orebody, but that the precise location (in space and time) of the two ore bodies were distinct. It is speculated that there may have been a time gap and/or physical distinction in the sub-basins in which bacteriogenic sulfide reduction was taking place. Whatever, the cause of the variation in seawater sulfate $\delta^{34}S$, the bacterial communities were likely similar in both cases – and more broadly in Ireland - when hydrothermal metals were being precipitated in a dynamic environment using bacteriogenic sulfide. Weber and Jorgensen (2002) note a dramatic increase in intensity of BSR activity and sulfide production in active hydrothermal centres in the Guaymas Basin, compared to off-mound production rates. We speculate that the extent of fractionation – and perhaps the intensity - seen in the Irish deposits is a reflection of such a hydrothermally stimulated bacterial community in the Mississippian sea of this region during ore deposition.

In contrast to Anderson et al. (1998), no simple correlation is observed between sphalerite and galena textures and S isotope signature, a feature which they noted in the Navan deposit. At Tara Deep this may reflect the dynamic nature of the depositing system, typically associated with fluid mixing, and with textures revealing an intimate relationship between hydrothermal and bacteriogenic signatures (Fig. 2.6C & 2.10). At Tara Deep, cavity fill, coarse galena, brecciated textures, and massive mineralization can possess both hydrothermal and bacteriogenic values. Thus, we argue that rapidly changing conditions, brought about by dynamic fluid mixing and thus modifying local physio-chemical conditions, were more important than the overall available S source for generating these textures (Fig. 2.11), the metals using whichever source was available at a given moment.

Coarse-grained galena with a hydrothermal $\delta^{34}S$ signature always have abundant Sb-sulfosalts and sporadic Cu-sulfosalt inclusions (Fig. 2.6C), in contrast to coarse-grained galena with a bacteriogenic $\delta^{34}S$ signature which only hosts minor Sb sulfosalt inclusions. This allows an accurate representation of the sulfur source at the petrographic scale. The occurrence of the abundant Cu and Sb sulfosalts reflects the ability for metalliferous fluids to mobilise copper, suggesting a temperature regime that is on the upper end of the spectrum (>250˚C) of fluid inclusion recorded at the Navan deposit (Lydon, 1988; Wilkinson, 2014).

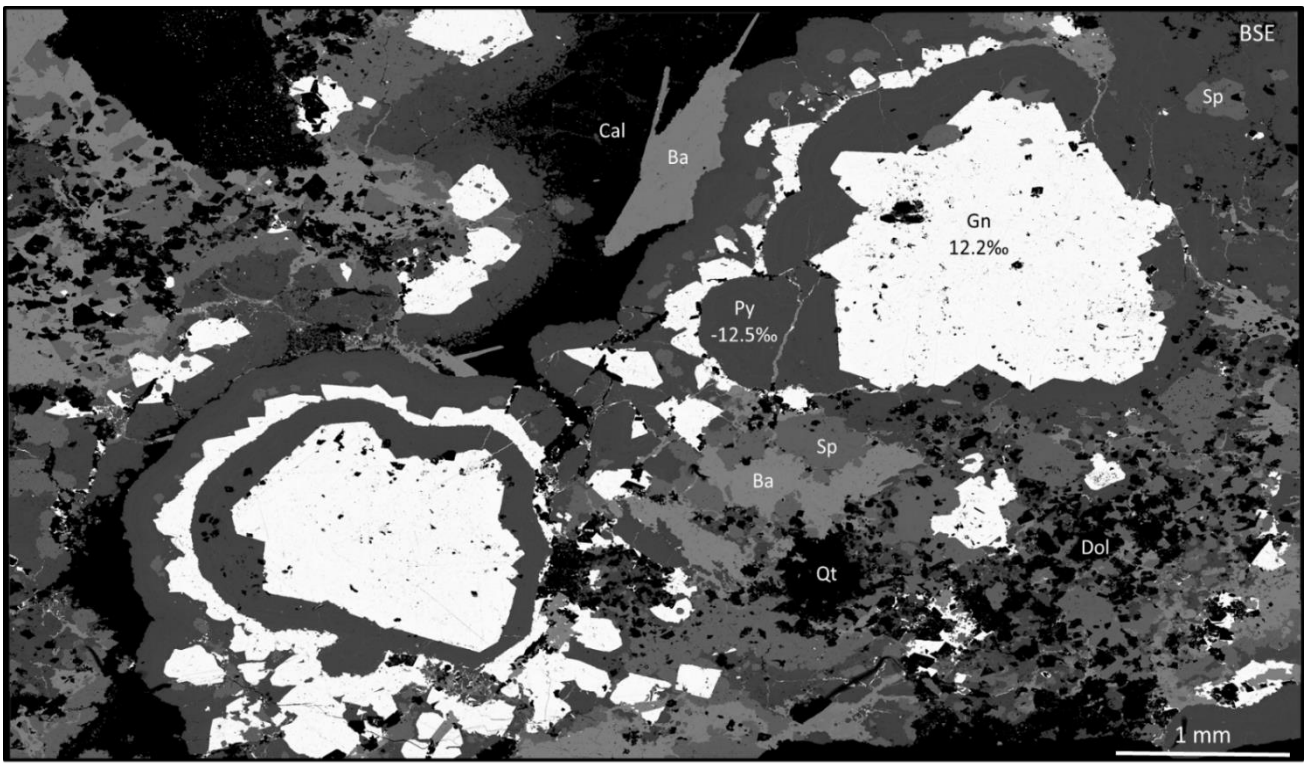

Figure 2.11 Back Scattered Electron (BSE) image of Pale Bed mineralization displaying the complex textures present at Tara Deep and the close relationship between bacteriogenic and hydrothermal base metal sulfides. Sphalerite is encased by colloform bacteriogenic pyrite which displays arsenic zonations (Py; -12.5‰), this is infilled by hydrothermal galena (12.2‰) with inclusions of Sb- and Cu-sulfosalts (N02428; 1473.6m). Mineral abbreviations; Barite (Ba), Calcite (Cal) Dolomite (Dol), Galena (Gn), Sphalerite (Sp) and Quartz (Qt).

Yesares et al., (in press) outlines that the TBU at Tara Deep displays a distinct S isotope pattern. In addition to the bimodal distribution in ore minerals similar to the Pale Bed and SFC counterparts, an extremely negative mode is also noted in pyrite of the TBU (<-20‰). This is also seen in the TBU-

equivalent levels at the Navan deposit (Anderson et al., 1998). Blakeman et al (2002) cogently argue that this reflects a bacterial consortium operating in more oxidizing conditions during "quieter" periods when the main mineralization is not taking place (instead, solely pyrite deposition), allowing increased disproportionation cycles during dissimilatory bacterial reduction of sulfate (Thamdrup et al., 1993; Canfield and Thamdrup, 1994; Finster, et al., 1998). As Blakeman et al (2002) points out, a corollary of this observation is that the sulfide in remobilized pyrite cannot be the source of this base-metal sulfide, as remobilized pyrite would simply retain its original $\delta^{34}S$ signature (see also Boyce et al., 1983b; Anderson et al., 1998).

2.7.3 Lead Isotopes

Data from Tara Deep display remarkably homogeneous $^{206}Pb/^{204}Pb$ of 18.2 ± 0.006 (2σ, n=25), which is coincident with Pb isotope data across the Navan deposits (Caulfield et al., 1986; O'Keeffe, 1986; Fallick et al., 2001). Fallick et al (2001) analysed bulk mine concentrates across all lenses at Navan ($^{206}Pb/^{204}Pb$=18.19 ± 0.03, 2σ), and agreed with earlier and subsequent interpretations of Pb isotope data from across the Irish Orefield (LeHuray et al., 1987; Mills et al., 1987; Dixon et al., 1990; Everett et al., 2003) that the Pb, and thus ore metals, were derived from leaching of the underlying Lower Paleozoic basement. Across Ireland, there is a systematic variation in lead isotope ratios from northwest to southwest Ireland, following the Caledonide inherited grain, which is seen in both Mississippian-hosted and basement-hosted mineralization. This variation across the Irish orebodies are interpreted to reflect mixing of lead extracted from Ordovician and Silurian volcanics and sediments during Caledonian accretion, derived from different crustal reservoirs north and south of the Iapetus suture (Boast et al., 1981b; Caulfield et al., 1986; O'Keeffe, 1986; LeHuray et al., 1987; Mills et al., 1987; Dixon et al., 1990; Fallick et al., 2001; Everett et al., 2003). A potential alternative source of lead from the Old Red Sandstone has been emphatically ruled out based on the experimental work of Everett et al., (2003).

2.7.4 Summary of Isotopic Constraints

Tara Deep and Navan show broadly similar Pb and S isotope characteristics, with both exhibiting a statistically identical Pb isotopic signature and a bimodal ore sulfide S isotopic distribution and homogeneous sulfate signature. An average isotopic fractionation between the contemporaneous marine sulfate and ore sulfide around 35‰ is found in both deposits, and is a signal found in all other economic Irish ore deposits. However, whilst they appear to be horses of the same colour, the shades are slightly different. Around 5‰ shifts to higher $\delta^{34}S$ in the subsurface-derived S isotope signatures (both sulfide and sulfate) indicate that Tara Deep's sulfur was sourced from a distinct seawater signature. In contrast, the Pb isotopes and the hydrothermal S isotopic signature show a similar hydrothermal influence, with derivation of both most likely from the Lower Paleozoic basement.

2.7.5 Differences Between Tara Deep and Navan

A series of additional mineralized lenses exist within the upper Pale Beds at the Main Navan Orebody; whilst for Tara Deep, the sedimentary sequence above the lower Pale Beds are principally lost or missing, and marker horizons within the Pale Beds are not preserved (Fig. 2.3A&B). Deciphering separate debris flows with the Navan deposit's Conglomerate Group Ore (CGO) is difficult (Ford, 1996), and so the unit is generally clumped as a homogenous package. At Tara Deep, particularly in Zone One, several distinct sedimentary breccias are clearly recognised in the TBU, with intervening thinly bedded limestones and shales that have consistent characteristics and are laterally persistent- highlighting that numerous slope instability events occurred in this region. Finally, seismic interpretation and initial drilling have revealed that the TBU has dramatically thickened over the Tara Deep region, and is interbedded with a series of slides, tuffaceous horizons, hydrothermal cherts and laminated iron sulfide mineralization. These features clearly highlight instability during rift-related basin margin sedimentation during the lower Viséan and have led to deposition of ~600m of TBU in the Tara Deep region (which has a thickness of 20m at the Navan Orebody). The increased thickness of TBU units in this area appears to reflect renewed peripheral faulting, potentially to the north (Ashton et al., 2018).

In summary, discrepancies exist between Tara Deep and Navan, but most of these differences can be explained by considering the variation in differential subsidence, sea-level variations, debrites/erosion, and subsequent removal of stratigraphy.

2.7.6 Genetic Implications

How Tara Deep formed has significant implications for the genesis of Irish-type base metal deposits and facilitates our understanding of the evolution of the Navan and Tara Deep systems. A schematic genetic model for the formation of Tara Deep is presented in Fig. 2.12. This model splits the broadly syn-rift mineralization relationships into three stages, early-rift, syn-rift and late-rift:

Stage 1 (early-rift): Basin rifting initiates, subsequently generating fault conduits for hot, buoyant metalliferous fluids from the basement. Structural lows developed where dense brines/connate fluids became trapped within the subsurface. In the Tara Deep region, NE trending faults (G and potentially the Navan fault) and the S Fault were important conduits, especially at the junctions between these faults. The onset of early-rift mineralization pre-dates the significant lower Viséan debris flows. Allochthonous clasts and rafts of Micrite Unit mineralization within the SFC agree with early extensional faulting, mineralization, and footwall failure pre-Boulder Conglomerate.

Stage 2 (syn-rift): Brines continued to pool within structural/topographic lows within the subsurface. The Pale Beds mineralization and the SFC mineralization are geographically and temporally distinct. The SFC likely represents a debrite in a region where mineralization was already occurring. The SFC records an evolving mineralization story, more acidic and reducing conditions, highlighted through the dominance of late phase marcasite and barite within the SFC matrix. There was a gradual shift to more Fe-dominant conditions with time. Exploration criteria at a regional scale should strongly favour highly productive, extensional basin margins, with focus on structural lows where debrites have occurred. These regions are insights into areas where faulting generated structural lows and locations where brines/connate fluids pooled. These structures also provided active conduits for metalliferous fluids to rise from the basement, and eventually generated footwall instability and collapse.

Stage 3 (late rift): Basin subsidence continued, with differential subsidence occurring between Tara Deep and Navan. This is highlighted by a remarkable thickening of the TBU stratigraphy between Tara Deep and Navan (Fig. 2.3). Late-rift debrites and turbidity currents dominated in the Tara Deep region. Fault conduits remained active, with the G Fault likely having a more crucial role. The system waned and became iron dominated with extensive iron sulfide lamination in the TBU, with only minor sphalerite and galena. Subsequently, the TBU provides a visual vector to potential underlying mineralization.

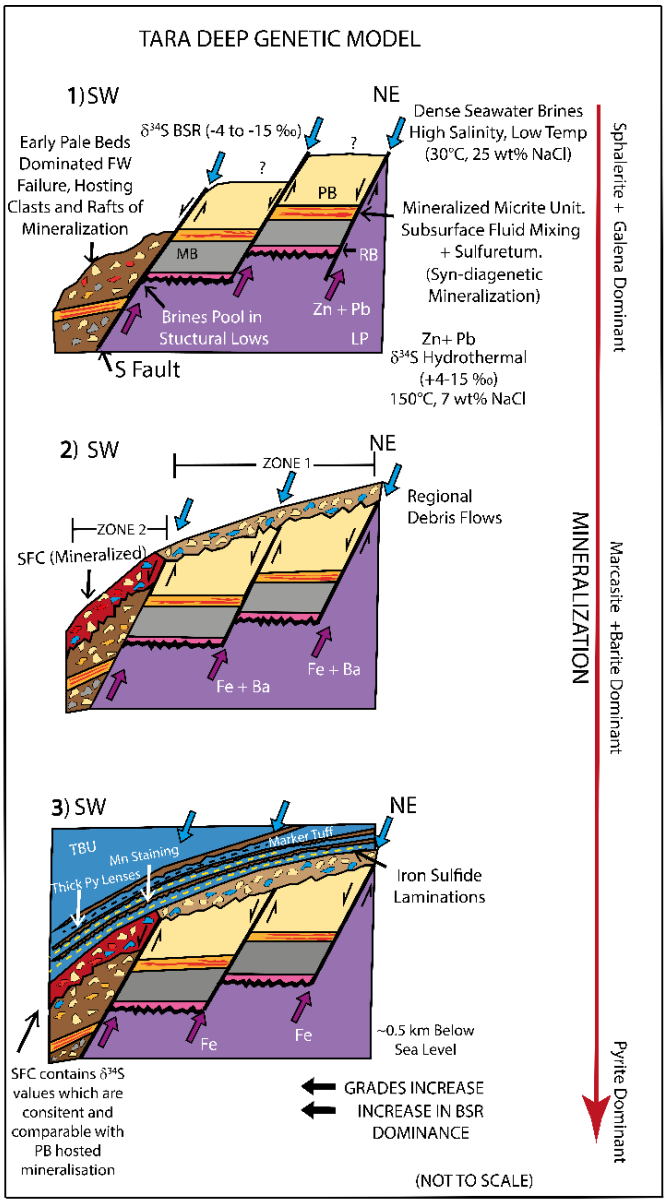

Figure 2.12 Tara Deep cartoon schematic model outlining the evolution of the deposit and showing the relationship between mineralization and the S Fault. Model highlights the close association between basin development, evolving carbonate depositional environments, and mineralization. A series of low angle faults likely exist which complicate this reconstruction. Abbreviations are, LP- Lower Paleozoics, MB- Mixed Beds, PB- Pale Beds, RB- Red Beds, SFC- S Fault Conglomerate, TBU- Thin Bedded Unit.

2.8 Conclusions

The Tara Deep deposit is hosted by Mississippian carbonates within complex fault-controlled terraces on the degrading footwall of a major normal fault system. These terraces have resulted from basin margin activity during the upper Tournaisian. The Tara Deep deposit has many similarities with the neighbouring Navan deposit that reflect comparable controls on the mineralizing process such as host rocks, Pb and S sources, and tectonic environment. Of crucial importance is the presence of eroded, transported and abraded clasts and rafts of sulfide entrained within syn-rift conglomerates in both the Navan (Conglomerate Group Ore) and Tara Deep (S Fault Conglomerate) deposits. This observation demonstrates that the onset of mineralization occurred during the upper Tournaisian, and relative to the stratigraphy, the timing of mineralization at Tara Deep is similar to Navan. Tara Deep and Navan are isotopically similar, showing both a statistically identical Pb isotopic signature and a bimodal sulfide S isotopic distribution and homogeneous sulfate signature. However, around 5‰ shifts to higher $\delta^{34}S$ in the subsurface-derived S isotope signatures (both bacteriogenic sulfide and sulfate) indicate that Tara Deep's sulfur was sourced from a distinct seawater signature. Close similarities with the Navan deposit allows Tara Deep to adopt a similar genetic model as Ashton et al., (2015). However, this research demonstrates that mineralization initiated during an early phase of the developing Dublin Basin and kept pace with rifting and subsequently an evolving basin. It develops the existing model to highlight the evolving basin and mineralization relationships, and also to outline that the Pale Beds mineralization is temporally distinct from the S Fault Conglomerate-host. Upper Tournaisian extensional faulting allowed dense brines to pool in structural lows, and also provided fault conduits for hot, metalliferous fluids from the basement to access the carbonate host rocks.

To discover more deposits like Tara Deep, it is vital to understand the basin margin architecture and to model existing debrites and structural lows where mineralization once occurred. Correlations with Navan are important encouragement for continuing exploration in the Tara Deep region and indeed in the areas to the south and west of Navan.

2.9 Acknowledgements

We thank Boliden Tara Mines who fully funded the PhD of DAD. Isotopic analyses were funded through NERC Facility award IP-1904-0619 to AJB. We thank Dave Coller and Mike Philcox for their comments on earlier versions of this manuscript. We thank the Grant Institute (University of Edinburgh) and John Craven in particular for access to SEM and CL microscope, and Peter Chung at the University of Glasgow for access to SEM. SUERC is supported by NERC and the Scottish Universities consortium. LY is funded by Science Foundation Ireland (SFI; grant number 18/IF/6347), and the European Regional Development Fund. We thank NEIF Facility staff Ian Millar and Alison McDonald for their help with the isotope analyses. Discussions with a number of individuals have also helped throughout the course of this research, we especially thank Adina Paytan, Cathy Hollis, Colin Braithwaite, Rachel Wood, Rob Raiswell, Steve Hollis, Will McCarthy and Tony Prave.

2.10 References

Altinok, E., 2005, Zn-Pb-Fe Mineralization process, evolution of sea water oxidation state in a restricted basin, and diagenesis of deep water calcareous sediments: geochemical and geological study of the Navan Deposit, Dublin Basin, Ireland. Unpublished PhD thesis, Colorado School of Mines, p. 160.

Anderson, I.K., 1990, Ore depositional processes in the formation of the Navan zinc-lead deposit, Co. Meath, Ireland. Unpublished PhD thesis, University of Strathclyde, p.290.

Anderson, I.K., Andrew, C.J., Ashton, J.H., Boyce, A.J., Caulfield, J.B.D., Fallick, A.E. and Russell, M.J., 1989, Preliminary sulphur isotope data of diagenetic and vein sulfides in the Lower Palaeozoic strata of Ireland and southern Scotland: implications for Zn + Pb +Ba mineralization. Journal of the Geological Society, London, 146, p. 715-720.

Anderson, I.K., Ashton, J.H., Boyce, A.J., Fallick, A.E. and Russell, M.J., 1998, Ore Depositional processes in the Navan Zn-Pb deposit, Ireland. Economic Geology 93, p. 535-563.

Andrew C.J., (1986) The tectono-stratigraphic controls to mineralization in the Silvermines area, County Tipperary, Ireland. In: Andrew CJ, Crowe RWA, Finlay S, Pennell WM, and Pyne J (eds.) Geology and Genesis of Mineral Deposits in Ireland. Dublin: Irish Association for Economic Geology. p. 377–417

Andrew C.J., 1993. Mineralization in the Irish Midlands. In: Pattrick RAD and Polya DA (eds.) Mineralization in the British Isles. London: Chapman and Hall. p. 208–269

Andrew, C.J., and Ashton, J.H., 1985. Regional setting, geology and metal distribution patterns of Navan orebody, Ireland: Trans. Inst. Min. Metall. (Sect.B: Appl. earth SCi.), v.94, p. 66-93.

Ashton, J.H., Beach, A., Blakeman, R.J., Coller, D., Henry, P., Lee, R., Hitzman, M., Hope, C., Huleatt-James, S., O'Donovan, B., Philcox, M.E., 2018. Discovery Of The Tara Deep Zn-Pb Mineralisation At The Boliden Tara Mine, Navan, Ireland: Success With Modern Seismic Surveys. In Seg Special Publications No 21, p. 365-381. Doi:10.5382/Sp.21.16.

Ashton, J.H., Black, A., Geraghty, J., Holdstock, M. and Hyland, E., 1992, The geological setting and metal distribution patterns of Zn-Pb-Fe mineralization in the Navan Boulder Conglomerate. In: Bowden, A.A., Earls, G., O'Connor, P.G. and Pyne, J.F. (Eds). The Irish Minerals Industry 1980-1990. IAEG, Dublin, p. 171-210.

Ashton, J.H., Holdstock, M.P., Geraghty, J.F., O'Keeffe, W.G., Peace, W. and Philcox, M.E., 2003, The Navan Orebody - Discovery and Geology of the South West Extension. In: Kelly, J.G., Andrew, C.J., Ashton, J.H., Boland, M.B., Earls, G., Fusciardi, L., Stanley, G. (Eds). Europe's Major Base Metal Deposits. IAEG, Dublin, p. 405-430.

Ashton, J.H.; Blakeman, R.J.; Geraghty, J.F.; Beach, A.; Coller, D.; Philcox, M.E. 2015 The Giant Navan carbonate-hosted Zn–Pb deposit—A review. In Current Perspectives on Zinc Deposits; Archibald, S.M.,Piercey, S.J., Eds.; Irish Association for Economic Geology: Dublin, Ireland, 2015; p. 85–122.

Ashton, J.H.; Downing, D.T.; Finlay, S. 1986. The geology of the Navan Zn–Pb orebody. In Geology and genesis of mineral deposits in Ireland; Andrew, C.J., Crowe, R.W.A., Finlay, S., Pennell, W.M., Pyne, J.F.,Eds.; Irish Association for Economic Geology: Dublin, Ireland, p. 243–280.

Banks, D.A., and Russell, M.J., 1992, Fluid mixing during ore deposition at the Tynagh base-metal deposit, Ireland: European Journal of Mineralogy, v. 4, p. 921–931.

Banks, D.A., Boyce, A.J., and Samson, I.M., 2002, Constraints on the origins of fluids forming Irish Zn-Pb-Ba deposits: Evidence from the composition of fluid inclusions. Economic Geology, 97, p. 441-480.

Barrie, C., Boyce, A., Boyle, A., Williams, P., Blake, K., Wilkinson, J., Lowther, M., McDermott, P. and Prior, D. 2009. On the growth of colloform textures: a case study of sphalerite from the Galmoy ore body, Ireland. Journal of the Geological Society, 166(3), p.563-582.

Blakeman, R.J., 2002, The Compositions and routes of the fluids generating the Navan giant base-metal orebody. Unpublished PhD thesis, University of Glasgow, p.207.

Blakeman, R.J., Ashton, J.H., Boyce, A.J., Fallick, A.E. and Russell, M.J., 2002, Timing of interplay between hydrothermal and surface fluids in the Navan Zn+Pb orebody, Ireland: Evidence from metal distribution trends, mineral textures and $\delta^{34}S$ analyses. Economic Geology, 97, p. 73-91.

Boast, A.M., Coleman, M.L., and Halls, C., 1981a, Textural and stable isotope evidence for the genesis of the Tynagh base metal deposit, Ireland: Economic Geology, v. 76, p. 27–55.

Boast, A.M., Swainbank, I.G., Coleman, M.L., and Halls, C. 1981b, Lead isotope variation in the Tynagh, Silvermines and Navan base-metal deposits, Ireland. Trans. Instn Min. Metall. (Sect B: Appl. Earth Sci.), 90, p. 115–119.

Boliden Summary Report. 2020 [online] Boliden.com. Available at: <https://www.boliden.com/globalassets/operations/exploration/mineral-resources-and-mineral-reserves-pdf/2020/resources-and-reserves-tara-2020-12-31.pdf> [Accessed 1 July 2021].

Boyce, A. J., Anderton, R. and Russell, M.J., 1983a, Rapid subsidence and early Carboniferous base-metal mineralization in Ireland. Trans. Instn Min. Metall. (Sect B: Appl. Earth Sci.), 92, p. 55-66.

Boyce, A, J. Coleman M.D. Russel, M.J. 1983b. Formation of fossil hydrothermal chimneys and mounds from Silvermines, Ireland: Nature, 306, p. 545 – 550.

Boyce, A.J., 1990, Exhalation, sedimentation and sulphur isotope geochemistry of the Silvermines Zn + Pb + Ba deposits, County Tipperary, Ireland. Unpublished PhD thesis, University of Strathclyde, p.354.

Boyce, A.J., Fallick, A.E., Fletcher, T.J., Russell, M.J., and Ashton, J.H., 1994, Detailed sulphur isotope studies of Lower Palaeozoic-hosted pyrite below the giant Navan Zn +Pb mine, Ireland: evidence of mass transport of crustal S to a sediment-hosted deposit: Mineralogical Magazine, v. 58A, p.109–110

Boyce, A.J., Fletcher, T.J., Fallick, A.E., Ashton, J., and Russell, M.J., 1993, Petrographic and $\delta^{34}S$ study of Lower Palaeozoic rocks under the Navan Zn + Pb deposits: A source of hydrothermal sulphur, *in* Fenoll Hach-Ali, P., Torres-Ruiz, J., and Gervilla, F., eds, current research in geology applied to ore deposits: Second Biennial SGA Meeting, Granada, 1993, Departa- mento de Mineralogia y Petrologia, Universidad de Granada, Proceedings, p. 53–56.

Boyce, A.J.; Stephen Little, C.; Russell, M. 2003. A New Fossil Vent Biota in the Ballynoe Barite deposit, Silvermines, Ireland: Evidence for Intracratonic Sea-Floor Hydrothermal Activity About 352 Ma.Econ. Geol., 98, p.649–656.

Braithwaite, C.J.R. and Rizzi, G., 1997, The geometry and petrogenesis of hydrothermal dolomites at Navan, Ireland. Sedimentology, 44, p. 421-440.

Canfield, D.E., and Thamdrup, B., 1994, The production of ^{34}S-depleted sulfide during bacterial disproportionation of elemental sulfur: Science, v. 266, p. 1973–1975.

Carboni, V., Walsh, J.J., Stewart, D.R.A., and Güven, J.F., 2003, Timing and geometry of normal faults and associated structures at the Lisheen Zn/Pb deposit, Ireland—investigating their role in the transport and trapping of: Society for Geology Applied to Mineral Deposits Meeting, 7th biennial, Athens, Greece, Proceedings, p. 665–668.

Caulfield, J.B.D., LeHuray, A.P. and Rye, D.M., 1986, A review of lead and sulphur isotopes investigations of Irish sediment-hosted base metal deposits, with new data from Keel, Ballinalack, Moyvoughly and Tatestown deposits. In: Andrew, C.J., Crowe, R.W.A., Finlay, S., Pennell, W.M. and Pyne, J. (Eds). Geology and Genesis of Mineral Deposits in Ireland. IAEG, Dublin, p. 591-616.

Claypool, J.B., Holser, W.T., Sakai, I.R., Zak, I., 1980, The age curves for sulfur and oxygen isotopes in marine sulfate and their mutual interpretation. Chemical Geology, 28, p. 199-260.

Coleman, M. and Moore, M., 1978. Direct reduction of sulfates to sulfate dioxide for isotopic analysis. *Analytical Chemistry*, 50(11), p.1594-1595.

Cook, H.E. and Mullins, H.T., 1983, Basin margin environment. Chap. 11. 540-617. In: Scholle, P.A., Bebout, D.G. and Moore, C.H. (Eds). Carbonate depositional environments. Tulsa OK, AAPG, p.708.

Cooke, D., Bull, S., Large, R. and McGoldrick, P., 2000. The Importance of Oxidized Brines for the Formation of Australian ProterozoicStratiform Sediment-Hosted Pb-Zn (Sedex) Deposits. Economic Geology, 95(1), p.1-18.

Coomer, P.G., and Robinson, B.W., 1976, Sulphur and sulphate-oxygen isotopes and the origin of the Silvermines deposits, Ireland: Mineralium Deposita, 11, p. 155-169.

Creaser RA, Wilkinson JJ, and Hnatyshin D, 2009. Re-Os dating of sulfide mineralization (pyrite) from the Lisheen Pb-Zn deposit, Ireland. Geoloical Society of America Abstracts with Programs 41(7): p.681.

Davidheiser-Kroll, B., Stuart, F. and Boyce, A., 2014. Mantle heat drives hydrothermal fluids responsible for carbonate-hosted base metal deposits: evidence from $^{3}He/^{4}He$ of ore fluids in the Irish Pb-Zn ore district. Mineralium Deposita, 49(5), p.547-553.

Dixon, P.R., LeHuray, A.P., and Rye, D.M., 1990, Basement geology and tectonic evolution of Ireland as deduced from Pb isotopes. Journal of the Geological Society, London, 147, p. 121-132.

Doran, A., Menuge, J. F., Hollis, P, S. and Güven, J. 2017. 'Enhancing understanding of Irish Zn-Pb mineralization : a closer look at the Island Pod orebody , Lisheen deposit', p. 597–600.

Elliot, H.A.L. Gernon, T.M. Roberts, S. Boyce, A.J., Hewson, C. 2019. Diatremes act as fluid conduits for Zn-Pb mineralization in the SW Irish ore field. Economic Geology, 114, p.117-125.

Everett, C.E., Rye, D.M. and Ellam, R.M., 2003, Source or sink? An assessment of the role of the Old Red Sandstone in the genesis of the Irish Zn-Pb Deposits. Economic Geology, 98, p. 31-50.

Everett,C. E., Wilkinson,J. J. Rye,D. M. 1999. Fracture-controlled fluid flow in the Lower Palaeozoic basement rocks of Ireland: implications for the genesis of Irish-type Zn-Pb deposits. In: McCaffreY,K. J. W., Lonergan,L. & Wilkinson,J. J. (eds) Fractures, Fluid Flow and Mineralization. Geological Society, London, Special Publications, 155, p.247-276.

Eyre, S.L., 1998, Geochemistry of dolomitization and Zn-Pb mineralization in the Rathdowney Trend,1225 Ireland: Unpub. Ph.D. thesis, Univ. London, p. 414.

Fallick, A.E., Ashton, J.H., Boyce, A.J., Ellam, R.M. and Russell, M.J., 2001, Bacteria were responsible for the magnitude of the world-class hydrothermal base metal sulfide orebody at Navan, Ireland. Economic Geology, 96, p. 885-890.

Finster, K., Liesack, W., and Thamdrup, B., 1998, Elemental sulfur and thiosulfate disproportionation by *Desulfocapsa sulfoexigens* sp. nov., a new anaerobic bacterium isolated from marine surface sediment: Applied Environmental Microbiology, v. 64, p.119–125.

Ford, C.V., 1996, The integration of petrologic and isotopic data from the Boulder Conglomerate to determine the age of the Navan orebody, Ireland. Unpublished PhD thesis, University of Glasgow, p.176.

Fritschle, T.; Daly, J.S.; McConnell, B.; Whitehouse, M.J.; Menuge, J.F.; Buhre, S.; Mertz-Kraus, R.; Döpke, D. 2018. Peri-Gondwanan Ordovician arc magmatism in southeastern Ireland and the Isle of Man:Constraints on the timing of Caledonian deformation in Ganderia. Geol. Soc. Am. Bull. 130, p.1918–1939.

Fusciardi, L.P., Guven, J.F., Stewart, D.R.A., Carboni, V., and Walshe, J.J., 2003, The geology and genesis of the Lisheen Zn-Pb deposit, Co. Tipper- ary, Ireland, in Kelly, J.G., Andrew, C.J., Ashton, J.H., Boland, M.B., Earls, G., Fusciardi, L., and Stanley, G., eds., Europe's major base metal deposits: Dublin, Irish Association for Economic Geology, p. 455–481.

Gagnevin, D. Menuge, J.F. Kronz, A. Barrie, C. Boyce, A.J. 2014, Minor Elements in Layered Sphalerite as a Record of Fluid Origin, Mixing, and Crystallization in the Navan Zn-Pb Ore Deposit, Ireland. Econ. Geol. v.109, p. 1513-1528

Gleeson, S.A., Banks, D.A., Everett, C.E., Wilkinson, J.J., Samson, I.M. and Boyce, A.J. 1999. Origin of mineralising fluids in Irish-type deposits: Constraints from halogens. In: Stanley, C.J. (ed.) Mineral Deposits: Processes to Processing, Vols 1 and 2. A.A. Balkema Publishers: Rotterdam, p. 857-860.

Gregg JM, Shelton KL, Johnson AW, Somerville ID, and Wright WR (2001) Dolomitization of the Waulsortian limestone (Lower Carboniferous) in the Irish Midlands. Sedimentology 48: p.745–766.

Grover, G., Read, J. F. 1978. Fenestral and Associated Vadose Diagenetic Fabrics of Tidal Flat Carbonates, Middle Ordovician New Market Limestone, Southwestern Virginia. *SEPM Journal of Sedimentary Research*, Vol. 48.

Henjes-Kunst, E., Raith, R.G. and Boyce, A.J. (2017) Micro-scale sulfur isotope and chemical variations in sphalerite from the Bleiberg Pb-Zn deposit, Eastern Alps, Austria. Ore Geology Reviews, 90, p.52-62.

Hitzman, M.W., and Beatty, D.W., 1996, The Irish Zn-Pb-(Ba) orefield, in Sangster, D.F., ed., Carbonate-hosted lead-zinc deposits: Society of Economic Geologists Special Publication, 4, p.112–143.

Hitzman, M.W., Earls, G., Shearly, E., Kelly, J, Cruise, M. and Sevastopulo, G., 1995, Ironstones (iron oxide-silica) in the Irish Zn Pb deposits and regional iron oxide-(silica) alteration of the Waulsortian limestone in southern Ireland. In: Anderson, I.K., Ashton, J.H., Earls, G., Hitzman, M. And Tear, S., (Eds). Irish carbonate-hosted Zn-Pb deposits: Society of Economic Geologists GuidebookSeries, 21, p.261-273

Hitzman, M.W., Redmond, P.B. and Beatty, D.W., 2002, The carbonate-hosted Lisheen Zn-Pb-Ag deposit, County Tipperary, Ireland. Economic Geology, 97, p.1627-1655.

Johnson, A.W., Shelton, K. L., Gregg, J.M., Somerville, I.D., Wright, W.R. and Nagy, Z.R., 2009, Regional studies of dolomites and their included fluids: recognizing multiple chemically distinct fluids during the complex diagenetic history of Lower Carboniferous (Mississippian) rocks of the Irish Zn- Pb ore field. Mineralogy and Petrology, 96, p. 1-18.

Johnston, J., Coller, D., Millar, G. and Critchley, M., 1996. Basement structural controls on Carboniferous-hosted base metal mineral deposits in Ireland. *Geological Society, London, Special Publications*, 107(1), p.1-21.

Kampschulte A, Bruckschen P, and Strauss H. 2001. The sulphur isotopic composition of trace sulphates in Carboniferous brachiopods: Implications for coeval seawater, correlation with other geochemical cycles and isotope stratigraphy. Chemical Geology 175: p. 149–173.

Lee, M.J. and Wilkinson, J.J., 2002, Cementation, hydrothermal alteration, and Zn-Pb mineralization of carbonate breccias in the Irish Midlands: textural evidence from the Cooleen Zone, near Silvermines, County Tipperary. Economic Geology, 97, p. 653-662.

LeHuray, A.P., Caulfield, J.B.D, Rye, D.M and Dixon, P.R., 1987, Controls on Sediment-Hosted Zn-Pb Deposits: A Pb Isotope Study of Carboniferous Mineralization in Central Ireland. Economic Geology, 82, p.1695-1709.

Lydon, J. W., 1988 Volcanogenic massive sulphide deposits, Part 2--Genetic models: Geoscience Canada, v. 15, p.43- 65.

McNestry A., Rees J. G. 1992. Environmental and palynofacies analysis of a Dinantian (Carboniferous) littoral sequence: the basal part of the Navan Group, Navan, County Meath, Ireland. Palaeogeography, Palaeoclimatology, Palaeoecology 96: p.175–193

Mills, H., Halliday, A.N., Ashton, J.H., Anderson, I.K., Russell, M.J., 1987, Origin of a giant orebody at Navan, Ireland. Nature, 327, p. 223-226.

Murphy, F.C., Anderson, T.B., Daly, J.S., Gallagher, V., Graham, J.R., Haroer, D.A.T., Johnston, J.D., Kennan, P.S., Kennedy, M.J., Long, C.B., Morris, J.H., O'Keeffe, W.G., Parkes, M., Ryan, P.D., Sloan, R.J., Stillman, C.J., Tietzch-Tyler, D., Todd, S.P., Wrafter, J.P., 1991. An appraisal of Caledonian suspect terranes in Ireland. Irish Journal of Earth Sciences, 11, p.11-41.

Nolan, S.C., 1989, The style and timing of Dinantian synsedimentary tectonics in the eastern part of the Dublin Basin, Ireland. In: Arthurton, R.S., Gutteridge, P. and Nolan,S. C. (Eds). The role of tectonics in Devonian and Carboniferous sedimentation in the British Isles. Yorkshire Geological Society, Occasional Publication 6, p. 83-97.

O'Keeffe, W.G., 1986, Age and postulated source rocks for mineralization in central Ireland, as indicated by lead isotopes. In: Andrew, C.J., et al. (Eds). Geology and Genesis of Mineral Deposits in Ireland. IAEG, Dublin, p. 617–624.

Paytan, A., Mearon, S., Cobb, K. and Kastner, M. 2002. Origin of marine barite deposits: Sr and S isotope characterization. Geology, 30(8), p.747.

Peace, W. and Wallace, M., 2000. Timing of mineralization at the Navan Zn-Pb deposit: A post-Arundian age for Irish mineralization. *Geology*, 28(8), p.711.

Philcox, M.E. 1984. Lower Carboniferous Lithostratigraphy of the Irish Midlands; Irish Association for Economic Geology: Dublin, Ireland. p.89.

Philcox, M.E., 1989, The mid-Dinantian unconformity at Navan, Ireland. In: Arthurton R.S., Gutteridge, P. and Nolan, S. C. (Eds). The role of tectonics in Devonian and Carboniferous sedimentation in the British Isles. Yorkshire Geological Society, Occasional Publication, 6, p. 67-81.

Phillips, W. E. A. & Sevastopulo, G. D. 1986. The Stratigraphic and Structural Setting Of Irish Mineral Deposits. In: Andrew, C. J., Growl, R. W. A., Finlay, S., Pennell, W. M. & Pyne, J. F. (Eds) Geology and Genesis Of Mineral Deposits In Ireland. Irish Association for Economic Geology, Dublin, p.1-30.

Rizzi, Giancarlo. 1992. *The sedimentology and petrography of Lower Carboniferous limestones and dolomites: host-rocks to the Navan zinc-lead deposit.* PhD thesis, University of Glasgow.

Robinson, B. W., and Kusakabe, M., 1975. Quantitative preparation of sulfur dioxide, for $^{34}S/^{32}S$ analyses, from sulfides by combustion with cuprous oxide. Anal. Chem., 47:1179.

Romano, M., 1980. The stratigraphy of the Ordovician rocks between Slane (County Meath) and Collon (County Louth), Eastern Ireland. J Earth Sci. Dubl. Soc. 3. p. 53-79.

Russell, M. J. 1968. Structural controls of base metal mineralization in relation to continental drift. Transactions of the Institution for Mining and Metallurgy, 77B, p.11-28.

Russell, M.J., 1978, Downward-excavating hydrothermal cells and Irish type ore deposits: Importance of an underlying thick Caledonian prism. Trans. Instn Min. Metall. (Sect B: Appl. Earth Sci.), 87, p. 168-171.

Russell, M.J., 1986, Extension and convection: a genetic model for the Irish Carboniferous base metal and barite deposits. In: Andrew, C.J., Crowe, R.W.A., Finlay, S., Pennell, W.M., Pyne, J.F., (Eds). Geology and Genesis of Mineral Deposits in Ireland. IAEG, Dublin, p. 545-554.

Samson, I.M., and Russell, M.J., 1987, Genesis of the Silvermines zinc-lead- barite deposit, Ireland: Fluid inclusion and stable isotope evidence: Economic Geology, v. 82, p. 371–394.

Schneider J, Von Quadt A, and Wilkinson JJ (2007) Age of the Silvermines Irish-type Zn-Pb deposit from direct Rb-Sr dating of sphalerite. In: Andrew CJ, et al. (eds.) Digging Deeper: Proceedings of the 9th Biennial Meeting of the Society for Geology Applied to Mineral Deposits, Dublin, Ireland, 20–23 August 2007. Dublin: Irish Association for Economic Geology. p. 373–376.

Schroll, E., Rantitsch, G., 2005. Sulphur isotope patterns from the Bleiberg deposit (Eastern Alps) and their implications for genetically affiliated lead–zinc deposits. Mineralogy and Petrology. 84, 1–18.

Singer D, A. 1995. World-class base and precious metal deposits; a quantitative analysis. Economic Geology 90: p.88–104

Steed, G, M. 1980. Silver in the Tara Mines Mineral Deposit at Navan- With Particular Emphasis On The Ore To The West Of The Main Shaft Pillar. Boliden Tara Mines Internal Report.

Strogen, P., Jones, G. And Somerville, I., 1990. Stratigraphy And Sedimentology Of Lower Carboniferous (Dinantian) Boreholes From West Co. Meath, Ireland. Geological Journal, 25(2), p.103-137.

Strogen, P., Somerville, I., Pickard, N., Jones, G. and Fleming, M., 1996. Controls on ramp, platform and basinal sedimentation in the Dinantian of the Dublin Basin and Shannon Trough, Ireland. Geological Society, London, Special Publications, 107(1), p.263-279.

Symons DTA, Pannalal SJ, and Kawasaki K (2007) Paleomagnetic age of the Magcobar Ba deposit, Silvermines, Ireland. In: Andrew CJ, et al. (eds.) Digging Deeper: Proceedings of the 9th Biennial Meeting of the Society for Geology Applied to Mineral Deposits, Dublin, Ireland, 20–23 August 2007. Dublin: Irish Association for Economic Geology. p. 377–380

Taylor S (1984) Structural and paleotopographic controls of leadzinc mineralization in the Silvermines orebodies, Republic of Ireland. Econ Geol 79: p.529–548

Thamdrup, B., Finster, K., Hansen, J.W., and Bak, F., 1993, Bacterial disproportionation of elemental sulfur coupled to chemical reduction of iron or manganese: Applied Environmental Microbiology, v. 59, p. 101–108.

Thirlwall, M., 2002. Multicollector ICP-MS analysis of Pb isotopes using a 207pb-204pb double spike demonstrates up to 400 ppm/amu systematic errors in Tl-normalization. Chemical Geology, 184(3-4), pp.255-279.

Torremans, K.; Kyne, R.; Doyle, R.; Guven, J.F.; Walsh, J.J. 2018.Controls on Metal Distributions at the Lisheen and Silvermines Deposits: Insights into Fluid Flow Pathways in Irish-Type Zn–Pb Deposits. Econ. Geol., 113, p.1455–1477.

Vaughan, A. and Johnston, J. D., 1992, Structural constraints on closure geometr across the Iaepetus suture in eastern Ireland. Journal of the Geological Society of London, 149, p. 65-74

Walshaw R, Menuge J, Tyrrell S 2006, Metal sources of the Navan carbonate-hosted base metal deposit, Ireland: Nd and Sr isotope evidence for deep hydrothermal convection. Minerium Deposita 41(8): p.803–819

Wanless, H. R. 1979. Limestone Response To Stress: Pressure Solution And Dolomitization. SEPM Journal Of Sedimentary Research, Vol. 49.

Wartho J-A, Quinn D, and Meere PA (2006) The timing of Variscan deformation: UV laser 40Ar/39Ar dating of syn late-orogenic intrusions from SW Ireland. *Geochimica et Cosmochimica Acta*, 70(18), p. 690.

Weber, A. and Jorgensen, B.B. 2002. Bacterial sufate reduction in hydrothermal sediments of the Guaymas Basin, Gulf of California, Mexico. Deep Sea Research Part I, 49, p. 827-841.

Wilkinson, J.J., 2010, A Review of Fluid Inclusion Constraints on Mineralization in the Irish Orefield and Implications for the Genesis of Sediment-Hosted Zn-Pb deposits. Economic Geology, 105, p. 417-442.

Wilkinson, J.J., 2014, Sediment-Hosted Zinc–Lead Mineralization: Processes and Perspectives, In Treatise on Geochemistry (Second Edition), edited by Heinrich D. Holland and Karl K. Turekian, Elsevier, Oxford, p. 219-249.

Wilkinson, J.J., Boyce, A.J., Everett, C.E., Lee, M.J., 2003, Timing and depth of mineralization in the Irish Zn–Pb orefield. In: Kelly, J.G., Andrew, C.J., Ashton, J.H., Boland, M.B., Earls, G., Fusciardi, L., Stanley, G. (Eds). Europe's Major Base Metal Deposits. IAEG, Dublin, p. 483-497.

Wilkinson, J.J., Eyre, S.L. and Boyce, A.J., 2005, Ore-forming processes in Irish-type carbonate-hosted Zn-Pb deposits: Evidence from mineralogy, chemistry and isotopic composition of sulfides at the Lisheen Mine. Economic Geology, 100, p. 63- 86.

Wilkinson, J.J.; Hitzman, M.W. The Irish Zn–Pb Orefield: The View from 2014. In Current Perspectives on Zinc Deposits; Archibald, S.M., Piercey, S.J., Eds.; Irish Association for Economic Geology: Dublin, Ireland, 2015; p. 59–72.

Yesares, L., Drummond, D., Hollis, S., Doran, A., Menuge J, F., Boyce, A. J., Blakeman, R. J., Ashton, J. H., 2019. Coupling mineralogy, textures, stable and radiogenic isotopes in identifying ore-forming processes and geochemical vectoring possibilities in Irish-type carbonate hosted Zn-Pb deposits.

Yesares, L.., Menuge, J., Blakeman, R, J., Ashton. J, H., Boyce, A., Coller, D., Drummond, D, A., Farrelly, I. (in press)., Pyrite Mineralization Halo Above The Tara Deep Zn-Pb Deposit, Navan, Ireland: Evidence For Sub-Seafloor Exhalative Hydrothermal Processes? [Accepted By Ore Geology Reviews in July, 2021].

Table 2.1: Conventional S Isotope Dataset for Tara Deep

SAMPLE	MIN	$\delta^{34}S_{VCDT}$ (‰)	UNIT	TEXURE	DATA
N02510/01	Anh	24	MICRITE UNIT	LATE INFILL PHASE IN BRECCIATED MINERALIZATION	NEW DATA
N02531/01	Anh	28.1	MICRITE UNIT	VEINING. CLOSELY ASSOCIATED WITH CALCITE	NEW DATA
N02531/02	Anh	27.8	MICRITE UNIT	COARSE BLADED ANH	NEW DATA
N02334/01	Ba	26.1	MICRITE UNIT	INFILL	NEW DATA
N02334/06	Ba	25.4	MICRITE UNIT	PODS/VEINING	NEW DATA
N02334/08	Ba	26.9	MICRITE UNIT	INFILL ASSOCIATED WITH HYDROBRECCIATION	NEW DATA
N02334/12A	Ba	27.5	MICRITE UNIT	INFILL	NEW DATA
N02334/18	Ba	27.4	MICRITE UNIT	LATE INFILL	NEW DATA
N02416/03	Ba	22.7	MICRITE UNIT	CAVITY INFILL/HYDROBRECCIATION	NEW DATA
N02417/01	Ba	27.8	MICRITE UNIT	LATE INFILL ASSOCIATED WITH MAR	NEW DATA
N02418/01	Ba	24.5	MICRITE UNIT	VEINING/INFILL (LATE; CROSS CUTTING MINERALIZATION)	NEW DATA
N02418/03	Ba	26.5	MICRITE UNIT	LATE CAVITY INFILL	NEW DATA
N02428/06	Ba	24.3	MICRITE UNIT	INFILL/GLOBULAR	NEW DATA
N02437/02	Ba	25	MICRITE UNIT	INFILL/VEINING	NEW DATA
N02437/08	Ba	23.1	MICRITE UNIT	INFILL PODS	NEW DATA
N02445/03	Ba	26.8	MICRITE UNIT	REWORKED/DISRUPTED MINERALIZATION	NEW DATA
N02445/07	Ba	28.1	MICRITE UNIT	INFILL ISOLATED BA	NEW DATA
N02334/01B	Gn	-9.9	MICRITE UNIT	COARSE	NEW DATA
N02334/03	Gn	-8.4	MICRITE UNIT	COARSE	NEW DATA
N02334/07	Gn	5.6	MICRITE UNIT	COARSE	YESARES ET AL. (2019) DATA
N02334/13	Gn	13.1	MICRITE UNIT	HYDROBRECCIATION	NEW DATA
N02334/14B	Gn	14.3	MICRITE UNIT	COARSE	NEW DATA
N02370/05	Gn	9.4	MICRITE UNIT	COARSE	YESARES ET AL. (2019) DATA
N02370/06A	Gn	7.5	MICRITE UNIT	CAVITY INFILL/REWORKED	NEW DATA
N02370/06B	Gn	10	MICRITE UNIT	CAVITY INFILL/REWORKED	NEW DATA
N02370/08	Gn	9.6	MICRITE UNIT	COARSE GN	NEW DATA
N02370/09	Gn	6.2	MICRITE UNIT	GEOPETAL GALENA	NEW DATA
N02416/02	Gn	-9.9	MICRITE UNIT	CAVITY INFILL/GEOPETAL	NEW DATA
N02428/04	Gn	9.8	MICRITE UNIT	COARSE CONCENTRIC GN	NEW DATA
N02428/06	Gn	-10.7	MICRITE UNIT	DENDRITIC GN	NEW DATA
N02428/06	Gn	-13	MICRITE UNIT	DENDRITIC GN	NEW DATA
N02437/02	Gn	-8.7	MICRITE UNIT	GEOPETAL/COARSE GN	NEW DATA
N02437/03	Gn	-6.6	MICRITE UNIT	COARSE ISOLATED CRYSTALS CUBIC	YESARES ET AL. (2019) DATA
N02437/08	Gn	-5.8	MICRITE UNIT	COARSE GEOPETAL GN IN MASSIVE MIN	NEW DATA
N02445/04	Gn	12.6	MICRITE UNIT	CAVITY INFILL MINERALIZATION ASSOCIATED WITH Cu-Sb-SULFOSALTS	NEW DATA
N02445/05	Gn	7.7	MICRITE UNIT	CAVITY INFILL REWORKED	YESARES ET AL. (2019) DATA
N02445/07	Gn	9.5	MICRITE UNIT	CAVITY INFILL REWORKED. COARSE	NEW DATA
N02454/04	Gn	3.4	MICRITE UNIT	HYDROBRECCIATION COARSE GN	NEW DATA
N02454/15	Gn	11.3	MICRITE UNIT	COARSE INFILL	NEW DATA
N02469/01	Gn	-11.6	MICRITE UNIT	COARSE GN ASSOCIATED WITH HYDROBRECCIATION	NEW DATA
N02499/13	Gn	-12.5	MICRITE UNIT	CAVITY INFILL DENDRITIC GALENA	NEW DATA
N02499/16	Gn	-13	MICRITE UNIT	CAVITY INFILL DENDRITIC GALENA	NEW DATA

N02505/19	Gn	10	MICRITE UNIT	CAVITY INFILL COARSE	NEW DATA
N02510/06	Gn	-8.7	MICRITE UNIT	MASSIVE MINERALIZATION	NEW DATA
N02370/03	Gn	7.1	MICRITE UNIT	GEOPETAL/CAVITY INFILL	NEW DATA
N02499/17	Gn	3.5	MICRITE UNIT	CAVITY INFILL COARSE GALENA	NEW DATA
N02499/18	Gn	7.5	MICRITE UNIT	CAVITY INFILL COARSE GALENA	NEW DATA
N02505/21	Gn	-11.1	MICRITE UNIT	MASSIVE MINERALIZATION/DENDRITIC	NEW DATA
N02505/23	Gn	10.3	MICRITE UNIT	CAVITY INFILL COARSE	NEW DATA
N02505/26	Gn	-9.9	MICRITE UNIT	CAVITY INFILL/COARSE	NEW DATA
N02417/01	Mrc	21.8	MICRITE UNIT	MARCASITE ASSOCIATED WITH BA/CALCITE. LATE INFILL PHASE	NEW DATA
N02464/01	Mrc	22.7	MICRITE UNIT	INFILL MARCASITE LATE. ASSOCIATED WITH Ba/Ca	NEW DATA
N02505/17	Mrc	28.3	MICRITE UNIT	LATE INFILL IN MASSIVE MINERALIZATION	NEW DATA
N02508/02	Mrc	21.7	MICRITE UNIT	LATE INFILL IN COLLOMORPHIC MINERALIZATION	NEW DATA
N02428/04	PY	-12.5	MICRITE UNIT	MICROCRYSTALLINE PY	YESARES ET AL. (2019) DATA
N02428/06	PY	-17.7	MICRITE UNIT	ELONGATED PY CYRTAL	YESARES ET AL. (2019) DATA
N02437/02	PY	8.8	MICRITE UNIT	VEINING	YESARES ET AL. (2019) DATA
N02454/04	PY	5.5	MICRITE UNIT	HYDROBRECCIATION	NEW DATA
N02418/02	SP	-6.9	MICRITE UNIT	MASSIVE MINERALIZATION	NEW DATA
N02469/01	SP	-9.1	MICRITE UNIT	HYDROBRECCIATION	NEW DATA
N02505/13	SP	-9.5	MICRITE UNIT	CAVITY INFILL/HYDROBRECCIATION	NEW DATA
N02505/20	SP	-8.1	MICRITE UNIT	CAVITY INFILL L DARK BROWN	NEW DATA
N02505/20	SP	5.3	MICRITE UNIT	CAVITY INFILL LIGHT COLOURED (LATE)	NEW DATA
N02505/21	SP	-8.1	MICRITE UNIT	MASSIVE MINERALIZATION	NEW DATA
N02505/23	SP	-3.6	MICRITE UNIT	CAVITY INFILL	NEW DATA
N02505/26	SP	-7.9	MICRITE UNIT	CAVITY INFILL/COLLOMORPHIC	NEW DATA
N02508/03	SP	-13.5	MICRITE UNIT	MASSIVE MINERALIZATION MED BROWN SP	NEW DATA
N02334/01B	SP	-2.6	MICRITE UNIT	CAVITY INFILL/COLLOFORM	NEW DATA
N02334/03	SP	-1.4	MICRITE UNIT	CAVITY INFILL/COLLOFORM	NEW DATA
N02334/04	SP	2.8	MICRITE UNIT	DISSEMINATED	NEW DATA
N02334/06	SP	11.1	MICRITE UNIT	CAVITY INFILL/LAMINATIONS	NEW DATA
N02334/07	SP	8.7	MICRITE UNIT	MASSIVE MIN (SOFT)	YESARES ET AL. (2019) DATA
N02334/08	SP	9.5	MICRITE UNIT	HYDROBRECCIATION (LIGHT COLOURED)	NEW DATA
N02334/09	SP	10.3	MICRITE UNIT	CAVITY INFILL/COLLOFORM (LIGHT COLOURED)	NEW DATA
N02334/10B	SP	-3.8	MICRITE UNIT	CAVITY INFILL (DARK)	NEW DATA
N02334/11	SP	-0.9	MICRITE UNIT	LAMINATED (LIGHT COLOURED)	NEW DATA
N02334/12A	SP	1.8	MICRITE UNIT	CAVITY INFILL	NEW DATA
N02334/12B	SP	5.7	MICRITE UNIT	CAVITY INFILL	NEW DATA
N02334/13	SP	2.9	MICRITE UNIT	HYDROBRECCIATION	NEW DATA
N02334/14B	SP	7.8	MICRITE UNIT	HYDROBRECCIATION	NEW DATA
N02334/14C	SP	0.7	MICRITE UNIT	HYDROBRECCIATION	NEW DATA
N02334/15B	SP	0.9	MICRITE UNIT	CAVITY INFILL/LAMINATIONS	NEW DATA
N02334/16	SP	1.1	MICRITE UNIT	CAVITY INFILL/LAMINATIONS (LIGHT COLOURED)	NEW DATA
N02334/19	SP	15.5	MICRITE UNIT	DISSEMINATED LIGHT COLOURED	NEW DATA
N02370/01	SP	9.6	MICRITE UNIT	DISSEMINATED LIGHT COLOURED	NEW DATA
N02370/02	SP	12	MICRITE UNIT	HYDROBRECCIATION (LIGHT-MID BROWN)	NEW DATA
N02370/03	SP	8.6	MICRITE UNIT	CAVITY INFILL	NEW DATA
N02370/04	SP	12.4	MICRITE UNIT	CAVITY INFILL	NEW DATA

N02370/05	SP	10.5	MICRITE UNIT	CAVITY INFILL/COLLOFORM	YESARES ET AL. (2019) DATA
N02370/06A	SP	12	MICRITE UNIT	CAVITY INFILL/REWORKED MINERALIZATION	NEW DATA
N02370/06B	SP	12.3	MICRITE UNIT	CAVITY INFILL/REWORKED	NEW DATA
N02370/07	SP	6.4	MICRITE UNIT	LIGHT COLOURED DISSEMINATED SP	NEW DATA
N02370/08	SP	9	MICRITE UNIT	LIGHT COLOURED DISSEMINATED SP	NEW DATA
N02370/09	SP	9.4	MICRITE UNIT	CAVITY INFILL	NEW DATA
N02404/04	SP	13.8	MICRITE UNIT	DISSEMINATED (LIGHT COLOURED)	NEW DATA
N02404/07	SP	16.2	MICRITE UNIT	DISSEMINATED (LIGHT COLOURED)	NEW DATA
N02404/09	SP	13.3	MICRITE UNIT	DISSEMINATED (LIGHT COLOURED)	NEW DATA
N02416/03	SP	-5.2	MICRITE UNIT	CAVITY INFILL LIGHT COLOURED	NEW DATA
N02417/02	SP	-0.1	MICRITE UNIT	LAYERED SP (NOT THIN SECTION REGION)	NEW DATA
N02418/01	SP	-5.9	MICRITE UNIT	CAVITY INFILL	NEW DATA
N02418/03	SP	-5.7	MICRITE UNIT	CAVITY INFILL	NEW DATA
N02428/03	SP	-6.4	MICRITE UNIT	CAVITY INFILL	NEW DATA
N02428/05	SP	-7.4	MICRITE UNIT	HYDROBRECCIATION	NEW DATA
N02428/06	SP	-6.3	MICRITE UNIT	HYDROBRECCIATION	NEW DATA
N02437/01	SP	-8.8	MICRITE UNIT	MASSIVE SOFT LIGHT COLOURED SP IN MATRIX	YESARES ET AL. (2019) DATA
N02437/02	SP	-2.2	MICRITE UNIT	LAMINATED SP	NEW DATA
N02437/03	SP	-8.3	MICRITE UNIT	MASSIVE MINE. SOFT REWORKED TEXTURES	NEW DATA
N02437/04	SP	-1.3	MICRITE UNIT	MASSIVE MINERALIZATION	NEW DATA
N02437/05	SP	-8.9	MICRITE UNIT	MASSIVE MINERALIZATION REWORKED	NEW DATA
N02437/06	SP	-6.6	MICRITE UNIT	CAVITY INFILL DARK BROWN	NEW DATA
N02437/06B	SP	-7	MICRITE UNIT	CAVITY INFILL LIGHT BROWN	NEW DATA
N02437/07	SP	-6	MICRITE UNIT	MASSIVE MINERALIZATION	NEW DATA
N02437/08	SP	-9.2	MICRITE UNIT	MASSIVE MINERALIZATION	YESARES ET AL. (2019) DATA
N02445/03	SP	10.7	MICRITE UNIT	REWORKED SP CLASTS	NEW DATA
N02445/04	SP	12.7	MICRITE UNIT	CAVITY INFILL.	NEW DATA
N02445/05	SP	-10.8	MICRITE UNIT	CAVITY INFILL REWORKED. COARSE	NEW DATA
N02445/07	SP	9.4	MICRITE UNIT	CAVITY INFILL REWORKED	NEW DATA
N02454/03	SP	14	MICRITE UNIT	HYDROBRECCIATION LIGHT COLOURED DISSEMINATED SP	NEW DATA
N02454/04	SP	12.4	MICRITE UNIT	HYDROBRECCIATION LIGHT COLOURED DISSEMINATED SP	NEW DATA
N02469/03	SP	-6.3	MICRITE UNIT	DISSEMINATED LIGHT COLOURED SP	NEW DATA
N02503/02	SP	-12.3	MICRITE UNIT	CAVITY INFILL/COLLOMORPHIC (DARK BROWN)	NEW DATA
N02505/16	SP	-8.8	MICRITE UNIT	CAVITY INFILL DARK BROWN REWORKED	NEW DATA
N02505/19	SP	-7.5	MICRITE UNIT	MASSIVE MINERALIZATION	NEW DATA
N02505/21	SP	-8.6	MICRITE UNIT	MASSIVE MINERALIZATION WITH HONEYBLEND SP IS INFILLING DENDRITIC GN SAMPLE	NEW DATA
N02508/03	SP	-10.1	MICRITE UNIT	HONEYBLENDE LATE PHASE MASSIVE MINERALIZATION	NEW DATA
N02505/17	SP	-1.6	MICRITE UNIT	MASSIVE MINERALIZATION	NEW DATA
N02427/05	Ba	29	S Fault Conglomerate (SFC)	MASSIVE MINERALIZATION INFILL	NEW DATA
N02427/02	Gn	8	SFC	CLAST OF INFILL	NEW DATA
N02427/04	Gn	-9.2	SFC	CLAST OF MINERALIZATION	YESARES ET AL. (2019) DATA
N02427/05	Gn	-6.9	SFC	MASSIVE MINERALIZATION	NEW DATA
N02427/06	Gn	-10.1	SFC	COARSE GN IN MASSIVE MIN	NEW DATA
N02427/11	Gn	-7.2	SFC	COARSE IN MASSIVE MINERALIZATION	NEW DATA
N02466/03	Gn	-12.5	SFC	MASSIVE MINERALIZATION MATRIX REPLACEMENT	NEW DATA

N02466/05	Gn	-11.5	SFC	MASSIVE MINERALIZATION MATRIX REPLACEMENT	NEW DATA
N02477/01	Gn	-10	SFC	REWORKED COARSE GN	NEW DATA
N02427/02	Mrc	21.5	SFC	MATRIX REPLACEMENT MASSIVE	NEW DATA
N02427/02	Mrc	28.4	SFC	MATRIX REPLACEMENT MASSIVE	NEW DATA
N02427/07	Mrc	22.2	SFC	BLADED EXPLOITS MATRIX	NEW DATA
n2409-17c	Mrc	24.6	SFC	NA	YESARES ET AL. (2019) DATA
N02465/03	PY	13.8	SFC	MASSIVE MINERALIZATION SOFT	NEW DATA
N02477/01	PY	-6	SFC	CUPIC PY IN MATRIX	NEW DATA
N02465/04	SP	-11	SFC	REWORKED SP IN MATRIX	NEW DATA
N02465/06	SP	-16	SFC	MASSIVE MINERALIZATION	NEW DATA
N02466/03	SP	-8.9	SFC	MASSIVE MINERALIZATION	NEW DATA
N02466/04	SP	-8.3	SFC	MASSIVE MINERALIZATION	NEW DATA
N02466/05	SP	-10	SFC	MASSIVE MINERALIZATION	NEW DATA
N02427/02	SP	-8.5	SFC	DISSEMINATED MATRIX LIGHT COLOURED	NEW DATA
N02427/02	SP	7.7	SFC	CLAST OF INFILL	NEW DATA
N02427/03	SP	-7.8	SFC	SP CLAST IN DEBRIS FLOW	NEW DATA
N02427/04	SP	-8.2	SFC	COARSE GLN IN CLAST	YESARES ET AL. (2019) DATA
N02427/05	SP	-5.9	SFC	MASSIVE MINERALIZATION	NEW DATA
N02427/06	SP	-8.6	SFC	MASSIVE MINERALIZATION	NEW DATA
N02439/03	SP	-8.3	SFC	INFILLING	NEW DATA
N02465/03	SP	-11.7	SFC	MASSIVE MINERALIZATION SOFT	NEW DATA
N02465/05	SP	-10.9	SFC	MASSIVE MINERALIZATION MATRIX REPLACEMENT	NEW DATA
N02465/06	SP	-13.3	SFC	MASSIVE MINERALIZATION SOFT MATRIX REPLACEMENT	NEW DATA
N02466/01	SP	-9.7	SFC	CLAST OF ALLOCHTHONOUS MINERALIZATION (DARK BROWN)	NEW DATA
N02466/02	SP	-11.1	SFC	MASSIVE MINERALIZATION MATRIX REPLACEMENT	NEW DATA
N02466/04	SP	-7.9	SFC	MASSIVE MINERALIZATION MATRIX REPLACEMENT	NEW DATA
N02466/04	SP	-9.4	SFC	MASSIVE MINERALIZATION MATRIX REPLACEMENT	NEW DATA
N02466/05	SP	-10.7	SFC	MASSIVE MINERALIZATION MATRIX REPLACEMENT	NEW DATA
N02477/01	SP	-8.8	SFC	REWORKED SP	NEW DATA
N02499/12	SP	-9.2	SFC	MASSIVE MINERALIZATION	NEW DATA

Table 2.2 Lead Isotope Dataset

Table.2 Measured $^{206}Pb/^{204}Pb$ from the Tara Deep Deposit.		
Sample Name	$^{206}Pb/^{204}Pb$	2s %
N02427/02	18.22	0.013
N02334/03	18.23	0.013
N02370/06B	18.24	0.013
N02370/09	18.21	0.013
N02427/04	18.22	0.013
N02427/05	18.22	0.013
N02427/06	18.22	0.013
N02427/11	18.22	0.012
N02428/04	18.24	0.012
N02428/06	18.23	0.012
N02437/08	18.22	0.013
N02445/07	18.23	0.012
N02445/04	18.23	0.012
N02454/15	18.22	0.012
N02466/03	18.22	0.012
N02466/05	18.22	0.012
N02469/01	18.23	0.013
N02499/13	18.23	0.015
N02499/16	18.23	0.015
N02499/17	18.23	0.015
N02499/18	18.23	0.014
N02505/19	18.23	0.015
N02505/20	18.22	0.015
N02505/21	18.23	0.015
N02505/23	18.23	0.015
N02510/06	18.23	0.015
Average	18.23	
Standard Deviation	0.006	

CHAPTER THREE: BACTERIOGENIC SULFIDE DOMINANCE & LEAD ISOTOPIC CONSTRAINTS AT TARA DEEP, CO. MEATH, IRELAND: IMPLICATIONS FOR GENESIS, CONTEXT AND POTENTIAL

Drummond[1], D. A., Ashton[2], J. H., Blakeman[3], R. J., Cloutier[4], J., Farrelly, I[3]., Pashley[5], V. H, Boyce[1], A. J.

[1]Scottish Universities Environmental Research Centre, Rankine Avenue, East Kilbride, Glasgow G75 0QF, United Kingdom.

[2]Consultant Boliden Tara Mines.

[3]Boliden Tara Mines, Exploration Department, Navan, County Meath, Ireland.

[4]Centre for Ore Deposits and Earth Science, University of Tasmania, Private Bag 79, Hobart, Tasmania, Australia.

[5]Geochronology & Tracers Facility, British Geological Survey, Nicker Hill, Keyworth, Nottingham, NG12 5GG, United Kingdom.

**Corresponding Author: drewdrummond59@gmail.com*

3.1 Abstract

Floatation concentrate samples were completed on representative drillholes from across the Tara Deep deposit by Boliden Tara Mines' Processing Plant to optimise ore recovery. The concentrates produced were analysed for S and Pb isotopes. The samples reveal limited variation with mean $\delta^{34}S$ = -6 ± 5.9 per mil (*n* = 38), and galena concentrate mean $^{206}Pb/^{204}Pb$=18.22 ± 0.004 (*n* = 19). Mass balance calculations suggest that ~90% of the Tara Deep sulfides were derived from bacteriogenic reduction of contemporaneous Lower Carboniferous seawater sulfate. Whereas metals were acquired from a local, orogenic crustal source beneath the orebody. These isotopic signatures at Tara Deep marginally differ from those associated with the Main Navan Orebody, suggesting that Tara Deep should be considered as an isolated deposit in space, and potentially time, and not an allochthonous block of the Navan deposit. As was reported for the world-class Navan deposit, enhanced bacterial activity was fundamental to ore deposition at Tara Deep.

3.2 Introduction

Boliden Tara Mines' Navan deposit is Europe's largest Zn-Pb deposit and is currently Ireland's only active base-metal mine. It is the largest of a class of Zn+Pb±Ag±Ba ore deposits known as "Irish-type", that were deposited syn-diagenetically with Mississippian limestone host rocks (Derry et al., 1965; Russell,

1975; Taylor and Andrew, 1978; Boast et al., 1981a; Boyce et al., 1983; Taylor, 1984; Ashton et al., 1986; Anderson et al., 1998; Chapter 2). When measured in terms of mass of metal per unit area of crust, the Irish Orefield is believed to constitute the world's largest known concentration of zinc and second largest concentration of lead on Earth (Singer, 1995). The Tara Deep prospect is a recently discovered companion of the Main Orebody and Southwest Extension (SWEX) deposits at Navan (see Ashton et al., 2018). The deposit is situated ~2 km SE of the SWEX (Fig. 3.1), where an ongoing drilling programme has steadily increased the inferred resource at Tara Deep to 26.2Mt @ 8.4% Zn and 1.6% Pb (Boliden Summary Report, 2020). Underground development is in progress to complement drilling, to upgrade the resources to indicated level, and to assist feasibility work.

Genetic models for Navan and Tara Deep, alongside the other Irish deposits have derived much detail from isotopic studies (Coomer and Robinson, 1976; Boast et al., 1981a; Boyce et al., 1983, 2003; Caulfield et al., 1986; O'Keeffe, 1986; Mills et al., 1987; Anderson et al., 1998; Wilkinson et al., 2005; Ashton et al., 2015; Chapter 2). In the Irish-type deposits, including Navan, there is a consensus that metals are derived from underlying Lower Paleozoic basement (Boast et al., 1981b; Caulfield et al., 1986; O'Keeffe, 1986; LeHuray et al., 1987; Mills et al., 1987; Dixon et al., 1990; Fallick et al., 2001; Everett et al., 2003), and that there is a dual source of sulfur, with a deep-derived, hydrothermal component arriving in the deposits with the ore fluid, which interacts with a subsurface fluid containing sulfur derived from bacterial reduction of seawater sulfate (Coomer and Robinson, 1976; Boyce et al. 1983; Caulfield et al., 1986; Anderson *et al*., 1998; Anderson, 1990; Ford, 1996; Fallick *et al*., 2001; Blakeman *et al*., 2002; Altinok, 2005, Wilkinson et al., 2005; Barrie et al., 2009; Gagnevin et al., 2014).

This research presents new sulfur and lead isotope data on drillhole concentrates from across the Tara Deep prospect (Fig. 3.1). Here, drillhole concentrates represent flotation test samples of assayed core splits, which were ground-down and homogenized by Boliden Tara Mines' laboratory to provide recovery data for future financial modelling. These Zn and Pb concentrates thus provide bulk snapshots of the ore in high grade regions of Tara Deep (Fig. 3.2). Isotopic data on these concentrates allows us not only to identify the dominant S and Pb isotopic signatures in Tara Deep, but also to

scrutinize the relationship of Tara Deep to other Irish-Type deposits. In particular - does the ratio of hydrothermal versus bacteriogenic sulfide carry over from Tara Deep to Navan? This is critical, as Fallick et al (2001) have shown that a dominant bacteriogenic signature was of central importance to the development of the Main Orebody.

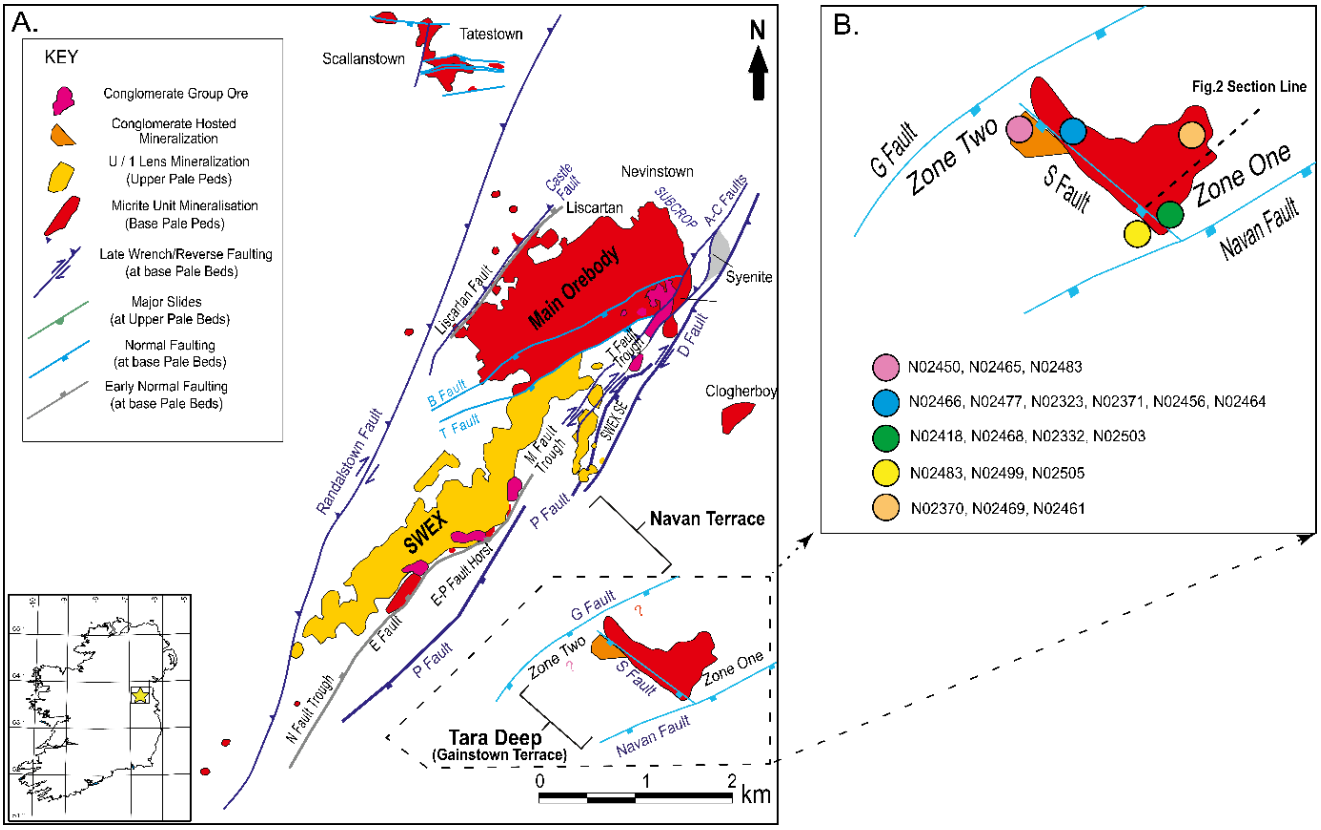

Figure 3.1 (A) Structural plan showing the positioning of Tara Deep relative to Navan, and the distribution of principal ore lenses and faults, modified from Ashton et al., (2015). (B) The location of DH concentrates from across the Tara Deep Deposit. Note the faults and drillhole (DH) concentrates are shown as plan projections from their intersections with the ore lenses, not as outcrop positions. SWEX is an abbreviation of Southwest Extension.

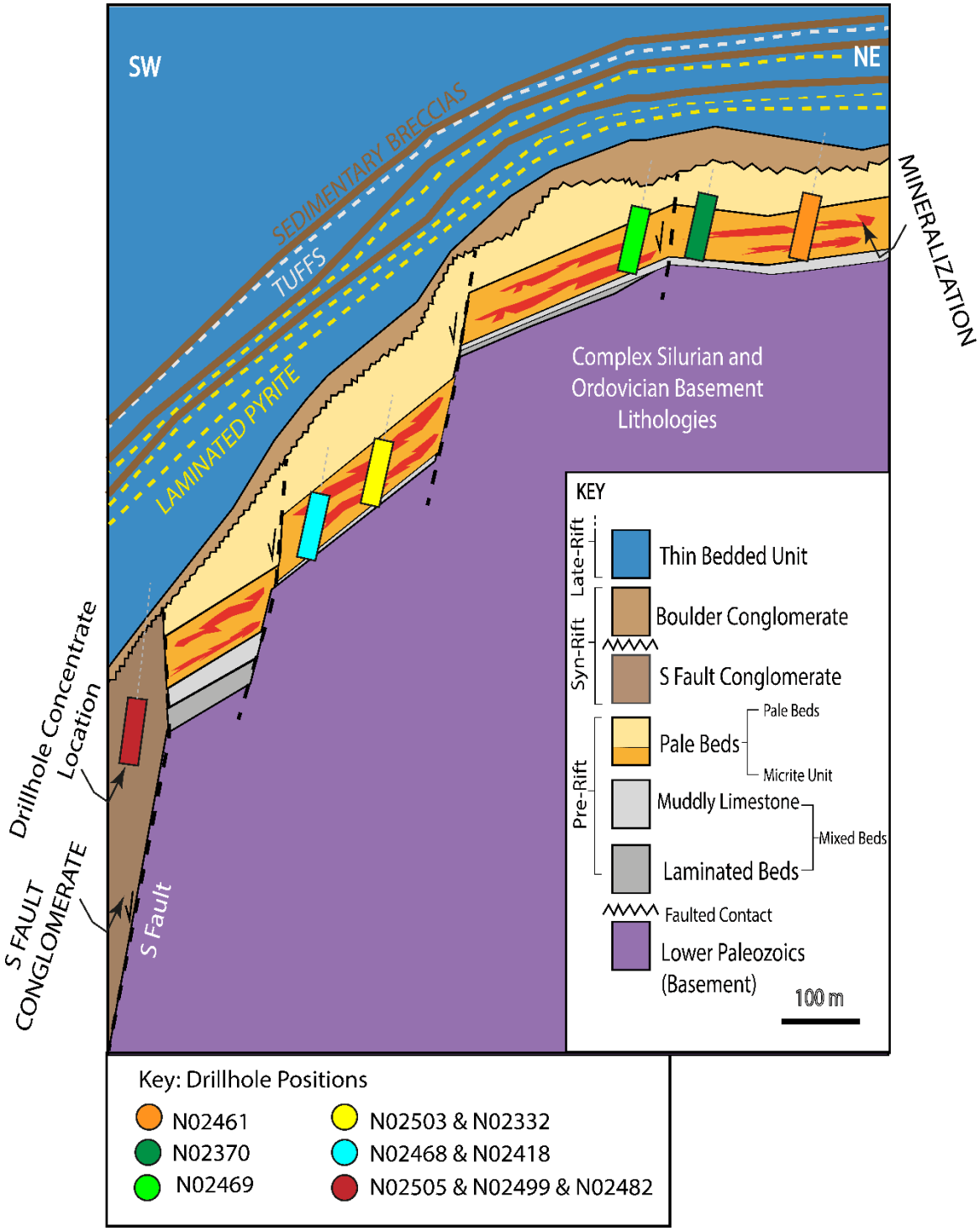

Figure 3.2 Schematic NE-SW cross section through the Tara Deep deposit. The location of DH Concentrates relative to this cross section have been plotted

3.3 Previous S Isotope Studies

An extensive stable isotope database exists for Navan (Anderson, 1990; Anderson *et al*., 1998; Ford, 1996; Fallick *et al*., 2001; Blakeman *et al*., 2002; Altinok, 2005) and other Irish-type deposits (Boyce et al., 1983; Caulfield et al., 1986; Wilkinson et al., 2005; Barrie et al., 2009; Wilkinson and Hitzman, 2014), but comparatively little work has been undertaken on Tara Deep (Yesares et al., 2019). Studies in the Navan Main Orebody have outlined two principal populations of δ^{34}S in ore sulfides, -26 to -4 ‰ and -4 to 16 ‰. The lightest δ^{34}S subgroup is interpreted as the product of contemporaneous bacterial reduction of seawater sulfate (BSR) during the Mississippian (Coomer and Robinson, 1976), with an average bacteriogenic isotopic fractionation factor $\delta^{34}S_{SO4\text{-}H2S}$ around 35‰ being typical for ore sulfides. The higher δ^{34}S sub-group likely represents hydrothermal sulfur which enters the orebody as metalliferous hydrothermal fluids, sourced dominantly from the Lower Paleozoic basement (Anderson et al., 1998; Boyce et al., 1993, 1994; O'Keeffe, 1986). This correlates with local sulfates (largely barite, and minor anhydrite) throughout the Main Orebody, that have an average δ^{34}S of +21±2‰ (n = 23; Andrew and Ashton, 1985; Anderson et al., 1998; Caulfield et al., 1986; Blakeman et al., 2002), which is indicative of the Mississippian seawater sulfate (Claypool et al., 1980; Kampschulte et al., 2001).

Mixing of the deep, basement-derived hydrothermal fluid, with limited reduced sulfide, with a surface fluid containing abundant bacteriogenic sulfide, was critical to the ore deposition at Navan, and in all other economic ore deposits in Ireland (Coomer and Robinson, 1976; Boyce et al., 1983 ; Caulfield et al., 1986; Anderson et al., 1998; Anderson, 1990; Ford, 1996; Fallick et al., 2001; Blakeman et al., 2002; Altinok, 2005; Wilkinson et al., 2005; Barrie et al., 2009; Wilkinson and Hitzman, 2014). This interpretation is also supported by fluid inclusion studies and radiogenic isotopes (Banks and Russell, 1992; Eyre, 1998; Everett et al., 1999; Samson and Russell, 1987 and see below).

Fallick et al., (2001) quantified the importance of BSR at the Navan Main Orebody using the δ^{34}S of Zn and Pb mine concentrates, taken from its principal ore lens, the 5-lens (constituting ~70% of all ore at that time, and representing up to 1Mt of ore per sample). The concentrates gave an isotopically homogeneous mean value of -13.6 ±2‰ (varying from -17.5 to -10‰), in contrast to the

wide range (-25 to +15‰) obtained from laser and conventional S isotope techniques on individual samples (Anderson et al., 1998), indicating through mass balance calculations that more than 90% of Navan sulfide was bacteriogenic. This dominance is reflected in other economic deposits in Ireland, creating a clear message: bacteriogenic sulfide dominance is a critical signature of economically viable carbonate-hosted Zn+Pb mines in Ireland (Coomer and Robinson, 1976; Boast *et al*., 1981a; Thamdrup *et al*., 1993; Boyce *et al*., 1983; Caulfield *et al*., 1986; Anderson, 1990; Ford, 1996; Anderson et al., 1998; Fallick et al., 2001; Banks *et al*., 2002; Blakeman, 2002; Blakeman et al., 2002; Weber and Jorgensen, 2002; Altinok, 2005; Wilkinson *et al*., 2005; Barrie *et al*., 2009; Anderson et al., 1998 and Yesares et al., 2019). At the same time, Fallick et al., (2001) also showed that the deposit had a rather homogenous Pb isotope signature across the Main Navan Orebody, and from top to bottom ore lens (in contrast with an earlier reconnaissance study, Mills et al., 1987). The former is typical of most Irish-type deposits (LeHuray et al., 1987).

Recently published work on Tara Deep has shown that sulfur isotope data from sphalerite (ZnS) and galena (PbS) analysed through *in situ* laser combustion and conventional analyses (Yesares et al., 2019; Chapter 2), displays a similar, but not identical, bimodal distribution. At Tara Deep, galena and sphalerite from Pale Beds-hosted mineralization reveal a dominant bimodal distribution of -13.5 ‰ to -3.6 ‰ and +3.4‰ to +16.2 ‰, reflective of the Main Orebody distribution. A similar pattern occurs in mineralization hosted in the S Fault Conglomerate (SFC) with BSR values of -16‰ to -5.9‰, and a minor hydrothermal component of +7.7‰ to +8‰ (Chapter 2). However, whilst this bimodal distribution is consistent with the same sulfide sources as interpreted for the Navan and other Irish-type deposits - BSR and hydrothermal - there is a clear distinction with the Main Orebody with regards to bacteriogenic sub-group: the distribution is shifted to less negative values, and their mean $\delta^{34}S$ is ~5‰ heavier in Tara Deep (a mean of -13.6 ± 2‰ for 5-lens, Fallick et al., 2001; versus -8.5 ± 2.4‰ and -9.7 ± 2.1‰ for Tara Deep Micrite Unit and SFC respectively). This resonates with the distinction in sulfate $\delta^{34}S$ at Tara Deep which has an overall mean of 26.2± 1.8‰ compared to the Main Orebody (21±2‰). These values are noticeably higher than the Irish Waulsortian-hosted deposits, which have a mean value of $\delta^{34}S$ of 18.2

± 2 ‰ (n=48; data from Boast et al., 1981a; Boyce, 1990; Wilkinson et al., 2005). Notwithstanding the distinction in modes of marine and bacteriogenic sulfide between Tara Deep and the Main Orebody, the bacteriogenic isotopic fractionation remains on average around 35‰, an extent consistent with BSR in both deposits. In contrast, the hydrothermal endmember mean and distribution closely match that of the Navan Main Orebody, averaging around 9‰ at Tara Deep.

Together, these data suggest that Tara Deep received a similar hydrothermal fluid input as the Main Orebody, but that the precise location (in space and time) of the two ore bodies were distinct. Tara Deep is not simply an allochthonous slice of the existing Navan deposits. It is speculated that there may have been a time gap and/or physical distinction in the sub-basins in which bacteriogenic sulfide reduction was taking place. Whatever the cause of the variation in seawater sulfate $\delta^{34}S$, the bacterial communities were likely similar in both cases when hydrothermal metals were being precipitated in a dynamic environment, using bacteriogenic sulfide exhibiting similar isotopic fractionation in both deposits.

3.4 Tara Deep Drillhole Concentrates S Isotopes

The concentrates were run by conventional methods with an error reproducibility better than ±0.3‰ based on repeat analyses of internal and international standards (Wagner et al., 2002). Lead concentrates reveal a bimodal S isotope distribution (Fig. 3.3) with a dominant BSR range of -16.8 to -5.8‰ (mean = -9.6±2.6; n=16) and minor hydrothermal component range of 1.9 to 6.6‰ (mean = 4.5±2; n=3). Zn concentrates reveal a bimodal distribution with a dominant BSR range of -11 to -1.9 (mean = -6.9±2.6 5.8; n=16) and a minor hydrothermal component range of 2.4 to 10.1‰ (mean = 7.1±3.5; n=3). Overall, the mean of the concentrate population is -6.0 ± 5.9‰ (1σ; n=38).

Conventional data from Tara Deep (Fig 3A & B) reveals a mean BSR signature of (–8.1‰) and hydrothermal signature of (9.0‰), based on the data presented, with an arbitrary division between the two populations at 0‰. Using these data, simple mass balance indicates that to achieve an overall mean bulk concentrate value of –6.0 ‰ (combining both Pb and Zn concentrates), ~88 % of the sulfide must

have been derived from the bacteriogenic source (~87%, if the two population modes (-8.3 and 9.4‰) are used).

The distribution of conventional data (Fig. 3.3A & B) is related more to technical aspects of sample preparation, than it is to the quantitative distribution of the S reservoir endmembers across the deposit. The majority of textures at Tara Deep are micro-scale, and thus less amenable to excision and single mineral conventional analyses. This relationship echoes with Anderson et al. (1998) and Fallick et al. (2001). However, microdrilling or in situ analyses remains very useful for defining end members and for correlating isotopic signatures with various textures (e.g. Barrie et al., 2009), which is something that is lost through analysing bulk drillhole (DH) concentrates.

Thus, insofar as the DH concentrates provide a reliable bulk representation of Tara Deep's sphalerite and galena, the sulfide sulfur is predominantly (>87%) bacteriogenic in origin. Furthermore, the Tara Deep concentrate S isotope signature correlates with conventional analyses, confirming that the BSR population is on average heavier by ~5‰, compared to the Navan Main Orebody and it's concentrates (-8.2 ± 3.0‰ for Tara Deeps DH concentrates versus -13.6 ± 2‰ for Main Orebody major 5-lens; Fallick et al., 2001).

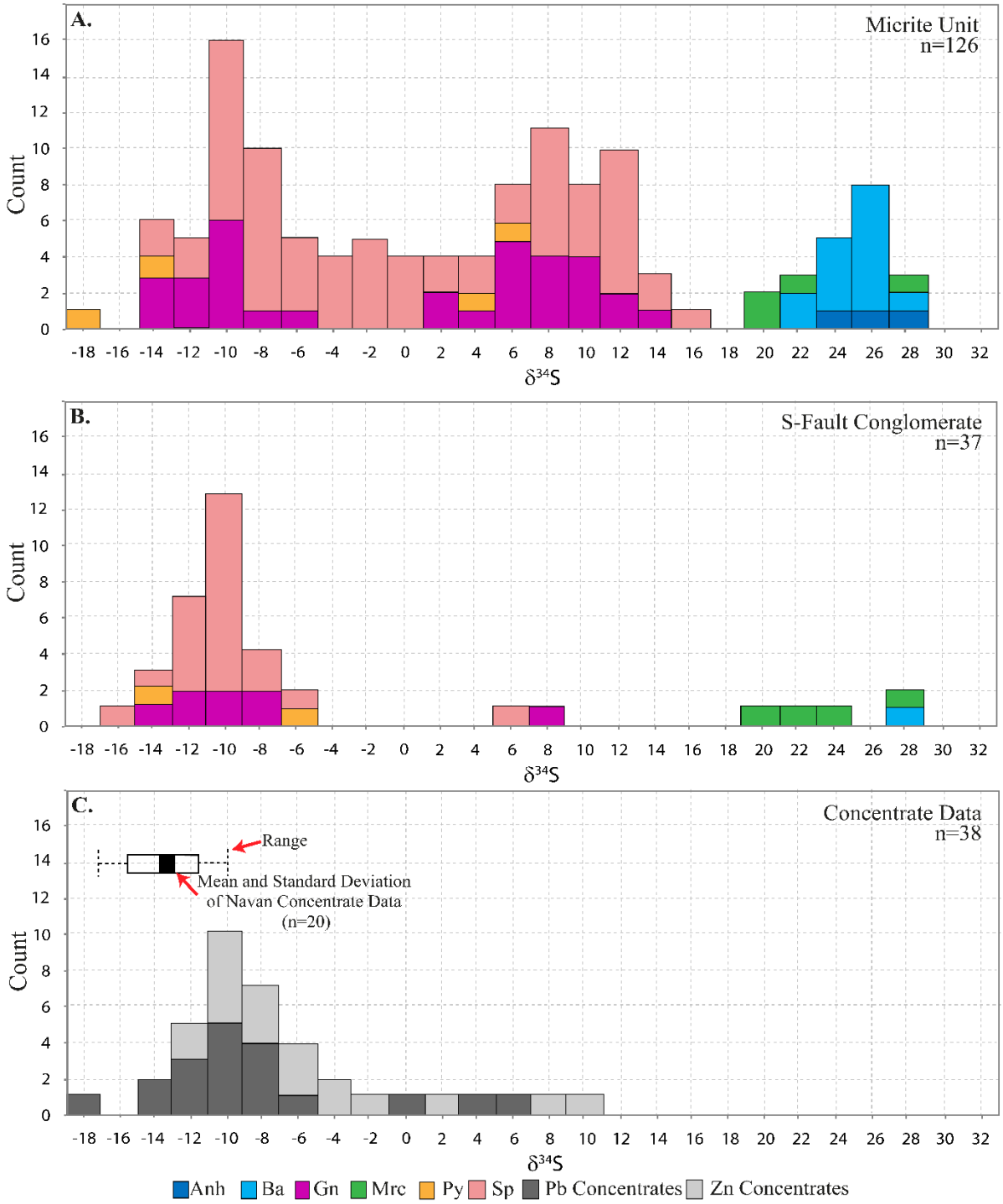

Figure 3.3 S isotope analyses of base metal sulfides from Tara Deep outlining a bimodal bacteriogenic (-16 to -4 ‰) and hydrothermal sulfur source (2 to 14 ‰) for both the (A) Micrite Unit and (B) the S Fault Conglomerate (Modified from Chapter 2) compared against (C) Drillhole concentrates, collected from across the entire Tara Deep Deposit. There are 19 drillholes with a Zn and Pb concentrate analysed for each (n=38). Also displaying the mean and standard deviation of Navan $\delta^{34}S$ data from Fallick et al., (2001).

3.5 Previous Pb Isotope Studies

Lead isotopic analyses are a key measure in the Irish-type genetic model, with galenas from the different orebodies having distinctive lead isotopic signatures reflecting those in the underlying local Lower Paleozoic basement, and in veins contained therein (Caulfield et al., 1986; O'Keeffe, 1986; Mills et al., 1987; Dixon et al., 1990; Everett et al., 2003). This, together with other evidence (e.g. Everett et al., 1999; Walshaw et al., 2006), requires hydrothermal convection cells circulating metalliferous fluid through the underlying Lower Paleozoic sequences (Russell, 1978; Mills et al., 1987; Dixon et al., 1990; Banks *et al*., 2002). A potential alternative source of lead from the Old Red Sandstone has been ruled out based on isotopic composition (Everett et al., 2003). At Navan, Pb isotopes have a homogeneous relationship across the deposits. Fallick et al., (2001) analysed bulk mine concentrates across all lenses at Navan ($^{206}Pb/^{204}Pb$=18.19±0.03, 2σ), and concluded that the isotopic signatures correlate with sulfides in veins hosted by the underlying Lower Paleozoic basement and that although a scattering of unradiogenic values have been previously recorded during single crystal analyses at Navan (see Mills et al., 1987), the representative signature is radiogenic. Furthermore, analyses by Caulfield et al., (1986) reveal similar radiogenic compositions at Tatestown (see Figure 3.1A for location) which have a mean $^{206}Pb/^{204}Pb$= 18.224 ± 0.006.

3.6 Tara Deep Drillhole Concentrates Pb Isotopes

Tara Deep reveals a homogenous Pb isotope signature from the concentrates (Fig. 3.4), with $^{206}Pb/^{204}Pb$=18.22±0.004 (2σ, n=19). This is statistically coincident with drilled out single crystal analyses completed on galena samples from Tara Deep (Chapter 2; which has $^{206}Pb/^{204}Pb$=18.23±0.006, 2σ, n=26). Broadly, the Tara Deep minerals and concentrate data statistically overlap the Navan Main Orebody and the Tatestown satellite data. Again, these data highlight that lead (and zinc; see Wilkinson et al., 2005) are sourced from the underlying Lower Paleozoic basement, agreeing with previous research (Boast et al., 1981b; Caulfield et al., 1986; O'Keeffe, 1986; LeHuray et al., 1987; Dixon et al.,

1990; Fallick et al., 2001; Everett et al., 2003). In harmony with the Main Orebody data, there is a lack of low $^{206}Pb/^{204}Pb$ ratios seen by Mills et al., (1987) in their reconnaissance study.

However, the subtle differences between the orebodies suggest each deposit has its own distinct source region. This is also seen in the variability of the hydrothermal signature from each deposit, which although having a coincident mode, shows significant variation. On a regional scale, a systematic variation in lead isotope ratios – "isoplumbs" (LeHuray et al., 1987, which would now be referred to as an isoscape) - from northwest to southwest Ireland, crossing the Caledonide grain, is seen in both Carboniferous-hosted and basement-hosted mineralization (Boast et al., 1981b; Caulfield et al., 1986; O'Keeffe, 1986; LeHuray et al., 1987; Mills et al., 1987; Dixon et al., 1990; Fallick et al., 2001; Everett et al., 2003). This variation across the Irish orebodies likely reflects the complexity of the basement across the region, and thus mixing of lead from different Ordovician and Silurian sediments north and south of the Iapetus suture, with Navan/Tara Deep likely located proximal to the suture zone (O'Keeffe, 1986; LeHuray et al., 1987; Dixon et al., 1990).

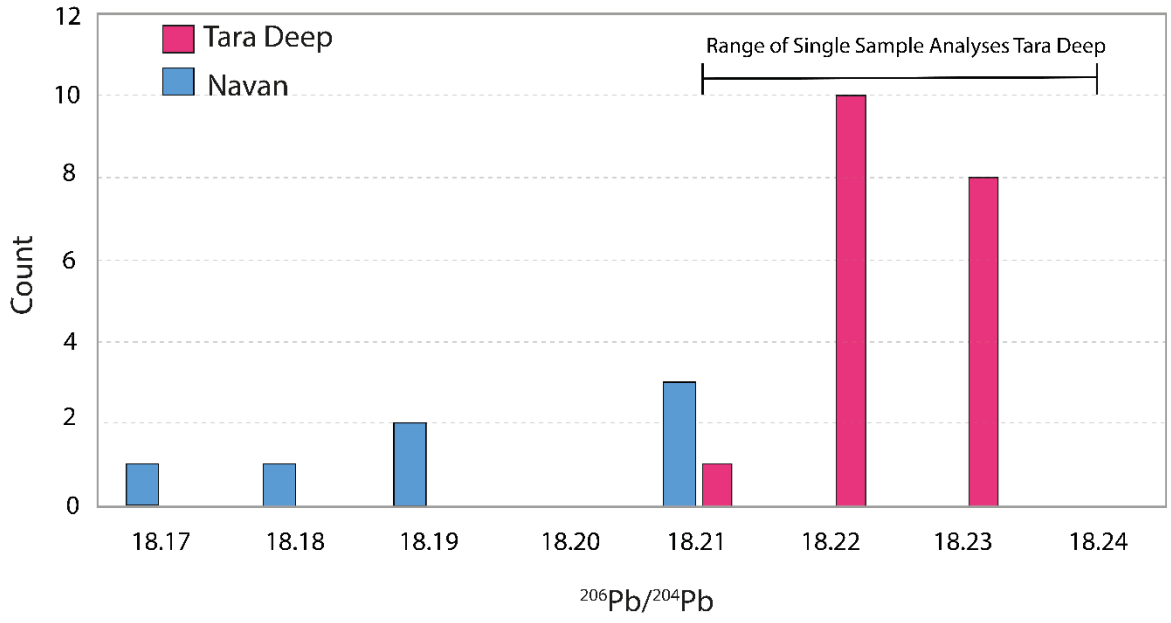

Figure 3.4 Pb Isotope Analyses for Tara Deep's Pb concentrates (n=19), versus Navan's bulk mine concentrate (Fallick et al., 2001)

3.7 Conclusions

The predominant Tara Deep S and Pb isotopic signatures are of 1) sulfur produced by the bacterial reduction of contemporaneous seawater sulfate, constituting no less than 87% of all sulfide in the deposit and 2) a homogeneous lead signature, reflective of derivation from underlying basement lithologies. Bacterial activity was thus critical to the establishment of Tara Deep, this in combination with interpretations made by Fallick et al., (2001) for the Navan deposit, are encouraging signs for exploration at Tara Deep, because to date, only Irish-type deposits with a strong bacteriogenic S isotope signature have gone into economic production. Whilst both the lead and sulfur isotope data are similar to the Navan Main Orebody, there is a distinct signature to the Tara Deep data, especially the bacteriogenic mode, which strongly suggests that Tara Deep is not an allochthonous slice off the Main Orebody, but rather a distinct deposit in space, and perhaps in time. Our data wholeheartedly agree with Fallick et al. (2001) who state that without the involvement of sulfate-reducing bacteria, there would not be the giant Zn + Pb orebody at Navan, Tara Deep, or indeed, other significant Irish orebodies of Mississippian age.

3.8 Acknowledgments

I wish to acknowledge the encouragement and permission of Boliden Tara Mines who facilitated this research. This research was conducted through funding of DAD by Boliden Tara Mines and a NERC Facility award to AJB (IP-1904-0619) for the isotopic analyses. SUERC is supported by NERC and the Scottish Universities consortium. I would also like to thank the British Geological Survey's Geochronology and Tracer Facility, in particular Ian Millar. Much of the data analyses and interpretation within this study was generated using Leapfrog© Software. I thank Seequent Limited for granting us an academic license.

3.9 References

Altinok, E., 2005. Zn-Pb-Fe Mineralization process, evolution of sea water oxidation state in a restricted basin, and diagenesis of deep water calcareous sediments: geochemical and geological study of the Navan Deposit, Dublin Basin, Ireland. Unpublished PhD thesis, Colorado School of Mines, p.160.

Anderson, I.K., 1990. Ore depositional processes in the formation of the Navan zinc-lead deposit, Co. Meath, Ireland. Unpublished PhD thesis, University of Strathclyde, p.290.

Anderson, I.K., Ashton, J.H., Boyce, A.J., Fallick, A.E., and Russell, M.J., 1998. Ore depositional processes in the Navan Zn-Pb deposit, Ireland: Economic Geology, v. 93, p. 535–563.

Andrew, C.J., and Ashton, J.H., 1985. Regional setting, geology and metal distribution patterns of Navan orebody, Ireland: Trans. Inst. Min. Metall. (Sect.B: Appl. earth SCi.), v.94, pp. 66-93.

Ashton, J.H., Beach, A., Blakeman, R.J., Coller, D., Henry, P., Lee, R., Hitzman, M., Hope, C., Huleatt-James, S., O'Donovan, B., Philcox, M.E., 2018. Discovery of the Tara Deep Zn-Pb mineralisation at the Boliden Tara Mine, Navan, Ireland: Success with modern seismic surveys. In SEG Special Publications no 21, pp. 365-381. doi:10.5382/sp.21.16: p.17.

Ashton, J.H., Downing, D.T., and Finlay, S., 1986, The geology of the Navan Zn-Pb orebody, in Andrew, C.J. et al., eds., Geology and genesis of mineral deposits in Ireland: Irish Association for Economic Geology, Dublin, p. 243–280.

Ashton, J.H.; Blakeman, R.J.; Geraghty, J.F.; Beach, A.; Coller, D.; Philcox, M.E. 2015 The Giant Navan carbonate-hosted Zn–Pb deposit—A review. In Current Perspectives on Zinc Deposits; Archibald, S.M.,Piercey, S.J., Eds.; Irish Association for Economic Geology: Dublin, Ireland, 2015; p. 85–122.

Banks, D.A., and Russell, M.J., 1992, Fluid mixing during ore deposition at the Tynagh base-metal deposit, Ireland: European Journal of Mineralogy, v. 4, p. 921–931.

Barrie, C., Boyce, A., Boyle, A., Williams, P., Blake, K., Wilkinson, J., Lowther, M., McDermott, P. and Prior, D. 2009. On the growth of colloform textures: a case study of sphalerite from the Galmoy ore body, Ireland. Journal of the Geological Society, 166(3), pp.563-582.

Blakeman, R.J., 2002. The Compositions and routes of the fluids generating the Navan giant base-metal orebody. Unpublished PhD thesis, University of Glasgow, p.207.

Blakeman, R.J., Ashton, J.H., Boyce, A.J., Fallick, A.E. and Russell, M.J., 2002, Timing of interplay between hydrothermal and surface fluids in the Navan Zn+Pb orebody, Ireland: Evidence from metal distribution trends, mineral textures and $\delta^{34}S$ analyses. Economic Geology, 97, p.73-91.

Boast, A.M., Coleman, M.L., and Halls, C., 1981a, Textural and stable isotopic evidence for the genesis of the Tynagh base metal deposit, Ireland: Economic Geology, v. 76, p. 27–55.

Boast, A.M., Swainbank, I.G., Coleman, M.L., and Halls, C. 1981b, Lead isotope variation in the Tynagh, Silvermines and Navan base-metal deposits, Ireland. Trans. Instn Min. Metall. (Sect B: Appl. Earth Sci.), 90, p. 115–119.

Boliden Summary Report. 2020 [online] Boliden.com. Available at: <https://www.boliden.com/globalassets/operations/exploration/mineral-resources-and-mineral-reserves-pdf/2020/resources-and-reserves-tara-2020-12-31.pdf> [Accessed 1 July 2021].

Boyce, A.J., 1990, Exhalation, sedimentation and sulphur isotope geochemistry of the Silvermines Zn + Pb + Ba deposits, County Tipperary, Ireland. Unpublished PhD thesis, University of Strathclyde, p.354.

Boyce, A.J., Coleman, M.L., and Russell, M.J., 1983, Formation of fossil hydrothermal chimneys and mounds from Silvermines, Ireland: Nature v. 306, p. 545–550.

Boyce, A.J., Fallick, A.E., Fletcher, T.J., Russell, M.J., and Ashton, J.H., 1994, Detailed sulphur isotope studies of Lower Palaeozoic-hosted pyrite below the giant Navan Zn +Pb mine, Ireland:

evidence of mass transport of crustal S to a sediment-hosted deposit: Mineralogical Magazine, v. 58A, p.109–110

Boyce, A.J., Fletcher, T.J., Fallick, A.E., Ashton, J.H. and Russell, M.J. 1993, Petrographic and $\delta^{34}S$ study of the Lower Palaeozoic under the Navan Zn+Pb deposit: A source of hydrothermal sulphur. In: Fenoll Hach-Alí, P., Torres-Ruiz, J. and Gervilla, F. (Eds.) "Current Research in Geology Applied to Ore Deposits", Proc. of the 2nd Biennial SGA Meeting, Publ. Univ. of Granada, Spain, p.53-56.

Boyce, A.J., Little, C.T.S. and Russell, M.J. 2003, A new fossil vent biota in the Ballynoe barite deposit, Silvermines, Ireland: evidence for intracratonic seafloor hydrothermal activity 352Myrs ago: Economic Geology v98, p. 649-656.

Caulfield, J.B., LeHuray, A.P. and Rye, D.M., 1986, A review of lead and sulphur isotope investigations of Irish sediment-hosted base metal deposits, with new data from the Keel, Ballinalack, Moyvoughly and Tatestown deposits, in Geology and genesis of mineral deposits in Ireland in Andrew, C.J., Crowe, R.W.A., Finlay, S., Pennell, W.M., and Pyne, J.F., eds., Dublin, Irish Association for Economic Geology, p. 591–615.

Claypool, J.B., Holser, W.T., Sakai, I.R., Zak, I., 1980, The age curves for sulfur and oxygen isotopes in marine sulfate and their mutual interpretation. Chemical Geology, 28, p. 199-260.

Coomer, P.G., and Robinson, B.W., 1976, Sulphur and sulphate-oxygen isotopes and the origin of the Silvermines deposits, Ireland: Mineralium Deposita, v. 11, p. 155–169.

Derry, D.R., Clark, G.R., and Gillat, N., 1965, The Northgate base-metal deposit at Tynagh, County Galway, Ireland: A preliminary study: Economic Geology, v. 60, p. 1218–1237.

Dixon, P.R., LeHuray, A.P., and Rye, D.M., 1990, Basement geology and tectonic evolution of Ireland as deduced from Pb isotopes: Journal of the Geological Society of London, v. 147, p. 121–132.

Everett, C.E., Rye, D.M. and Ellam, R.M., 2003, Source or sink? An assessment of the role of the Old Red Sandstone in the genesis of the Irish Zn-Pb Deposits. Economic Geology, 98, p. 31-50.

Everett,C. E., Wilkinson,J. J. Rye,D. M. 1999. Fracture-controlled fluid flow in the Lower Palaeozoic basement rocks of Ireland: implications for the genesis of Irish-type Zn-Pb deposits. In: McCaffreY,K. J. W., Lonergan,L. & Wilkinson,J. J. (eds) Fractures, Fluid Flow and Mineralization. Geological Society, London, Special Publications, 155, p.247-276.

Eyre, S.L., 1998, Geochemistry of dolomitization and Zn-Pb mineralization in the Rathdowney Trend, Ireland: Unpub. Ph.D. thesis, Univ. London, p.414.

Fallick, A.E., Ashton, J.H., Boyce, A.J., Ellam, R.M. and Russell, M.J., 2001, Bacteria were responsible for the magnitude of the world-class hydrothermal base metal sulfide orebody at Navan, Ireland. Economic Geology, v.96, p. 885-890.

Ford, C.V., 1996, The integration of petrologic and isotopic data from the Boulder Conglomerate to determine the age of the Navan orebody, Ireland. Unpublished PhD thesis, University of Glasgow, p.176.

Gagnevin, D., Menuge, J.F., Kronz, A., Barrie, C., and Boyce, A.J., 2014, Minor Elements in Layered Sphalerite as a Record of Fluid Origin, Mixing, and Crystallization in the Navan Zn-Pb Ore Deposit, Ireland: Economic Geology, v. 109, p.1513-1528.

Kampschulte A, Bruckschen P, and Strauss H. 2001. The sulphur isotopic composition of trace sulphates in Carboniferous brachiopods: Implications for coeval seawater, correlation with other geochemical cycles and isotope stratigraphy. Chemical Geology 175: 149–173.

LeHuray, A.P., Caulfield, J.B.D, Rye, D.M and Dixon, P.R., 1987. Controls on Sediment-Hosted Zn-Pb Deposits: A Pb Isotope Study of Carboniferous Mineralization in Central Ireland. Economic Geology, v. 82, p. 1695-1709.

Mills, H., Halliday, A.N., Ashton, J.H., Anderson, I.K., and Russell, M.J., 1987, Origin of a giant orebody at Navan, Ireland: Nature, v. 327, p. 223–226.

O'Keeffe, W.G., 1986, Age and postulated source rocks for mineralization in central Ireland, as indicated by lead isotopes, in Andrew, C.J., et al., eds., Geology and genesis of mineral deposits in Ireland: Dublin, Irish Association for Economic Geology, p. 617–624.

Russell, M.J., 1975, Lithogeochemical environment of the Tynagh base-metal deposit, Ireland, and its bearing on ore deposition: Transactions of the Institution of Mining and Metallurgy, v. 84B, p. 128–133.

Russell, M.J., 1978, Downward-excavating hydrothermal cells and Irish type ore deposits: Importance of an underlying thick Caledonian prism. Trans. Instn Min. Metall. (Sect B: Appl. Earth Sci.), 87, p. 168-171.

Samson, I.M., and Russell, M.J., 1987, Genesis of the Silvermines zinc-lead- barite deposit, Ireland: Fluid inclusion and stable isotope evidence: ECONOMIC GEOLOGY, v. 82, p. 371–394.

Singer D, A. 1995. World-class base and precious metal deposits; a quantitative analysis. Economic Geology v. 90: 88–104

Taylor, S. 1984. Structural and paleotopographic controls of lead zinc mineralization in the Silvermines orebodies, Republic of Ireland. Econ Geol 79: p.529–548

Taylor, S and Andrew, C.J., 1978. Silvermines orebodies, Co. Tipperary, Ireland: Transactions of the Institution of Mining and Metallurgy, v. 87B, p. 111–124.

Thamdrup, B., Finster, K., Hansen, J.W., and Bak, F., 1993. Bacterial disproportionation of elemental sulfur coupled to chemical reduction of iron or manganese: Applied Environmental Microbiology, v. 59, p. 101–108.

Wagner, T., Boyce, A.J. and Fallick, A.E. 2002, Laser combustion analysis of $\delta^{34}S$ of sulfosalt minerals: determination of the fractionation systematics and some crystal-chemical considerations. Geochimica et Cosmochimica Acta, v. 66, p.2855-2863.

Walshaw R. D., Menuge J. F. and Tyrrell S. 2006, Metal sources of the Navan carbonate-hosted base metal deposit, Ireland: Nd and Sr isotope evidence for deep hydrothermal convection: Mineralium Deposita v. 41(8), p.803–819.

Weber, A. and Jorgensen, B.B. 2002. Bacterial sufate reduction in hydrothermal sediments of the Guaymas Basin, Gulf of California, Mexico. Deep Sea Research Part I, 49, p. 827-841.

Wilkinson, J.J., Eyre, S.L. and Boyce, A.J., 2005, Ore-forming processes in Irish-type carbonate-hosted Zn-Pb deposits: Evidence from mineralogy, chemistry and isotopic composition of sulfides at the Lisheen Mine. Economic Geology, 100, p. 63- 86.

Wilkinson, J.J.; Hitzman, M.W. 2014. The Irish Zn–Pb Orefield: The View from 2014. In Current Perspectives on Zinc Deposits; Archibald, S.M., Piercey, S.J., Eds.; Irish Association for Economic Geology: Dublin, Ireland, p. 59–72.

Yesares, L., Drummond, D., Hollis, S., Doran, A., Menuge, J., Boyce, A., Blakeman, R. and Ashton, J., 2019. Coupling Mineralogy, Textures, Stable and Radiogenic Isotopes in Identifying Ore-Forming Processes in Irish-Type Carbonate-Hosted Zn–Pb Deposits. *Minerals*, 9(6), p.335.

Table 3.1 S Isotope Concentrate Data Per Hole

DH Concentrate Sample	**$\delta^{34}S$ (‰)**
N02323 Pb Concentrate	-6.4
N02323 Zn Concentrate	-3.9
N02332 Pb Concentrate	-10.2
N02332 Zn Concentrate	-8.8
N02370 Pb Concentrate	5
N02370 Zn Concentrate	10.1
N02371 Pb Concentrate	1.9
N02371 Zn Concentrate	2.4
N02418 Pb Concentrate	-7.8
N02418 Zn Concentrate	-4.8
N02450 Pb Concentrate	-10.2
N02450 Zn Concentrate	-9.5
N02456 Pb Concentrate	-12.5
N02456 Zn Concentrate	-10.6
N02461 Pb Concentrate	6.6
N02461 Zn Concentrate	8.7
N02464 Pb Concentrate	-8.5
N02464 Zn Concentrate	-6.3
N02465 Pb Concentrate	-12.1
N02465 Zn Concentrate	-11
N02466 Pb Concentrate	-9.9
N02466 Zn Concentrate	-8.2
N02468 Pb Concentrate	-8.6
N02468 Zn Concentrate	-8.3

N02469 Pb Concentrate	-11
N02469 Zn Concentrate	-2.8
N02477 Pb Concentrate	-7.6
N02477 Zn Concentrate	-7.7
N02482 Pb Concentrate	-5.8
N02482 Zn Concentrate	-1.9
N02483 Pb Concentrate	-16.8
N02483 Zn Concentrate	-7.2
N02496 Pb Concentrate	-7.6
N02496 Zn Concentrate	-8.8
N02503 Pb Concentrate	-9.2
N02503 Zn Concentrate	-4.8
N02505 Pb Concentrate	-9
N02505 Zn Concentrate	-5.9
Overall Mean	**-6**
Standard Deviation	**5.9**

Table 3.2 Pb Isotope Concentrate Data Per Hole

Sample Name	$^{206}Pb/^{204}Pb$
N02323	18.22
N02332	18.23
N02370	18.22
N02371	18.23
N02418	18.23
N02450	18.22
N02456	18.22
N02461	18.21
N02464	18.22
N02465	18.22
N02466	18.22
N02468	18.23
N02469	18.23
N02477	18.22
N02482	18.23
N02483	18.22
N02496	18.22
N02503	18.23
N02505	18.23
Overall Mean	18.22
Standard Deviation	0.004

CHAPTER FOUR: CARBONATE DEPOSITIONAL PROCESSES AT THE TARA DEEP Zn-Pb DEPOSIT, CO. MEATH, IRELAND. NEW INSIGHTS FOR THE EVOLUTION OF THE DUBLIN BASIN MARGIN.

Drummond[1], D. A., Hollis[2], C., Ashton[3], J. H., Blakeman[4], R. J., Farrelly[4], I., Cloutier[5], J., D., Boyce[1], A. J.

[1]Scottish Universities Environmental Research Centre, Rankine Avenue, East Kilbride, Glasgow G75 0QF, United Kingdom.

[2]School of Earth and Environmental Science, University of Manchester, Manchester M13 9PL, UK

[3]Consultant Boliden Tara Mines.

[4]Boliden Tara Mines, Exploration Department, Navan, County Meath, Ireland.

[5]Centre for Ore Deposits and Earth Science, University of Tasmania, Private Bag 79, Hobart, Tasmania, Australia.

**Corresponding Author: drewdrummond59@gmail.com*

4.1 Abstract

The Tara Deep Zn-Pb deposit (currently 26.2 Mt @ 8.4% Zn, 1.6% Pb; Boliden Summary Report, 2020) is hosted by Mississippian carbonates within the Dublin Basin, situated 2 km south of the world-renowned Navan deposit. Tara Deep is located at depths of between 1.2-1.9 km within fault-controlled terraces on the degraded footwall of a major normal fault system. The system formed as a result of a rapidly subsiding basin margin during the upper Tournaisian extension. The region's long lived and dynamic evolution has resulted in a complex architecture of large normal and strike slip faults. The complexity of the Dublin Basin margin evolution at Navan can be divided into three distinct phases: pre-rift ramp sedimentation in the lower Mississippian (upper Tournaisian), syn-rift abrupt detachment and destructive debris flows in the lower Viséan, and finally late-rift basin infill sedimentation during the lower Viséan to Mid-Mississippian. Diagenetic processes include dolomitization, mineralization and extensive pressure solution, which complicate the lithofacies reconstruction by occluding pre-existing textures. Dolomitization occurs in four phases: D1 – D4. D1 predates mineralization and represents early replacement by non-ferroan euhedral dolomite (30 μm), this dolomite typically has cloudy cores (often associated with Mn), with clear ferrous rims. D2 represents interparticle infill by anhedral (50 μm), ferroan dolomite. D3 occurs as late, coarse, non-ferroan saddle dolomite cement which occurs in vugs. D4 occurs as the last phase throughout the Tara Deep succession, is nanocrystalline, and is related to burial dolomitization evidenced by its close association with pressure solution seams. Pressure solution is also partially responsible for the generation of common and distinct stylo-nodular textures in the Pale Beds and can lead to occlusion of the original host rock fabric in the Thin Bedded Unit. Oxygen and carbon isotopes are used to constrain these interpretations. Mineralization, dominated by bacteriogenic sulfide, is also intimately linked to basin margin development and architecture, and is recorded across early syn-rifting textures to late-rifting textures, highlighting the complexity and longevity of the mineralizing system within the Mississippian carbonates. Together these processes speak of a dynamic sedimentary, tectonic and microbiological environment which have culminated in an exceptional accumulation and preservation of base metals during the Mississippian.

4.2 Introduction

The Tara Deep Zn-Pb deposit (Fig. 4.1; Inferred Resources currently 26.2 Mt @ 8.4% Zn, 1.6% Pb) is a recent discovery by Boliden Tara Mines which significantly adds to the greater Navan resource (total Navan resource >125 Mt at ~8% Zn and 2% Pb). Located 2 km south of the Navan Orebody in Co. Meath, Ireland, the deposit occurs immediately south of the Longford Down Lower Paleozoic Inlier, within a major ENE-trending structural corridor that is related to the Iapetus Suture (Morris and Max, 1995). To the south and southwest, Mississippian platform carbonates and calc-turbidites of the Dublin Basin sub-crop. The Tara Deep deposit remains open to exploration, with the majority of the mineralization situated at depths of 1.2 to 1.9 km.

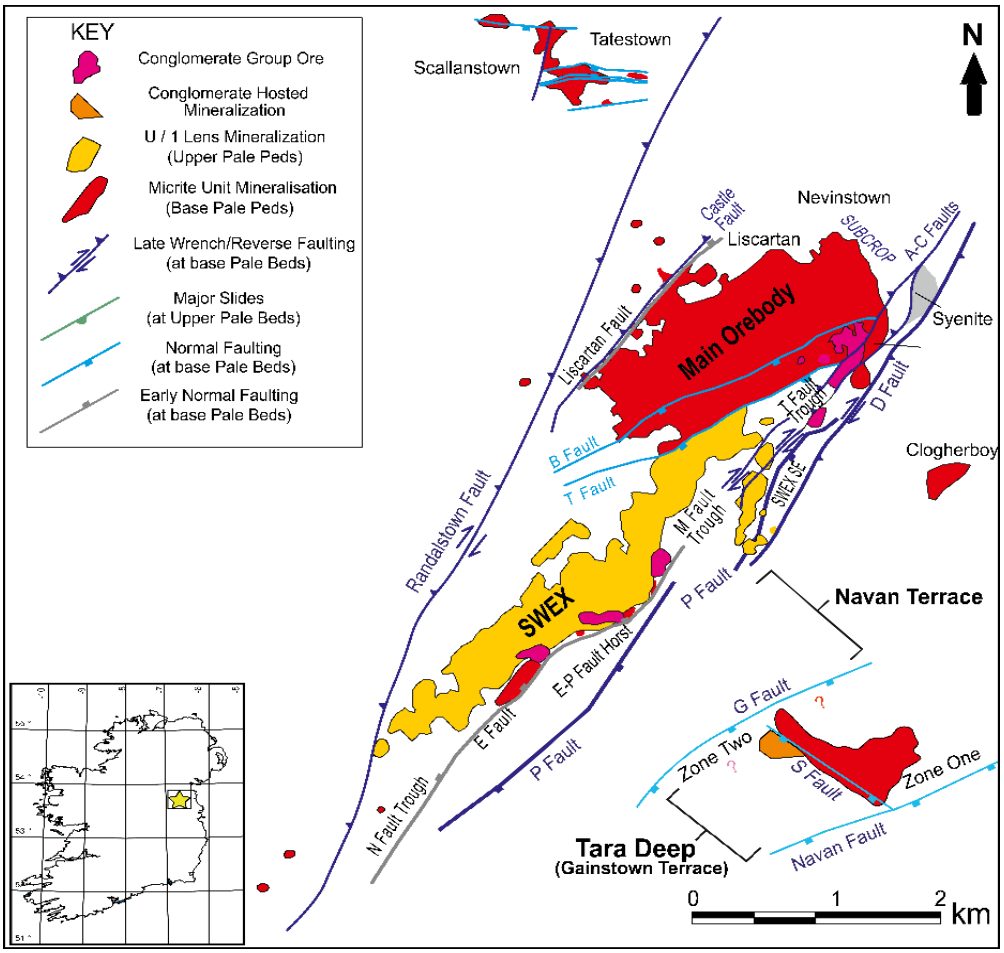

Figure 4.1 Structural plan showing the positioning of Tara Deep relative to the Navan Orebody, and the distribution of principal ore lenses and faults, modified from Ashton et al., (2015). Note the faults are shown as plan projections from their intersections with the ore lenses, not as outcrop positions. SWEX is an abbreviation of Southwest Extension.

More broadly, Irish Mississippian carbonates host numerous Zn-Pb±Ba deposits of economic importance, with the world-class Navan deposit being Europe's largest zinc producer for over 40 years. After more than 60 years of intensive exploration, the next generation of Zn-Pb deposits within Ireland will almost certainly be deeper and less readily detectable from the surface. This study unravels the carbonate depositional processes at the heart of the Tara Deep deposit. What emerges is a story of a complex, dynamic carbonate depositional and diagenetic environment, heavily impacted by major basin margin subsidence in the Dublin Basin. This study will help facilitate future exploration and guide basin analysts.

4.3 Geological Context

Navan is located 45km NW of Dublin. Geologically it is located immediately south of the Longford Down Lower Paleozoic Inlier, adjacent to a major NE-trending fault zone forming the southern margin to the inlier. The stratigraphic and palaeogeographical settings of the Mississippian sequences are described in detail by Philcox (1989) and Phillips and Sevastopulo (1986). A formal stratigraphy has been erected for the Mississippian of the region (Rees 1987; Strogen et al., 1990) but since this study deals exclusively with the Navan Mine area, the informal mine nomenclature is retained here (Fig. 4.2). Due to the proximity of the Navan deposit and the complexity of basin evolution, it is vital to outline the setting and stratigraphy of the Navan deposit before a comparison is made with Tara Deep (Fig. 4.1).

During the Mississippian, the Navan area was located on the southern margin of Laurussia, just north of the equator. It was separated from the Gondwanan supercontinent by the Rheic Ocean and eastern and western arms of the Theic and Paleo-Tethys oceans (Scotese, 2001). These were separated by the Armorican continental plate, which was bordered by opposite-facing subduction zones (Matte, 2001).

The geophysical signature (Murphy, 1974, 1981) and seismic signature (Ashton et al., 2018) of the Lower Paleozoic basement of the Dublin Basin is complex on both gravity and magnetic maps (Morris and Max, 1995), and a plethora of Pre-Mississippian faults have been detected (Andrew 1993;

Russell, 1968; Strogen et al., 1996; Ashton et al., 2003, 2015). The basement rocks stratigraphically below the Navan area, constitute a structurally complex, lithologically varied series of Ordovician and Silurian sedimentary, volcanic and intrusive rocks (Strogen et al., 1996; Everett et al., 1999, 2003; Ashton et al., 2015). This basement was deformed in the late Silurian-Early Devonian by the Caledonian Orogeny resulting in NE-SW structural fabrics which were subsequently reactivated and inherited by the overlying Mississippian sequences (Russell 1968; Johnston et al., 1996; Strogen et al., 1996; Worthington and Walsh, 2011). In general, the basement displays evidence of low-grade metamorphism, associated with anchimetamorphic to zeolite facies, with greenschist facies metamorphism in regions (Vaughan and Johnston, 1992).

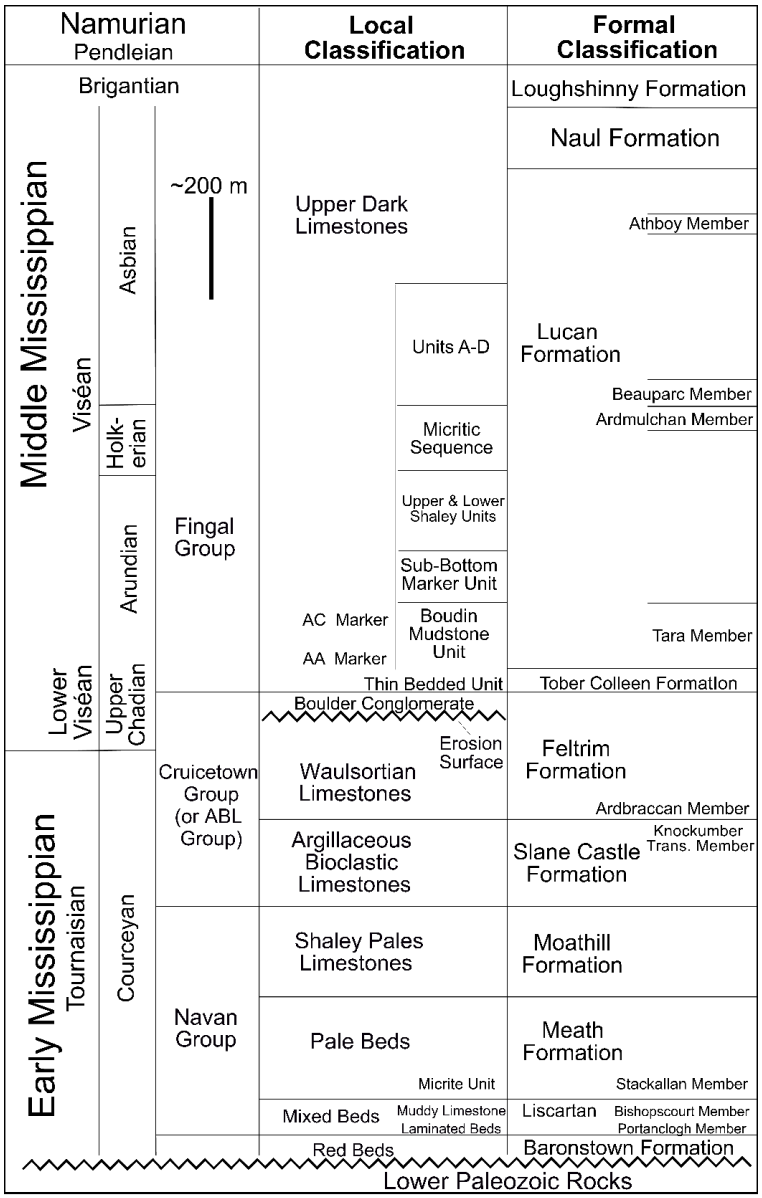

Figure 4.2 Formal and informal stratigraphy table of Mississippian rocks in the Navan and Tara Deep area (after Philcox 1984, 1989; Strogen et al., 1990 and Ashton et al., 2015). Local classification is used throughout this study due to its acceptance with Irish economic geologists.

The Lower Paleozoic basement is unconformably overlain by early Mississippian locally-termed Red Beds, comprising impure red sandstones and polymict pebble conglomerates that in regions contain caliche horizons, alongside cross-bedded and rippled sandstones, siltstones and mudstones. They are interpreted as fluvial or alluvial fan deposits (Strogen et al., 1990; Rizzi, 1992). There is little evidence for any appreciable palaeorelief at this time (Fig. 4.2; Romano, 1980; O'Keeffe, 1986, Murphy et al, 1991; Ashton et al., 2015; Fritschle et al 2018). The Red Beds represent the transition from subaerial to submarine deposition, and are diachronous due to a northward-advancing transgression that led to the establishment of shallow marine conditions across most of south and central Ireland. Consequently, the Red Beds are overlain by Mixed Beds which comprise the Laminated Beds and Muddy Limestone. The Laminated Beds are a varied suite of thinly bedded (millimetre scale), often bioturbated, dark argillaceous siltstones and mudstones with local paler siltstones, sandstones and calcarenites. They record the initial transgression of the early Mississippian sea (Philcox, 1989; Andrew and Ashton 1985). The Laminated Beds were deposited in a variety of emergent, peritidal to shallow subtidal environments (McNestry and Rees 1992; Rizzi, 1992). The overlying Muddy Limestone is a dark, well-bedded argillaceous and crinoidal limestone with prominent bioclastic horizons. Syringopora reticulata, brachiopods and other bioclasts reflect deposition in a clastic-influenced shallow marine to lagoonal environment (Anderson, 1990; Rizzi, 1992; Ashton et al., 2015).

Stratigraphically above the Muddy Limestone are the Pale Beds; these rocks are the main host for Zn+Pb mineralization, particularly within the locally termed Micrite Unit sub-group (Fig. 4.1 & Fig. 4.2). The Pale Beds comprise medium grey micrite, oolitic and bioclastic grainstones, dolostones, with some calcareous sandstones and minor argillaceous siltstone layers, interpreted to represent subtidal deposition (Strogen et al., 1996; McNestry and Rees, 1992). Several distinctive sandstone, siltstone and shale layers, each up to several metres thick, form marker horizons within the overlying Pale Beds at the Navan deposit, which are vital for ore lens classification and structural interpretation (Philcox, 1989, Braithwaite and Rizzi, 1997; Ashton et al 2015). Rizzi and Braithwaite (1997) state that the Pale Beds contain at least 44 peritidal, emergent and shallow-shelf depositional cycles.

In the north of the Navan deposit a series of channels exist within the Laminated Beds, Muddy Limestone, and Micrite Unit. Various authors have described these as having a similar size and shape to coastal channel systems which dissect modern tidal flats, lagoons and barrier island deposits (see Rizzi and Braithwaite, 1997; but also, Anderson, 1990; Strogen, 1996; Ashton et al., 2015). The channel assembly within these units trends generally N-S. Within the Laminated Beds the channel sequence is about 20 m deep and 100-500 m wide. Cross-sections correlating cycles indicate that there are at least five minor channels stacked vertically within the sequence. Within the Muddy Limestone channelling occurs over an area of 1200m across (generally east-west) and 20 m deep. These channels contain sand to small-pebble grade, burrowed and cross-bedded grainstones, which display fining-upwards cycles and cross-bedding consistent with deposition in such channels. Lithoclasts and siliciclastic grains are deemed to have originated from the northern hinterland, whereas bioclasts and ooliths likely derived from adjacent marine environments. A third channel assembly is present towards the base of this succession, between the two lowest siliciclastic markers. Isopach data reveals that it occupies a N-S trending depression whose axis lies in the same geographical area as those channels below. The channel fill consists of at least 13 individual channels, each up to 1.5 km wide and 8 m deep. Significantly, these channels, at four stratigraphic levels, formed in essentially the same palaeogeographic position, pointing to a well-established and long-lived drainage system to the north of Navan at this time (Phillips and Sevastopolo, 1986; Rees 1987).

Increasing water-depth in the upper Tournaisian led to the deposition of the Shaley Pales and Argillaceous Bioclastic Limestone (ABL) which are overlain by Waulsortian mudbank limestones. The Shaley Pales consist of repeated wackestone, packstone and shale cycles, with a few sandstones and thin graded grainstones (the latter with sharp, eroded bases). These were likely deposited below fair-weather wave-base, with the grainstones representing storm deposits (Philcox, 1989, 1991; Strogen et al., 1990; Rizzi and Braithwaite, 1996). The Argillaceous Bioclastic Limestone, consist of shaley wackestone, shales and a few packstones, with the siliciclastic content decreasing vertically. Abundant bioclasts, typically crinoid ossicles, are present throughout, some forming sharp-based beds a few

centimetres thick. Generally, these rocks reflect a continuation of deep-water outer ramp sedimentation with the thin limestones again representing storm deposits (Strogen et al., 1990). No evidence of emersion has been found in the Shaley Pales, the ABL or younger rocks at Navan; water depths were likely too great to result in emergence. The ABL is overlain by the Waulsortian limestone. At Navan, the Waulsortian limestone forms only isolated knolls (Ashton et al., 1992) and unlike in other areas of the Irish Orefield, the Waulsortian limestones is poorly developed and unmineralized at Navan (see Lees and Miller, 1995).

Two-dimensional seismic data across the Navan region demonstrates that the rate of basin subsidence accelerated during the deposition of the ABL, marked by changes in the thickness of this unit across extensional structures (Ashton et al., 2015). The same relationship is observed in the NW of the Navan deposit where the Waulsortian limestone thickens in the hanging walls of syn-sedimentary faults (Fig. 4.3A). Both of these observations reveal that extension began during the upper Tournaisan/lower Viséan around the time of ABL deposition.

Crucially, a marked change in basin evolution in the Navan deposit area occurs abruptly around the timing of Waulsortian limestone deposition. Gravitational instability is witnessed by large collapse events, subsequently reworking and redepositing the lower Mississippian stratigraphy as large allochthonous blocks and debrites, known locally as the Boulder Conglomerate (Ford, 1996; Ashton et al., 2015). Thick accumulations of shale-rich Arundian-Holkerian calc-turbidites and debris flows of the Upper Dark Limestone (UDL) fill the basin (Nolan, 1989; Philcox, 1989; Ashton et al 2015).

Regionally, the Dublin Basin was inverted likely during the Variscan Orogeny but, in general, the level of overall tectonic deformation is low grade (Strogen et al., 1996; Ashton et al. 2015). Details of the structure of the Variscan compression are given by Dolan (1983), Sanderson (1984), Coller (1984), Cooper et al. (1984, 1986) and Rothery (1988).

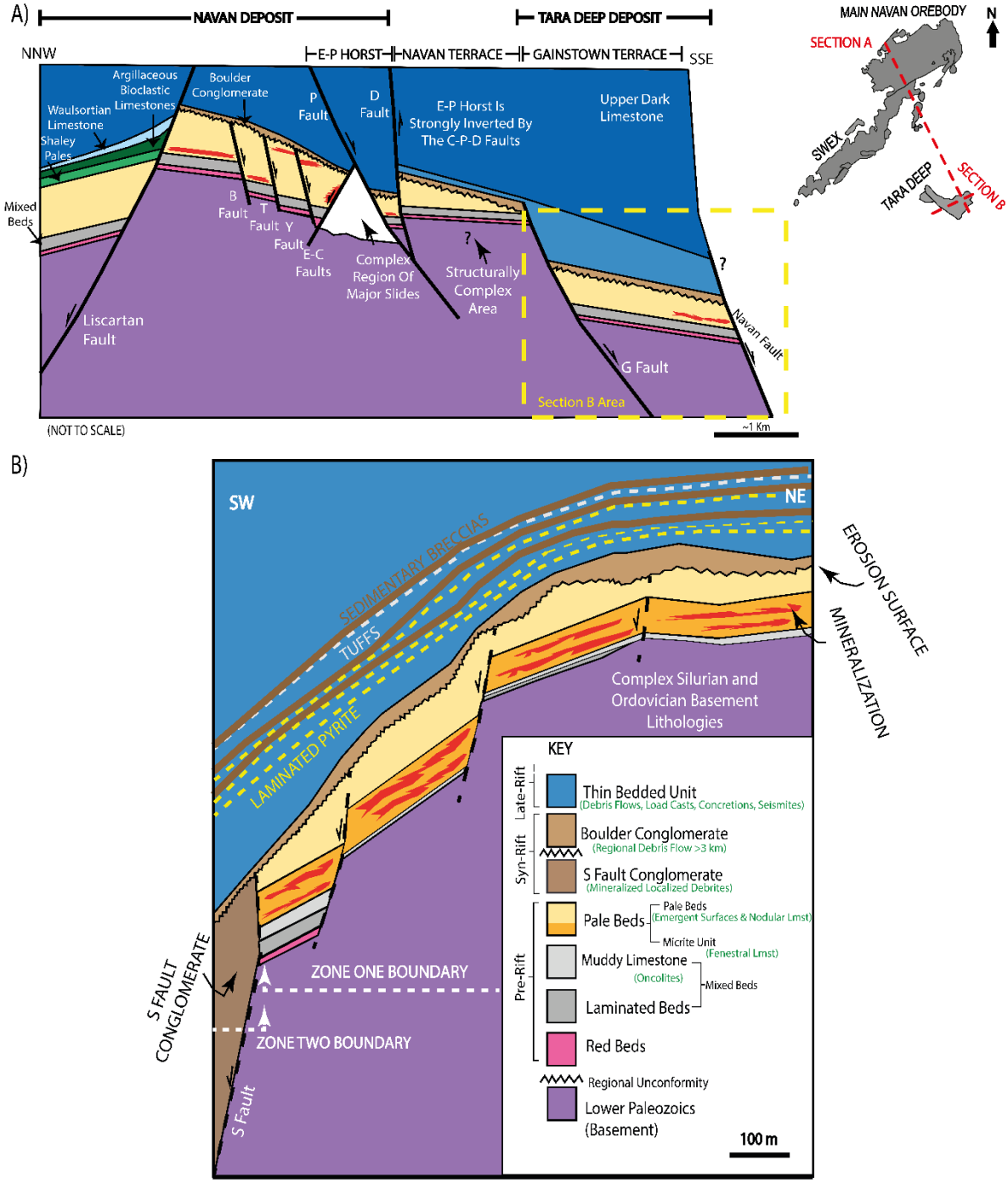

Figure 4.3: Modified cross sections from Chapter 2. Tara Deep is located within a terrace between the G and Navan faults. A) Highly schematic post-inversion cross section across the Navan to Tara Deep region, highlighting the principal controlling faults. B) SW-NE schematic section outlining the setting of the Tara Deep deposit within the Gainstown Terrace; a region consisting of a series of fault-controlled terraces. A faulted contact likely exists between the Laminated Beds and the underlying Lower Paleozoics. The S Fault divides the deposit into Zone One (S Fault footwall) and Zone Two (S Fault hanging wall). Zone One has a similar Mississippian stratigraphy to that of the Main Orebody, but the upper Pale Beds, Shaley Pales, Argillaceous Bioclastic Limestone and Waulsortian limestone have been completely removed by sliding and debrites which may pre-date the overlying Boulder Conglomerate. Zone Two hosts at least two significant debris flow events, a localized debrite (S Fault Conglomerate) and the Boulder Conglomerate.

4.4 Structural Framework

Broadly N-S extension led to several major faults trending generally ENE and defining a horst and two terraces (Fig. 4.3A). The southern margin of the Navan deposit, is defined by the major E-P horst, involving the NW dipping E Fault (>500m normal throw) and the SE dipping P Fault (>800m apparent normal throw; see Ashton et al., 2018; Fig. 4.1). Southwards (~1.5 km), the SE dipping G Fault is developed (>500m normal throw) with the intervening area termed the Navan Terrace. Both the E-P horst and the Navan Terrace are not fully defined due to low resolution drilling, but the orebody host rocks appear to be largely absent from both regions due to southwards-directed sliding and erosion (Ashton et al., 2015). The Navan Terrace is strongly dislocated by a complex zone of major SE dipping post-mineral faulting termed the D-Q Fault Zone (Fig. 4.1). Late compression, and subsequently inversion, complicates the reconstruction of pre-inversion relationships between Navan and Tara Deep (a significant dextral offset is suspected; Johnston et al, 1996; Strogen et al., 1996).

Stepping down towards the Tara Deep deposit (Fig. 4.3A&B), a further ~1.5km south of the G Fault lies the SE dipping Navan Fault, this is the largest structure in the area and displays a normal displacement of at least 3km, as estimated from seismic data (Ashton et al., 2018). Tara Deep occurs on the Gainstown Terrace between the G and Navan faults, where strongly mineralized host rocks have been subjected to several episodes of faulting and sliding. The terrace is dissected by several SW-dipping, low-angle listric normal faults with vertical displacements of <50m, trending broadly perpendicular to the G and Navan faults. More significantly, in the SW parts of the Tara Deep deposit, a large complex zone of sliding and planar faulting cuts obliquely NNW-SSE across the Gainstown Terrace and is termed the S Fault (Fig. 4.3). This structure dips steeply WSW with a normal throw of >600m. Seismic and drilling data indicate that the G, Navan and S Faults do not significantly displace the lower Viséan debris flows and basal units of the UDL that overlie the truncated Pale Beds (Fig. 4.3).

4.5 Methods

4.5.1 Drill Core Analyses and Sampling

Detailed logging of Tara Deep core was undertaken during exploration drilling. Two hundred and thirty-one samples were collected to represent the different stratigraphical units, carbonate textures and mineralization styles. One hundred seventy polished thin sections were prepared. Petrographic analyses of the textures and their paragenetic relationships were carried out using standard transmitted and reflected light microscopy. Detailed scanning electron microscopy (SEM) was completed at the University of Glasgow, using a Quanta 200F Environmental SEM with EDAX microanalysis. Cold cathodoluminescence was completed at the GRANT Institute, University of Edinburgh using a CITL 8200 Mk 3A mounted on a Nikon Optiphot petrological microscope in order to discriminate between the various dolomitization and cement phases. Dolomite textures were described according to the scheme of Sibley and Gregg (1987).

4.5.2 Oxygen and Carbon Isotope Method

The oxygen and carbon isotope composition of calcite and dolomite samples drilled from offcuts were analyzed on an Analytical Precision AP2003 mass spectrometer equipped with a separate acid injector system. CO_2 was released from carbonates by reaction with 105% H_3PO_4 under a helium atmosphere at 70°C, after reacting for a minimum of 1 day in the case of calcites, or 3 days in the case of dolomites. Measured O isotope ratios are reported as per mil deviations relative to Vienna standard mean ocean water (VSMOW) and C isotopes relative to Vienna PeeDee Belemnite (VPDB) using conventional delta notation. Mean analytical reproducibility based on replicates of the SUERC laboratory standard MAB-2 (Carrara Marble) was around ±0.2% for both carbon and oxygen. MAB-2 is an internal SUERC laboratory standard extracted from the same Carrara Marble quarry as the IAEA-CO-1 international standard. It is calibrated against IAEA-CO-1 and NBS-19 and has exactly the same C and O isotope values as IAEA-CO-1 (–2.5% and 2.4% VPDB, respectively).

4.6 Results

4.6.1 Tara Deep Stratigraphy

The S Fault separates Tara Deep's stratigraphy into Zone One (S Fault Footwall) and Zone Two (S Fault hanging-wall; see Fig. 4.2 & 4.3). Within Zone One the Navan stratigraphy, up to the lower Pales Beds, is intact but the superseding Shaley Pales, Argillaceous Bioclastic Limestone and Waulsortian limestone have been removed completely by sliding and associated debrites. These debrites are similar in nature to the Boulder Conglomerate at Navan, which overlies a distinct Erosion Surface (Fig. 4.3B). While to the west, Zone Two displays complex sedimentary breccias (e.g the S Faut Conglomerate; SFC) and large rotated blocks of Mixed Beds, Pale Beds and Shaley Pales in the S Fault hanging-wall. Description of the stratigraphy within both zones will be separated into pre-, syn- and late-rift classifications; where the SFC and Boulder Conglomerate are regarded as syn-rift, the lithologic packages beneath this and the basement are pre-rift, and everything above the Boulder Conglomerate until the youngest sedimentary breccia in the Thin Bedded Unit is regarded as late-rift (Fig. 4.3B).

4.6.2 Zone One's Pre- and Syn- lower Mississippian Statigraphy:

Situated north of the Navan fault and within the hanging wall of the S Fault, Zone One (Fig. 4.3) hosts a truncated sequence which is locally equivalent to the Navan deposits lower Mississippian stratigraphy. Crucially, SE dipping, low-angle faults, and associated sliding, dissect the majority of Tara Deep (Fig. 4.3), meaning a faulted contact likely exists between the Laminated Beds (Fig. 4.4A) and the underlying Ordovician and Silurian Basement. These are overlain by oncolite rich Muddy Limestone (Fig. 4.4B), which often displays a gradational contact with the underlying Laminated Beds.

Pale Beds

The principal host for mineralization within Zone One is a lateral equivalent of the Micrite Unit at the Navan deposit (Fig. 4.4C; ~60 m in thickness), which is the lowest sub-unit of the Pale Beds. This package is a distinct manifestation of the same intertidal Micrite Unit horizon as described in the Navan deposit (see Rizzi, 1992; Anderson et al., 1998; Ashton et al., 2015). However, whereas at Navan this intertidal

unit is variable across the deposit and also hosts channelling in the northern mine area, at Tara Deep this same interval is far more consistent with no current evidence for channelling. Characteristic features of the Micrite Unit include fine-grained, organic-rich, navy/dark grey colour, and abundant fenestral (birds-eye) textures. The Micrite Unit is interbedded with a series of oolitic-calcarenite horizons (up to three). Early, replacement dolomitization in the Micrite Unit completely replaces these oolitic-calarenite horizons (Fig. 4.4D), but replacement of the surrounding micrite is highly variable. This replacement dolomitization predates mineralization (Fig. 4.4E; see dolomitization section below). At Tara Deep, an Upper and Lower Micrite can be distinguished on either side of a laterally continuous central dolomitized oolitic grainstone horizon across the entire Zone One. This, together with a consistency of thickness in the Micrite Unit (around 50m) across the Navan and Tara Deep deposits, suggests a strong similarity in depositional environment across the entire area.

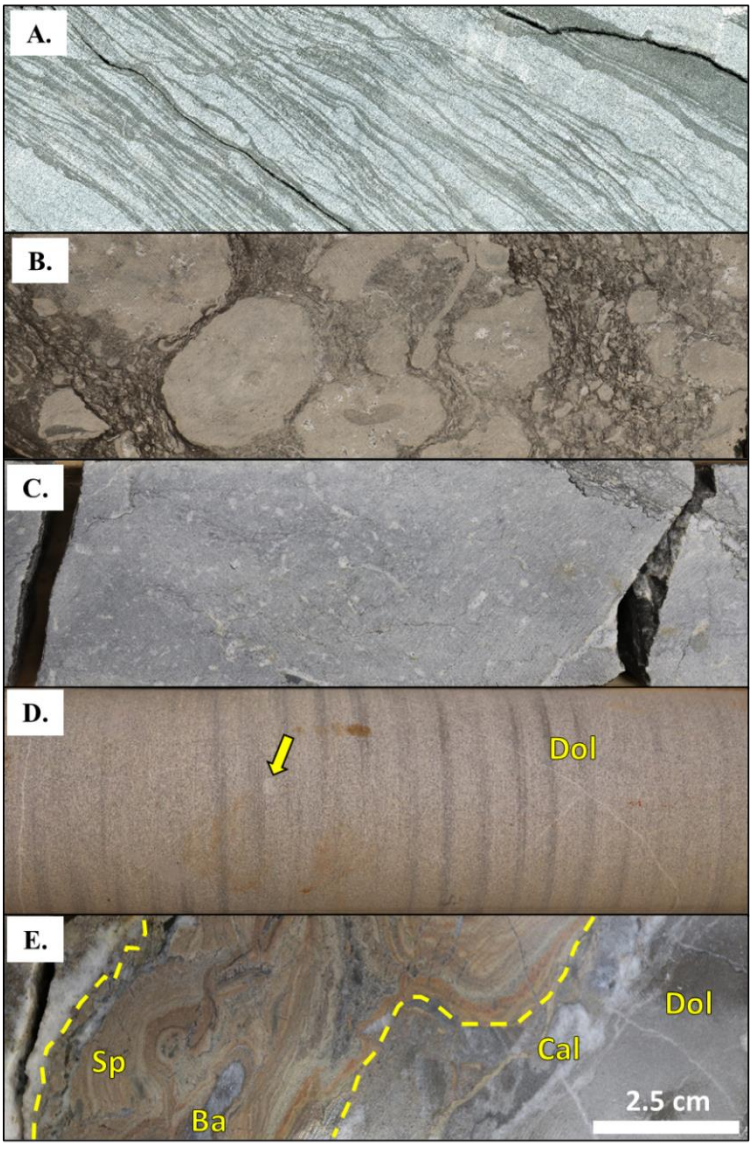

Figure 4.4 Upper Tournaisian peritidal to shallow marine, pre-rift, facies hosted at Tara Deep. A) Laminated Beds consisting of fine laminations of calcsilitite and mud (N02505/ 29; 1921.2 m). B) Oncolites hosted within the Muddy Limestone (N02505/28; 1904.15m). C) Undolomitized Micrite Unit with fenestral textures. In the top right pressure solution seams exists (N02428/09, 1404.9 m). D) Dolomitized Micrite Unit, dolomitization has occluded the original fenestral fabric. The yellow arrow reveals a ghost fenestral texture. Note the vertical markings on the core are drillmarks not bedding (N02445/06; 1772.6m). E) Cavity fill mineralization, within a dolomitized Micrite Unit, with dominantly sphalerite mineralization and minor barite. These cavities have likely been generated through fluid enhancement (N02334; 1775.3 m)

Overlying the Micrite Unit, the remaining Pale Beds consist dominantly of oolitic grainstones. The true thickness of the Pale Beds is unknown as they are capped by a palaeo-erosive surface, known locally as the Erosion Surface. Two important textures exist within the remaining Pale Beds: A) emergent surfaces (Fig 4.5 & 4.6) and B) an equivocal texture locally termed 'Healed Conglomerates' (Fig. 4.7 A-F).

A) Emergent surfaces typically occur as complex subvertical irregular mud filled fissures, with a width of 1-3 cm and a length of <30 cm. They represent marine carbonates that have been periodically exposed above the sea floor. Carbonate mud typically infills these fissures. In the southeast of Tara Deep, particularly at the Navan-S Fault junctions, these textures are often exploited by iron oxide (Fig. 4.5A). Cross-cutting relationships reveal early-diagenetic fissure fills, associated with carbonate mud (see also oxygen and carbon isotope data section below), are co-genetic with iron oxide alteration (Fig. 4.5B). Sometimes these surfaces can be observed reworked (Fig. 4.5C). Geopetal relationships on the fissure walls can be identified (Fig. 4.6A), outlining fissures were once open and subsequently infilled by carbonate mud. The geopetal textures also reveal that a sub-vertical orientation once existed to these fissures. Petrographic observations of grain-scale textures from these textures often highlight an absence of early marine cements with compaction between ooids and grain bridging via meniscus cements (Fig. 4.6B). In some of these iron oxide-rich examples, there is evidence of branching (200µm in length) hollow tube structures, which may represent filamentous bacteria and frutexites (Figs 4.6B & 4.6C), but abiotic textures are dominant (Fig. 4.6E). Future work which is beyond the scope of this study will look into these textures (Appendix 2).

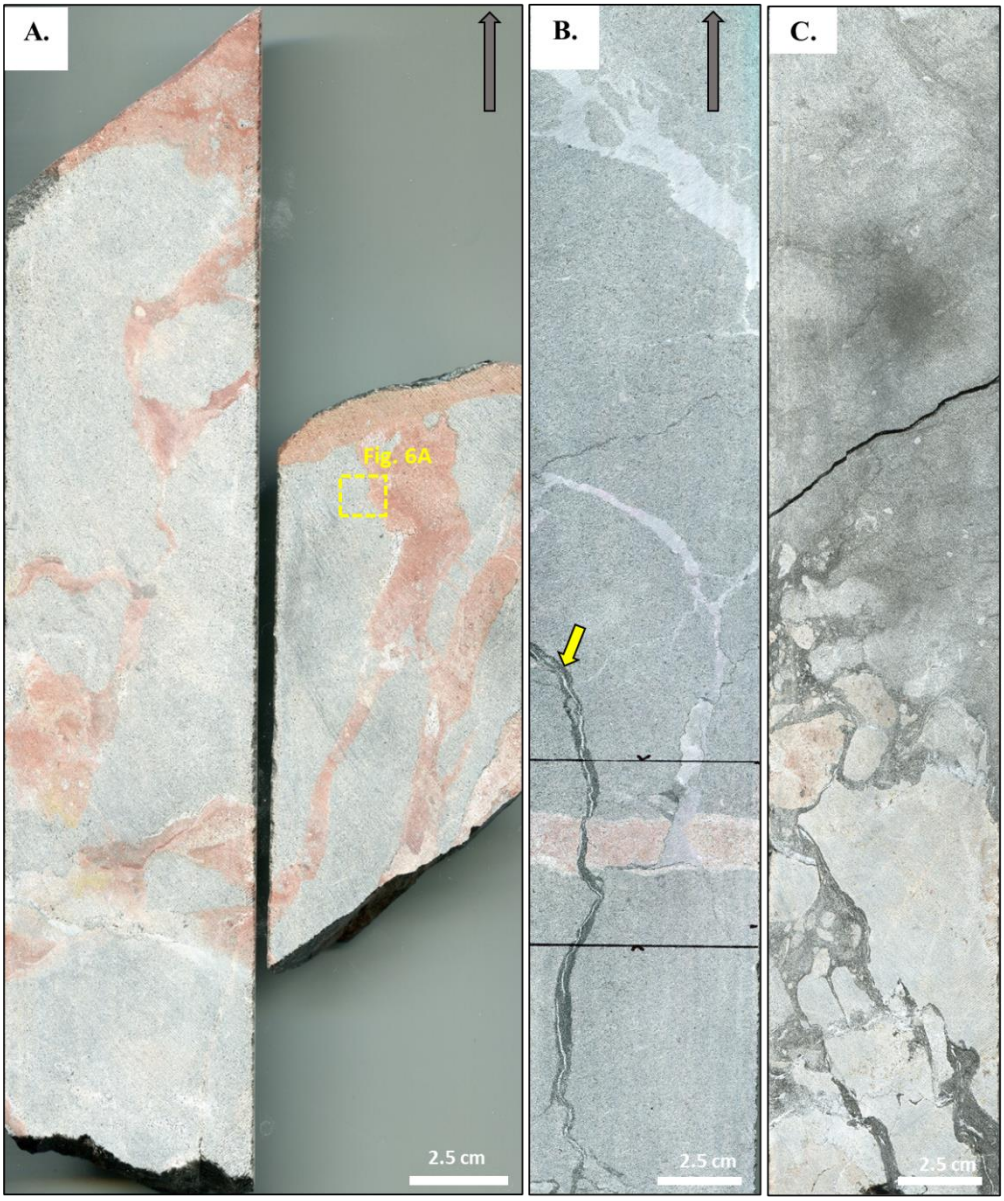

Figure 4.5 Evidence for emergent surfaces present within the Pale Beds at Tara Deep. A) Drill core image (way up arrow noted) outlining the complexity of the mud filled fissures within the oolitic grainstone. These emergent surface cavities has been infilled by carbonate mud and then altered by iron oxide. Note the iron oxide preferentially exploits the emergent surfaces, but it can also be observed exploiting interparticle porosity within the oolitic grainstones, highlighting early diagenetic processes, and the semi-lithified nature of the host rock (N02505/04; 1723.25m). B) Halved NQ-drillcore showing the way up direction (grey arrow). Iron oxide emergent surface is crosscut by a marginally later carbonate mud infill associated with later emergence, thus revealing that both iron oxide and micrite infill are early diagenetic processes and they are existing almost co-genetic. Both of these textures are cross-cut by late pressure solution (yellow arrow; N02510/03, 1529.6). (C) Reworked emergent surface highlighting fluctuating depositional conditions

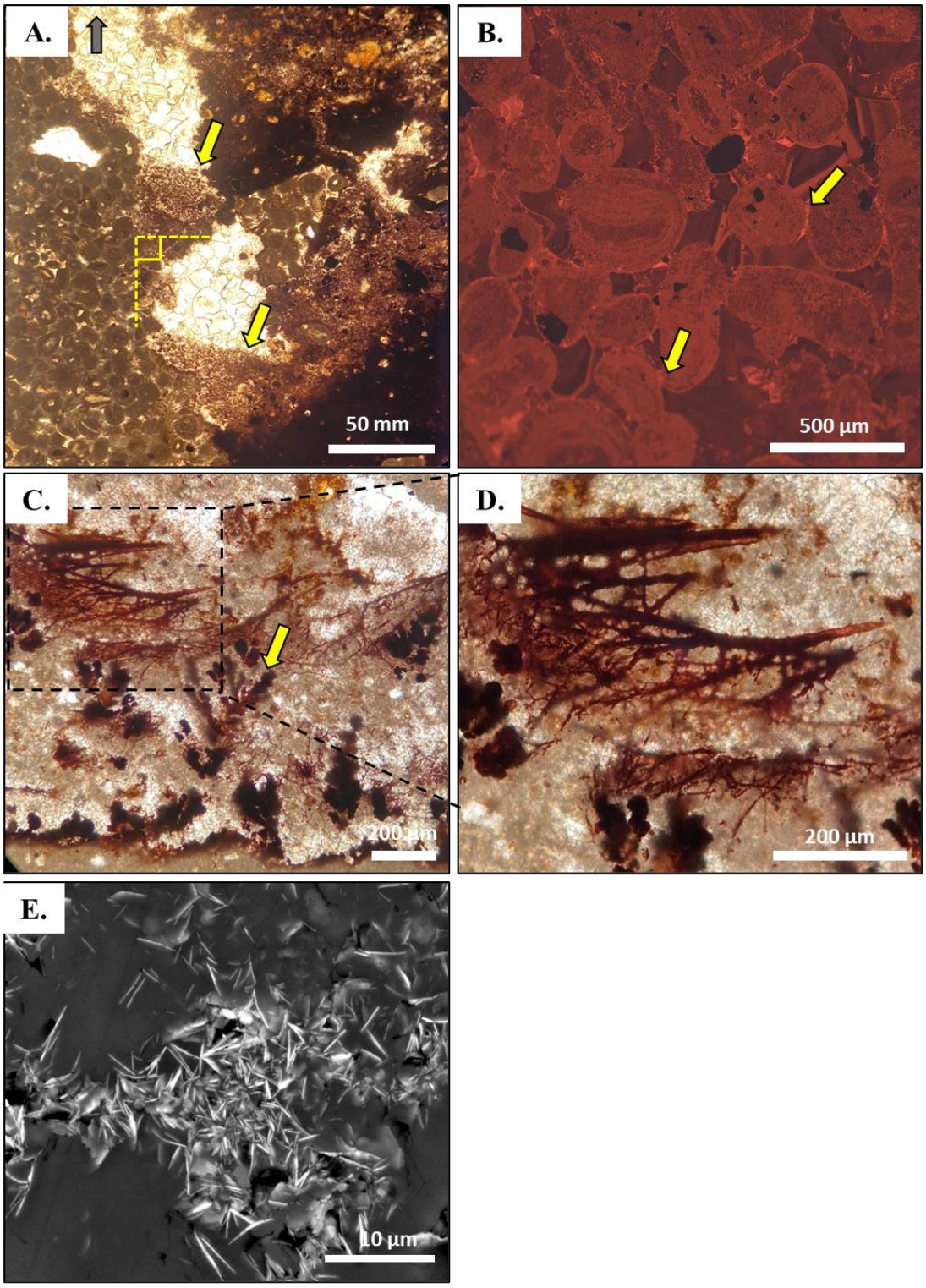

Figure 4.6 Detailed petrography of emergent surface textures A) Geopetal textures (arrows) on cavity walls. Note the way up direction (grey arrow), and that the geopetal infill forms at right angles to this, revealing that the textures were once subvertical. The host rock matrix displays an absence of marine cements and is infilled by micrite (N02505/04 1723.25m) B) An absence of marine cements within these oolitic grainstones are suggested by grain compaction and bridging cements (arrow; N02513/01, 949.7m). C) Frutexites (arrow) and potential filamentous bacteria (box) occurring within emergence cavities within the Pale Beds, in many cases nucleating on initial cavity walls (N02510/05 1664.5m). D) Zoomed in version of Fig.4.6C highlighting branching relationship to filamentous bacteria and hollow tube structures. E) Abiotic alteration textures with disc shaped iron oxide encased by clays (N02505/04 1723.25m).

B) Stylo-nodular limestones: At Tara Deep the locally-termed 'Healed Conglomerate' consists of undolomitised 'ghost nodules' that have diffuse margins sitting within an argillaceous dolomitised matrix (Figs 4.7A & 4.7B). The matrix consists of swarms of interconnected microstylolites which make up a dolomitic stylocumulate matrix. Stylocumulate here refers to insoluble residue accumulated along a pressure-solution surface (Fig. 4.7C). Swarms of microstylolites extend into the sides of nodules and fade out, giving the nodule margin a faint appearance, hence the local mine nomenclature 'Healed Conglomerate', but in some examples autobreccia or mottled textures (Wanless 1979) occur and nodules can tesselate into their original positions (if pictured without the stylocumulate matrix; see Fig. 4.7D & E). Other observations made regarding these textures include, monomict clast composition, and veins/bioclasts are able to be traced across various nodules (separated only by the stylocumulate matrix). Late-phase mineralization has likely enhanced these textures (Fig 4.7F).

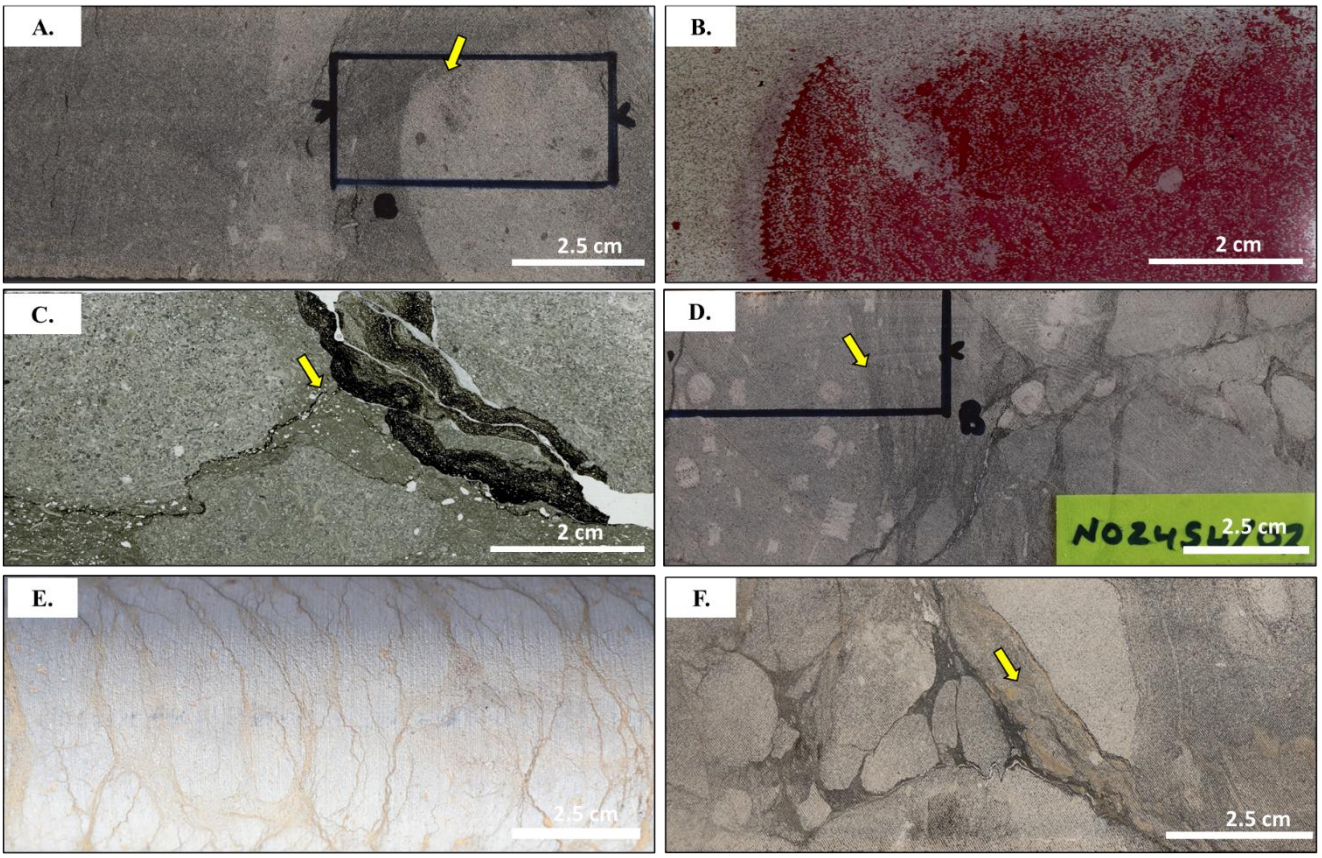

Figure 4.7 Stylo-nodular textures preserved in the Pale Beds at Tara Deep. A) Undolomitized host rock nodule is encased by dolomitized pervasive pressure solution, creating a faint margin to the nodule (arrow). Note thin section region marked (N02454/12, 1083.5 m). B) Thin section scan from Fig. 4.7A stained with alizarin red and potassium ferricyanide, highlighting the stark contrast between the undolomitized nodule and the non-ferrous dolomite stylocumulate matrix. Also note the faint margin to the nodules (N02454/12, 1083.5 m). C) Thin section scan revealing a distinct stylolite with pressure solution seams exploiting and anastomosing (arrow) through the partially lithified matrix of the stylo-nodular textures (N02416/10A, 1401.3 m). D) Stylo-nodular texture, if pressure solution seams were removed, one could tesselate the individual monomict nodules into their original position. Note the margin to the left-hand side nodule (arrow) which shows a faint margin as a function of numerous pressure solution propagating through the sample (N02454/02, 1080.2 m). E) Autobreccia within the Pale Beds, similar examples can be found in the Micrite Unit, this weathered core outlines the anastomosing nature to these pressure solution seams and the high iron content within stylolites (N02531, 931 m). F) Sphalerite, and very minor galena, mineralization (arrow) exploiting and enhancing the stylocumulate matrix between stylo-nodular textures. Note pyrite can also be observed exploiting these textures (N02499/09, 1739.5m).

The Pale Beds, and the associated textures discussed above, are highly variable petrographically. Clean limestones with isopachous marine cements occur within Healed Conglomerate nodules (Fig. 4.8A), whereas in regions where emergent surfaces exist, there is an absence of early marine cements and meniscus cements occur between compacted ooids (Fig. 4.8B -4.8D). Thus, in these emergent surfaces, the absence of marine cements have facilitated compaction and pressure solution at grain contacts (Fig. 4.8F). In regions of clean limestones away from the stylo-nodular textures, well-developed isopachous marine cements exist. The stylo-nodular textures typically occur in regions with a higher

argillaceous content. Many of the pressure solution textures associated with the stylo-nodular Pale Beds, cross-cut bioclasts on nodule margins (Fig. 4.8F) and they themselves are associated with insoluble grains from the original host rock (e.g., jadeite, apatite, quartz, albite, muscovite, illite and zircon; Fig. 4.8E). These minerals are minor components of the Pale Beds and suggest that significant thickness reduction has occurred as a function of pressure solution. These stylolites are always associated with late microcrystalline and framboidal pyrite, with rare sphalerite and galena. These sulfides typically nucleate on pre-existing early sulfides, and in some regions significant iron sulfide mineralization (plus minor late sphalerite) have exploited these textures (Fig. 4.8G & 4.8H).

It is interpreted that these Healed Conglomerate textures are pseudobreccias, created through pervasive pressure solution of a pre-exiting nodular limestone, so called stylo-nodular textures. The texture and processes involved are described in detail by various authors (Logan and Semeniuk, 1976; Wanless, 1979). The origin of the nodular limestone is difficult to constrain through drillholes at a depths of 1.6 km. The close association between this late dolomite (D4; see below) and pressure solution seams suggest it formed as a reactate mineral as a result of burial dolomitization. Reactate is defined by Logan and Semeniuk (1976) as a mineral formed in association with, and because of pressure solution conditions. There is no obvious evidence of bioturbation within these textures.

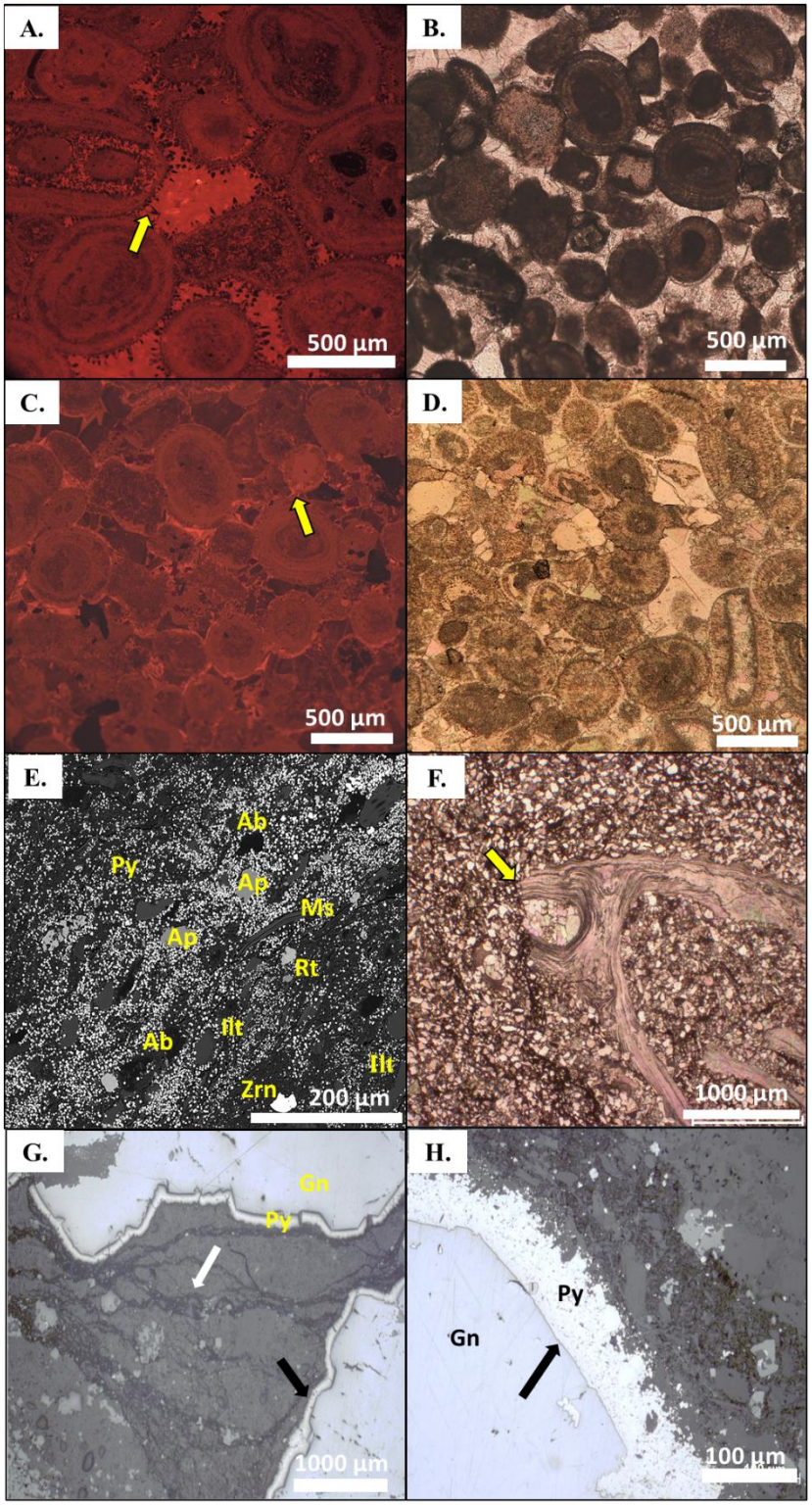

Figure 4.8 Detailed petrography from the Pale Bed stylo-nodular textures. A) Undolomitized oolitic grainstone revealing minor compaction and distinct isopachous marine cements (arrow; N02416/12A, 1459.7) B and C) Plane polarized light image and CL image revealing an absence of early marine cements. Minor compaction and meniscus cements bridge ooids (arrow; N02513/01, 949.7) D) Compaction and subsequent dissolution of ooids at grain contacts due to an absence of early marine cements (N02469/11; 1088.6 m) E) Detailed back scattered electron image from a stylolite within the Pale Beds, highlighting concentrated insoluble minerals from the host rock alongside microcrystalline iron sulfides, suggesting that significant reduction has occurred as these detrital minerals are a minor component of the host rocks. Note mineralization is still able to exploit these stylolite textures. Mineral abbreviations: Albite (Ab), Apatite (Ap), Muscovite (Ms), Rutile (Rt), illite (Ilt), pyrite (Py) Zircon (Zrn) (N02416/10, 1401.3 m). F) Pressure solution reworking pre-existing bioclast. G) and H) Both reflected light images highlight that pressure solution postdates the main phase of Micrite Unit mineralization. Horsetail stylolites (white arrow) is associated with microcrystalline pyrite. Microcrystalline pyrite can be observed nucleating on the margins of pre-existing hydrothermal galena (black arrows; N02445; 1788.1 m)

4.6.3 Zone Two's Syn-rift Stratigraphy:

Zone Two occurs immediately west of the S Fault (Fig. 4.3B), as a steeply dipping (70-80°), structurally complex region of syn-rift origin associated with the Gainstown Terrace.

S Fault Conglomerate (SFC)

In the common hanging-wall of the G and S Faults, a distinct clast-supported sedimentary breccia, known locally as the S Fault Conglomerate (SFC), is composed almost exclusively of sub-angular Pale Beds clasts (~2-10 cm; Fig. 4.9A & 4.9B) and minor Waulsortian limestone clasts. Large (>20m) blocks/rafts of Pale Beds, appear to rest within the upper parts of this package. Within these breccias, clasts of Pale Beds host emergent textures as described above, and the breccia matrix is occasionally exploited by iron oxide staining. However, no stylo-nodular clasts have been found within the SFC. In contrast, when a clast supported matrix occurs, compaction has resulted in inter-suturing between clasts (Fig. 4.9B). The nature of these breccia suggest a local, early debrite origin.

This region is also host to clasts of detrital sulfide and rafts of displaced cavity-fill Micrite Unit mineralization (Chapter 2). Mineralization is also recorded replacing the matrix and encasing pre-existing mineralized clasts within this debrite (Fig. 4.9C). In areas where the SFC is dominated by Pale Beds clasts, the unit contains very high Zn+Pb grades with stringer style replacement mineralization, and allochthonous Pale Beds mineralization (Fig. 4.9C). Detrital sulfide clasts unequivocally reveal that mineralization initiated pre-SFC and the overlying Boulder Conglomerate, highlighting an early syn-rift minimum age for the onset of mineralization (see also Ford 1996; Anderson et al., 1998; Chapter 2). Toward the southeastern end of the S Fault hanging-wall, the S Fault Conglomerate dies out.

4.6.4 Main Rifting Event: Catastrophic Boulder Conglomerate

Stratigraphically above the SFC conglomerates of Zone Two, and the complicated Pale Bed textures of Zone One, much of the upper Tournaisian sediments are absent compared to the normal Navan stratigraphy due to basin subsidence and associated sliding/debrites. Now a complex array of polymict rafts (>6 m thickness) and clasts exist (≥ 3 cm), either as matrix supported (Fig 4.9D) or clasts supported

(Fig 4.9E). These are dominated by the missing limestone units, but locally also contain minor Lower Paleozoic clasts. These have been interpreted as debris flows of at least lower Viséan age (Fig. 4.9D & 4.9E), due to their polymict clast composition and their irregular basal contact. This unit is equivalent to the Boulder Conglomerate at Navan. These slides and associated debrites have scoured through the succession from the north and north-east, subsequently ca.500m of upper Tournaisian pre-rift stratigraphy has been removed (mid-upper Pale Beds, Shaley Pales, Argillaceous Bioclastic Limestone and Waulsortian limestones).

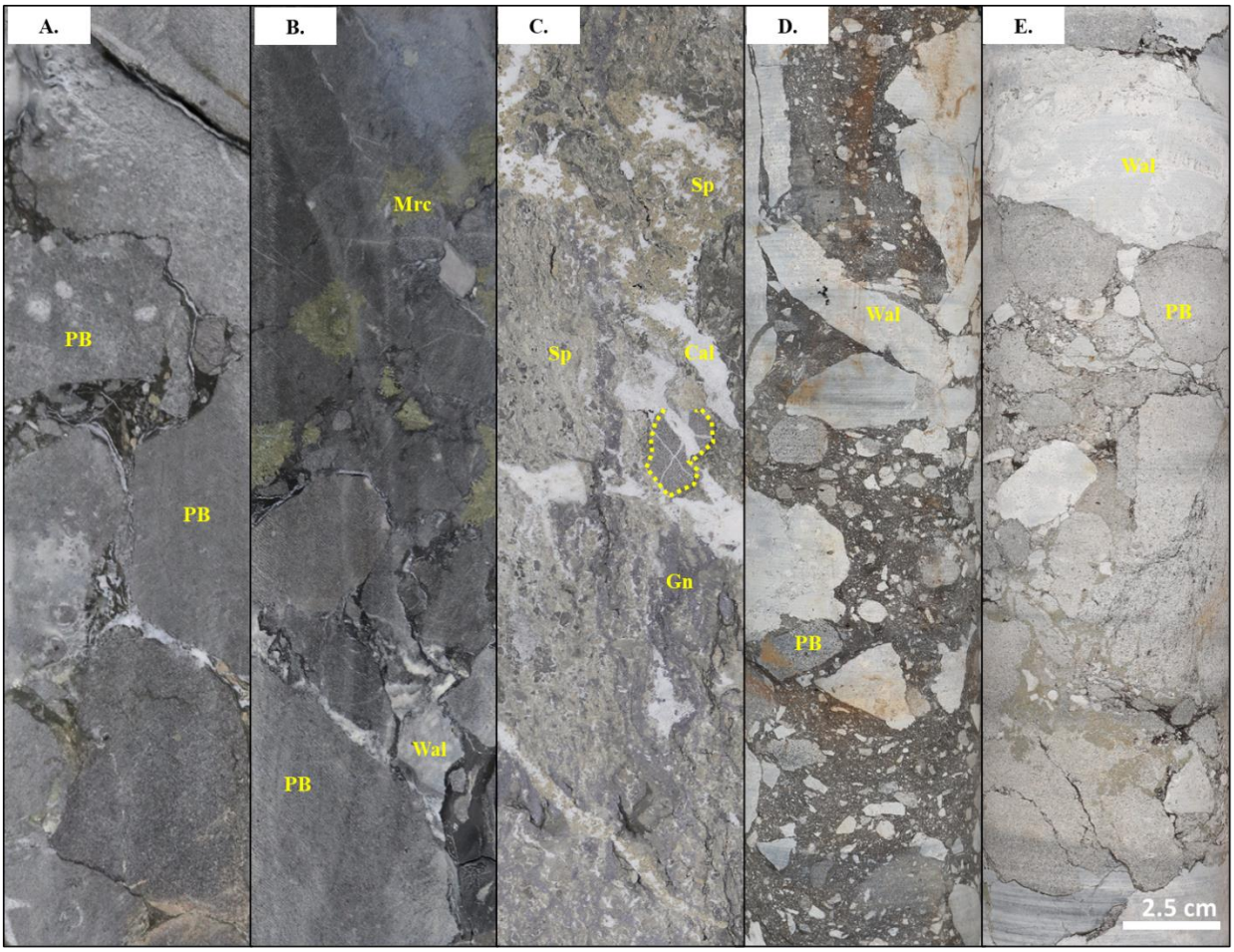

Figure 4.9 Photographs of debris flows in drillcore within the Tara Deep system. A) S Fault Conglomerate (SFC) with Pale Beds (PB) dominated clasts and no preservation of stylo-nodular relationships within clasts. Note the compaction and suturing of clasts as a function of compression. B) SFC with marcasite (Mrc) exploiting the matrix between dominantly Pale Beds (PB) clasts with very minor Waulsortian-like (Wal) clasts C) High grade stringer-style mineralization within the SFC, with sphalerite (Sp), galena (Gn) and microcrystalline pyrite replacing the host rock matrix. Note the small Pale Beds clast (dashed line) highlighting that the initial S Fault Conglomerate has almost been completely replaced. D and E) Lower Viséan rifting event is epitomized by a polymitc conglomerate, equivalent to the Boulder Conglomerate, dominanted by Pale Beds and Waulsortian limestone (associated with stromatactis cavities) clasts. These debris flows can either be matrix supported or clast supported, but they host clasts of the missing upper Tournaisian units eg. Shaley Pales, Argillaceous Bioclastic Limestone, Waulsortian and occasionally Lower Paleozoics.

4.6.5 Late-rift Viséan Stratigraphy: Upper Dark Limestone (Thin-Bedded Unit)

The entire Zone One and Zone Two stratigraphy is overlain by the basal units of the Upper Dark Limestone (UDL), locally termed the Thin Bedded Unit (TBU; Fig. 4.3), which stratigraphically overlies the Boulder Conglomerate. The TBU at the Navan deposit barely exceeds 20m in thickness, however seismic interpretation and drilling reveals that the Thin Bedded Unit at Tara Deep (often termed New-TBU) thickens dramatically across the P and G faults, from around 120m in the east of Zone One, to >600m in the west of Zone Two (Ashton et al., 2018). The TBU can be broken down into several sub-units separated by sedimentary breccias, each of which host variable iron sulfide laminations, manganese staining, and hydrothermal cherts (Yesares et al., 2019, in press). From oldest to youngest, they are termed the TBU-5, TBU-4, TBU-3, TBU-2 and TBU-1, their upper surfaces are defined by distinct polymict breccias which laterally vary in thickness across the region. These breccias have a very similar nature to the underlying Boulder Conglomerate, being both clast and matrix supported and hosting polymict clasts of upper Tournaisian units. However, stylo-nodular textures have been observed within the debrites of the TBU. The TBU in general at Tara Deep shows an absence of bioturbation. It also hosts three prominent tuff intervals (Fig. 4.10A), of which the uppermost is the best preserved just beneath the youngest sedimentary breccia; others have been recorded beneath each respective sedimentary breccia but are poorly preserved. These tuffs do not occur as one thick band, but occur as multiple packages of fine layers (0.5 cm-10 cm in thickness), repeatedly interbedded with calcareous mudstone over intervals of 2 m.

Alongside distinct breccias, numerous soft sediment deformation and early diagenetic textures are preserved in the TBU, these include; load casts (Fig. 4.10B-F), concretions (Fig. 4.10G & 4.10H) and seismites (Fig. 4.10I), all of which are closely related. It is important to note, that similar to the textures observed in the Pale Beds, pervasive pressure solution has exploited these host rocks, and associated textures, and has significantly changed the original fabric. So much so that in places, it has altered the appearance of the initial host rock due to the abundance of pervasive pressure solution seams (Fig. 4.11).

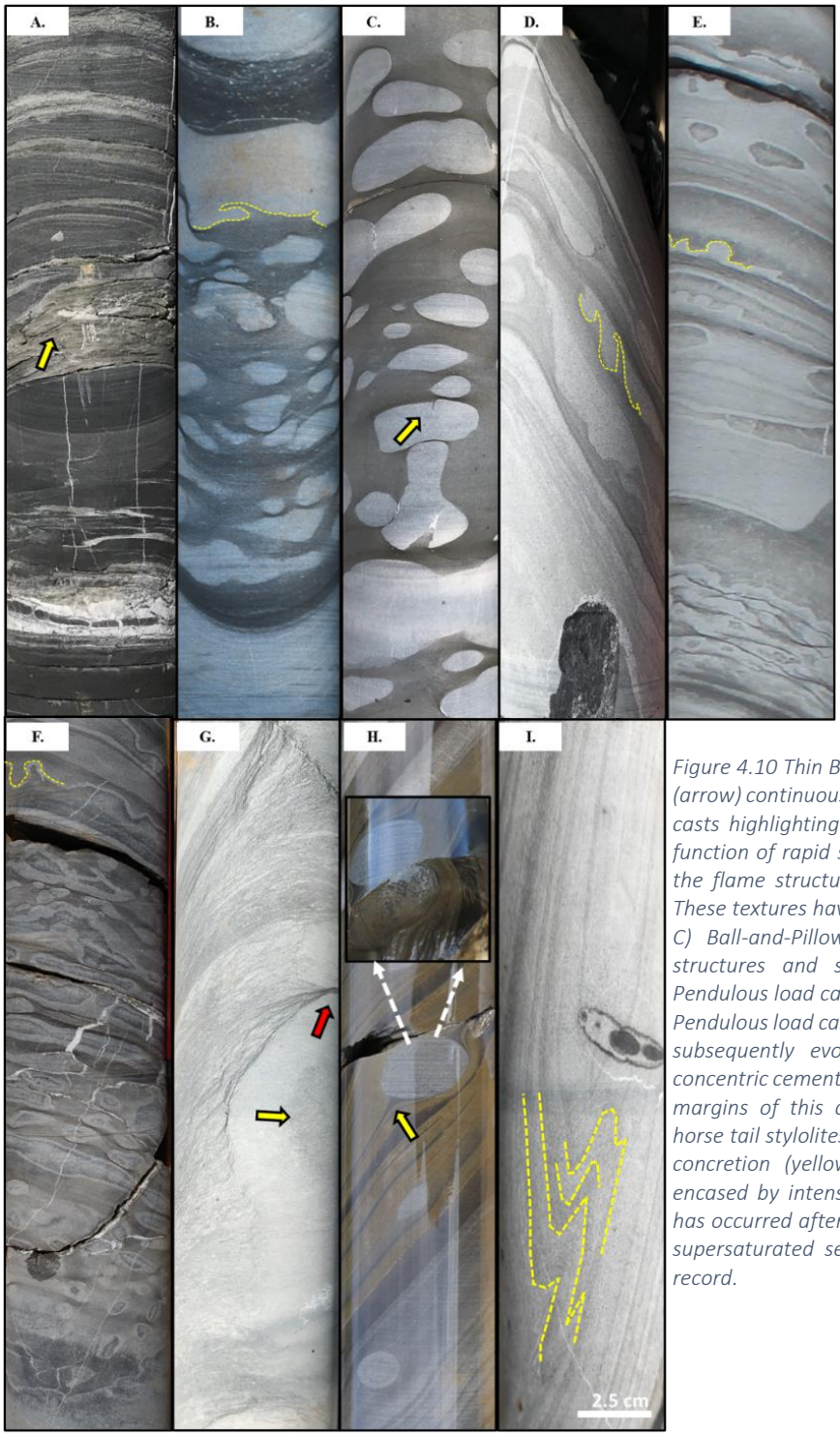

Figure 4.10 Thin Bedded Unit (TBU) drillcore images. A) Tuffs (arrow) continuously interbedded between calcisiltite. B) Load casts highlighting extreme soft sediment deformation as a function of rapid sedimentation and density contrasts. Note the flame structure on the upper contact (yellow outline). These textures have also been exploited by pressure solution. C) Ball-and-Pillow structures within the TBU. D) Flame structures and soft sediment deformation features. E) Pendulous load casts and minor ball-and pillow structures. F) Pendulous load casts and ball-and-pillow structures that have subsequently evolved into zoned concretions. Note the concentric cementation history. G) Zoned concretion, the dark margins of this concretions highlight an accumulation of horse tail stylolites (red arrow). Note the internal core to the concretion (yellow arrow). H) Concretion that has been encased by intense iron sulfide, highlighting mineralization has occurred after an early phase of diagenesis and within a supersaturated sediment. I) Seismites in the TBU drillcore record.

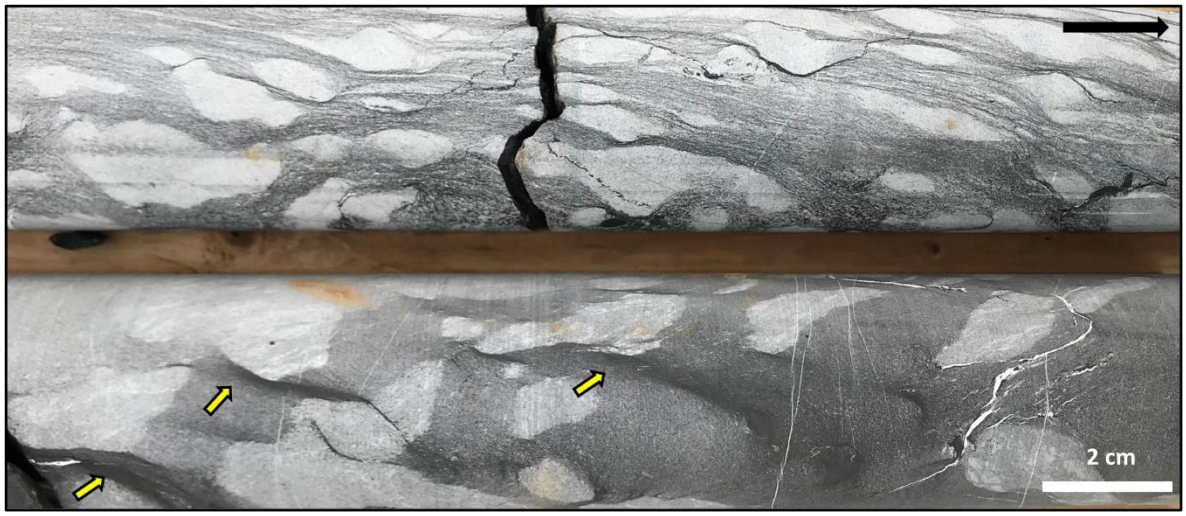

Figure 4.11 NQ drillcores from the same hole (1 m apart) highlighting load casts within the TBU that have been exploited by intense pressure solution. In the lower core, the original host rock fabric is almost completely occluded by pressure solution, but dark shaded regions highlight areas where an amalgamation of pressure solution seams have occurred, similar in nature to the concretion in Fig. 4.10G (N02505, 992.9m).

The load cast classification used here retains the nomenclature and develops descriptive criteria proposed by Allen (1982) and Owen (1987; 2003). Load casts in the TBU, overlying the Tara Deep deposit, occur as laterally continuous undulations at an interface between layers, that once varied in density, with relatively denser sediment above and less dense below (see Anketell et al., 1970). They appear as isolated masses of the overlying material 'floating' in the lower bed. Five varieties of load structures exist within the TBU at Tara Deep, simple load casts, pendulous load casts, attached pseudonodules, detached pseudonodules and ball-and-pillow structures. The most common textures at Tara Deep are globular (~1-6 cm) ball-and-pillow structures, which comprise vertically stacked pseudonodules (Fig. 4.10B & 10C). Many of the pseudonodules show small indents where the neck associated with pendulous load casts have detached. Flame structures (Fig. 4.10D) and pendulous load casts (Fig. 4.10E & 4.10F) are less abundant. These pendulous load casts have narrow necks that attach upper and lower layers, terminating in a bulbous, rounded crest and producing a morphology of teardrops and diapirs.

Many of these load casts develop into concretions (Fig. 4.10G & 4.10H). These concretions reveal marginal zonations from cores to margins. Many of these concretions are encased by iron sulfide (Fig. 4.10H & 4.12A). Both the ball-and-pillow and subsequently the concretion textures are

petrographically similar, they preserve the original fabric and composition of the host rock, dominated by recrystallised calcispheres, which preserve little evidence of compaction prior to lithification (Fig. 4.12B). These calcispheres are several 10s of microns in diameter, preserve a spherical morphology and have simple wall structures which consist of thin concentric layers of radial calcite. Conversely, the host rock, surrounding the concretions, has been significantly compacted, flattened and exploited by pressure solution (associated with nanocrystalline dolomitization and microcrystalline pyrite), ultimately deforming and occluding any pre-existing fabrics (Fig. 4.11 & 4.12 C-F). Some of the ball-and-pillow textures display an elongated augen shape with pressure shadows. Finally, these textures are often closely associated with seismites (30-50 cm) which show a sigmoidal relationship and are commonly found within argillaceous regions of the TBU and attest to seismic activity at the time (Fig. 4.11L).

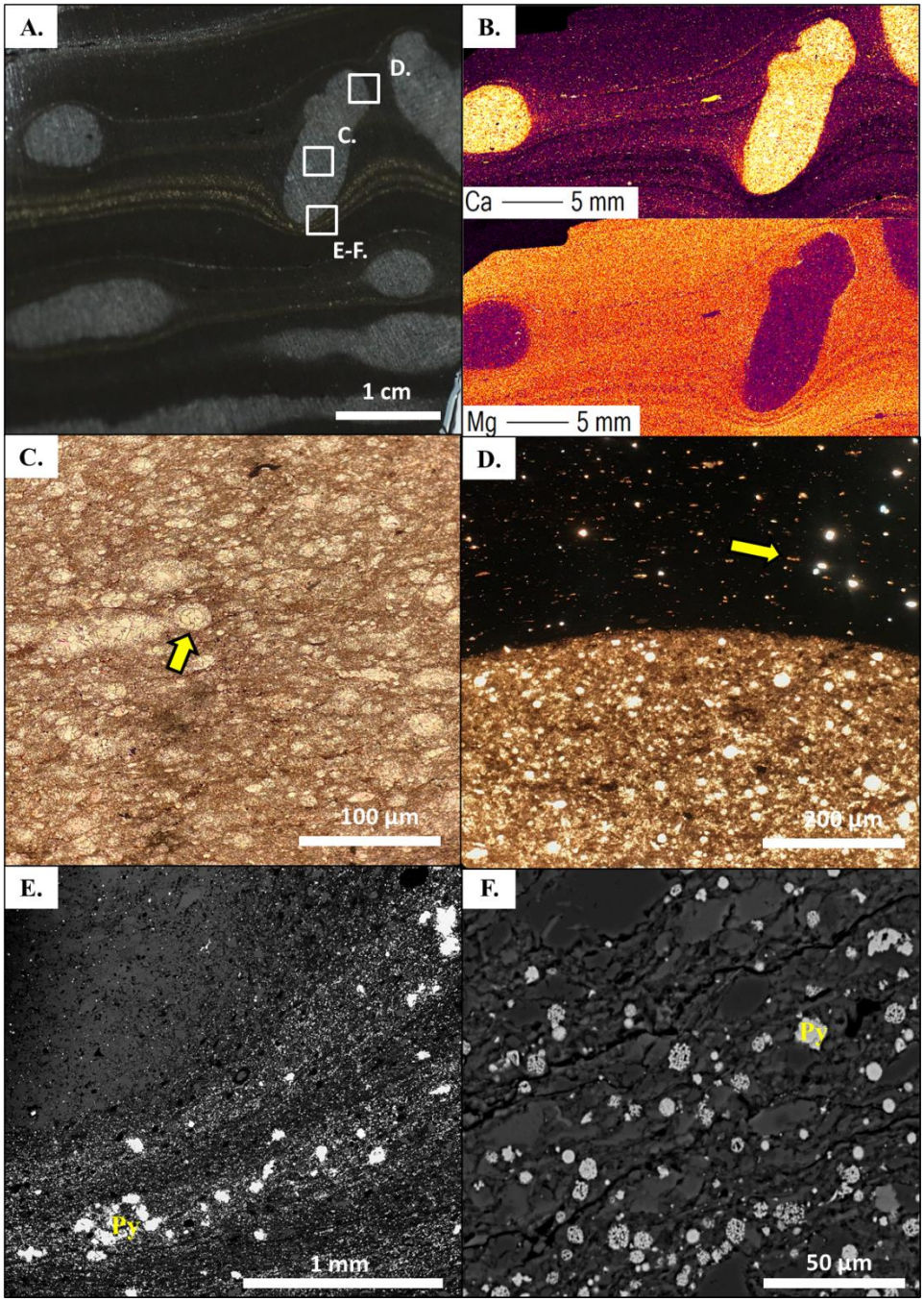

Figure 4.12 Detailed petrography of a ball-and-pillow textures in the TBU (N02454/04; 1103.9 m) A) Ball-and-pillow textures with microcrystalline pyrite associated with regions of pervasive microstylolitization; importantly revealing an element of the mineralization in the TBU was late and during burial and compaction. Boxes show location of figures 4.12C-F. B) Calcium and magnesium elemental maps of this sample highlighting the contrast in chemistry between the load cast and the matrix of the host rock, which has been exploited by pervasive pressure solution, with associated burial dolomitization (D4). C) Recrystallised calcispheres hosted within ball-and-pillow textures, which reveal no evidence of compaction. D) Contrast in cement fabric between the concretions and host matrix. The concretion shows little evidence of internal compaction and is an early diagenetic fabric, whereas the matrix has been compacted, exploited by pressure solution, and calcispheres are now lobate shaped (white arrow). E) Back Scattered Electron (BSE) image highlighting horsetail stylolites are packed full of microcrystalline and framboidal pyrite. F) Zoomed in BSE image from E) highlighting micro-intersuturing of stylolites, associated with framboidal pyrite.

4.6.6 Dolomitization

Dolomitization at Tara Deep is multistage (D1-D4) and occurs across the entire stratigraphic record:

- *D1 early replacement dolomitization* is the dominant dolomite phase within the Pale Beds, particularly within the Micrite Unit subgroup. In plane polarized light, D1 comprises euhedral (30 μm) crystals with cloudy cores, which luminesce pink under cathodoluminescence (CL), indicating Mn enrichment (based on semi-quantitative SEM analyses), they are typically associated with non-luminescent clear rims which quench luminescence, outlining iron-rich margins (Fig. 4.13A & 4.13B). Within the Micrite Unit, this early replacement dolomitization is highly variable and often fabric retentive. It typically preferentially replaces the oolitic-calcarenite horizons within the Micrite Unit; subsequently ghost oolites (Fig. 4.13E) are commonly observed. A distinct dolomitized oolitic-calcarenite horizon in the centre of the Micrite Unit, equivalent to the 5-lens dolomite at the Navan deposit, can be used to divide the package into upper and lower regions, highlighting the laterally continuity of this dolomitization across the region. Replacement dolomitization (D1) of the surrounding Micrite Unit can occur as wholescale replacement or be completely absent. Where complete replacement occurs, the original fenestral textures are occluded - only able to be clearly observed through CL/SEM (Fig. 4.13F-H). D1 dolomite crystal margins have been observed reworked by iron oxide alteration within emergent surface textures and late calcite veining, highlighting an early origin (Fig. 4.13C & 4.13D).
- *D2 dolomite* consists of subhedral (~50 μm), non-luminescent, Fe-rich dolomite (~5 wt% Fe, through semi-quantitative SEM analyses) which infills both interparticle porosity between D1 crystals and fenestral porosity (Fig. 4.13IJ). Both D1 and D2 dolomite are post-dated by Zn-Pb mineralization (Chapter 2).
- *D3 dolomite* is rare within the Pale Beds, consisting of coarsely crystalline (0.5 cm) saddle dolomite (Fig. 4.13K & 4.13L) present within vugs of the oolitic horizons within the Pale Beds. It is often closely associated with coarse locally termed honeyblende sphalerite.

- *D4 dolomite* is nanocrystalline and is closely associated with pressure solution seams that exploit the matrix of both the Pale Beds and TBU. Dolomitization in these regions is scattered throughout the host rock stylocumulate matrix. D4 dolomite does not stain with a combination of alizarin red and potassium ferricyanide, revealing its non-ferrous character (Fig 4.7B; Fig. 4.14).

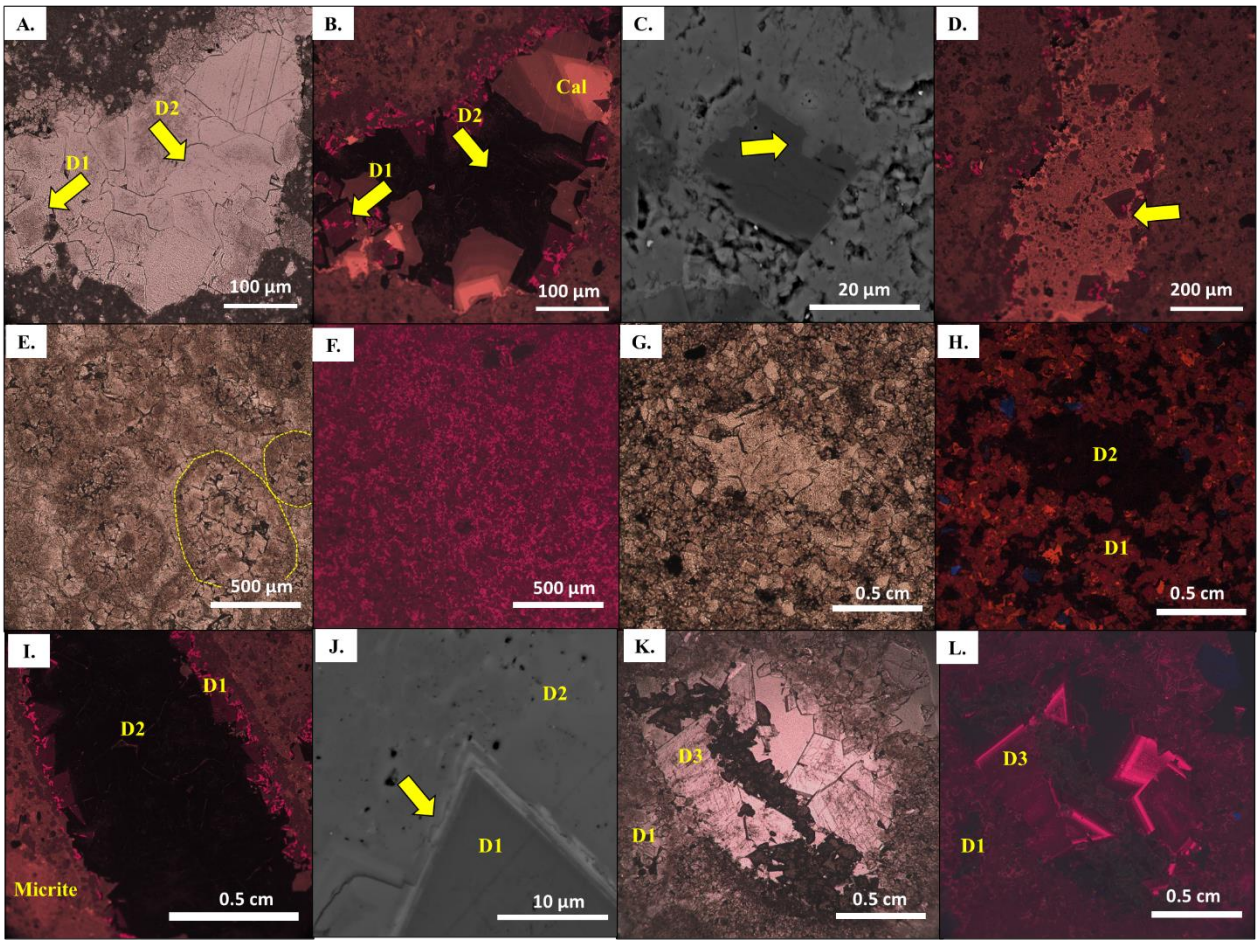

Figure 4.13. Dolomitization relationships (D1-D3) within the Micrite Unit and Pale Beds. A) Fenestral texture within the Micrite Unit. Early, replacement dolomitization (D1) reveals euhedral crystals on fenestral walls, with cloudy cores and a clear rims (black arrow). Subhedral ferroan dolomite crystals infill the remaining space (D2). A final phase of late zoned calcite (cal) exploits any remaining interstitial space (N02454/13, 1095.3 m) B) Same field of view under cold cathodoluminescense revealing that early replacement dolomite (D1) are characterised by Mn enrichment (pink luminescense) with a black Fe rich rim that quenches luminescence. This is later infilled by ferroan dolomite (D2; N02454/13, 1095.3). C) Early diagenetic replacement dolomite (D1) is crosscut by iron oxide that exploits emergence surface cavities and the host rock matrix). D) Early replacement dolomitization (D1) is crosscut by calcite veining. E) Fabric retentive replacement dolomitization (D1), highlighted through ghost ooids (plane polarized light; N02499/14, 17262.25 m); and F) the same field of view through cathodoluminescense revealing a complete replacement of the host rock fabric (N02499/14, 17262.25 m) G and H) Plane polarized light and cathodoluminescent image revealing a preservation of the original texture. Dolomitization has completely replaced the host rock (D1) whereas the fenestral texture has been infilled by ferrous dolomite (D2) which quenches luminescence. On the hand sample scale any evidence of fenestral textures are lost see Figure 4.4D. I) Fenestral texture from the Micrite Unit. The initial micritic mud has been partially replaced by dolomite (D1), whereas the fenestral porosity has been infilled by ferrous dolomite (D2; N02454/13, 1095.3 m). J) Early replacement dolomite (D1) has been marginally corroded by ferroan dolomite infill (D2; N02334/13 1815). K) Plane polarized light and L) cathodoluminescent image of late, zoned saddle dolomite (D3) occurring within a vuggy oolitic grainstone within the Micrite Unit (N02505/18, 1815.8m).

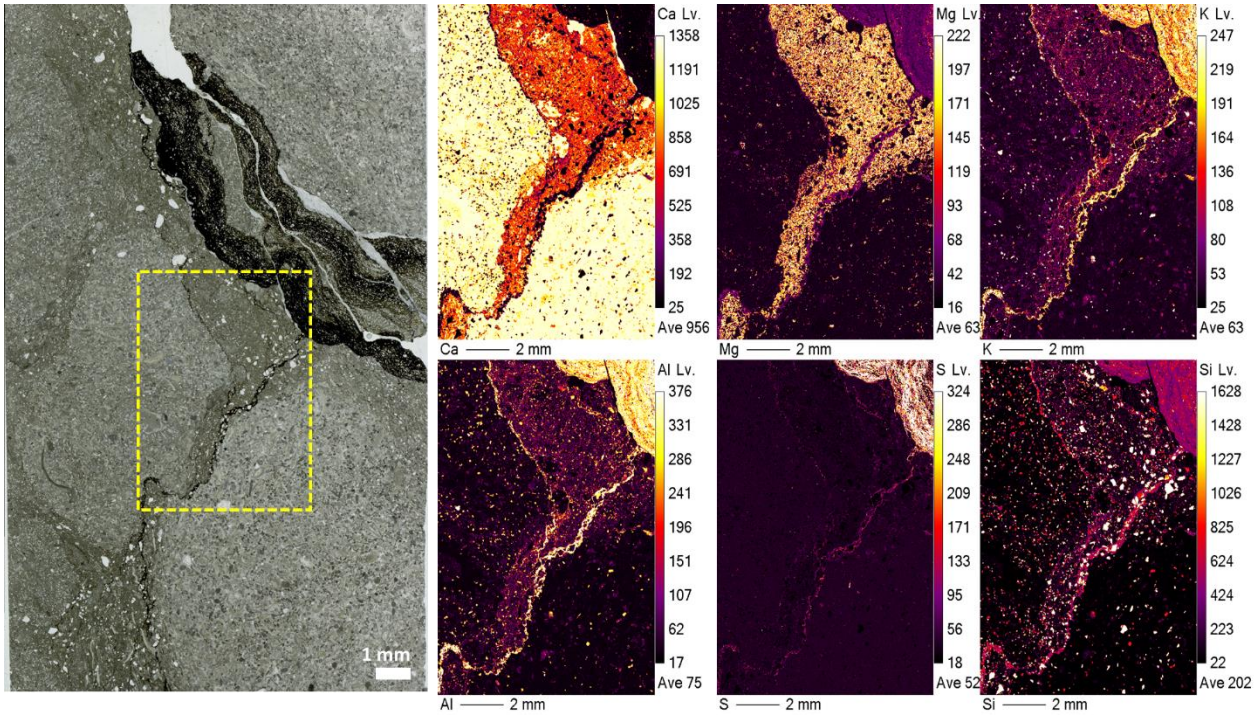

Figure 4.14 Thin section scan of stylo-nodular textures within the Pale Beds with associated energy-dispersive X-ray spectroscopy maps. Stylolite (arrow) can clearly be seen anastomosing its way through the nodular carbonate, thus changing the chemistry and appearance of the host rock matrix. Pressure solution is associated with burial dolomitization (D4; Mg) and the formation of clays (Al, Si, K). These textures have been enhanced and exploited by metalliferous fluids, dominantly microcrystalline iron sulfide (S).

4.6.7 Oxygen and Carbon Isotopes

Analyses of oxygen and carbon isotopes within these paragenetically well-constrained carbonates reveal that undolomitized Pale Beds have $\delta^{18}O$ ranges of 24 ‰ to 26.9 ‰ and $\delta^{13}C$ = 0.9 ‰ to 4.1 ‰ (n=12), and TBU primary calcite ranges from 25 ‰ to 26.9 ‰ and 2.4 ‰ to 3.3 ‰ (n=3). Micrite mud which infills emergent surface textures show $\delta^{18}O$ from 25.3 ‰ to 27.9 ‰ and $\delta^{13}C$ from -5.1 ‰ to 3.9 ‰ (n=9). Two concretions in the TBU show the heaviest O isotope values and lowest C isotope values of all carbonates at Tara Deep, ranging from 26.3 ‰ to 28.2 ‰, and -14.2 ‰ to -8.3 ‰ respectively. The nodules, within the stylo-nodular texture, have $\delta^{18}O$ ranging 24 ‰ to 28.1‰ and $\delta^{13}C$ from 1.6 ‰ to 4.5 ‰ (n=7), almost identical to those associated with undolomitized regions of the Pale Beds, whereas the surrounding dolomitized stylocumulate matrix have $\delta^{18}O$ from 22.8 ‰ to 25.5 ‰ and $\delta^{13}C$ of 1 ‰ to 4.6 ‰ (n=6). At the scale of the technique (~1-2mg per sample), it proved impossible to separate the D1 and D2 phases of dolomitization, so their signatures - $\delta^{18}O$ from 20.8 ‰ to 22.9 ‰ and $\delta^{13}C$ from

0.8‰ to 3.4 ‰ (n=16) - represents an amalgamation of these two phases. These ranges are similar to calcite veining in Tara Deep which vary from $\delta^{18}O$ 19.1 ‰ to 23.2 ‰ and $\delta^{13}C$ -2.5 ‰ to 2.3 ‰ (n=14) in areas with significant mineralization, to $\delta^{18}O$ from 20.6 ‰ to 22.1 ‰ and $\delta^{13}C$ of 0.3 ‰ to 1.8 ‰ (n=5) in regions without mineralization.

4.7 Discussion

4.7.1 Genetic Model for the Pre-Rift to Late-Rift Stratigraphy at Tara Deep

Tara Deep is located within a complex, tectonically active rift basin, in which primary depositional textures have been pervasively overprinted by dolomitization, mineralization and pressure solution processes. These diagenetic processes not only occlude the original fabric, but they also generate textures which add complexity and foster misinterpretation, and consequently they are discussed last. A number of key lithofacies and associated textures can be used to outline the depositional environment associated with the Tara Deep deposit. A schematic genetic model for the formation of Tara Deep is presented in Fig. 4.15. This model splits the stratigraphy into three stages (1) Pre-rift sequences: a shallow dipping carbonate ramp (2) syn-rift: platform detachment, debrites and footwall failure and (3) late rift: basin infill. These will now be discussed in turn.

Pre-Rift Sequences At Tara Deep: Shallow Dipping Carbonate Ramp

A number of features within the upper Tournaisian sequences define a shallow intertidal carbonate and inner ramp setting. The Laminated Beds host a distinctive opaline quartz horizon, interpreted as a diagenetic replacement of anhydrite (also seen at the Navan deposit; see Rizzi, 1992), suggesting a peritidal to subtidal, and occasionally emergent environment, when the region was situated just north of the equator (Rizzi, 1992; Scotese, 2001). The overlying Muddy Limestone (Fig. 4.4B) hosts dark, well-bedded argillaceous and crinoidal limestone with prominent bioclastic horizons and oncolites. Syringopora reticulata, brachiopods and other bioclasts reflect deposition in a shallow marine or lagoon setting. The Micrite Unit is a fenestral limestone (Fig. 4.4C) which is interpreted to be a low energy,

peritidal unit. The central oolitic horizon that divides the Micrite Unit, likely represents a shift to higher energy conditions. The Micrite Unit is succeeded by thick packages of higher energy, shallow marine (<10m), oolitic grainstones of the overlying Pale Beds (Fig. 4.5). Emergent surfaces within the Pale Beds (Fig. 4.5) attest to this shallow marine depositional environment, with geopetal textures on cavity walls (Fig 4.6A) revealing that they were once open fissures and likely formed perpendicular to the sea-floor. These surfaces are interbedded by thick packages of nodular limestone. Both emergent surfaces (Fig. 4.5 & 4.6) and the overlying nodular limestone textures (Fig. 4.7) repeat themselves several times. The exact number of packages and thickness of the Pale Beds is unknown at Tara Deep due to the overlying erosion surface which truncates the pre-rift stratigraphy. However, Rizzi and Braithwaite (1996) record up to 44 peritidal to shallow shelf depositional packages within a complete sequence of Pale Beds within the Navan deposit. The high degree of lateral continuity, albeit with minor local variation, of these carbonate packages across the Navan (Philcox 1989; Rizzi, 1992; Strogen et al., 1996) and Tara Deep area (~ 5 km^2) suggests that these units were likely once extensive and deposited within the inner part of a shallow dipping carbonate ramp. No channels have yet been identified at Tara Deep, but to the north of the Navan deposit a series of channels exist within the Laminated Beds, Muddy Limestone, and Micrite Unit. Various authors have described these as having a similar size and shape to coastal channel systems which dissect modern tidal flats, lagoons and barrier island deposits (Phillips and Sevastopolo, 1986; Rees 1987; Rizzi and Braithwaite, 1997; but also, Anderson, 1990; Strogen, 1996; Ashton et al., 2015). The channel assembly within these units trends generally N-S. Significantly, these channels, at four stratigraphic levels, formed in essentially the same palaeogeographic position, pointing to a well-established and long-lived drainage system to the north of Navan at this time. In addition, there is no regional evidence for significant topographic relief at this time, but the preservation of local clastic/detrital sediments within these channels suggests that Navan and Tara Deep once represented a land-attached platform with the hinterland to the north (Anderson, 1990; Rizzi, 1992; Ashton et al., 2015).

Evidence of subaerial emergence and shallow marine conditions have already been referred to elsewhere in the North Irish Midlands. Harwood and Sullivan (1991) document palaeosols from the upper Tournaisian Moyvoughly Beds, at Moyvoughly, 50 km west of Navan. Pickard et al. (1992) described the oolitic grainstones at Kentstown, ~15 km ESE of Navan in which meniscus cements and rhizoliths are well developed. Rizzi and Braithwaite (1996) document a green mudstone within the Micrite Unit in the NE of the Navan deposit area which hosts clay cutans, a sepic-plasmic fabric, circum-granular cracks, micritized grains and faecal pellets filling burrows, which the authors deem to provide evidence of pedogenesis.

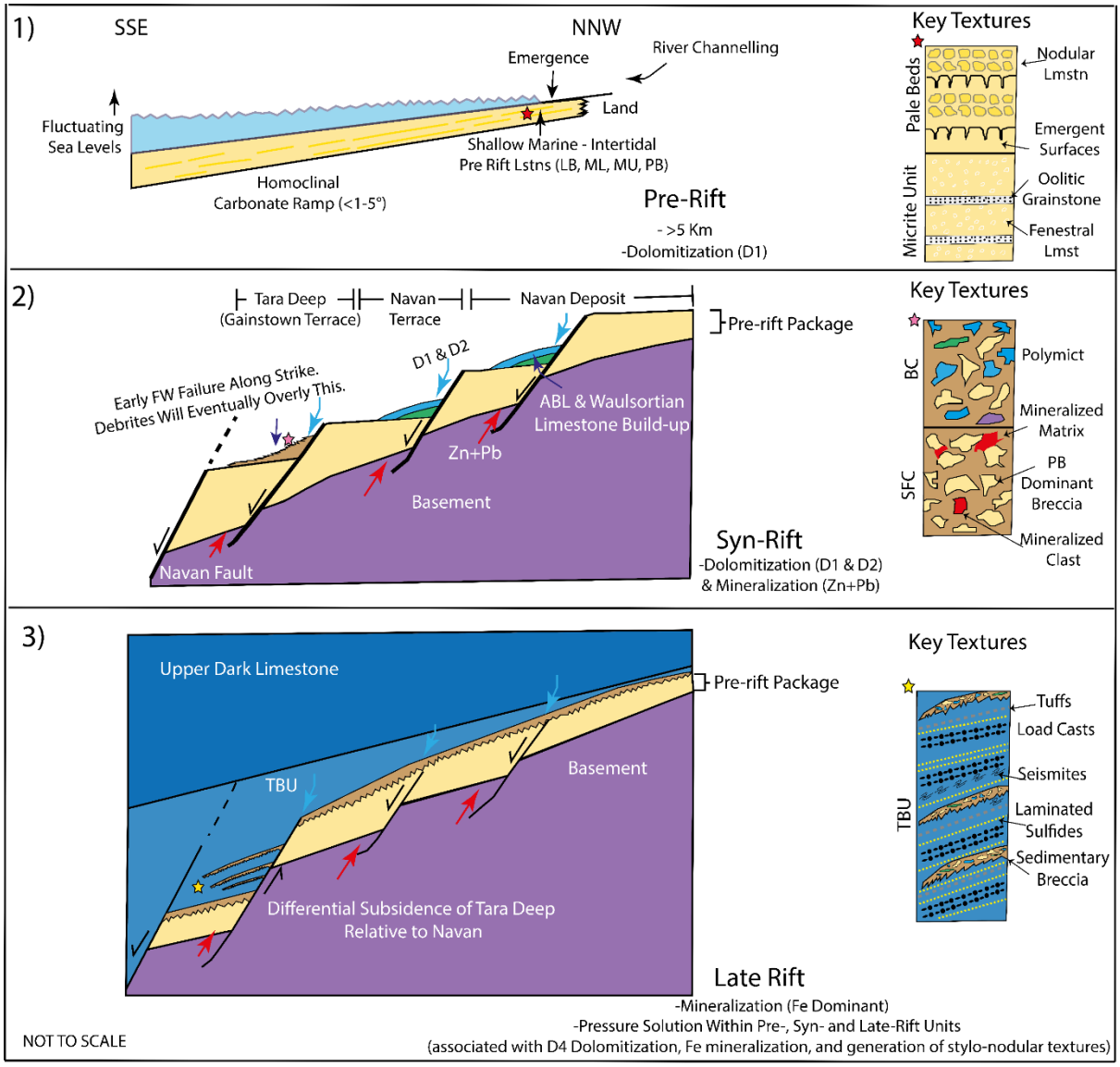

Figure 4.15 Cartoon schematic showing generalized concept of footwall degradation at Tara Deep and Navan. Broken down into 1) Pre-rift: Shallowly Dipping Carbonate Ramp, 2) Syn-rift: Platform Detachment, Debrites and Footwall Failure and 3) Late rift: Basin Infill. Model highlights the close association between basin development, evolving carbonate depositional environments, and mineralization.

Syn-Rift Sequences At Tara Deep: Platform Detachment, Debrites and Footwall Failure

From the upper Tournaisian to lower Viséan, growth faulting along this northern margin of the Dublin Basin began to exert a significant influence on the type and thickness of sediment deposited, particularly with regards to the Argillaceous Bioclastic Limestones and Waulsortian limestone. Signs of tectonic instability became increasingly marked through the lower Viséan. During this period across the Dublin Basin, differentiation into platform and basin facies becomes increasingly marked due to rifting (Strogen et al., 1996). At Tara Deep, the earliest debrites (e.g., SFC) and intraformational debris flows (e.g Boulder Conglomerate; see also Ford, 1996), highlight footwall instability associated with basin margin subsidence. For the Dublin Basin, it is generally accepted that the Boulder Conglomerate, represents the most catastrophic phase of rifting, however the Boulder Conglomerate likely represents numerous catastrophic basin margin processes (Boyce et al., 1983). The Boulder Conglomerate represents a more regional (~5km), rather than localized (<0.5km) event, constituting various debris flows, slumps and sliding events.

Three lines of evidence suggest that a palaeotopography, associated with early rift-related syn-sedimentary faulting, existed well before the formation of the Boulder Conglomerate: 1) Debrites at both Tara Deep and Navan are gravity driven, usually triggered by seismicity and/or oversteepening of slopes (Read, 1985; Barnaby and Read, 1990; Moscardelli and Wood, 2008; Tournadour et al., 2015), and slope instability had to be generated prior to this catastrophic event. 2) Early syn-sedimentary faults appear to be cross-cut by the Boulder Conglomerate (Fig. 4.3) and since the S Fault Conglomerate at Tara Deep stratigraphically underlies the Boulder Conglomerate, early faulting and sliding were clearly occurring within the Pale Beds well before this. Subsequently rafts of Pale Beds and Micrite Unit mineralization are now displaced into the S Fault hanging wall (see also Chapter 2). 3) Finally, the Argillaceous Bioclastic Limestone and Waulsortian limestone, to the NW of the Navan deposit (Fig. 3A), thickens on the hanging wall of syn-sedimentary faults, highlighting differential subsidence before the lower Viséan debris flows (see also Ashton et al., 2018).

Late Rift: Basin Infill

After the regional debris flow events that truncated much of the upper Tournaisian stratigraphy, the Tara Deep area remained seismically active. The Thin Bedded Unit comprises the TBU-5, TBU-4, TBU-3, TBU-2 and TBU-1, each of which are overlain by distinct debris flows. Tectonic events had the greatest control on the gross pattern of carbonate facies distribution, with the TBU displaying a series of soft sediment deformation features (Owen, 2003; Allen 1982; Barnaby and Read, 1990), seismites and debrites (Fig. 4.9 & 4.10). At Navan, the Thin Bedded Unit barely exceeds 20m in thickness, however seismic interpretation and drilling reveals that the Thin Bedded Unit at Tara Deep thickens dramatically across the P and G faults, from around 120m in the east of Zone One, to >600m in the west of Zone Two.

Experimental evidence indicates that there is a progressive increase in the extent of soft sediment deformation from simple load casts, also known as flame structures, to ball-and pillow structures (see Owen, 2003; but also Kuenen 1958; Anketell *et al.* 1970; Allen 1982; Moretti et al., 1999). The Tara Deep examples mostly resemble extreme soft sediment deformation load casts, so called ball-and-pillow textures (Fig. 4.10C), where the hanging lobe has become almost or completely detached from the overlying bed, resulting in apparently isolated masses of the overlying material 'floating' in the lower bed. However, more simple flame textures (Fig. 4.10B) and pendulous load (Fig. 4.10D-E) casts can also be observed. The geometry of these ball-and-pillow structures are typically rounded to augen shaped with associated pressure shadows (Fig. 4.11 & 4.12), which may reflect an element of shearing, however their geometry can also be modified by lateral stresses related to slopes, currents or hydraulic gradients affecting the flow of pore water (Allen 1985; Dasgupta 1998; Moretti *et al.* 2001).

Preliminary attempts have been made to identify criteria that allow the identification of triggering agents from the characteristics and context of preserved soft sediment textures (Sims 1975; Seilacher 1984; Alfaro et al. 1997; Molina et al., 1998; Rossetti 1999; Jones & Omoto 2000). Notwithstanding the fact that these stratigraphic observations are made from drill cores taken at depth,

it appears that the Tara Deep load casts are laterally extensive, recurring horizons, and that they also occur in close association with seismites and between debrites, suggesting that seismic activity was the most likely triggering agent for soft sediment deformation within the TBU package at Tara Deep. Furthermore, these textures are hosted within a tectonically active basin margin and are both underlain and overlain by large debrites. The thickness of the TBU at Tara Deep reveals a high rate of movement on the G Fault. It seems improbable that the enormous amount of new accommodation- well over 600m - could be accommodated in a single tectonic event, thus the region likely remained seismically active for a considerable length of time. All in all, the TBU indicates rapid sedimentation of packages that contrast in density and rheology – a highly unstable sedimentological setting, below the level of benthic carbonate production (>200 m).

4.7.2 Diagenetic Modification of the Stratigraphy at Tara Deep

Dolomitization

The Pale Bed and TBU textures at Tara Deep suggest that at least four generations of dolomitization occurred. These stages can be broken down into early replacement (D1), ferroan dolomite interparticle infill (D2), with later phases involving saddle (D3) and burial dolomitization (D4).

Understanding the timing of dolomitization within this tectonically dynamic region is complex, but similar to mineralization (Chapter 2), dolomitization is multiphase and has occurred over a significant period of time, synchronous with basin margin development. The close link between mineralization and dolomitization (Ashton et al., 2015) highlights similar fluid flow processes - with fluids capable of exploiting fault conduits (Blakeman et al., 2002), intraparticle porosity and stylolite seams (Fig. 4.13 & 14). D1 replacement dolomitization (30 μm) likely reflects reflux dolomitization (Warren, 2000) because of the shallow marine-intertidal setting and because of its laterally extensive (>5 km), stratabound and fabric retentive nature. Both D1 and D2 (50 μm) predate mineralization, thus they are early and not related to deep basin dolomitization processes. D3 (>1cm) is rare but appears much later because it occurs in vugs and is closely associated with late honeyblende sphalerite (Chapter 2). The origin of both D2 and D3 is ambiguous but they are deemed to reflect higher temperature,

potentially hydrothermal dolomitization, because D2 is ferrous and infills interparticle/fenestral porosity, whereas D3 is closely associated with vuggy porosity and mineralization. However, it is likely that D2 and D3 are temporally distinct. The rare preservation of D3 within the Pale Beds may be a function of the occlusion of porosity through earlier dolomitization and mineralization events. Finally, D4 is nanocrystalline and occurs as a function of burial dolomitization due to its close association with pressure solution seams (see Wanless 1979, McHargue and Price 1982; Sternbach and Friedman 1984).

TBU Concretions

Concretions in the TBU at Tara Deep record pre-compaction textures, where concretion cements formed early in the diagenetic history, i.e., before significant burial. No significant compaction to internal microfossils has been observed. Some concretions developed from initial load cast structures, which have been used as nucleation sites to act as the main growing point for concretions (Fig. 4.10F). There is a clear overlap between load cast development and concretion formation because their internal compositions are identical, and because concretions have been observed forming around pendulous load casts (Fig. 4.10E &F). From the abundance of soft sediment textures in the TBU, the region was likely supersaturated with respect to marine water, and subsequently concretion growth has been facilitated by these super-saturated conditions, which enable transport of ions to nucleation sites via diffusion (Marshall and Pirrie, 2013)

Pressure Solution

Pressure solution has been recognised for many years as the cause of sutured stylolites seams and grain contact structures (e.g Sorby 1879, 1908; Stockdale, 1922, 1926, 1936, 1943; Dunnington, 1954); yet assessment of the general significance of pressure solution in limestones or how it fits specifically into a general scheme of diagenesis is rarer (Folks, 1965; Logan and Semeniuk, 1976; Wanless, 1979). Specific limestone units (beds, structures, or grains) may be preferentially resistant or responsive to change, and with or without impurities that will strongly influence the character of change (especially magnesium ions and clay particles). This is crucial to understand because pressure solution is recorded throughout the entire Tara Deep stratigraphy; within the Micrite Unit (Fig. 4.4C), between clasts in the

SFC (Fig. 4.9A), and across various TBU textures (Fig. 4.10 & 4.11). Each unit will have responded differently depending on the stress enforced, the rock composition and the responsiveness of various horizons within and between each unit (Wanless, 1979).

Pervasive pressure solution of a pre-existing nodular limestone, is the likeliest interpretation to explain the origin of the locally termed 'Healed Conglomerates' within the Pale Beds. These textures resemble stylo-nodular textures, or non-seam solution as described by Wanless (1979), formed by pervasive solution thinning of a unit that has little or no structural resistance to stress. Other origins such as large-scale breccia structures associated with collapse of epigenetic karsts (Hamilton and Ford, 2002; Lucia, 1995), cavern collapse sinkholes (Salvati, 2002), channelling, bioturbation, and minor debris flows, can be ruled out because they are inconsistent with A) the monomict clast composition (Fig. 4.7C). B) The laterally continuous nature of the Healed Conglomerates (>2 km^2), C) the lack of evidence for internal clast rotation associated with bioturbation, D) the absence of regolith material, and E) the subrounded often isolated nodule shape. Furthermore, these other mechanisms do not explain the faint clast margins (Fig. 4.7D), the ability to tessellate nodules into their original position if imagined without stylocumulate matrix, the relatively homogeneous size (5-10 cm) and shape, and the pressure solution relationship that exists with subsequent dolomitization of the stylocumulate matrix, whereas the nodule remains undolomitized (Fig. 4.14). Finally, the stratigraphic contact between the Pale Beds and the underlying Micrite Unit shows no evidence of erosion.

In summary, the stylo-nodular textures within the Pale Beds are brought about because the nodular limestone matrix has no internal structural resistance to stress, and thus responded to compaction by pervasive pressure solution through the matrix, whereas the nodules remain competent and are not exploited by pressure solution. The repeating packages of nodular and emergent textures within the Pale Beds reveals the unit was deposited under fluctuating condition. The stylocumulate matrix between nodules now consists of pre-existing grains that are concentrated as an insoluble residue (Fig. 4.8E) and are associated with nanocrystalline dolomite which formed as a reactate mineral (D4; Fig. 4.7B).

Similar textures to the stylo-nodular limestones at Tara Deep exist within the Upper Silurian Tonoloway-Keser Ls., Mifflin Co., Pennsylvania (Scholle and Ulmer-Scholle, 2003), Kayin Stat, Southeast Myanmar (Udchachon et al., 2018), Argentine Precordillera (Gomez and Astini, 2015) and Southern England (Garrison and Kennedy, 1977). A similar nodular, clayey limestone facies occurs in the Middle Cambrian Muav Limestone through the Grand Canyon, Arizona (Wanless, 1979). It appears these nodular limestones are also documented within a range of environments, such as foreslope environments from Miette and Ancient Wall Build-ups (Upper Devonian), Alberta (McIlreath and James ,1978) to shallow marine settings with examples discussed in South Tibet, China (Kahsnitz and Willems, 2019) and even restricted intrashelf, mixed shallow subtidal and peritidal environments (Gomez and Astini, 2015). It is clear that more work needs to go into cataloguing these textures globally.

A number of key conclusions can be made from these textures 1) The recognition that these are pseudobreccias, and not debrites, rules out any misinterpretation for basin reconstruction, especially in terms of interpreting palaeotopography or interpreting very early rifting of the Dublin Basin. 2) A large volume reduction is anticipated as a result of compaction. Logan and Semeniuk, (1976) document that reductions of up to 80% can occur. The volume loss at Tara Deep is unknown, but it has important implications for interpreting lithology thickness variations and textures. Differential compaction may reduce the true thickness of facies. 3) The ability for pressure solution seams to exploit and propagate extensively through the Pale Beds matrix (Fig 4.7C), and soft sediment textures in the TBU (Fig. 4.11), highlights that these facies were likely partially lithified, and subsequently rapidly buried and exposed to significant stress relatively early in their diagenetic history, this suggests that basin subsidence occurred relatively quickly and aggressively in the Tara Deep region. Although the stylo-nodular textures have never been reported for Navan, there are similar examples recorded in the literature as 'Nodular Markers' (Anderson et al., 1998; Rizzi, 1992). These textures display similar relationships as the stylo-nodular textures at Tara Deep. However, the textures are clearly much more widespread (>2 km^2) and better developed at Tara Deep, likely reflecting differential subsidence between the two areas. 4) Tara Deep clearly shows late phase sphalerite and iron sulfide (with minor

galena) exploiting pressure solution regions (Fig. 4.7F, 4.8G & H) suggesting that metalliferous fluids are still capable of exploiting these late diagenetic textures.

4.7.3 Isotopic Constraints

Textural complexity and consequences for isotope data: Given the intimate intergrowth of carbonate phases, for example D1 and D2 dolomite in the Micrite Unit (Fig. 4.13H), and ghost margins to the Healed Conglomerates encased by a dolomitized (D4) stylocumulate matrix (Fig. 4.7B), in conjunction with the scale of isotopic analyses (1-2mg), it was difficult to ensure that the results were from single phases of carbonate. Consequently, the interpretation of the data should be viewed with caution. Nonetheless, some process parameters can be outlined.

Early diagenetic cements: Calcite in earliest phases of the Micrite Unit and Pale Beds range from $\delta^{13}C$ of 0.9 ‰ to 4.1 ‰ and $\delta^{18}O$ from 24 ‰ to 26.9 ‰ (n=12), with averages of 2.2 ± 0.9‰ and 25.5 ± 0.8‰ respectively. Geopetal micrite infill of early emergent surfaces $\delta^{18}O$ ranges up to 27.9‰, averaging 26.1 ± 0.8.‰, with $\delta^{13}C$ averaging 1.7 ± 2.6‰. In the TBU unit, calcilutite $\delta^{18}O$ averages 26.0 ± 0.8‰, and $\delta^{13}C$ 2.8 ± 0.4‰. Assuming Mississippian seawater has a $\delta^{18}O$ similar to today around 0‰ (Mii et al., 1999), then these early diagenetic cements precipitated around temperatures of 30 to 40°C (Fig, 4.16A). Similarly early calcisiltite calcite in the TBU indicates equilibrium temperature of deposition around 20-40°C. This is consistent with deposition of these carbonates in a tropical, emergent settings from marine Carboniferous carbonates (Keith and Weber, 1964; Sheppard et al, 1986). The $\delta^{13}C$ composition of carbonate cements reflects the source of the carbonate, and for the vast majority of Navan carbonates the source is dominated by marine bicarbonate.

Concretions: In the TBU concretions record $\delta^{18}O$ averages 27.3 ± 1 and $\delta^{13}C$ -11.2± 2.9 ‰, revealing a similar early diagenetic equilibrium temperature of deposition of 20-40°C. This data also agrees with Raiswell et al., (2002) who looked at carbonate concretions in the Lower Carboniferous Craton Shale Formation. The low C isotope value recorded in these concretions demands a microbial, organic carbon contribution. The precipitation of organic matter produces dissolved carbonate with

distinctive low isotopic compositions. Initially, sulphate reduction (see Raiswell et al., 2002) produces carbonate with a $\delta^{13}C$ that is essentially inherited from the source organic matter (typically -28 to -26‰). It is thus reasonable to speculate that the values measured are a mixture of locally available light carbon from bacteriogenic sulfide reduction, and marine carbonate. However, a contribution from methanogenesis cannot be ruled out on isotopic grounds alone (Raiswell et al., 2002). By contrast, the matrix carbonate surrounding the concretions, are dominated by marine carbonate.

D1 and D2: Given the intimate relationship between these two dolomite phases (Fig. 4.13F-H), it was not possible to guarantee single dolomite composition in any given Micrite Unit sample. However, we note the consistency of values across a variety of samples, resulting in a relatively narrow range of both $\delta^{18}O$ and $\delta^{13}C$ with resultant means of 22 ± 0.6‰ and 2.0 ± 0.7‰. This suggests that the two generations have similar values. The average temperature of deposition, assuming deposition in equilibrium with Mississippian seawater of 0‰, is around 80°C (Fig. 4.16A). Both the D1 and D2 dolomitization phases and the host limestone temperatures discussed here, correlate with calculated temperatures within Shelton et al., (2019) from "host dolomites (~40-100°C)" and "host limestones (20-40°C)" located on the NE margin of the Dublin Basin.

Healed Conglomerate: Taking average compositions here would not provide a direct insight into the primary calcite and D4 composition, because of the faint nodule margin has resulted in the co-occurrence of primary calcite in the nodule mixing with reactate dolomite focused in the stylocumulate matrix associated with pressure solution. Instead, we note an example where the clasts and matrix are distinct (Fig. 16B). In this example, the clast clearly shows $\delta^{13}C$ and $\delta^{18}O$ averaging 2.5‰ and 24.7‰, with associated D4 dolomite showing values of 3.0‰ and 21.6‰ respectively. Here temperatures of deposition in equilibrium with Mississippian seawater are around 40°C and 85°C respectively.

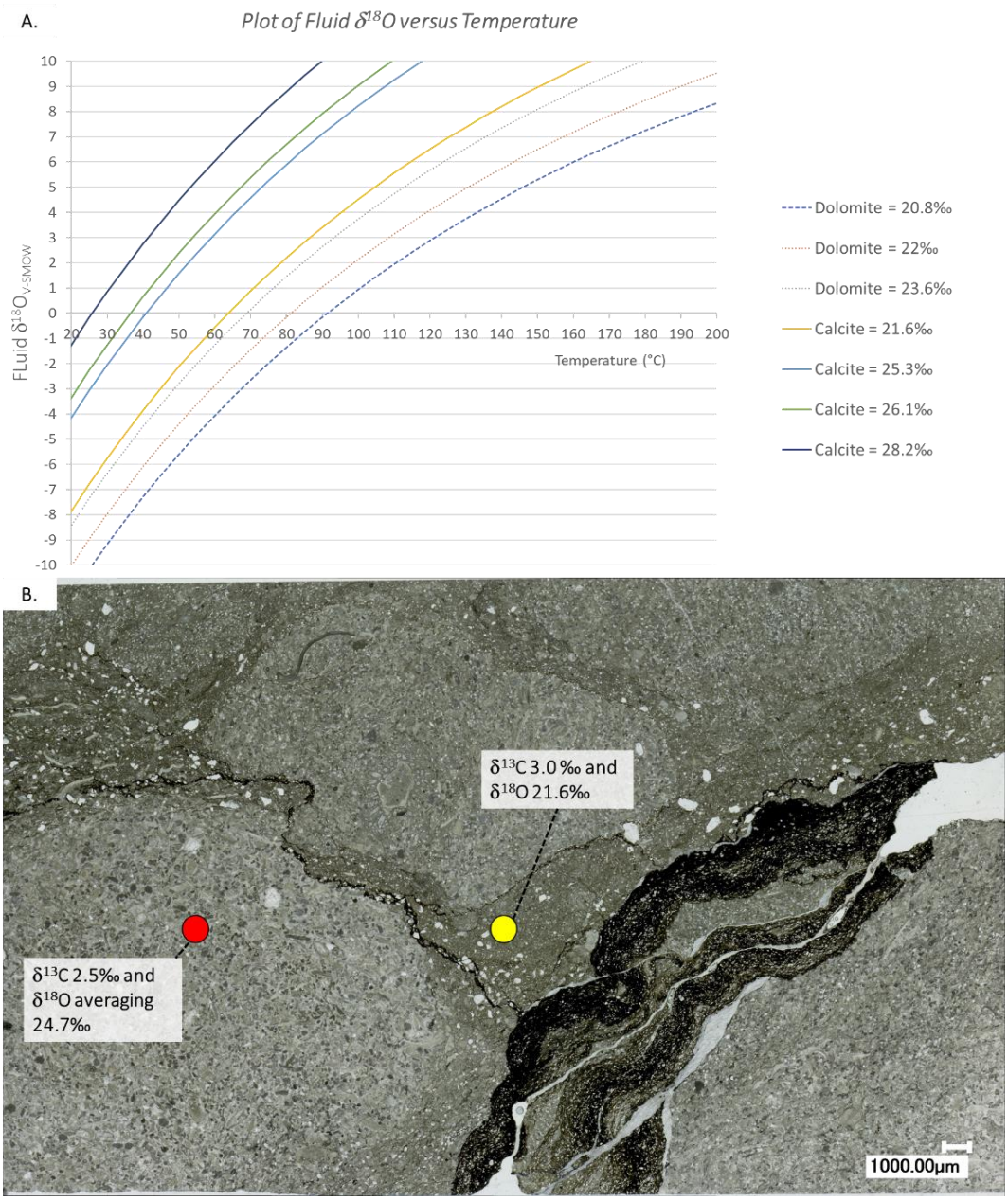

Figure 4.16 A) Graphs of temperature versus $\delta^{18}O$, showing the calculated range of precipitation temperatures of the carbonate minerals obtained from measured values of carbonate textures, assuming Mississippian seawater has a $\delta^{18}O$ around 0‰ (Mii et al., 1999). Equations used for dolomite and calcite found in Vasconcelos et al. (2005) and Horita (2014) respectively. B) Scanned thin section of healed conglomerate texture. Pressure solution seams from stylolite has exploited through host rock matrix.

Calcite veining: There is a noted homogeneity of C and O isotope composition between those veins occurring with or without areas of mineralization, averaging $\delta^{18}O$ of 21.3‰ in each type, typically within ±1.2‰, and $\delta^{13}C$ averaging around 0.6‰. It is not possible to determine the likely fluid in equilibrium with these veins as there are no fluid inclusion data available. Nonetheless depositional temperatures must have been above a calculated minimum value of 65°C, which is that calculated from

equilibrium with un-interacted marine water around 0‰; if later basinal or hydrothermal fluids were responsible for vein deposition, then higher temperatures would ensue, given that these waters are likely to have been significantly isotopically heavier (Sheppard et al, 1986).

4.7.4 Mineralization

Large orebodies, such as Navan and Tara Deep, are major geochemical anomalies within Earth's crust whose existence reflects an unusual convergence of numerous geological events and conditions. It is thus vital to understand the link between basin evolution and mineralization in order to vector toward further deep basin margin mineralization in the Irish Orefield. What are the key linkages between the carbonate diagenetic history of the Navan region and the generation of these Zn-Pb ore deposits?

Timing: Clasts of mineralization entrained in the SFC provide unambiguous evidence that the onset of mineralization occurred during the upper Tournaisian at Tara Deep. The same relationship is recorded within the Boulder Conglomerate at Navan (Boyce et al., 1983; Anderson et al., 1998, Ford, 1996 and Ashton et al., 2015), suggesting that early ramp detachment at both Navan and Tara Deep triggered initial mineralization, whereas later debrites have been prompted by footwall instability and subsequently entered palaeo-structural lows where mineralization was already occurring. Chapter 2 shows evidence of rapid, early, extensive mineralization such as colloform sphalerite within cavity fill textures within the Micrite Unit of the Pale Beds (Fig. 4.4E), alongside mineralization hosted as clasts and matrix replacement in the SFC, and finally as laminated iron sulfides in the TBU (Fig. 4.10H). Highlighting that mineralization was intimately linked to basin margin evolution in the Navan area, and that it occurred over a long period of time within the Tara Deep system. Here, the evidence of iron sulfide draping concretions in the TBU (Fig. 10H) reveals that mineralization was occurring beneath the subsurface, after an early phase of diagenesis. The calc-turbidites, debris flows and load casts within the TBU, attest to an unstable, rapid sedimentation, and it is possible that these packages also provided a stratigraphic trap for the waning mineralization system (McCaffrey and Kneller, 2001; Kneller et al., 2016). Other textural implications are also important; early diagenetic (Fig. 4.5A and Fig. 4.5B) iron

oxide alteration of the Pale Beds stresses the semi-lithified nature of these units and highlights their porosity and permeability- with iron oxide capable of utilizing both emergent surface cavities, and the semi-lithified host rock cements (Fig. 4.5C). D1 and D2 dolomitization predate mineralization, subsequently constraining the timing and highlighting they are not deep burial dolomitization processes. Interestingly, Shelton et al., (2019) agrees with a lower Viséan age for hydrothermal activity by documenting reworked zebra dolomites (associated with hydrothermal dolomitization) within syn-rift Viséan debrites at Loughshinny on the NE margin of the Dublin Basin. The timing of pressure solution is unclear. The absence of stylo-nodular textures within the SFC clasts (Fig. 4.9A & 4.9B), and the overlying Boulder Conglomerate, suggest that it postdates the main phase of rifting, and thus formed during burial. However, stylo-nodular textures have been observed within the debrites of the TBU, highlighting that they must have formed at some stage after the SFC, but before the TBU debrites. These late phase pressure solution seams (Fig.4.14) are also exploited by metalliferous fluids (dominantly Fe-bearing but minor Zn and Pb), highlighting that metalliferous fluids were capable of utilizing all levels of primary and secondary porosity.

Biology: It is important to note that at both Navan and Tara Deep, alongside every other economic orebody in the Irish Orefield, there is extensive evidence for bacteriogenic sulfide reduction of seawater sulfate (Fallick et al., 2001; Chapter 3), which appears entirely invisible from the dolomite carbon isotopic signatures. Thus, a number of congruent processes are involved within the northern margin of the Dublin Basin, and it is the confederacy and dynamism of all of these processes that proved critical for development of these Zn-Pb orebodies.

4.7.5 Significance for Exploration

From an exploration perspective within the Irish Orefield, focus should not only be paid to regions on the margins of the tectonically active basins, but should also look to identify regions where pre-rift facies still exist and where debrites and syn-sedimentary faulting occurred. These regions could contain areas where structural lows once developed. In these volatile regions, metalliferous fluids could have

once risen and interacted with connate fluids/seawater, ultimately precipitating Zn-Pb mineralization. These Zn-Pb deposits likely initiated during the upper Tournaisian but are now buried deep beneath the subsided basin fill. The next generation of Zn-Pb deposits within Ireland will principally be deeper and less readily detectable from the surface, thus modelling debris flows, detailed 3D seismics (see Tournadaour et al., 2015), and using vectors such as laminated pyrite in the TBU will play a key role in highlighting structures where mineralization was once occurring.

4.8 Conclusions

Tara Deep is located in a segmented normal fault system on the northern margin of the Dublin Basin. The evolution of the carbonate diagenetic history is intimately linked to a rapidly subsiding basin. The textures discussed within this study outline the complexity of the Tara Deep system. The northern margin of the Dublin Basin initiated as a shallow ramp setting in the upper Tournaisian, shallowly dipping from NE to SW. Detachment and debris flows occurred during the upper Tournaisian/lower Viséan reflecting regional extension. These unstable conditions continued during the mid-Mississippian, with basin infill dominating. The Tara Deep region of the Dublin Basin is far from discrete, it is chaotic, abrupt and hosts numerous complicated debris flow events and associated calc-turbidites. Overlying these debrites, within the Thin Bedded Unit, load casts and seismites attest to continued rapid sedimentation within a subsiding basin. Diagenetic processes, such as multiphase dolomitization and extensive pressure solution, add complexity and fosters misinterpretation, by occluding the original host rock fabric. However, most importantly, as the region adapts to this dynamic tectonic setting, and associated subsidence, they become host to world-renowned deposits. The intimate integration of all these congruent processes has resulted in one of the most fertile Zn-Pb regions in the world.

4.9 Acknowledgements

We wish to acknowledge the encouragement and permission of Boliden Tara Mines who generously funded and facilitated this research. We would also like to thank the Grant Institute (University of Edinburgh), and the University of Glasgow. This research was conducted through funding of D A

Drummond by Boliden Tara Mines. SUERC is supported by NERC and the Scottish Universities consortium. A J Boyce is part funded by NERC's National Environmental Isotope Facility (NEIF) at SUERC. Alison McDonald and Julie Dougans are thanked for assistance with the isotope analyses. We were fortunate to benefit from discussions of this research with Mike Philcox, Dave Coller, Colin Braithwaite, Rachel Wood, Rob Raiswell, Steve Hollis, Giancarlo Rizzi and Tony Prave.

4.10 References

Alfaro, P., Moretti, M., & Soria, J. M. 1997. Soft sediment deformation structures induced by earthquakes (seismites) in Pliocene lacustrine deposits (Guadix-Baza Basin, Central Betic Cordillera). Eclogae Geologicae Helvetiae, 90, p.531–540.

Allen, J.R.L, 1985. Wrinkle Marks: An Intertidal Sedimentary Structure Due To Aseismic Soft-Sediment Loading. Sedimentary Geology, 41, p.75-95.

Allen, J.R.L. 1982. Sedimentary Structures: Their Character And Physical Basis. Developments In Sedimentology, 30. Elsevier, Amsterdam.

Anderson, I.K., 1990, Ore Depositional Processes In The Formation Of The Navan Zinc-Lead Deposit, Co. Meath, Ireland. Unpublished Phd Thesis, University Of Strathclyde, p.290.

Anderson, I.K., Ashton, J.H., Boyce, A.J., Fallick, A.E. And Russell, M.J., 1998. Ore Depositional Processes In The Navan Zn-Pb Deposit, Ireland. Economic Geology 93, p. 535-563.

Andrew C.J., 1993. Mineralization in the Irish Midlands. In: Pattrick RAD and Polya DA (eds.) Mineralization in the British Isles. London: Chapman and Hall p. 208–269.

Andrew, C.J., and Ashton, J.H., 1985. Regional setting, geology and metal distribution patterns of Navan orebody, Ireland: Trans. Inst. Min. Metall. (Sect.B: Appl. earth SCi.), v.94, p. 66-93.

Anketell, J. M., Cegla, J., & Dzulynski, S. (1970). On the deformational structures in systems with reversed density gradients. Annales Societatis Geologorum Poloniae, 40, p.3–30.

Ashton, J.H., Beach, A., Blakeman, R.J., Coller, D., Henry, P., Lee, R., Hitzman, M., Hope, C., Huleatt-James, S., O'donovan, B., Philcox, M.E., 2018. Discovery Of The Tara Deep Zn-Pb Mineralisation At The Boliden Tara Mine, Navan, Ireland: Success With Modern Seismic Surveys. In Seg Special Publications No 21, Pp. 365-381. Doi:10.5382/Sp.21.16: p. 17.

Ashton, J.H., Black, A., Geraghty, J., Holdstock, M. and Hyland, E., 1992, The geological setting and metal distribution patterns of Zn-Pb-Fe mineralization in the Navan Boulder Conglomerate. In: Bowden, A.A., Earls, G., O'Connor, P.G. and Pyne, J.F. (Eds). The Irish Minerals Industry 1980-1990. IAEG, Dublin, p. 171-210.

Ashton, J.H., Holdstock, M.P., Geraghty, J.F., O'keeffe, W.G., Peace, W. And Philcox, M.E., 2003, The Navan Orebody - Discovery And Geology Of The South West Extension. In: Kelly, J.G., Andrew, C.J., Ashton, J.H., Boland, M.B., Earls, G., Fusciardi, L., Stanley, G. (Eds). Europe's Major Base Metal Deposits. Iaeg, Dublin, p. 405-430.

Ashton, J.H.; Blakeman, R.J.; Geraghty, J.F.; Beach, A.; Coller, D.; Philcox, M.E. 2015 The Giant Navan Carbonate-Hosted Zn–Pb Deposit—A Review. In Current Perspectives On Zinc Deposits; Archibald, S.M.,Piercey, S.J., Eds.; Irish Association For Economic Geology: Dublin, Ireland, 2015; p. 85–122.

Barnaby, R. And Read, J., 1990. Carbonate Ramp To Rimmed Shelf Evolution: Lower To Middle Cambrian Continental Margin, Virginia Appalachians. Geological Society Of America Bulletin, 102(3), p.391-404.

Blakeman, R.J., Ashton, J.H., Boyce, A.J., Fallick, A.E. And Russell, M.J., 2002, Timing Of Interplay Between Hydrothermal And Surface Fluids In The Navan Zn+Pb Orebody, Ireland: Evidence

From Metal Distribution Trends, Mineral Textures And $\delta^{34}S$ Analyses. Economic Geology, 97, p. 73-91.

Boliden Summary Report. 2020 [online] Boliden.com. Available at: <https://www.boliden.com/globalassets/operations/exploration/mineral-resources-and-mineral-reserves-pdf/2020/resources-and-reserves-tara-2020-12-31.pdf> [Accessed 1 July 2021].

Boyce, A. J., Anderton, R. And Russell, M.J., 1983, Rapid Subsidence And Early Carboniferous Base-Metal Mineralization In Ireland. Trans. Instn Min. Metall. (Sect B: Appl. Earth Sci.), 92, p. 55-66.

Braithwaite, C.J.R. And Rizzi, G., 1997, The Geometry And Petrogenesis Of Hydrothermal Dolomites At Navan, Ireland. Sedimentology, 44, p. 421-440.

Coller, D. W. 1984. Variscan Structures In The Upper Palaeozoic Rocks Of West Central Ireland. *In:* Hutton, D. H. W. & Sanderson, D. J. (Eds) *Variscan Tectonics Of The North Atlantic Region.* Geological Society, London, Special Publication, 14, p.185-194.

Cooper, M.A., Collins, D.A., Ford, M., Murphy, F.X., Trayner, P.M., O'Sullivan, M.J., 1984. Structural style, shortening estimates and the thrust front of the Irish Variscides. In: Hutton, D.H.W., Sanderson, D.J. (Eds.), Variscan Tectonics of the North Atlantic Region Special Publication, 14. Geological Society of London, London, p. 167–175.

Cooper, M.A., Collins, D.A., Ford, M., Murphy, F.X., Trayner, P.M., O'Sullivan, M.J., 1986. Structural evolution of the Irish Variscides. Journal of the Geological Society, London 143, p.53–61.

Dasgupta, P. 1998. Recumbent Flame Structures In The Lower Gondwana Rocks Of The Jharia Basin, India – A Plausible Origin. Sedimentary Geology, 119, p.253-261.

Dolan, J. M. 1983. A structural cross-section through the Carboniferous of northwest Kerry. *Irish Journal of Earth Sciences,* 6, p.95-108.

Dunnington, H. V., 1954, Stylolite Development Postdates Rock Induration: Jour. Sed. Petrology, V. 24, p. 27--49.

Everett, C.E., Rye, D.M. And Ellam, R.M., 2003, Source Or Sink? An Assessment Of The Role Of The Old Red Sandstone In The Genesis Of The Irish Zn-Pb Deposits. Economic Geology, 98, p. 31-50.

Everett,C. E., Wilkinson,J. J. Rye,D. M. 1999. Fracture-Controlled Fluid Flow In The Lower Palaeozoic Basement Rocks Of Ireland: Implications For The Genesis Of Irish-Type Zn-Pb Deposits. In: Mccaffrey,K. J. W., Lonergan,L. & Wilkinson,J. J. (Eds) Fractures, Fluid Flow And Mineralization. Geological Society, London, Special Publications, 155, p.247-276.

Fallick, A.E., Ashton, J.H., Boyce, A.J., Ellam, R.M. and Russell, M.J., 2001, Bacteria were responsible for the magnitude of the world-class hydrothermal base metal sulfide orebody at Navan, Ireland. Economic Geology, 96, p. 885-890.

Folk, R. L., 1965, Some Aspects Of Recrystallization In Ancient Limestones: Soc. Econ. Paleontologists Mineralogist Spec. Pub. No. 13, p. 14-48.

Ford, C.V., 1996, The Integration Of Petrologic And Isotopic Data From The Boulder Conglomerate To Determine The Age Of The Navan Orebody, Ireland. Unpublished Phd Thesis, University Of Glasgow, p.176.

Fritschle, T.; Daly, J.S.; Mcconnell, B.; Whitehouse, M.J.; Menuge, J.F.; Buhre, S.; Mertz-Kraus, R.; Döpke, D.2018. Peri-Gondwanan Ordovician Arc Magmatism In Southeastern Ireland And The Isle Of Man: Constraints On The Timing Of Caledonian Deformation In Ganderia. Geol. Soc. Am. Bull., 130, p.1918–1939.

Garrison, R. And Kennedy, W., 1977. Origin Of Solution Seams And Flaser Structures In Upper Cretaceous Chalks Of Southern England. Sedimentary Geology, 19, p.107-137.

Gomez, F. And Astini, R., 2015. Sedimentology And Sequence Stratigraphy From A Mixed (Carbonate–Siliciclastic) Rift To Passive Margin Transition: The Early To Middle Cambrian Of The Argentine Precordillera. Sedimentary Geology, (316), p.39-61.

Hamilton, J., Ford, D., 2002. Karst Geomorphology And Hydrogeology Of The Bear Rock Formation—A Remarkable Dolostone And Gypsum Megabreccia In The Continous Per- Mafrost Zone Of Northwest Territories, Canada. Carbonates And Evaporites 17, p.114–115.

Harwood, G. M. & Sullivan, M. 1991. Sedimentary History Of The Moyvoughly Area, County West-Meath: Evidence For Syn-Sedimentary Fault Move- Ments In A Mixed Carbonate Siliciclastic System Of Courceyan Age. In: Lomando, A. & Harris, P. M. (Eds) Mixed Carbonat~Siliciclastic Sequences. Society Of Economic Palaeontologists And Miner- Alogists, Core Workshop. No. 15, p.253-384.

Horita, J., 2014. Oxygen and carbon isotope fractionation in the system dolomite–water–CO2 to elevated temperatures. *Geochimica et Cosmochimica Acta*, 129, p.111-124.

Johnston, J., Coller, D., Millar, G. and Critchley, M., 1996. Basement structural controls on Carboniferous-hosted base metal mineral deposits in Ireland. Geological Society, London, Special Publications, 107(1), p.1-21.

Jones, A.E & Omoto, K. 2000. Towards Establishing Criteria For Identifying Trigger Mechanisms For Soft-Sediment Deformation: A Case Study Of Late Pleistocene Lacustrine Sands And Clays, Onikobe And Nakayamadaira Basins, Northeastern Japan. Sedimentology, 47, p.1211-1226.

Kahsnitz, M. And Willems, H., 2019. Genesis Of Paleocene And Lower Eocene Shallow-Water Nodular Limestone Of South Tibet (China). Carbonate Evaporites, (34), p.199-218.

Keith, M. and Weber, J., 1964. Carbon and oxygen isotopic composition of selected limestones and fossils. Geochimica et Cosmochimica Acta, 28(10-11), p.1787-1816.

Kneller, B., Dykstra, M., Fairweather, L. and Milana, J., 2016. Mass-transport and slope accommodation: Implications for turbidite sandstone reservoirs. *AAPG Bulletin*, 100(02), pp.213-235.

Kuenen, Ph. H. 1958. Experiments In Geology. Transactions Of The Geological Society Of Glasgow, 23, p.1-28.

Lees, A. And Miller, J., 1995, Waulsortian Banks. In Monty, C.L.V., Bosence, D.W.J., Bridges, P.H. And Pratt, B. R., (Eds). Carbonate Mud-Mounds. Int Assoc Sediment Spec Pub 23, Blackwell Science, Oxford, p.191-271.

Logan, B.W., Semeniuk, V. 1976: Dynamic Metamorphism; Process And Products In Devonian Carbonate Rocks; Canning Basin, Western Australia. – Geological Society Of Australia, Spec. Publ., 6, p.138.

Lucia, J.F., 1995. Lower Paleozoic Cavern Development, Collapse, And Dolomitization. American Association Of Petroleum Geologists, Franklin Mountains, El Paso, Texas. https://doi.org/10.1306/M63592

Marshall, J. And Pirrie, D., 2013. Carbonate Concretions-Explained. Geology Today, 29(2), p.53-62.

Matte P (2001) The Variscan Collage And Orogeny (480_290 Ma) And The Tectonic Definition Of The Armorica Microplate: A Review. Terra Nova 13: p.122–128.

McCaffrey, W.D. and Kneller, B.C. 2001. Process controls on the development of stratigraphic trap potential on the margins of confined turbidite systems and aids to reservoir evaluation. AAPG Bulletin, 85 (6). p. 971-988. ISSN 0149-1423

Mchargue, T.R. And Price, R.C., 1982, Dolomite From Clay In Argillaceous Or Shale Associated Marine Carbonates: Journal Ofsedimentary Petrology, V. 48, p. 799-814.

McIlreath, I. A., & James, N. P. 1978. Facies Models 13. Carbonate Slopes. Geoscience Canada, 5(4).

McNestry A., Rees J. G. 1992. Environmental and palynofacies analysis of a Dinantian (Carboniferous) littoral sequence: the basal part of the Navan Group, Navan, County Meath, Ireland. Palaeogeography, Palaeoclimatology, Palaeoecology 96: p.175–193

Mii, H., Grossman, E.L., And Yancey, T.E., 1999, Carboniferous Isotope Stratigraphies Of North America: Implications For Carboniferous Paleoceanography And Mississippian Glaciation: Geological Society Of America, Bulletin, V. 111, p. 960–973.

Molina, J.M., Alfaro, P., Moretti, M. Gz Stria, J.M. 1998. Soft-Sediment Deformation Structures Induced By Cyclic Stress Of Storm Waves In Tempestites (Miocene, Guadalquivir Basin, Spain). Terra Nova, 10, p.145-150.

Moretti, M., Alfaro, P., Caselles, O. Canas, J.A. 1999. Modelling Seismites With A Digital Shaking Table. Tectonophysics, 304, p.369-383.

Moretti, M., Stria, J.M., Alfaro, P. & Walsh, N. 2001. Asymmetrical Soft-Sediment Deformation Structures Triggered By Rapid Sedimentation In Turbiditic Deposits (Late Miocene, Guadix Basin, Southern Spain). Facies, 44, p.283-294.

Morris, P. & Max, M. D. 1995. Magnetic Crustal Character In Central Ireland. Geological Journal, 30, 49-67

Moscardelli, L. And Wood, L., 2008. New Classification System For Mass Transport Complexes In Offshore Trinidad. Basin Research, 20(1), p.73-98.

Murphy, F.C., Anderson, T.B., Daly, J.S., Gallagher, V., Graham, J.R., Haroer, D.A.T., Johnston, J.D., Kennan, P.S., Kennedy, M.J., Long, C.B., Morris, J.H., O'keeffe, W.G., Parkes, M., Ryan, P.D., Sloan, R.J., Stillman, C.J., Tietzch-Tyler, D., Todd, S.P., Wrafter, J.P., 1991. An Appraisal Of Caledonian Suspect Terranes In Ireland. Irish Journal Of Earth Sciences, 11, p.11-41.

Murphy, T. 1974 Gravity anomaly map of Ireland. Communications of the Dublin Institute for Advanced Studies, Series D, Geophysical Bulletin No. 32. Dublin.

Murphy, T. 1981 Geophysical evidence. In C.H. Holland (ed.), A geology of Ireland, 225-9. Edinburgh. Scottish Academic Press.

Nolan, S.C., 1989, The Style And Timing Of Dinantian Synsedimentary Tectonics In The Eastern Part Of The Dublin Basin, Ireland. In: Arthurton, R.S., Gutteridge, P. And Nolan,S. C. (Eds). The Role Of Tectonics In Devonian And Carboniferous Sedimentation In The British Isles. Yorkshire Geological Society, Occasional Publication 6, p. 83-97.

O'Keeffe, W.G., 1986, Age And Postulated Source Rocks For Mineralization In Central Ireland, As Indicated By Lead Isotopes. In: Andrew, C.J., Et Al. (Eds). Geology And Genesis Of Mineral Deposits In Ireland. Iaeg, Dublin, p. 617–624.

Owen, G. 1987. Deformation Processes In Unconsolidated Sands. In: Jones, M.E. & Preston, R.E (Eds) Deformation Of Sediments And Sedimentary Rocks. Geological Society, London, Special Publications, 29, p.11-24.

Owen, G., 2003. Load Structures: Gravity-Driven Sediment Mobilization In The Shallow Subsurface. Geological Society, London, Special Publications, 216(1), p.21-34.

Philcox M. E. 1991. The Geology Of The Clogherboy And 'Ep-East' Areas, South Of Navan. Boliden Tara Mines Internal Report.

Philcox, M.E. 1984. Lower Carboniferous Lithostratigraphy Of The Irish Midlands; Irish Association For Economic Geology: Dublin, Ireland, p.89.

Philcox, M.E., 1989. The Mid-Dinantian Unconformity At Navan, Ireland. In: Arthurton R.S., Gutteridge, P. And Nolan,S. C. (Eds). The Role Of Tectonics In Devonian And Carboniferous Sedimentation In The British Isles. Yorkshire Geological Society, Occasional Publication, 6, p. 67-81.

Phillips, W. E. A. & Sevastopulo, G. D. 1986. The stratigraphic and structural setting of Irish mineral deposits. In: ANDREW, C. J., GROWL, R. W. A., FINLAY, S., PENNELL, W. M. & PYNE, J. F. (eds) Geology and Genesis of Mineral Deposits in Ireland. Irish Association for Economic Geology, Dublin, p.1-30.

Pickard, N. A. H., Jones, G. Ll., Rees, J. G., Somerville, I. D. & Strogen, P. 1992. Lower Carboniferous (Dinantian) Stratigraphy And Structure Of The Walterstown-Kentstown Area, Co. Meath, Ireland. *Geological Journal,* 27, p.35-58.

Raiswell, R., Bottrell, S., Dean, S., Marshall, J., Carr, A. and Hatfield, D., 2002. Isotopic constraints on growth conditions of multiphase calcite-pyrite-barite concretions in Carboniferous mudstones. Sedimentology, 49(2), p.237-254.

Read. J,F., 1985. Carbonate Platform Facies Models. AAPG Bulletin, 69.

Rees, J. G. 1987. The Carboniferous Geology Of The Boyne Valley Area, Ireland. Phd Thesis, Trinity College, Dublin.

Rizzi, G. and Braithwaite, C.J.R., 1996, Cyclic emersion surfaces and channels within Dinantian limestones hosting the giant Navan Zn-Pb deposit, Ireland. In: Strogen P., Somerville, I.D. & Jones, G.Ll. (eds), Recent Advances in Lower Carboniferous Geology, Geological Society Special Publication No. 107, p. 207-219.

Rizzi, G. And Braithwaite, C.J.R., 1997. Sedimentary cycles and selective dolomitization in limestones hosting the giant Navan zinc-lead ore deposit, Ireland. Exploration and Mining Geology, v. 6, p.63-77.

Rizzi, Giancarlo. 1992. The Sedimentology And Petrography Of Lower Carboniferous Limestones And Dolomites: Host-Rocks To The Navan Zinc-Lead Deposit. Phd Thesis, University Of Glasgow

Romano, M., 1980. The Stratigraphy Of The Ordovician Rocks Between Slane (County Meath) And Collon (County Louth), Eastern Ireland. J Earth Sci. Dubl. Soc. 3. P. 53-79.

Rossetti, D.F. 1999. Soft-Sediment Deformation Structures In Late Albian To Cenomanian Deposits, Sat Lufs Basin, Northern Brazil: Evidence For Palaeoseismicity. Sedimentology, 46, p.1065-1081.

Rothery, E. 1988. En-Echelon Vein Array Development In Extension And Shear. *Journal Of Structural Geology,* 10, p.63-71.

Russell, M. J. 1968. Structural Controls Of Base Metal Mineralization In Relation To Continental Drift. Transactions Of The Institution For Mining And Metallurgy, 77b, p.11-28.

Salvati, R. And Sasowsky, I., 2002. Development Of Collapse Sinkholes In Areas Of Groundwater Discharge. Journal Of Hydrology, 264(1-4), p.1-11.

Sanderson, O. J. 1984. Structural Variation Across The Northern Margin Of The Variscides In Nw Europe. *In:* Hutton, D. H. W. & Sanderson, D. J. (Eds) *Variscan Tectonics Of The North Atlantic Region.* Geological Society, London, Special Publication, 14, p.149-166.

Scholle, P. And Ulmer-Scholle, D., 2003. A Color Guide To The Petrography Of Carbonate Rocks. Tulsa, Okla.: American Association Of Petroleum Geologist.

Scotese, C. R, 2001. Atlas of Earth History, PALEOMAP Project, Arlington, Texas, p.52.

Seilacher, A. 1984. Sedimentary Structures Tentatively Attributed To Seismic Events. Marine Geology, 55, p.1-12.

Shelton, K., Hendry, J., Gregg, J., Truesdale, J. and Somerville, I., 2019. Fluid Circulation and Fault- and Fracture-related Diagenesis in Mississippian Syn-rift Carbonate Rocks On the Northeast Margin of the Metalliferous Dublin Basin, Ireland. Journal of Sedimentary Research, 89(6), p.508-536.

Sheppard, S. M. F. 1986. Characterization And Isotopic Variations In Natural Waters. In Stable Isotopes In High Temperature Geological Processes (Eds J. W. Valley, H. P. Taylorand J. R. O'Neil). Miner. Soc. Am., Rev. Miner. 16, p. 165-184.

Sibley, D. F. And Gregg, J. M., 1987, Classification Of Dolomite Rock Textures. Journal Of Sedimentary Petrology, V. 57, p. 967-975

Sims, J.D. 1975. Determining Earthquake Recurrence Intervals From Deformational Structures In Young Lacustrine Sediments. Tectonophysics, 29, p.141-152.

Sorby H. C. 1908, On The Application Of Quantitative Methods To The Study Of The Structure And History Of Rocks. Quarterly Journal Of The Geological Society, London 64: p.171–232

Sorby, H. C. 1879, On The Structure And Origin Of Limestones: Quart. Jour. Geol. Soc. London, V. 35, p.56-95.

Sternbach, Ga. And Friedman, G.M., 1984, Felman Carbonates Formed At Depth Require Porosity Well-Log Correction: Hunton Group, Deep Anadarko Basin (Upper Ordovician To Lower Devonian) Of Oklahoma And Texas. Transactions Of Southwest Section, American Association Petroleum Geology, p.167-173

Stockdale, P. B., 1922, Styiolites: Their Nature And Ortgin: Indiana Univ. Studies, V. 9, p. 1-97.

Stockdale, P. B., 1926, The Stratigraphic Significance Of Solution In Rocks: Jour. Geology, V. 34, p.399-414.

Stockdale, P. B., 1936, Rare Stylolites: Am. Jour. Sci., V. 32, p. 129-133.

Stockdale, P. B.,1943, Stylolites: Prtmary Or Secondary?: Jour. Sed. Petrology, V. 13, p. 3-12.

Strogen, P., Jones, G. And Somerville, I., 1990. Stratigraphy And Sedimentology Of Lower Carboniferous (Dinantian) Boreholes From West Co. Meath, Ireland. Geological Journal, 25(2), p.103-137.

Strogen, P., Somerville, I., Pickard, N., Jones, G. and Fleming, M., 1996. Controls on ramp, platform and basinal sedimentation in the Dinantian of the Dublin Basin and Shannon Trough, Ireland. Geological Society, London, Special Publications, 107(1), p.263-279.

Tournadour, E., Mulder, T., Borgomano, J., Hanquiez, V., Ducassou, E. and Gillet, H., 2015. Origin and architecture of a Mass Transport Complex on the northwest slope of Little Bahama Bank (Bahamas): Relations between off-bank transport, bottom current sedimentation and submarine landslides. *Sedimentary Geology*, 317, p.9-26.

Udchachon, M., Charusiri, P., Thassanapak, H. And Burrett, C., 2018. A New Section Of Lower Palaeozoic Rocks In Kayin State (Southeast Myanmar). Proceedings Of The Geologists' Association, (129), p.215-226.

Vasconcelos, C., McKenzie, J.A., Warthmann, R. and Bernasconi, S.M. (2005) Calibration of the $\delta^{18}O$ paleothermometer for dolomite precipitated in microbial cultures and natural environments. Geology, 33, p.317–320.

Vaughan, A. And Johnston, J. D., 1992, Structural Constraints On Closure Geometr Across The Iaepetus Suture In Eastern Ireland. Journal Of The Geological Society Of London, 149, p. 65-74

Wanless, H. R. 1979. Limestone Response To Stress: Pressure Solution And Dolomitization. Sepm Journal Of Sedimentary Research, Vol. 49.

Warren, J., 2000. Dolomite: occurrence, evolution and economically important associations. *Earth-Science Reviews*, 52(1-3), p.1-81.

Worthington, R. And Walsh, J., 2011. Structure Of Lower Carboniferous Basins Of Nw Ireland, And Its Implications For Structural Inheritance And Cenozoic Faulting. Journal Of Structural Geology, 33(8), p.1285-1299.

Yesares, L., Drummond, D., Hollis, S., Doran, A., Menuge J, F., Boyce, A. J., Blakeman, R. J., Ashton, J. H., (2019). Coupling Mineralogy, Textures, Stable And Radiogenic Isotopes In Identifying Ore-Forming Processes And Geochemical Vectoring Possibilities In Irish-Type Carbonate Hosted Zn-Pb Deposits.

Yesares, L.., Menuge, J., Blakeman, R, J., Ashton. J, H., Boyce, A., Coller, D., Drummond, D, A., Farrelly, I. (in press)., Pyrite Mineralization Halo Above The Tara Deep Zn-Pb Deposit, Navan, Ireland: Evidence For Sub-Seafloor Exhalative Hydrothermal Processes? [Accepted By Ore Geology Reviews in July, 2021].

Data Table 4.1: Carbon & Oxygen Isotopes

Sample Name	**Category**	**UNIT**	**$\delta^{13}C$ VPDB (‰)**	**$\delta^{18}O_{VPDB}$ (‰)**	**$\delta^{18}O_{VSMOW}$ (‰)**	**Correction Applied**
D4 N02416/10A	Calcite Veining (No Mineralization)	PALE BEDS	1.5	-10.0	20.6	Corrected as calcite
N02416/13A	Calcite Veining (No Mineralization)	PALE BEDS	1.2	-9.5	21.1	Corrected as calcite
N02469/03	Calcite Veining (No Mineralization)	PALE BEDS	0.3	-9.4	21.2	Corrected as calcite
Z1 N02469/09A	Calcite Veining (No Mineralization)	PALE BEDS	1.8	-8.5	22.1	Corrected as calcite
Z16 N02469/11A	Calcite Veining (No Mineralization)	PALE BEDS	1.6	-9.1	21.5	Corrected as calcite
N02505/23	Calcite Veining (Associated With Mineralization)	MICRITE UNIT	-2.5	-8.8	21.9	Corrected as calcite
N02508/02	Calcite Veining (Associated With Mineralization)	MICRITE UNIT	0.1	-10.0	20.6	Corrected as calcite
K04 N02417/01	Calcite Veining (Associated With Mineralization)	MICRITE UNIT	-0.6	-9.6	21.0	Corrected as calcite
K01 A N02464/01	Calcite Veining (Associated With Mineralization)	PALE BEDS	0.8	-11.4	19.2	Corrected as calcite
L13 N02454/04A	Calcite Veining (Associated With Mineralization)	MICRITE UNIT	1.6	-8.4	22.2	Corrected as calcite
L20 N02454/14	Calcite Veining (Associated With Mineralization)	MICRITE UNIT	-0.6	-7.5	23.2	Corrected as calcite

L38 N02334/08	Calcite Veining (Associated With Mineralization)	MICRITE UNIT	-0.2	-7.5	23.2	Corrected as calcite
L48 N02454/03	Calcite Veining (Associated With Mineralization)	MICRITE UNIT	0.6	-9.2	21.4	Corrected as calcite
N02370/01	Calcite Veining (Associated With Mineralization)	MICRITE UNIT	2.3	-7.9	22.8	Corrected as calcite
N02370/04	Calcite Veining (Associated With Mineralization)	MICRITE UNIT	0.9	-10.0	20.6	Corrected as calcite
N02465/04	Calcite Veining (Associated With Mineralization)	SFC	2.1	-11.4	19.1	Corrected as calcite
Z27 N02466/04	Calcite Veining (Associated With Mineralization)	SFC	0.5	-10.8	19.7	Corrected as calcite
N02428/06	Calcite Veining (Associated With Mineralization)	MICRITE UNIT	-0.9	-7.8	22.9	Corrected as calcite
Z29 N02466/05	Calcite Veining (Associated With Mineralization)	SFC	1.0	-10.4	20.2	Corrected as calcite
N02499/08 (3)	Pressure Solution (D4 Dolomite)	PALE BEDS	3.0	-7.1	23.6	Corrected as dolomite
N02505/10	Pressure Solution (D4 Dolomite)	PALE BEDS	1.6	-6.0	24.7	Corrected as dolomite
N02508/01	Pressure Solution (D4 Dolomite)	PALE BEDS	4.7	-5.3	25.5	Corrected as dolomite
D2 N02416/10A	Pressure Solution (D4 Dolomite)	PALE BEDS	3.0	-9.0	21.6	Corrected as dolomite
Z3 N02469/09A	Pressure Solution (D4 Dolomite)	PALE BEDS	2.4	-7.6	23.1	Corrected as dolomite
N02510/02	Pressure Solution (D4 Dolomite)	PALE BEDS	1.0	-7.8	22.8	Corrected as dolomite
N02505/10	Healed Conglomerate Nodule	PALE BEDS (HC)	1.6	-5.8	24.9	Corrected as calcite
N02508/01	Healed Conglomerate Nodule	PALE BEDS (HC)	4.5	-2.7	28.1	Corrected as calcite

N02510/02	Healed Conglomerate Nodule	PALE BEDS (HC)	3.2	-6.7	24.0	Corrected as calcite
N02510/04	Healed Conglomerate Nodule	PALE BEDS (HC)	1.8	-6.6	24.1	Corrected as calcite
D1 N02416/10A	Healed Conglomerate Nodule	PALE BEDS (HC)	2.5	-6.4	24.3	Corrected as calcite
D3 N02416/10A	Healed Conglomerate Nodule	PALE BEDS (HC)	2.4	-5.6	25.2	Corrected as calcite
Z2 N02469/09A	Healed Conglomerate Nodule	PALE BEDS (HC)	2.8	-5.0	25.7	Corrected as calcite
N02499/11	Dolomite (D1 & D2 Bulk Signature)	MICRITE UNIT	2.7	-7.8	22.9	Corrected as dolomite
N02499/14	Dolomite (D1 & D2 Bulk Signature)	MICRITE UNIT	1.2	-8.7	21.9	Corrected as dolomite
N02499/15	Dolomite (D1 & D2 Bulk Signature)	MICRITE UNIT	1.8	-9.8	20.8	Corrected as dolomite
N02499/20	Dolomite (D1 & D2 Bulk Signature)	MICRITE UNIT	1.9	-8.6	22.1	Corrected as dolomite
N02505/15	Dolomite (D1 & D2 Bulk Signature)	MICRITE UNIT	1.7	-8.7	22.0	Corrected as dolomite
N02505/18	Dolomite (D1 & D2 Bulk Signature)	MICRITE UNIT	1.0	-8.7	21.9	Corrected as dolomite
N02505/22	Dolomite (D1 & D2 Bulk Signature)	MICRITE UNIT	1.6	-8.2	22.5	Corrected as dolomite
N02505/25	Dolomite (D1 & D2 Bulk Signature)	MICRITE UNIT	0.8	-8.5	22.1	Corrected as dolomite
N02505/26	Dolomite (D1 & D2 Bulk Signature)	MICRITE UNIT	3.4	-9.3	21.4	Corrected as dolomite
N02517/02	Dolomite (D1 & D2 Bulk Signature)	MICRITE UNIT	1.7	-9.1	21.5	Corrected as dolomite
N02370/05	Dolomite (D1 & D2 Bulk Signature)	MICRITE UNIT	2.2	-8.4	22.3	Corrected as dolomite
N02370/06B	Dolomite (D1 & D2 Bulk Signature)	MICRITE UNIT	2.2	-8.3	22.3	Corrected as dolomite
N02445/06	Dolomite (D1 & D2 Bulk Signature)	MICRITE UNIT	3.0	-9.2	21.4	Corrected as dolomite

N02505/27	Dolomite (D1 & D2 Bulk Signature)	MICRITE UNIT	1.4	-7.8	22.8	Corrected as dolomite
N02469/03	Dolomite (D1 & D2 Bulk Signature)	MICRITE UNIT	2.0	-9.6	21.0	Corrected as dolomite
L20 N02454/14	Dolomite (D1 & D2 Bulk Signature)	MICRITE UNIT	3.1	-8.0	22.6	Corrected as dolomite
N02499/01	Host Rock Early Diagenetic Cement	PALE BEDS	2.9	-5.8	24.9	Corrected as calcite
N02499/02	Host Rock Early Diagenetic Cement	PALE BEDS	1.1	-3.9	26.9	Corrected as calcite
N02499/03	Host Rock Early Diagenetic Cement	PALE BEDS	1.3	-5.2	25.5	Corrected as calcite
N02499/08 (4)	Host Rock Early Diagenetic Cement	PALE BEDS	0.9	-5.5	25.3	Corrected as calcite
N02505/02	Host Rock Early Diagenetic Cement	PALE BEDS	1.4	-5.0	25.7	Corrected as calcite
N02505/04	Host Rock Early Diagenetic Cement	PALE BEDS	2.9	-5.1	25.7	Corrected as calcite
N02505/06 (1)	Host Rock Early Diagenetic Cement	PALE BEDS	2.4	-6.2	24.5	Corrected as calcite
N02505/07 (3)	Host Rock Early Diagenetic Cement	PALE BEDS	2.5	-6.0	24.8	Corrected as calcite
N02505/11	Host Rock Early Diagenetic Cement	PALE BEDS	2.6	-4.9	25.9	Corrected as calcite
N02505/12	Host Rock Early Diagenetic Cement	PALE BEDS	1.8	-4.3	26.4	Corrected as calcite
N02510/03	Host Rock Early Diagenetic Cement	PALE BEDS	2.3	-6.7	24.0	Corrected as calcite
N02513/01	Host Rock Early Diagenetic Cement	PALE BEDS	4.1	-4.5	26.2	Corrected as calcite
N02510/05	Geopetal Micrite Infill	PALE BEDS	-5.1	-5.4	25.3	Corrected as calcite
N02505/12	Geopetal Micrite Infill	PALE BEDS	2.1	-5.4	25.3	Corrected as calcite
N02505/02	Geopetal Micrite Infill	PALE BEDS	3.2	-4.1	26.7	Corrected as calcite
N02505/04	Geopetal Micrite Infill	PALE BEDS	2.3	-4.2	26.6	Corrected as calcite
N02505/07	Geopetal Micrite Infill	PALE BEDS	3.9	-2.9	27.9	Corrected as calcite

N02505/08	Geopetal Micrite Infill	PALE BEDS	2.6	-4.8	25.9	Corrected as calcite
N02505/11	Geopetal Micrite Infill	PALE BEDS	0.6	-5.0	25.7	Corrected as calcite
N02510/03	Geopetal Micrite Infill	PALE BEDS	2.3	-5.3	25.5	Corrected as calcite
N02510/04	Geopetal Micrite Infill	PALE BEDS	3.8	-5.0	25.8	Corrected as calcite
N02513/03	TBU Host Rock	TBU	3.3	-4.7	26.0	Corrected as calcite
N02416/04	TBU Host Rock	TBU	2.5	-3.9	26.9	Corrected as calcite
N02448/01	TBU Host Rock	TBU	2.4	-5.7	25.0	Corrected as calcite
N02416/04	TBU Concretion	TBU	-14.2	-2.6	28.2	Corrected as calcite
N02448/01	TBU Concretion	TBU	-8.3	-4.5	26.3	Corrected as calcite

CHAPTER FIVE: CONCLUSIONS, FUTURE WORK AND EXPLORATION POTENTIAL.

5.1 Conclusions

Tara Deep is located in a segmented normal fault system on the northern margin of the Dublin Basin. The evolution of the carbonate diagenetic history is intimately linked to a rapidly subsiding basin. The carbonate textures discussed within this study outline the complexity of the Tara Deep system. The northern margin of the Dublin Basin initiated as a shallow ramp setting in the upper Tournaisian, likely shallowly dipping from NE to SW. Detachment and debris flows occurred during the upper Tournaisian/lower Viséan reflecting regional extension. These unstable conditions continued during the mid-Mississippian, with basin infill dominating. The Tara Deep region of the Dublin Basin is far from discreet, it is chaotic, abrupt and hosts numerous complicated debrites and associated calc-turbidites. Overlying these debrites, within the Thin Bedded Unit, load casts and seismites attest to continued rapid sedimentation within a subsiding basin. Diagenetic processes, such as multiphase dolomitization and extensive pressure solution, adds complexity, and potential misinterpretation, by occluding the original host rock fabric. However, most importantly, as the region adapts to this dynamic tectonic setting and associated subsidence, it becomes host to world-renowned ore deposits. The extension which led to this profound tectonic activity was a response to enhanced mantle heat flow (Davidheiser-Kroll, 2014). This thinned the crust and facilitated downward-excavating hydrothermal cells (Russell, 1978) moving seawater (likely evaporated; Banks et al., 2002) down through reactivated syn-sedimentary faults, into the thick metalliferous basement to ultimately become the principal ore fluid for Tara Deep/Navan. The intimate integration of all these congruent processes has thus resulted in one of the most fertile Zn-Pb regions in the world.

Tara Deep's mineralization is hosted by Mississippian (Lower Carboniferous) carbonates, within complex fault-controlled terraces on the degrading footwall of a major normal fault system. These terraces have resulted from basin margin activity during the upper Tournaisian. The Tara Deep deposit has many similarities with the neighbouring Navan deposit that reflect comparable controls on the

mineralizing process such as host rocks, Pb and S sources, and tectonic environment. Of crucial importance is the presence of eroded, transported and abraded clasts and rafts of sulfide entrained within syn-rift conglomerates in both the Navan (Conglomerate Group Ore) and Tara Deep (S Fault Conglomerate) deposits. This observation demonstrates that the onset of mineralization occurred during the upper Tournaisian, and relative to the stratigraphy, the timing of mineralization is similar to Navan. Conventionally drilled analyses reveals Tara Deep and Navan are isotopically similar, showing both a statistically equivalent Pb isotopic signature and a bimodal sulfide S isotopic distribution and homogeneous sulfate signature. However, around 5‰ shifts to higher $\delta^{34}S$ in the subsurface-derived S isotope signatures (both bacteriogenic sulfide and sulfate) indicate that Tara Deep's sulfur was sourced from a distinct seawater signature, highlighting Tara Deep should be considered a separate deposit to Navan in space, and potentially time. In addition, both the new sulfur and lead isotope data from Tara Deep's drillhole concentrates, from across the entire deposit, reiterates this message and highlights that the predominant Tara Deep signatures are of 1) sulfur produced by BSR of seawater sulfate (~90%) and 2) a homogeneous lead signature, reflective of derivation from underlying basement lithologies. Bacterial activity was of central importance to the establishment of Tara Deep, this in combination with interpretations made by Fallick et al., (2001) for the Navan deposit, are encouraging signs for exploration at Tara Deep. As Fallick et al. (2001) states, without the involvement of sulfate-reducing bacteria, there would be no giant Zn + Pb orebody at Navan, Tara Deep, or indeed, other economically significant Irish orebodies of Mississippian age. Furthermore, both the lead and sulfur isotope data reveal a marginally distinct signature, for both the conventionally drilled and drillhole concentrate analyses, suggesting Tara Deep should be considered as its own isolated deposit, and not an allochthonous block of the Navan deposit.

Close similarities with the Navan deposit allows Tara Deep to adopt a similar genetic model as Ashton et al., (2015). However, this research stresses that mineralization initiated during an early phase of the developing Dublin Basin and kept pace with rifting and subsequently an evolving basin. Thus Pale

Beds mineralization is temporally distinct from the S Fault Conglomerate-host. This research develops the existing model to highlight the evolving basin and multi-phase mineralization relationships.

Overall, this thesis has outlined, in detail, the carbonate and mineralization processes that led to the formation of the exciting Tara Deep prospect beside the giant Navan Zn+Pb deposit, by detailing the ore petrography and stable isotope geochemistry, and their intimate relationship with basin margin evolution. It has revealed the genesis of the deposit, particularly determining its tectonic, geological and genetic relationship to the neighboring Navan orebody. Whilst exploring these relationships, the project has informed prospectivity for further ore discovery in the Dublin Basin, around and beyond this deposit. To discover more deposits like Tara Deep, it is vital to understand the basin margin architecture and to model existing debrites and structural lows where mineralization once occurred. Correlations with Navan are important encouragement for continuing exploration in the Tara Deep region and indeed in the areas to the south and west of Navan.

5.2 Remaining Questions and Future Work

- When did mineralization start and finish? This research shows that mineralization initiated early syn-rifting and continued until rifting ceased. Rb-Sr dating of sphalerite and Re-Os dating of pyrite should be used to constrain the mineralization window. An Rb-Sr study on sphalerite, similar in nature to Schneider et al., (2007), should focus on early coarse colloform sphalerite textures and aim to avoid late coarse honeyblende sphalerite. Re-Os dating of pyrite should focus on minor early pyrite veins that can occasionally be found exploiting colloform pyrite, and a comparison with the laminated pyrite in the Thin Bedded Unit would be an excellent project.
- The next generation of discoveries within the Irish Orefield will principally be deeper. Understanding of Tara Deep reveals that although early-rift mineralization can be displaced into the depths of the Dublin Basin, the mineralizing system was still capable of evolving as rifting took place. Through understanding how the system has evolved, pathfinders to target future deposits can be constrained. Local and regional debris flows appear to act as an

important vector for future exploration, they highlight structural lows where faults scarps existed, and dense saline fluids could interact with buoyant hydrothermal solutions, subsequently depositing base metal sulfides. These debris flows have a distinct impedance contrast on the seismic dataset and should be correlated with the extensive drillhole dataset. A detailed structural understanding will continue to be the most important control for identifying high-priority targets. It is safe to assume that the pre-rift facies at Tara Deep and Navan would once have been largely laterally continuous across much of the basin margin, but similar to modern carbonate platforms, the pre-rift facies likely become poorly developed further south, and may abruptly change.

- Due to the complexity of processes involved at Tara Deep (mineralization, dolomitization and extensive pressure solution), many of the host rock fabrics are overprinted or lost, so correlations on a regional scale are very difficult. This has led to an overlap in local nomenclature across the region. It is suggested that hyperspectral reflectance, alongside detailed core imaging, should be used to help correlate units across the Tara Deep and Navan region. Hyperspectral reflectance of debris flows at Tara Deep would allow a correlation of breccias on a regional scale and would help understand their chemical and mineralogical variation, alongside helping to understand their links to ore formation. Hyperspectral reflectance would not only complement existing macro- to microscopic observations, but would also highlight 1) geochemical pathfinders for mineralization, 2) differences between mineralization in the S Fault Conglomerate and Conglomerate Group Ore, and 3) may reveal different infrared spectral signatures that could outline the relationship between hydrothermal dolomite versus replacement dolomitization, and possibly a chemical difference between early colloform sphalerite and late coarse honeyblende sphalerite. An added bonus is that detailed core images could be stored on an online platform, allowing for cross-examination of various units, and to view their 3D relationships.

- A substantial reduction in unit thickness at Tara Deep is expected as a function of extensive pressure solution. However, exactly how much reduction has occurred is unknown. Furthermore, exactly when this pressure solution occurred is difficult to constrain.

- The behaviour of the Dublin Basin is closely comparable with many of the Dinantian basins in England (Gawthorpe et al., 1989; Breislin et al., 2020), however many of these carbonate platforms lie on tectonic blocks cored by granites. Igneous intrusions have been intersected by drilling ~3 km SE of Navan, beneath similar platform facies to those present at Tara Deep. Work should be completed to decipher the age and significance of this igneous intrusion, or whether it is merely an intersection of the Kentstown granite (c.430 Ma).

- 3D seismics could have the potential to significantly enhance the structural understanding of Tara Deep and decipher the lateral displacement that likely exists between Tara Deep and Navan. The origin of local and regional debrites is complex, and they can result from several combined processes (Moscardelli and Wood, 2008; Tournadour et al., 2015). Future 3D seismics could shine light on these processes.

- Future work should attempt to date the tuffs in the TBU at Tara Deep using U-Pb dating. However, care is required to avoid contamination with the surrounding host rocks. These tuffs are hosted within calc-turbidites, and so many of the tuff intervals repeat, and are only 2-6 cm thick. To avoid contamination, the stratigraphically lowest tuff horizon with the thickest interval should be selected for zircon separation, and only euhedral zircons should be picked for dating. A sieve fraction of >60 to <120 microns should be initially used to locate zircons (based on preliminary observations made during this research).

- Microfossils in the Pale Beds appear to occur within the iron oxide textures of the emergent surfaces, however identifying exactly what these microfossils are is incredibly difficult due to alteration and reworking. Further detailed work is required for identifying these textures. Many abiotic textures can create features which are mistaken as being biotic (Pinti et al., 2009;

Marshall et al., 2011). It would be useful to attain more chemistry, or biomarkers, on these fabrics. In addition, a better 3D understanding e.g. micro-CT, is necessary. An initial look at these textures can be found in Appendix 2.

- It is known that a deep circulating metalliferous fluid, carrying metals from the basement is a key player within both the Tara Deep and Navan systems. However, I do not rule out the minor involvement of the regional debrites that truncate much of the upper Tournaisian stratigraphy as a driver for later phases of metalliferous fluids. Davidheiser-kroll (2014) revealed at Navan that high Zn-Pb ratios occurred in regions where the Boulder Conglomerate existed and suggested an unroofing model for mineralization. However, although this could be deemed a '"chicken-and-egg"' argument, in that the Boulder Conglomerate likely entered structural lows proximal to faulting, where mineralization was already occurring (based on clasts of mineralization encased by matrix replacement mineralization in both the CGO at Navan and SFC at Tara Deep), recent work on the Little Bahama Bank highlights that fluid escape can occur due to the compressive nature of debrites, subsequently deforming the infilling sediments, and forming pockmarks (Tournadour et al., 2015). Thus, it is quite possible that a minor late driver for mineralization also involved the Boulder Conglomerate.

5.3 Implications for Further Discovery within the Dublin Basin

Carbonate slope models focus on the abruptness of the margin to basin transition. Tara Deep evolved from a shallow marine ramp setting during the upper Tournaisian, to a detached carbonate platform, and then by the time of the Thin Bedded Unit into a basin associated with a highly unstable sedimentary environment coupled with debrites as basin infill dominated (Chapter 4).

Mineralization is intimately linked to basin development and is prolonged. Clasts of mineralization in the Boulder Conglomerate, alongside an evolving paragenetic sequence, and evidence of rapid precipitation textures such as dendritic galena and colloform sphalerite within cavities of the Micrite Unit, highlight that an early phase of rapid mineralization occurred before the catastrophic

debris flow events (Chapter 2). Whereas Chapter 4 highlights the longevity of the waning sub-economic mineralization within the Tara Deep system; mineralization in the TBU occurs within once supersaturated sediments, where it encases early-diagenetic concretions and exploits late pressure solution seams. From an exploration perspective, focus should not only be paid to regions on the margins of tectonically active basins within the Irish Orefield, but should also look to constrain regions where debrites and syn-sedimentary faults were occurring. These regions highlight areas where structural lows once developed, metalliferous fluids could rise, and fluid mixing could occur leading to significant Zn-Pb deposits. Thus, debris flows and laminated pyrite mineralization in the TBU should be used to vector towards prospects within the Dublin Basin and beyond.

5.4 References

Ashton, J.H.; Blakeman, R.J.; Geraghty, J.F.; Beach, A.; Coller, D.; Philcox, M.E. 2015. The Giant Navan Carbonate-Hosted Zn–Pb Deposit—A Review. In Current Perspectives On Zinc Deposits; Archibald, S.M.,Piercey, S.J., Eds.; Irish Association For Economic Geology: Dublin, Ireland, 2015; p. 85–122.

Banks, D.A., Boyce, A.J., and Samson, I.M., 2002, Constraints on the origins of fluids forming Irish Zn-Pb-Ba deposits: Evidence from the composition of fluid inclusions. Economic Geology, 97, p. 441-480.

Breislin, C., Crowley, S., Banks, V., Marshall, J., Millar, I., Riding, J. and Hollis, C., 2020. Controls on dolomitization in extensional basins: An example from the Derbyshire Platform, U.K. *Journal of Sedimentary Research*, 90(9), p.1156-1174.

Davidheiser-Kroll, B. 2014. Understanding the fluid pathways that control the Navan ore body. PhD thesis, University of Glasgow.

Fallick, A.E., Ashton, J.H., Boyce, A.J., Ellam, R.M. And Russell, M.J., 2001. Bacteria Were Responsible For The Magnitude Of The World-Class Hydrothermal Base Metal Sulfide Orebody At Navan, Ireland. Economic Geology, 96, p. 885-890.

Gawthorpe, R. L. Gutteridge, P. and Leeder, M. R. 1989. Late Devonian and Dinantian basin evolution in northern England and North Wales. In: Arthurton, R. S., Gutteridge, P. and Nolan, S. C. (eds.), The role of tectonics and Carboniferous sedimentation in the British Isles. Yorkshire Geological Society Occasional Publication, 6, p.1-23.

Marshall, C., Emry, J. and Olcott Marshall, A., 2011. Haematite pseudomicrofossils present in the 3.5-billion-year-old Apex Chert. Nature Geoscience, 4(4), p.240-243.

Moscardelli, L. And Wood, L., 2008. New Classification System For Mass Transport Complexes In Offshore Trinidad. Basin Research, 20(1), p.73-98.

Pinti, D., Mineau, R. and Clement, V. 2009. Erratum: Hydrothermal alteration and microfossil artefacts of the 3,465-million-year-old Apex chert. Nature Geoscience, 2(12), p.897-897.

Russell, M.J., 1978, Downward-excavating hydrothermal cells and Irish type ore deposits: Importance of an underlying thick Caledonian prism. Trans. Instn Min. Metall. (Sect B: Appl. Earth Sci.), 87, p. 168-171.

Schneider J, Von Quadt A, and Wilkinson JJ (2007) Age of the Silvermines Irish-type Zn-Pb deposit from direct Rb-Sr dating of sphalerite. In: Andrew CJ, et al. (eds.) Digging Deeper: Proceedings of the 9th Biennial Meeting of the Society for Geology Applied to Mineral Deposits, Dublin, Ireland, 20–23 August 2007. Dublin: Irish Association for Economic Geology. p. 373–376

Tournadour, E., Mulder, T., Borgomano, J., Hanquiez, V., Ducassou, E. and Gillet, H., 2015. Origin and architecture of a Mass Transport Complex on the northwest slope of Little Bahama Bank (Bahamas): Relations between off-bank transport, bottom current sedimentation and submarine landslides. *Sedimentary Geology*, 317, p.9-26.

APPENDIX 1: STANDARD LABORATORY PROCEDURES

A1.1 Creating Polished Thin Sections:

Polished thin sections were created for petrographic analyses, microprobe analyses, and mineral identification.

1) Regions of interest were photographed and measured to the appropriate length.

2) A diamond blade was used to cut the samples into appropriately sized cubic blocks. Extra care was required to ensure a clean cut was completed.

3) Three stages of mechanical polishing were then carried out; a course, medium, and finally a fine polish was completed. It was important to ensure that a detailed, equal polish was observed across the sample. This polishing was finished off with a manual polish using 300 µm.

4) Thin section glass slides were polished using 600 µm in order to provide a cohesive surface to glue the samples onto.

5) The samples were left to dry on a heated plate overnight. Once dry, samples were glued onto individual thin sections. The appropriate labels were scratched onto the slides.

6) Sections were then cut to remove the excess thickness of sample material. The samples were polished to an appropriate thickness of 60-100 µm. To achieve an appropriate finish for SEM and microprobe analyses, the samples were lapped to begin with, but were finished using manual polishing. An orange-yellow birefringence to quartz crystals was used as an approximate indicator that the samples were of an appropriate thickness for SEM/microprobe analyses.

A1.2 Sulfur Isotope Analyses

The process is carried out in a glass vacuum line using cryogenics to transfer, separate, purify, and measure the yield and isolate the gas of interest. The presence or absence of gas in each section of the

line is monitored using pirani gauges. Standard techniques for sulfides (Robinson and Kusakabe, 1975) and sulfates (Coleman and Moore, 1978) were used.

The line consists of the following components:

-Pumping system capable of evacuating each section of the line.

-High temperature furnace to combust the sample.

-Copper furnace for reduction of SO_3 to SO_2

-Dry ice/ acetone trap to remove water from the gases produced.

-n-Pentane trap to enable cryogenic separation of CO_2 from the SO_2

-CO_2 isolation finger.

-Calibrated cold finger with a pressure transducer to measure gas yield

-Port connection for gas sample tube to transfer the gas to a mass spectrometer.

-Pentane trap pirani gauge display.

-Calibrated cold finger transducer display.

General overview of the analysis includes:

-Moisture is retained in the slush trap (dry ice/acetone slurry) at minus 78°C

-Non-condensable gas is removed when the gas is frozen into the liquid nitrogen trap and pumped using the high vacuum system.

-Carbon dioxide is removed from the pentane trap when it is allowed to warm up to minus -130°C, at this temperature sulfur dioxide remains in the trap.

-The yield of sulfur dioxide gas is determined by freezing the gas into the calibrated cold finger section and isolating the gas in that section. When the liquid nitrogen is removed and the cold finger is allowed

to warm to room temperature, the reading on the cold finger transducer display is directly proportional to the number of micromoles of gas present.

-The sulfur dioxide is then frozen into the collection tube so that it can be transferred to the mass spectrometer for isotope ratio analyses.

Preparation of Cu_2O: The copper oxide is obtained from the suppliers in black powder CuO form. Before using as an oxidising agent for the sulfur mineral, it is essential to reduce the powder to Cu_2O. This is achieved by heating the powder (700°C) in a vacuum for several hours. When the powder is ready to be used it has a dull red colour.

Sulfur Isotope Analysis Method: the sample (4-10 mg) is mixed with 200mg copper oxide (Cu_2O oxidising agent) and heated to produce sulfur dioxide. The evolved gas also contains moisture, non-condensable gas and carbon dioxide. All equipment was calibrated according to Edwards Calibration Procedure VE-CAL-001, which involves direct comparison with reference gauges that are traceable to national standards.

Sample preparation:

Pure sulfides: weigh out 4-10mgs and mix thoroughly with 200mgs of Cu_2O using a mortar and pestle. Place in a quartz tube (~3.0 cm long) and hold it in place using quartz wool.

Purification and isolation of the sulfur dioxide for pure sulfides: switch on furnace and allow to heat up to the required temperature (1025°C). While this is happening, load the sample into the combustion tube and pump down slowly to prevent the sample being drawn into the line, at this point a mass spectrometry tube can be pumped as well. The acetone slush trap is made and put on the double U bend. Before starting the analysis, it is important to make sure there are no leaks in the system. The line should pump down to 4.0E-3. Make sure there is enough n-Pentane in the pentane trap.

To begin, close the vacuum valves and place your sample into the furnace. For sulfides, react the sample for ~25 mins; CO_2, H_2O and SO_2 will be produced. All water will freeze into the slush trap and the CO_2 and SO_2 will freeze into the pentane trap.

When the reaction is complete, pump away any non-condensable gases and isolate the pentane trap. Remove the liquid nitrogen from the pentane trap and warm it gently with a hot-air gun from top to bottom. Heat until you see vapours beginning to form in the pentane, do not overheat as the pentane will start to boil. Refreeze the pentane trap for 5 mins or until the gauge recovers. Pump the pentane trap for a few seconds. Finally, close the vacuum trap, then remove the liquid nitrogen and place it on the CO_2 coldfinger for 3 minutes. During this time there will be a small deflection and then a large one on the gauge. At the end of the 3 minutes close the coldfinger and check to make sure all CO_2 has frozen down. If the gauge continues to fall, then a second 3 minute separation will need to be carried out, this is particularly important on carbonate rich samples. Warm the pentane trap and freeze the sample into the manometer. Measure the pressure, and then freeze the samples into the mass spectrometer tube.

Sulfide+Cu_2O → SO_2+CO_2 → Measure+ Collect

Pure Sulphates- weigh out 10-15 mgs, mix with 200 mgs Cu_2O and 600 mgs of sand. Place in quartz tube as explained above. When heated with Cu_2O these produce SO_3 that requires reduction to SO_2. When running sulphates, a piece of Cu wire should be placed in the furnace alongside the sample. The furnace temperature should be 1120°C. Make sure the Cu wire inside is not oxidised. When the sample is reacted it should be held in the Cu furnace for 15 mins. This is to ensure that any SO_3 is reduced to SO_2. The gas should then be frozen into the pentane trap for 15 mins. After this the procedure is the same as the sulfides.

Sulphate+Cu_2O+SiO_2 → SO_2+SO_3+CO_2 → SO_2+CO_2→ Measure +Collect

When finished: leave the line pumping and remove the slush trap so that any water collected will be pumped away. New Cu_2O can be made up overnight if required. In addition, quartz sample tubes and

Cu wire should be changed when necessary. The bench on which the line is mounted must be kept clean and free of waste materials. After every 12-15 sulphate analyses, the copper in the furnace should be changed. Removal and cleaning of the pentane trap and the water trap is required from time to time. The need for cleaning will be apparent by the staining that builds up on the inside of these components

A1.3 Lead Isotope Analyses

Powdered samples of sulfides from mineralized drill core were dissolved using 1 ml 2% HNO_3 at the British Geological Survey in Nottingham. Dissolved samples were converted to bromide using 2 mls of concentrated HBr. Pb was separated using columns containing 100 microlitres of Dowex AG1x8 anion exchange resin using standard bromide separation methods. Prior to Pb isotope analyses each sample was spiked with a thallium solution, which was added to allow for the correction of instrument-induced mass bias. Samples were then introduced into a Nu Plasma HR multicollector ICP-MS (inductively coupled plasma-mass spectrometer). For each sample, five ratios were simultaneously measured ($^{206}Pb/^{204}Pb$, $^{207}Pb/^{204}Pb$, $^{208}Pb/^{204}Pb$, $^{207}Pb/^{206}Pb$ and $^{208}Pb/^{206}Pb$). Each individual acquisition consisted of 75 sets of ratios, collected at 5-second integrations, following a 60 second de-focused baseline. The precision and accuracy of the method was assessed through repeat analyses of an NBS 981 Pb reference solution (also spiked with thallium). The average values obtained for each of the measured NBS 981 ratios were then compared to the known values for this reference material (Thirlwall, 2002). All sample data were subsequently normalised, according to the relative daily deviation of the measured reference value from the true, with the aim to cancel out the slight daily variations in instrumental accuracy. Internal uncertainties (the reproducibility of the measured ratio) were propagated relative to the external uncertainty.

A1.4 Cathodoluminescence (CL)

Cathodoluminescence (CL) is an optical and electromagnetic phenomenon in which electrons impacting on a luminescent material, instigate the emission of photons which may have wavelengths in the visible

spectrum. It is a form of luminescence (the emission of visible light from an object when it is bombarded with some other form of energy), which was first described by Crookes (1880). Visible emissions emanating from trace elements or mineral defects are conventionally observed through an optical microscope. Similar to other optical techniques, CL provides qualitative information on the chemical composition, crystal growth forms and relationships between cements, fractures, and stylolites etc. from which the mineral paragenetic relationships can be obtained (Witkowski et al., 2000). The CL colours depend largely on the trace element or defect responsible for the emission and the mineral host. Within carbonates, these can be readily observed because of the relatively low energy of electrons required to excite luminescence. Luminescence of carbonates is controlled by the relative abundance of Fe^{2+} and Mn^{2+} in the crystal lattice (Savard et al., 1995). Carbonates such as calcite and dolomite tend to grow layer by layer in voids, and during their growth incorporate different quantities of activators and quencher elements depending on; the ions present in the depositing fluid, temperature, pH and Eh. Since these condition change over time the resulting crystals are often banded or zoned. In general, calcite usually displays a bright yellow-orange luminescence, whereas most dolomite luminesces pale blue or red, or not at all in ferrous (or higher operating voltages may be needed to generate its colours). Although staining techniques are capable of distinguishing calcite and dolomite, stains do not always work uniformly, and they do not work at all for siliceous material. However, using CL various common minerals have quite distinctive CL colours which permits them to be recognised even in trace amounts (Kopp, 1981). For many academic and industrial geological applications, it is useful to determine the sequence and environment of porosity evolution, the relative timing of porosity occlusion and its possible effects on ore migration (Witkowski et al., 2000). It is crucial to understand the paragenetic sequence of the host stratigraphy as minerals are often precipitated within the pore space of a sedimentary rock during diagenesis.

A1.5 3D Modelling

Data validation, exploration and visualisation was processed using Seequent's Leapfrog Geo 4.4 software. Three-dimension analyses were carried out to investigate the structural controls of the Tara Deep deposit to identify the controlling structures on the geology, and fluid flow within the deposit. Boliden Tara Mines' Exploration Department have extensive drilling, assay analyses, historical analytical records etc., allowing detailed 3D modelling of the complex structural geology. In regions of interpretation, the locations of each lithology, as well as their extents, was delineated from the diamond drillhole records, historic reports, publications, and underground mapping. It was particularly useful to allow comparisons to be made between Tara Deep and the main Navan deposit (including the SWEX). It is vital to understand the structural controls of Tara Deep in order to investigate the processes at which the deposit likely formed under, and most importantly from an industry perspective, pinpointing the regions with the highest grades of ore. Through analyses of these structural geometries and location of best ore grades, future exploration will be able to accurately determine where the most economic grades of ore will be located.

References

Coleman, M. and Moore, M., 1978. Direct reduction of sulfates to sulfate dioxide for isotopic analysis. Analytical Chemistry, 50(11), p.1594-1595.

Crookes, W., 1880, Magnetic Deflection Of Molecular Trajectory Laws Of Magnetic Rotation In High And Low Vacua Phosphorgenlc Properties Of Molecular Discharge. Philosophical Transactions Of The Royal Society Of London, V. 170, Part Ii, p. 641-662. [First Description of Cl Phenomena.]

Kopp, O. C., 1981, Cathodoluminescence Petrography-A Valuable Tool For Teaching And Research: Journal Of Geological Education, V 29, p.108-113

Robinson, B. W., and Kusakabe, M., 1975. Quantitative preparation of sulfur dioxide, for $^{34}S/^{32}S$ analyses, from sulfides by combustion with cuprous oxide. Anal. Chem., 47:1179.

Savard, M., Veizer, J. And Hinton, R., 1995. Cathodoluminescene At Low Fe And Mn Concentrations; A Sims Study Of Zones In Natural Calcites. Journal Of Sedimentary Research, 65(1a), p.208-213.

Thirlwall, M., 2002. Multicollector Icp-Ms Analysis Of Pb Isotopes Using A 207pb-204pb Double Spike Demonstrates Up To 400 Ppm/Amu Systematic Errors In Tl-Normalization. Chemical Geology, 184(3-4), p.255-279.

Witkowski, F. W., Blundell, D. J., Gutteridge, P., Horbury, A. D., Oxtoby, N. H., And Quing, H., 2000. Video Cathodoluminescence Microscopy Of Diagenetic Cements And Its Applications. Marine And Petroleum Geology, 17, p.1085–1093.

Appendix 2: SUBSURFACE FILAMENTOUS FABRICS FROM THE TARA DEEP Zn-Pb DEPOSIT, CO. MEATH, IRELAND.

A2.1 Introduction

Tara Deep is the latest carbonate-hosted Zn-Pb discovery by Boliden Tara Mines, which is located 2km to the SE of the world-class Navan deposit. Tara Deep and Navan are located within the northern margin of the Dublin Basin, and they offer a rare opportunity to assess in detail syn-rift diagenesis and the complexities that come with basin evolution. Within the Tara Deep system, the basin margin evolves from a shallow marine intertidal environment, associated with fenestral limestones and emergent surfaces, into a highly unstable basin fill succession by the lower Viséan. This section will focus on subsurface filamentous fabrics (SFFs) that are hosted within emergent surface textures within early pre-rift facies, locally-termed Pale Beds (see Chapter 4). These textures are now located on a series of fault-controlled terraces on the southern margin of the Tara Deep's Zone One (8 drillhole intersections made to date), where they offer early insight into the depositional environment and the palaeoconditions that existed. Iron oxide has preferentially exploited these emergent surfaces (Fig. A2.1), but it can also be observed exploiting interparticle porosity in the host rock. Within these iron oxide exploited cavities, a series of complicated filamentous fabrics exist, the morphometric characteristics of which are very similar to those of microbial filaments and the fabrics formed from them. However, filamentous fabrics can be very controversial (Pinti et al., 2009; Marshall et al., 2011) because it is difficult to determine whether they are of biological (microbial filaments) or nonbiological origin (chemical gardens, fibrous crystals, filamentous pseudofossils etc; Sayed and Polshettiwar, 2015; Barge et al., 2015; McMahon, 2019), and these fabrics can occur in the microporosity of any type of rock. Here I present initial observations and interpretations to help explore the biogenicity of these textures and to highlight what they reveal in terms of the depositional environment. Due to the Covid-19 pandemic, it has proved impossible to complete detailed chemistry, isotopic analyses and CT-scans on these textures.

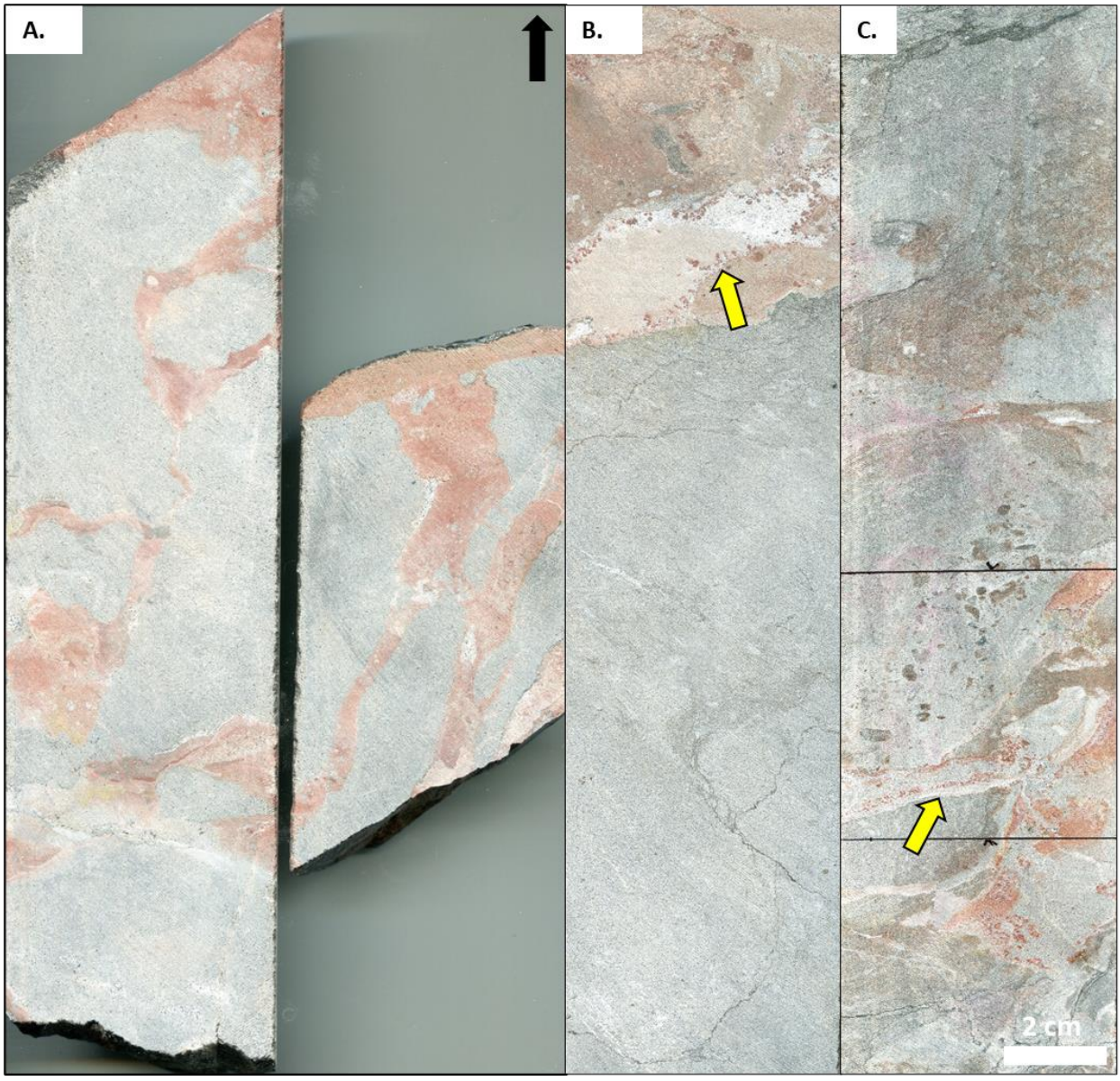

Figure A2.1 Halved drillcores displaying emergent surface textures within the Pale Beds at Tara Deep. A) Cavities within the Pale Beds emergent surfaces are often infilled by micritic mud, but these cavities have also been preferentially exploited by iron oxide. Arrow denotes the way up direction (N02505/04; 1723.25 m). B) Emergent surface cavity has subsurface filamentous fabrics nucleating on cavity walls (yellow arrow; N02499/02; 1674.5 m). C) Note iron exploits both the fissure cavity and host rock matrix. Again, note subsurface filamentous fabrics nucleating on cavity walls (yellow arrow; N02510/05; 1664. 5 m)

A2.2 Background

Subsurface filamentous fabrics (SFFs) as defined by Hoffman et al., (2008) as microscopic to macroscopic mineral fabrics that result from the precipitation of minerals on a substrate of filamentous (thread-like) geometric units in subterraneous environments. Typical dimensions of the filamentous units are widths in the range of microns and lengths of hundreds of microns. SFFs are widespread in several terrestrial subsurface environments. Despite the variability of host environments, the morphology of SFFs are very similar (Hofmann et al., 2008). Hoffman et al., (2008) propose that microbial life-forms can produce distinctive fabrics structurally organized in ways fundamentally different from abiogenic formations. A number of criteria, most prominently filament width, bending and number of direction changes in filaments, show that most SFFs are more closely related to microbial filaments than to abiogenic textures. In conjunction, isotopic analyses can provide an important line of evidence when evaluating biogenicity (Neubeck et al., 2021).

Bacteria have long been known to play a pivotal role in the complex mineralization story present within Irish-Type deposits (Fallick et al., 2001). Despite this, no known fossiliferous bacteria have ever been reported proximal to mineralization within the Navan or Tara Deep deposits. However, observations of biological activity have been made within other Irish-type deposits, e.g. Silvermines (Boyce et al., 2003) and Tynagh (Banks, 1985).

A2.3 Methods:

Detailed logging of Tara Deep drillcore was undertaken during the exploration drill core campaign. Two hundred and thirty-one samples were collected that epitomised different stratigraphical units, carbonate textures and mineralization styles. From these, twelve large (6 cm x 4 cm) polished thin sections were created from iron oxide altered regions. Petrographic analyses of these textures and their paragenetic relationships were carried out using standard transmitted and reflected light microscopy. Detailed scanning electron microscopy (SEM) was completed at the University of Glasgow, using a Quanta 200F Environmental SEM with EDAX microanalysis, and remotely at the Aberdeen Centre for

Electron Microscopy, Analysis and Characterisation (ACEMAC) facility, at the University of Aberdeen, using a Carl Zeiss GeminiSEM 300 VP Field Emission instrument equipped with Deben Centaurus CL detector, an Oxford Instruments NanoAnalysis Xmax80 Energy Dispersive Spectroscopy (EDS) detector and AZtec software suite. Prior to electron microscopy samples were sputter coated with a thin coat of gold-palladium under vacuum

Carbon Isotopes

Micro-drilled emergent surface cavities that have been exploited by iron oxide, were acid washed with hydrochloric acid to remove any carbonate. Bulk subsamples of 12-15 mg of leached iron oxide were weighed into 5 × 3 mm tin capsules and combusted in a Pyrocube elemental analyzer (Elementar, Hanau, Germany). Sample gases were transferred via helium carrier gas to a Thermo Delta XP Plus isotope ratio mass spectrometer (Thermo, Bremen, Germany). Drift correction using a 3-point normalization was performed using three in-house standards (GEL, ALAGEL and GLYGEL) encompassing a range of isotope compositions, run every ten samples, and a suite of GELs of different sizes were used to correct samples for linearity (Werner & Brand, 2001). GEL is a gelatin solution, ALAGEL an alanine-gelatine solution spiked with 13C-alanine, and GLYGEL a glycine-gelatine solution spiked with 15N-alanine. Four differently sized USGS 40 glutamic acid international reference materials (Qi et al., 2003; Coplen et al., 2006) were used as independent checks of accuracy and to acquire the calibration for N and C content. All data are reported with respect to the international V-PDB for $\delta^{13}C$. Results are reported in δ notation (McKinney et al., 1950). Analytical precision (SD) of GEL (Gelatin) was $\delta^{13}C$ = 0.08‰.

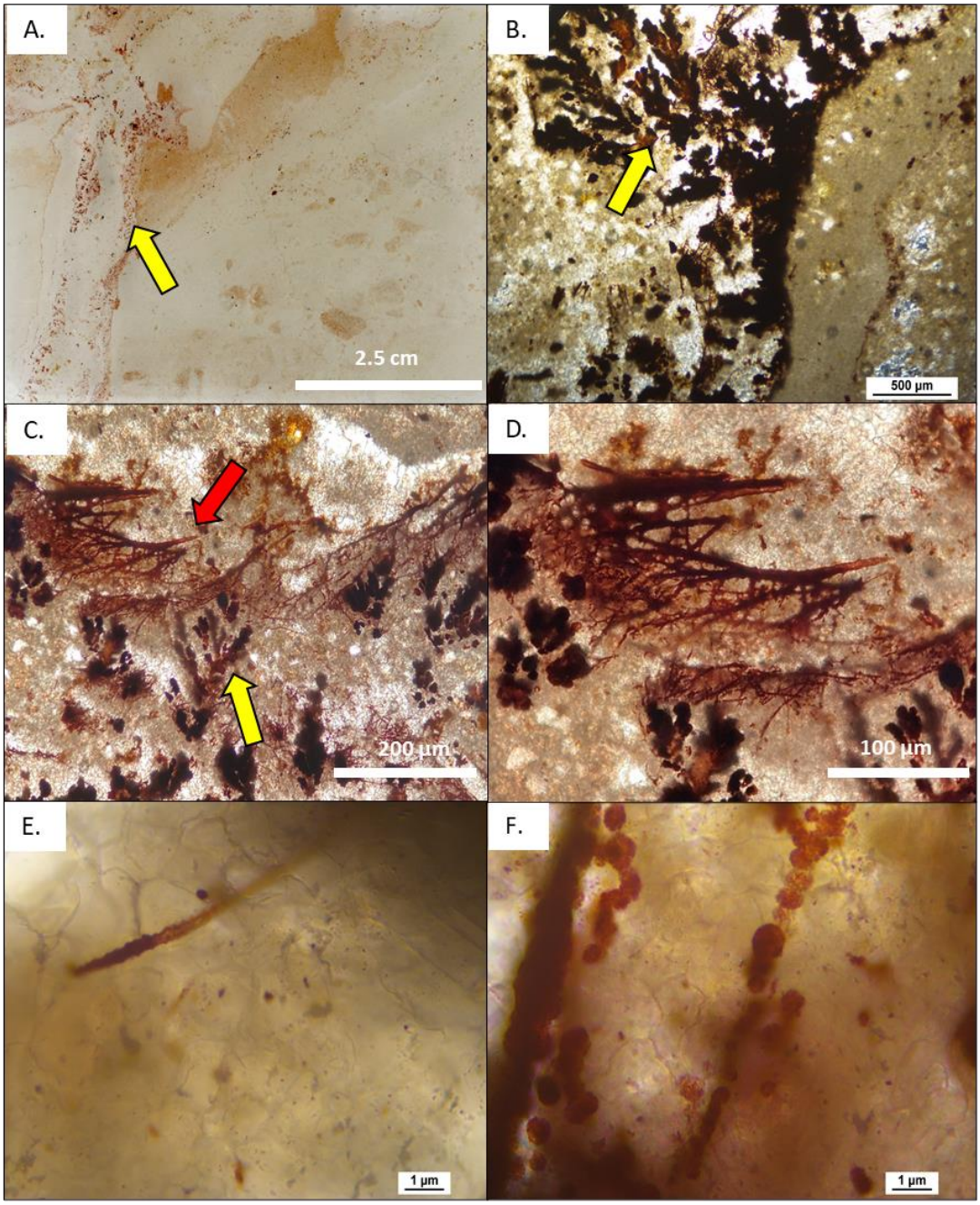

Figure A2.2 Detailed standard petrography images from example N02510/05 (for region of interest see yellow arrow on Fig. A2.1C). (A) Thin section scan from region marked in figure A2.1C, note subsurface filamentous fabrics nucleating on palaeocavity wall (yellow arrow). B) Frutexite-like structure can be observed nucleating on cavity walls (yellow arrow). C and D) Branching filamentous structure (red arrow), which appears to have a hollow tip, are closely associated with frutexites (yellow arrow). E and F) High magnification image of structure of filamentous tubes.

A2.4 Initial Observations and Preliminary Interpretations

-In transmitted light, some of these textures reveal a branching cauliflower-like morphology, ranging in length from 200-500 µm. These textures are very similar to microstromatolites or frutexites (Fig. A2.2A-B; Neubeck et al., 2021). These textures can be observed nucleating on pre-existing cavity walls. However, chemical data is required to supplement these observations, especially since complicated textures can be generated abiotically in iron oxide.

- These textures were closely associated with webs of filaments, all of which appeared to be replaced by iron oxide. Many of the filamentous fabrics (Fig. A2.2C-D) also show considerable branching, bending and a dendritic appearance. They range in length from 10 µm to 200 µm, with the central stalk typically displaying a width of 20 µm. Detailed SEM analyses (Fig. A2.3 & A2.4) of these structures reveal that they are typically isolated features that do not connect. Some of these filamentous fabrics show evidence of having hollow tubes in both standard petrography (Fig. A2.2C) and detailed SEM analyses (Fig. A2.4A&B). All of these filamentous structures appear to be composed of microcrystalline Fe-oxyhydroxide grains (Fig. A2.4C). These Fe-oxyhydroxide grains are ubiquitous and often appear embedded in calcite (Fig. A2.4D).

-To determine the biogenicity of these structures conventional organic carbon analyses on micro-drilled and leached samples were completed. These samples were collected from micro-drilled regions where these textures existed, not from individual isolated textures, thus they should be handled with caution as they represent a bulk signature. All samples analysed contained organic carbon, ranging from 0.14-0.96 wt%. Isotopic analyses revealed significantly negative $\delta^{13}C$ values for the samples. The $\delta^{13}C$ values range from -22.9 to -28.5 ‰ (n=11), which an average $\delta^{13}C$ of -26.1 ‰± 1.9.

-Distinct abiotic textures are more dominant and easier to identify within these emergent surface cavities (Fig. A2.6). Abiotic textures consist of disc shaped iron oxide alteration, bladed crystals and microcrystalline and framboidal pyrite.

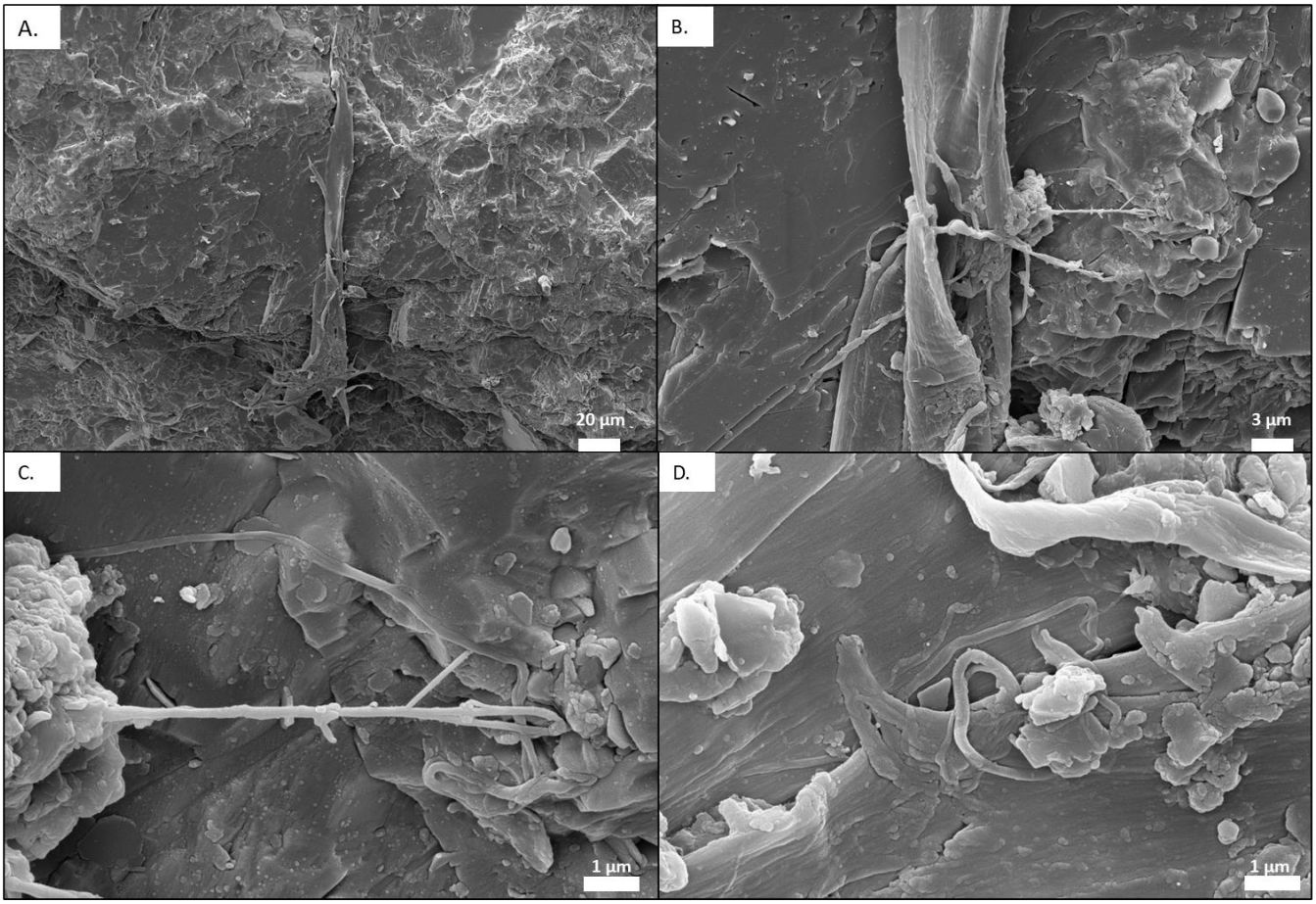

Figure A2.3. Back scattered electron image conducted on an emergent surface rock chip from sample N02510/05 (see Fig. A2.1C) that has been exploited by iron oxide. A) The fabric in the centre of the image displays an isolated branching morphology with a length of 200 microns and a width of 20 microns. B) A closer look at the structure in Fig.A2.3A reveals a series of bending tubes and branches. C) A closer look at one of the branches in Fig. A2.3B. D) A series of sinuous textures can be identified in the fabric which reveals numerous complicated bends.

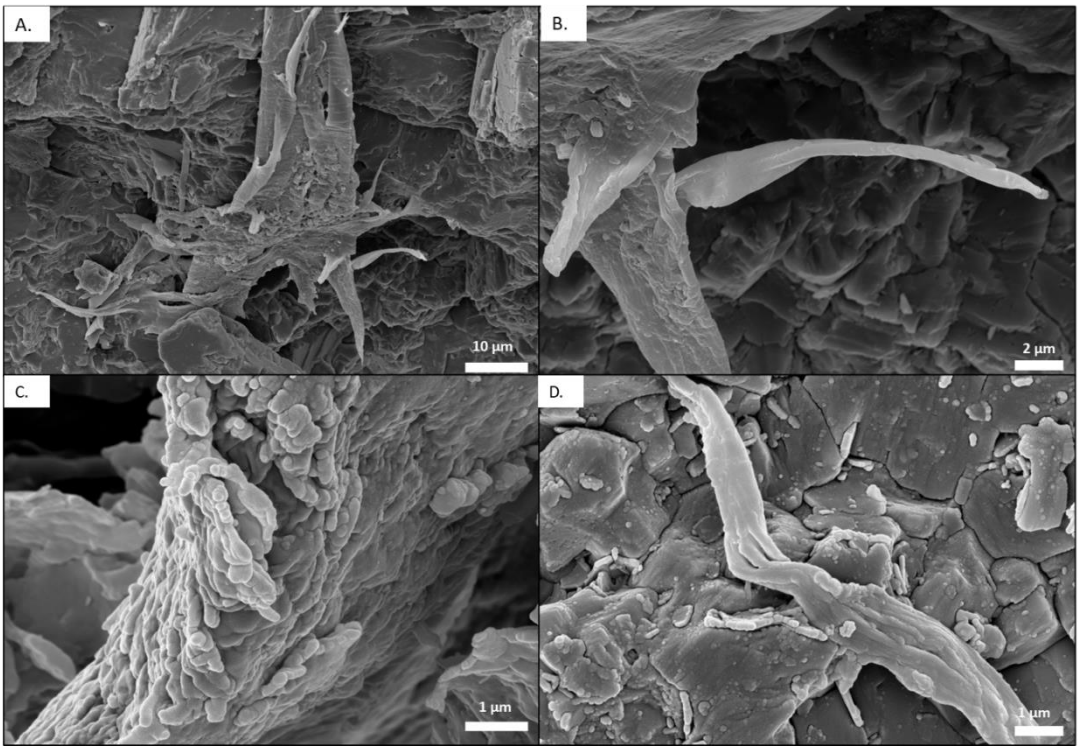

Figure A2.4. Backscattered electron image form N02510/05. A and B) A closer examination of the isolated 'root' of one of these structures. The specimen displays complicated bending and numerous branches. C) These fabrics appear to be encrusted or built from a series of sub-micron Fe-oxyhydroxide grains. D) An additional bending structure composed of numerous Fe-oxyhydroxide grains, displaying complicated bending. This texture is comparable to a Gallionella stalk.

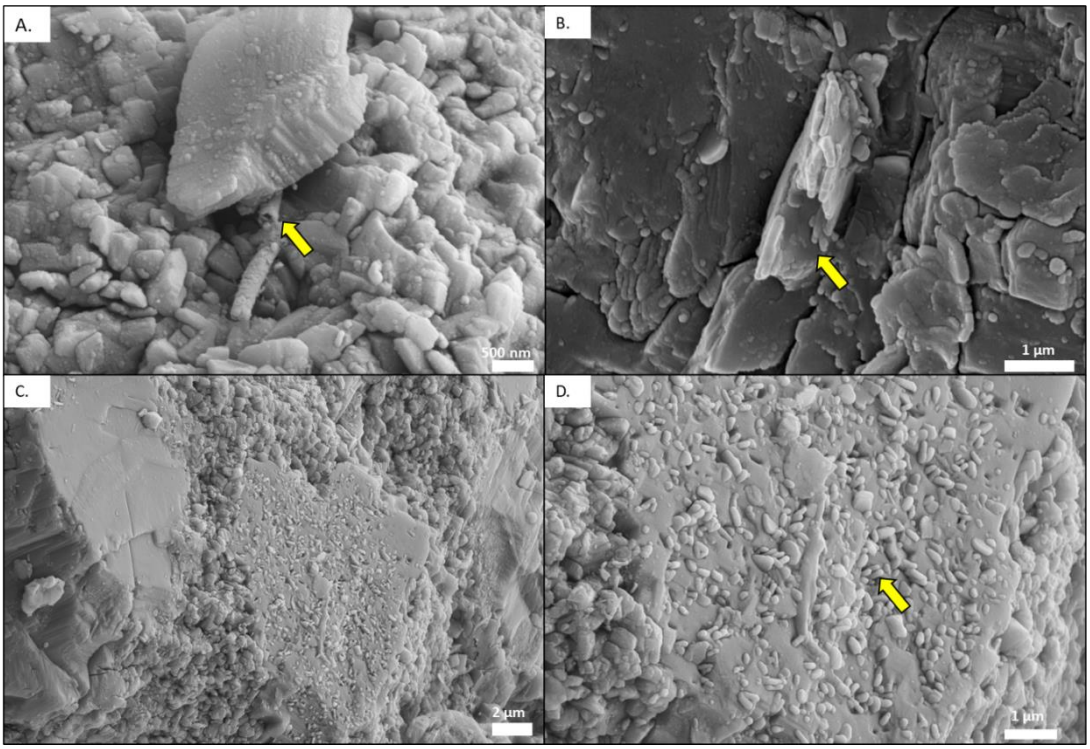

Figure A2.5. More images from N02510/05 A) a broken hollow tube can be identified under a calcite crystal. B) A hollow tube built from Fe-oxyhydroxide grains which propagate out of the host rock matrix. C and D) These Fe-oxyhydroxide grains are ubiquitous and can be found embedded in calcite.

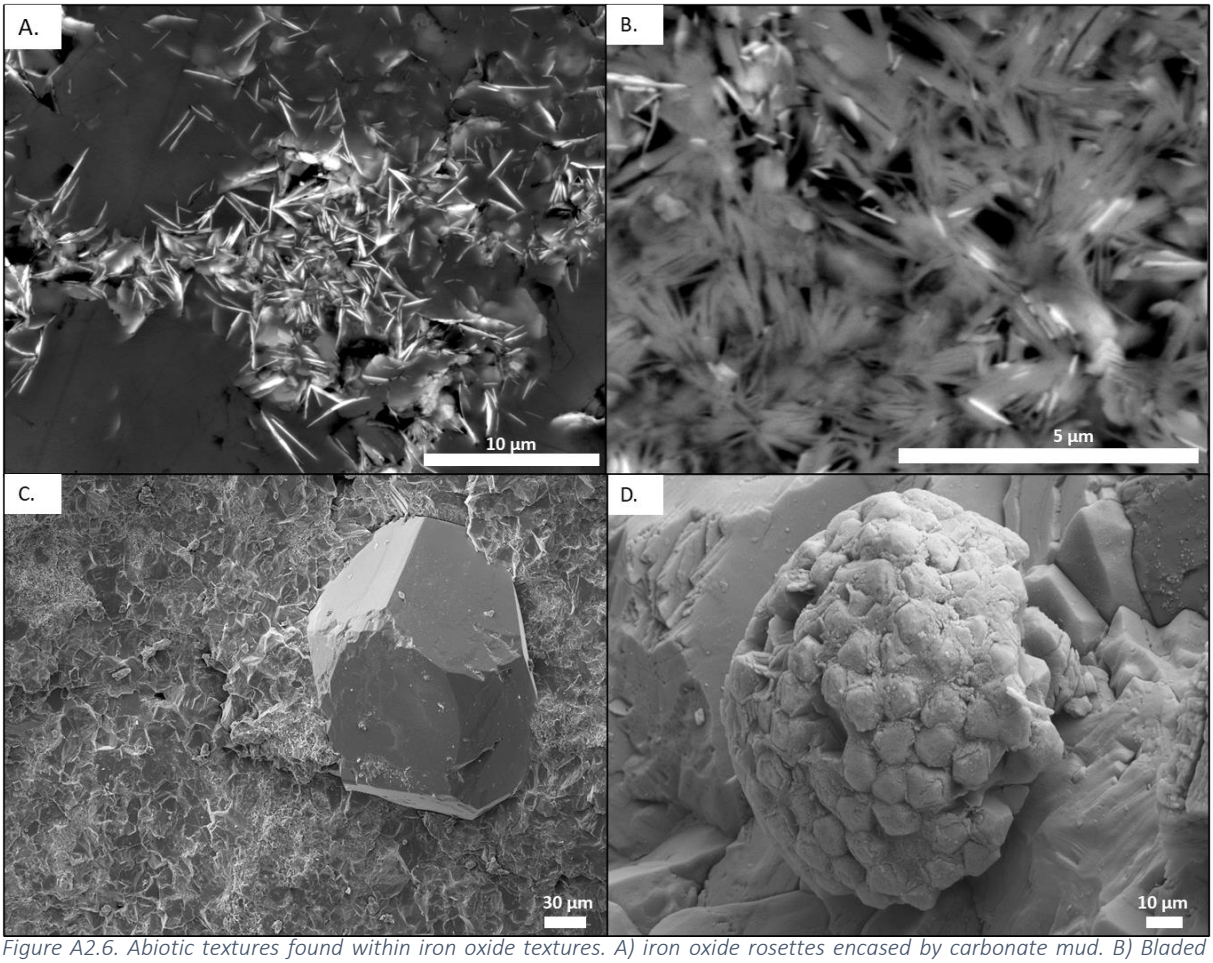

Figure A2.6. Abiotic textures found within iron oxide textures. A) iron oxide rosettes encased by carbonate mud. B) Bladed crystals C) microcrystalline pyrite. D) Framboidal pyrite.

A2.5 Significance and Implications

-The morphometric characteristics of certain SFFs at Tara Deep are very similar to those of microbial filaments and fabrics in terms of dimensions, numerous structural bends, hollow isolated structures, and evidence of branching. Frequent branching and anastomoses connections are in favour of a biological origin.

-These Tara Deep examples are very similar to filamentous structures that have been observed in a large variety of environments, such as cavities in volcanics, oxidized ore deposits, palaeokarst environments and even pipelines carrying acid mine effluent (Hofmann et al., 2008; Williams et al., 2015; Williams et al., 2017; Götze et al., 2020).

-The easiest explanation for the 'webby networks' is that they are fossil biofilms originally composed of filamentous microorganisms (perhaps including but not necessarily limited to iron-oxidizing bacteria).

-The variation in filament thickness is interesting. It is assumed thicker filaments have accumulated more Fe-oxyhydroxide than the fabrics that are thinner. Fe-oxidizing bacteria can accumulate rather flocculent sheath-like coatings of ferric oxyhydroxides.

- If these samples are confirmed to be fossilized bacteria, it could provide crucial evidence for active microbial communities during early phases of the Dublin Basin evolution. Assuming microbial activity during the beginning of SFF formation, the upper temperature limit of initial SFF formation was probably ~100-150°C, similar temperatures were suggested by Götze et al., (2020).

- Tara Deep's C isotope values observed (mean $\delta^{13}C$ of -26.1 ‰± 1.9) are similar to those reported in Neubeck et al., (2021) for frutexites, and Kennedy et al., (2010). Kennedy et al., (2010) report one of the first investigations focused on the utility of carbon isotopes as a biosignature in iron oxide. They report similar C isotope data from iron oxide samples collected from hydrothermal vents, subterranean and surficial groundwater seeps and cultures of *Gallionella ferruginea*. They highlight that iron-oxidising bacteria are capable of significantly fractionating carbon isotopes and that this isotopic ratio holds promise as a viable biosignature in contemporary environments and palaeoenvironments.

-The presence of subsurface filamentous fabrics may also be used to infer the possible former presence of subsurface life not only in different types of environments, but potentially also in geologically similar situations on other planetary bodies such as Mars.

-While these results are preliminary in nature, they are also promising and warrant further investigation. It would be rash to conclude here that these textural assemblages exclusively represent biological textures, especially given the lack of chemical data and because numerous studies have shown that inorganic chemical reactions can produce iron-mineralized filaments and tubes similar in

both morphology and composition to examples which have been interpreted in the past as fossil microorganisms (Oaki and Imai, 2003; McMahon, 2019). However, given the morphological features (in particular complicated bending), the shallow marine/emergent depositional setting and context (which is favourable for life), and bulk $\delta^{13}C$ analyses of these textures, the initial indication is that these fabrics are biological in origin.

A2.6 Acknowledgments

I am very thankful to Aberdeen University for remotely analysing these polished thin sections with me during the Covid-19 pandemic, with particular thanks to Alex Brasier and John Still. I thank the ISAAC facility at the University of Glasgow for SEM access. SUERC is supported by NERC and the Scottish Universities consortium. I also wish to thank Magnus Ivarsson, Nicola McLoughlin, Aubrey Zerkle and Sean McMahon for their advice and opinion on these textures.

A2.7 References

Banks, D. A. 1985. A fossil hydrothermal worm assemblage from the Tynagh lead-zinc deposit in Ireland. Nature, 313, p.128-131.

Barge, L. M., Cardoso, S. S. S., Cartwright, J. H. E., Cooper, G. J. T., Cronin, L., De Wit, A., Doloboff, I. J., Escribano, B., Goldstein, R. E., Haudin, F., Jones, D. E. H., Mackay, A. L., Maselko, J., Pagano, J. J., Pantaleone, J., Russell, M. J., Sainz-Díaz, C. I., Steinbock, O., Stone, D. A., ••• Thomas, N. L. (2015). From chemical gardens to chemobrionics. *Chemical Reviews*, *115*(16), p.8652 – 8703.

Boyce, A.J.; Stephen Little, C.; Russell, M. 2003. A New Fossil Vent Biota in the Ballynoe Barite deposit, Silvermines, Ireland: Evidence for Intracratonic Sea-Floor Hydrothermal Activity About 352 Ma.Econ. Geol., 98, p. 649–656.

Coplen TB, Brand WA, Gehre M, Gröning M, Meijer HAJ, Toman B, Verkouteren RM. 2006 New guidelines for $\delta^{13}C$ measurements. *Analytical Chemistry.* 2006;78:2439–2441. doi: 10.1021/ac052027c.

Fallick, A.E., Ashton, J.H., Boyce, A.J., Ellam, R.M. And Russell, M.J., 2001. Bacteria Were Responsible For The Magnitude Of The World-Class Hydrothermal Base Metal Sulfide Orebody At Navan, Ireland. Economic Geology, 96, p. 885-890.

Götze, J., Hofmann, B., Machałowski, T., Tsurkan, M., Jesionowski, T., Ehrlich, H., Kleeberg, R. and Ottens, B., 2020. Biosignatures in Subsurface Filamentous Fabrics (SFF) from the Deccan Volcanic Province, India. *Minerals*, 10(6), p.540.

Hofmann, B.A., Farmer, J.D., von Blanckenburg, F., Fallick, A.E., 2008. Subsurface filamentous fabrics: An evaluation of possible modes of origins based on morphological and geochemical criteria, with implications for exopalaeontology. Astrobiology 8, p.87-117.

Kennedy, C., Gault, A., Fortin, D., Clark, I., Pedersen, K., Scott, S. and Ferris, F., 2010. Carbon isotope fractionation by circumneutral iron-oxidizing bacteria. Geology, 38(12), p.1087-1090.

Marshall, C., Emry, J. and Olcott Marshall, A., 2011. Haematite pseudomicrofossils present in the 3.5-billion-year-old Apex Chert. *Nature Geoscience*, 4(4), p.240-243.

McKinney CR, McCrea JM, Epstein S, Allen HA, Urey HC. 1950. Improvements in mass spectrometers for the measurement of small differences in isotope abundance ratios. Review of Scientific Instruments, 21(8), p.724-730.

McMahon, S., 2019. Earth's earliest and deepest purported fossils may be iron-mineralized chemical gardens. Proceedings of the Royal Society B: Biological Sciences, 286(1916). http://dx.doi.org/10.1098/rspb.2019.2410

Neubeck, A., Ivarsson, M., Broman, C., Lima-Zaloumis, J., Bach, W. and Whitehouse, M., 2021. Carbon isotopic composition of Frutexites in subseafloor ultramafic rocks. *Biogeochemistry*, 154(3), p.525-536.

Oaki, Y. and Imai, H., 2003. Experimental Demonstration for the Morphological Evolution of Crystals Grown in Gel Media. Crystal Growth & Design, 3(5), p.711-716.

Pinti, D., Mineau, R. and Clement, V., 2009. Erratum: Hydrothermal alteration and microfossil artefacts of the 3,465-million-year-old Apex chert. *Nature Geoscience*, 2(12), p.897-897.

Qi H, Coplen TB, Geilmann H, Brand WA, Böhlke JK. 2003 Two new organic reference materials for $\delta^{13}C$ and $\delta^{15}N$ measurements and a new value for the $\delta^{13}C$ of NBS 22 oil. *Rapid Communications in Mass Spectrometry.* 2003;17: p.2483–2487.

Sayed, F. and Polshettiwar, V., 2015. Facile and Sustainable Synthesis of Shaped Iron Oxide Nanoparticles: Effect of Iron Precursor Salts on the Shapes of Iron Oxides. *Scientific Reports*, 5(1).

Werner RA, Brand WA. 2001. Referencing strategies and techniques in stable isotope ratio analysis. *Rapid Communications in Mass Spectrometry.* 2001; 15: p.501–519.

Williams, A.J., Alpers, C.N., Sumner, D.Y., Campbell, K.M., 2017. Filamentous Hydrous Ferric Oxide Biosignatures in a Pipeline Carrying Acid Mine Drainage at Iron Mountain Mine, California. Geomicrobiology, Journal ,34, p.193-206.

Williams, A.J., Sumner, D.Y., Alpers, C.N., Karunatillake, S., Hofmann, B.A., 2015. Preserved Filamentous Microbial Biosignatures in the Brick Flat Gossan, Iron Mountain, California. Astrobiology 15, p.337-668.

Table A2.1: Organic Carbon $\delta^{13}C$ Data

Sample ID	$\delta^{13}C$ (‰)	Organic Carbon (mg)	wt% C
n02505-07	-27.08	0.042	0.30
n02505-08	-26.00	0.082	0.65
n02499-02	-28.07	0.110	0.89
n02505-11	-28.49	0.110	0.75
n02505-10	-28.28	0.126	0.88
n02505-04	-26.71	0.136	0.96
n02510-05	-23.41	0.050	0.36
n02499-08	-26.66	0.073	0.57
n02510-04	-22.87	0.031	0.21
n02499-06	-24.58	0.031	0.22
n02510-05b	-24.50	0.020	0.14
Average	-26.06	0.07	0.54
Standard Deviation	1.87	0.04	0.29

APPENDIX 3: EVIDENCE FOR CLUMPED C-O ISOTOPE REORDERING AT THE TARA DEEP Zn-Pb OREBODY, NAVAN, IRELAND.

Drummond[1], D. A.,Clog[1], M., McDonald[1], A., Hollis[2], C., Boyce[1], A. J.

[1]Scottish Universities Environmental Research Centre, Rankine Avenue, East Kilbride, Glasgow G75 0QF, United Kingdom.

[2]School of Earth and Environmental Science, University of Manchester, Manchester M13 9PL, UK.

A3.1 Abstract

Understanding fluid temperatures associated with an orebody provides critical insights into the processes that drive metal transport and deposition within ore deposits. Tara Deep provides an early opportunity to explore the systematics of clumped isotope palaeothermometry in paragenetically well-defined calcite and dolomite within Irish-Type mineralization, in a region where obtaining conventional fluid inclusions has proved notoriously difficult. The message emerging is that post-depositional solid-state reordering of C–O bonds in the calcite lattice has significantly altered the primary clumped isotope composition of paleotemperatures at the Tara Deep Zn-Pb deposit. Calcite samples within Tara Deep have been exposed to temperatures greater than 120°C or more for 10^6–10^8 years timescales which has partially modified the solid-state C–O bond reordering within calcite, thus inhibiting their use as a measure of the primary hydrothermal temperature during ore deposition. This has been achieved without inducing visible changes in crystal microstructure and trace element concentrations, metrics commonly used to gauge preservation quality. Because re-equilibration during exhumation and cooling will draw the TΔ47 towards lower values, the temperatures recorded in our samples place a lower bound on the peak paleotemperatures at 175°C. Dolomites record a lower apparent temperature to the re-ordered calcites, suggesting that the Δ47 of our dolomite samples were not completely reset during the geological history of those rocks. Overall, what emerges is a cautionary tale, calcite at Tara Deep do not preserve the primary depositional temperature and have undergone significant reordering, meaning that they should not be considered as primary ore depositional

temperatures. Detailed petrography of textures support this, highlighting that it is highly unlikely for early diagenetic cements to record apparent temperature of 93°C to 147°C.

A3.2 Introduction

The Tara Deep Zn-Pb deposit (26.2 Mt @ 7.8% Zn and 1.6% Pb; Boliden Summary Report, 2020) is the most recent major discovery of the world-renowned Navan Orebody cluster (Ashton et al., 2018). Tara Deep is located 2km south of the Navan Orebody, on the footwall of a large south-dipping basin margin fault, where mineralization is found at a depth of 1.2-1.9 km (see Ashton et al. 2018; Chapter 2).

Clumped isotope thermometry of marine carbonates has provided new insight into the paleotemperatures and oxygen isotope compositions of ancient seawaters (Came et al., 2007; Keating-Bitonti et al., 2011; Price and Passey, 2013) and have even revealed evidence for large global climatic shifts (e.g., the Late Ordovician-Early Silurian glaciation; Finnegan et al., 2011). There is potential for clumped isotopes to reconstruct temperatures and fluid properties in hydrothermal ore deposits. Delineation of fluid temperatures associated with an orebody provides critical constraints on the processes that drive transport and deposition of metals (Mering et al., 2018) and would provide limitations to phase stability models, and the proportion of metals capable of being transported in fluids (Cooke et al., 2000; Boyce et al, 2015). This is particularly useful in regions like Navan, where workable fluid inclusions prove elusive and/or unrepresentative of the main mineralizing event (Everett et al., 1999). Here we present the first measured Δ47 in paragenetically well-constrained, carbonate generations from the Tara Deep system, that sits alongside the giant Navan Orebody. What emerges is a cautionary tale, stressing that C-O bond reordering has occurred, resulting in temperature data which reflect extended post-deposition heating of the area, rather than reflecting the hydrothermal history of the ore depositional event.

A3.3 Previous Studies at Navan

Categorised as Irish-type deposits, mineralization within the Irish Orefield is comparable to carbonate-hosted SEDEX deposits, that were deposited syn-diagenetically with their Mississippian (Lower

Carboniferous) limestone host rocks (Derry et al., 1965; Russell, 1975; Taylor and Andrew, 1978; Boast et al., 1981; Boyce et al., 1983a; Taylor, 1984; Ashton et al., 1986; Anderson et al., 1998; Chapter 2). There is dispute about the timing of mineralization at Navan and Tara Deep, with the most widely accepted theory being that mineralization began in the Irish Orefield at ~355 Ma and lasted some 10 m.y. (Anderson et al., 1998; Boyce et al., 2003; Wilkinson et al., 2003). Genetic models for Navan and Tara Deep, alongside other Irish deposits have derived much detail from isotopic studies (Coomer and Robinson, 1976; Boast et al., 1981; Boyce et al., 1983b, 1993; Caulfield et al., 1986; O'Keefe, 1986; Mills et al., 1987; Anderson et al., 1998; Ashton et al., 2015; Chapter 2).

Tara Deep is located immediately south of the Longford Down Lower Paleozoic Inlier, within a major NE to ENE-trending structural corridor approximately coincident with the underlying Iapetus Suture (Vaughan & Johnston, 1992). To the south and west of the Navan area, Mississippian platform carbonates and calc-turbidites of the developing Dublin Basin sub-crop. The local stratigraphy at Navan and Tara Deep records an overall marine transgression during the upper Tournaisian and contains pre-, syn-, and post-rift elements. These rocks lie on a regional unconformity overlying Ordovician and Silurian volcano-sedimentary and igneous rocks, originally deposited on the Laurentian and Avalonian margins of the Iapetus Ocean (Romano, 1980; O'Keeffe, 1986, Murphy et al, 1991; Fritschle et al 2018). The Tournaisian Old Red Sandstone (ORS) of the Irish Midlands, locally termed Red Beds, represents the base of the lower Mississippian and marks the start of the transition from subaerial to marine deposition.

The upper Tournaisian (pre-rift) stratigraphy at Navan and Tara Deep, records shallow marine carbonate deposition within a developing peritidal environment (Ashton et al., 2015). This encapsulates the deposition of 200m of micrites, bioclastic calcarenites and oolites, which appear to display a cyclicity, with numerous emergent surfaces observed which have been suggested to have developed on a shallow, homoclinal ramp (Rizzi, 1992; Chapter 4). In local nomenclature, these 'Pale Beds' are the principal host for mineralization, particularly within the Micrite Unit sub-group. The Micrite Unit is a

fenestral limestone, exhibiting birds-eye textures and representing deposition in a dominantly intertidal environment (Strogen et al., 1990; McNestry and Rees, 1992).

Overlying the Micrite Unit at Tara Deep the remaining Pale Beds comprise higher energy, but yet still shallow marine, oolitic grainstones which still reveals evidence for emergence and nodular limestone features, which have later been enhanced by pervasive pressure solution. Across the Dublin Basin, increasing water-depth during the upper Tournaisian led to the deposition of the Shaley Pales and Argillaceous Bioclastic Limestones (ABL), followed by the deep-water Waulsortian mudbank limestones, which unlike some other areas in Ireland, are poorly developed and unmineralized at Navan (Boyce et al., 1983a; Caulfield et al., 1986; Wilkinson et al., 2005; Barrie et al., 2009; Ashton et al., 2015; Wilkinson and Hitzman, 2014). However, at Tara Deep these units are no longer preserved, and the destructive dynamic nature of the Dublin Basin is evident. Within Irish geology the main phase of rifting is generally accepted as being the generation of the catastrophic Boulder Conglomerate (BC). These laterally extensive debris flows are the key expression of the main rift event in the lower Viséan, where rapid subsidence resulted in gravitational instability that has truncated much of the upper Tournaisian stratigraphy (upper Pale Beds, Shaley Pales, Argillaceous Bioclastic Limestone and Waulsortian limestone), subsequently reworking and re-deposition of material as large allochthonous blocks and submarine sedimentary breccias (Philcox, 1989; Andrew, 1993; Boyce et al., 1983b; Ford, 1996; Chapter 2). Although the Boulder Conglomerate is classified as one unit, it is likely composed of many individual sedimentary breccias related to prolonged extension (Ford, 1996). Thick accumulations of Arundian-Holkerian calc-turbidites and minor conglomerates later form the rapid infill to the Dublin Basin, known locally as the Upper Dark Limestone (Nolan, 1989; Philcox, 1989; Ashton et al 2015). Basal parts of the Upper Dark Limestone (locally termed the Thin Bedded Unit; TBU) show a remarkable increase from 20m thick at the Navan deposit, to over 500m thick at Tara Deep. At Tara Deep, the TBU reveals complex soft sediment deformation features associated with calc-turbidites, and minor debris flows, attesting to rapid unstable basin infill, likely associated with continued seismic activity (Chapter 4). Finally, later

Variscan compression led to inversion, and a local dip of 15-20° SW was also probably imparted (Ashton *et al*. 2018).

Extensive petrographic studies of the Navan and Tara Deep stratigraphy have been completed involving drill core logging, thin section petrography, cathodoluminescence (CL), fluid inclusion and isotopic analyses (Anderson, 1990; Redmond, 1991; Rizzi, 1992; Farrelly, 1993; Braithwaite and Rizzi, 1997; Rizzi and Braithwaite, 1997; Anderson et al., 1998; Everett and Wilkinson, 2001; Thorpe, 2001; Peace, 1999; Peace et al. 2003; Knight, 2012; Chapter 2 & 4). Researchers typically outline the complexity of rifting basins, with early marine pre-rift facies being characterized by fenestral micrites, and observations of isopacheous marine cements within oolitic grainstones (Wilkinson et al., 2003; Chapter 4). Occurrences of emergent surfaces have been noted in the lower Pale Beds (Anderson, 1990; Rizzi, 1992; Rizzi and Braithwaite, 1996; Chapter 4). These textures are occluded by a series of processes that complicate depositional environment reconstruction, these include dolomitization, mineralization and pressure dissolution.

Dolomitization is evident in nearly all of the carbonate-hosted Zn+Pb deposits in Ireland, however, relationships between dolomite formation and ore deposition are varied. It is generally accepted that dolomitization likely occurred in stages in deposits such as Navan (Anderson, 1990), Tara Deep (Chapter 4), Silvermines (Andrew, 1986), and Tynagh (Boast et al. 1981), and formation of pre-ore dolomite may have been an important controlling factor in ore genesis, acting as seals for metalliferous fluids (Anderson, 1990). Although dolomite is closely associated with mineralization at Navan, a model has never been constrained. Chapter 4 reveals that dolomitization can be broken down into D1-D4 stages at Tara Deep. The D1 phase represents fabric retentive euhedral (30 µm size) replacement dolomitization that is constrained to the Pale Beds, it preferentially replaces oolitic horizons and occludes the fenestral fabric of the Micrite Unit and is laterally extensive for >3km. D2 dolomitization is ferroan dolomite (50 µm size) that infills any remaining interparticle porosity remaining after D1 dolomitization. Clasts of replacive dolomitization and mineralization have been observed within the Boulder Conglomerate (Ford, 1996; Anderson et al., 1998). These allochthonous

dolomite and sulfide clasts provide evidence that the mineralizing and dolomitizing system started prior to the onset of the Boulder Conglomerate and continued during its formation. D3 is a late rare, coarse (~0.5 cm) saddle dolomite phase that is associated with vuggy porosity and is closely associated with a phase of late sphalerite, locally termed honeyblende sphalerite. The acidity of this late metalliferous fluid can generate vuggy porosity in pre-existing dolomitized units, and it is within these vugs that saddle dolomite crystals can be found. Finally, the D4 phase is closely associated with late pressure solution. D4 likely represents burial dolomitization, where dolomite forms as a reactate mineral (Chapter 4).

Significant oxygen and carbon isotopic analyses have been attempted for the Navan carbonates (limestone and gangue; Rizzi, 1992; Braithwaite and Rizzi, 1997; and Peace, 1999), with limited work completed on the Tara Deep system (Chapter 4). These studies are consistent with deposition of these carbonates in a tropical, emergent settings from marine Carboniferous carbonates (Keith and Weber, 1964), and in subsequent diagenetic events related to basin subsidence. The $\delta^{13}C$ composition of carbonate cements reflects the source of the carbonate, and for the vast majority of Navan carbonates the source is dominated by marine bicarbonate. Oxygen isotope data show a variation in which early diagenetic phases are modelled in equilibrium with Mississippian marine water at temperatures between about 20-85°C (Chapter 4). Vein calcite temperature signatures are lacking fluid inclusion data, and consequently the hydrothermal fluid O isotope signature is ambiguous. However, temperatures in excess of 65°C can be modelled from the $\delta^{18}O$ (Chapter 4).

Maturation studies indicate that the Navan host-rocks should have passed through the oil-window. Despite this, small amounts of crude oil show limited distribution within vugs and carbonate veins in the Boulder Conglomerate, Waulsortian, and Upper Dark Limestones at Navan, suggesting that maturation may have been lower in the Navan area than thermal indicators suggest. Survival of low homogenisation temperatures and monophase fluid inclusions in minerals like calcite and barite at Navan, are suggested as evidence that the Variscan heating event, at least locally, did not exceed ~150°C (Wilkinson et al., 2003; Wilkinson, 2010).

A3.4 Clumped Isotope Background

Carbonate clumped isotope thermometry is based on the distribution of heavy isotopes in the carbonate lattice (Eiler 2011). In aqueous fluids, the proportion of carbonate ions bearing two heavy isotopes (one ^{13}C and one ^{18}O) is related not only to the abundance of those heavy isotopes but also to temperature. Those isotope distributions are recorded and preserved when precipitation as carbonate minerals occur. Carbonate minerals can then be dissolved in phosphoric acid in the laboratory, and the resulting CO_2 analyzed by mass spectrometry to measure the proportion of CO_2 isotopologues of various masses, and specifically the excess of isotopologues of mass 47 relative to a stochastic distribution of heavy isotopes among isotopologues, noted Δ47. Well-characterized or lab-grown carbonates are used to calculate crystallisation temperatures (Ghosh et al 2006). However, there are limitations to the preservation of the clumped isotope signatures in carbonate minerals. Open system recrystallisation (for example because of an influx of hot fluid) can reset Δ47 towards the temperatures of recrystallisation and modify the $\delta^{13}C$ and $\delta^{18}O$ of the mineral (Ryb and Eiler 2018, Stolper et al 2018). Modification of the Δ47 can also occur in closed-system conditions, through diffusion of isotopes in the lattice of the crystal, towards re-equilibration to the new ambient temperature (e.g., Dennis and Schrag 2010). The kinetics of re-equilibration of Δ47 have been studied experimentally for calcite and dolomite (Passey and Henkes 2012, Henkes et al 2014, Stolper and Eiler 2015, Lloyd et al 2018), with the conclusion that Δ47 in calcite would be significantly modified when temperatures rise above 100°C for long geological timescales (10^6–10^8 years), with dolomite potentially able to withstand temperatures of up to 150°C over geological timescales (Lloyd et al 2018). This constitutes both a challenge to the use of clumped isotope geothermometry to recover crystallisation temperatures and as a potential tool to understand thermal histories (e.g., Ryb et al 2021).

A3.5 Clumped Isotopes Method

Clumped isotope measurements were performed at the Scottish Universities Environmental Research Centre (SUERC) with a Thermo Fisher 253 Isotope Ratio Mass Spectrometer (IRMS), using a manual

extraction line. Samples (typical size: 3.5mg for pure carbonate) were digested in >103 % H_3PO_4 at 90°C for 13 min in a common acid bath for calcites, and 30 minutes for dolomites. A glass coil cooled at -76 °C with a mixture of ethanol and dry ice was placed immediately after the acid bath to trap the water produced during the acid digestion. The CO_2 produced was also condensed continuously during the acid digestion in a subsequent glass coil submerged in liquid N_2. During the last 3 minutes (5 for dolomites) of acid digestion, incondensable gases were evacuated by pumping with a turbomolecular pump. The resulting CO_2 was further transferred to a calibrated volume attached to a strain gauge using liquid N_2. The gas was then thawed until it reached room temperature, after which the acid digestion volume yield was measured. The CO_2 was then passed through a 4 m Gas Chromatography column held at 40 °C with a He carrier flow before being diverted to the IRMS, where it was measured in 7 blocks of 6 dual-inlet measurements (26 s integration time) recording intensities of masses 44 to 48.

Data reduction was done using the Easotope software (John and Bowen, 2016), the IUPAC parameters (Brand et al 2010, Petersen et al 2019), and the ^{18}O acid fractionation of Kim et al (2007) for calcites and Rosenbaum and Sheppard (1986) for dolomites. After the pressure base-line (PBL) background correction the difference between the standards ETH1 and ETH2 was less than 0.005 ‰. To define the empirical transfer function (ETF) from the measured Δ47 to the absolute reference frame, we use the values from Bernasconi et al. (2021) for the ETH1-ETH4 carbonate standards. The reprojected Δ_{47} values were used to calculate apparent temperatures using the calibration of Anderson et al. (2021).

$$\Delta_{47\ RAFC(Br,P,AFF)} = 0.0391(\pm0.0004)*10^6/T^2 + 0.154(\pm0.004)$$

Analytical uncertainties on Δ47 were calculated by taking the larger of the standard deviation of the ETH carbonate standards Δ47 and the standard deviation on replicates of each sample, and dividing by the square root of the number of replicates.

Detailed logging of Tara Deep core was undertaken during the exploration drill core campaign. Representative samples were collected that outlined different stratigraphical units and various textural styles. Focus was paid to early diagenetic cements, multi-phase dolomitization, regions hosting calcite

veining (with and without mineralization) and regions of pressure solution, with an aim to better constrain the depositional environment associated with Tara Deep.

A3.6 Results

We present here the results of stable isotope analyses, including clumped isotopes at mass 47, from 17 carbonate samples from Tara Deep as described in the previous section. The samples were selected to span the range of units, facies and mineralogy at Tara Deep (10 calcites and 7 dolomites). In the rest of the manuscript, all $\delta^{13}C$ are relative to VPDB, all $\delta^{18}O$ to VSMOW and all $\Delta47$ to an absolute reference frame based on the ETH carbonate standards as described above.

The bulk $\delta^{13}C$ and $\delta^{18}O$ values are broadly in agreement with previous measurements conducted at Tara Deep (Chapter 4). In more detail, the undolomitized host rocks signatures (one sample for each) in the Micrite Unit, Pale Beds and Thin Bedded Unit (TBU) have $\delta^{13}C$ and $\delta^{18}O$ values covering small ranges, 1.8 to 2.9 ‰ and 24.9 to 25.7 ‰ respectively. Iron oxide which has exploited early micritic cements within Pale Bed's emergent surfaces (n=1) reveals a slightly altered signature of $\delta^{13}C$ 2.0 ‰ and $\delta^{18}O$ values 25.2 ‰. In the Pale Beds with stylo-nodular texture, the carbonate nodules (n=3) have slightly higher $\delta^{13}C$ (2.1 to 2.7 ‰) and $\delta^{18}O$ values (25.7 to 27 ‰).

A concretion (n=1) in the TBU showed a carbon isotopic composition markedly depleted compared to all other samples ($\delta^{13}C$ = -14.2 ‰), suggesting a bacteriogenic involvement (Raiswell et al., 2002), and an oxygen isotopic composition ($\delta^{18}O$ = 29.2 ‰) consistent with early diagenesis at low temperatures. Carbon and oxygen isotope values measured in calcite veining associated with regions of mineralization are markedly different from the host rocks and nodules ($\delta^{18}O$= 21.5 ‰ to 22.5‰; $\delta^{13}C$ = -0.1‰ to 0.4; n=2), consistent with either a hotter and/or isotopically distinct fluid.

The dolomite samples are from two different broad types, D1/D2 and D4 as summarized in Chapter 4. D1/D2 represent early replacement dolomitization (D1) and ferroan dolomite infill (D2), whereas D4 is associated with pressure solutions around nodules in the Pale Bed's Healed Conglomerates. The bulk signatures of early replacement and minor infill dolomitzation (D1/D2; n=4)

display $\delta^{13}C$ values of 1.7 to 2.3 ‰ and $\delta^{18}O$ values of 23 to 24.6 ‰, suggesting crystallization at higher temperatures and/or due to the influence of fluids with relatively low $\delta^{18}O$. The extensive dolomitized pressure solution (D4) surrounding the Healed Conglomerate nodules (n=3) reveal an altered signature of $\delta^{13}C$ (1.1 to 2.5 ‰) and $\delta^{18}O$ values (23.7 to 24.5 ‰).

The Δ47 values in the undolomitized, early diagenetic cements within the Micrite Unit, Pale Beds and TBU host rocks range from 0.376 to 0.446‰, corresponding to apparent temperatures (in the rest of the manuscript, TΔ47) of 93 to 147°C. Similarly for the nodules within the Pale Beds and concretions in the TBU, the Δ47 values range from 0.370 to 0.399‰ (TΔ47 between 126 °C and 152°C). Those apparent temperatures strongly contrast with the bulk isotope signatures, clearly suggesting resetting, and thus are no longer reflecting the low temperature diagenetic conditions.

Iron oxide exploiting an emergent surface texture has a signature of 0.349‰, with an apparent temperature of 175°C. Calcite veining associated with mineralization has a range of 0.351 to 0.396‰ with an apparent temperature of 129 to 173°C. Early replacement dolomitization associated with ferroan infill has a Δ47 range of 0.377 to 0.424‰, suggesting temperatures in the range of 108-146°C. It is suggested within Chapter 4, that this early replacement dolomitization is unlikely to be related to hydrothermal dolomitization due to the fabric retentive replacement and the fact that dolomitization is laterally continuous within the Micrite Unit for >3 km, thus dolomitization here is more suggestive of reflux dolomitization. Subsequently indicating that these dolomitization (D1/D2) temperatures recorded have also been reset. Finally, later D4 dolomitization associated with pressure solution seams have a Δ47 range of 0.388 to 0.464‰ (TΔ47 between 82 to 136°C).

A3.7 Discussion

The $\delta^{13}C$ and $\delta^{18}O$ isotope compositions of the samples investigated in this study are comparable to those measured in Chapter 4 for each phase of carbonate investigated. Along with the petrographic relationships observed in the drill cores, the stable isotope compositions of the calcite host rocks were calculated as reflecting formation during the early stages of diagenesis, at temperatures of 40°C or lower, while early dolomites (D1/D2) would have been formed around 80°C (see Table A3.1). These

temperatures (typically 20-85°C) were calculated assuming equilibrium with Mississippian seawater ($\delta^{18}O$ = 0 ‰; Mii et al., 1999), which could be incorrect if the Tournaisian seawater was unique, or if diagenetic fluids had isotopic compositions markedly different from seawater, as was suggested by Shelton et al (2019) for carbonate veins in the north-east of the Dublin Basin. The main advantage of the clumped isotope geothermometer is that it is not necessary to know the $\delta^{18}O$, of the co-existing fluid during precipitation to calculate the crystallisation temperature. However, the TΔ47 calculated for the calcites with the highest $\delta^{18}O$ range from 90 to 150°C, which does not seem plausible with the petrological observations and would require the earliest diagenetic fluids to have a $\delta^{18}O$ >7 ‰.

Clumped isotope paleotemperatures from primary carbonates are susceptible to alteration via C–O bond reordering in the solid mineral lattice. Specifically, such 'reordering' must involve the breakage of existing C–O bonds, and reforming the C–O bonds with allochthonous C or O originating from, for example, neighbouring carbonate groups. Such reordering is related to solid-state diffusion of C and O atoms through the mineral lattice. Regardless of the exact mechanism(s), the net result is a gradual change in the abundance of ^{13}C–^{18}O bonds (and other isotope-specific bonds; Henkes et al. 2014) towards equilibrium values for carbonate minerals heated to a sufficient temperature (about 100°C for calcite, Stolper et al 2015, Hemingway and Henkes 2021; and about 150°C for dolomite, Lloyd et al 2018, Hemingway and Henkes 2021). This process can reset primary clumped isotope compositions without visibly changing the texture and, crucially, the $^{18}O/^{16}O$, $^{13}C/^{12}C$, or trace element composition of the calcite (Henkes et al 2014). As the process involves reordering of C–O bonds at the molecular to unit cell scale, it does not require mass exchange with external fluids or gases, as would be required to alter $^{18}O/^{16}O$ and $^{13}C/^{12}C$ via self-diffusion (e.g., Anderson, 1969; Kronenberg et al., 1984; Farver, 1994, Henkes et al. 2014). Additionally, recrystallization through dissolution-reprecipitation can potentially alter the Δ47 during diagenesis towards burial temperatures, which can leave the bulk isotopic compositions seemingly unaffected if the fluid/rock ratio is small (e.g., Bergmann et al 2018, Ryb and Eiler 2018). This can be potentially useful to constrain paleotemperature profiles by looking at the final distribution of Δ47 recorded in samples along with numerical models of the kinetics of bond-reordering

(Ryb et al 2021). Independent constraints on the thermal history of the carbonate rocks studied can thus be critical for the interpretation of the observed Δ47 values when re-equilibration is possible, with the two most important parameters affecting the final Δ47 being the maximum temperature reached and the rate of exhumation (e.g., Ryb et al 2021 and references therein). However, Mering et al (2018) were able to use carbonate clumped isotopes to recover temperatures in ore deposits of up to ~350°C, consistent with fluid inclusion data, highlighting the potential for carbonate rocks to record high temperatures in some geological settings, possibly where cooling rates are faster than those caused by erosion and exhumation.

The thermal history of the Dublin Basin has been studied previously, mainly based on vitrinite reflectance and fluorescence (Jones, 1992; Fernandes and Clayton, 2003), which are proxies for the maximum temperature reached during the diagenetic history. Fernandes and Clayton (2003) observed that in most of the Dublin Basin, the Viséan packages within the basin reached conditions compatible with the dry-gas window. The notable exception was the borehole closest to Navan and Tara Deep (near the Kingscourt Outlier) where the heating was not as pronounced and suggested a position within the oil window. The presence of crude oil in vugs and fragile fluid inclusions from Navan (Wilkinson 2010) would also suggest that the maximum temperatures reached did not exceed 150°C during the maximum burial and heating, although it is unclear if this maximum P-T conditions were reached during the Variscan orogeny, which caused folding and complex deformation in the area (Ashton et al., 2015). In any case, the inferred maximum paleotemperatures are above the 'blocking temperature' for Δ47 in calcite, and potentially dolomite as well. The calculated temperatures for our samples are therefore likely not primary formation temperatures but modified to variable extents during heating and burial, and potentially during exhumation as well. Another indication that the variations in Δ47 of the calcite or dolomite samples are mainly due to secondary processes (recrystallization and/or bond re-ordering) is that there are no correlations between the Δ47 and bulk isotopic compositions globally or among the different sample types present. Because re-equilibration during exhumation and cooling will draw the

TΔ47 towards lower values, the temperatures recorded in our samples place a lower bound on the peak paleotemperatures at 175°C.

Clumped isotope signatures recorded in dolomites are more resistant to modification by heating than those in calcites, although the magnitude of the difference is not precisely known and has been investigated by recent studies (e.g., Lloyd et al 2018, Hemingway and Henkes 2021). Nevertheless, it means that if calcite and dolomite minerals are heated to temperatures of 150°C or more (which are inferred for other regions of the Dublin basin; Fernandes and Clayton, 2003), for long periods of time (10^6–10^8 years), the Δ47 of both calcites and dolomites will completely reset to reflect equilibrium at the burial temperature and will be modified during cooling. Assuming both mineral types have a common exhumation history, then dolomites should record higher apparent temperatures than the calcites. However, in our samples, we observe that the temperatures recorded by the dolomites cover a lower apparent temperature range (82 to 146°C) than the calcites (93 to 175°C), with an overall lower average (118±21°C and 140±25°C respectively). This means that the Δ47 of our dolomite samples were not completely reset during the geological history of those rocks.

A3.8 Conclusion

Understanding fluid temperatures associated with an orebody provides critical insight into the processes that drive transport and deposition of metals, and has the potential to provide limitations to phase stability models and the proportion of metals capable of being transported in fluids. Tara Deep offered a rare opportunity to look at clumped isotope palaeothermometry within Irish-Type mineralization, a region where obtaining conventional fluid inclusions has proved very difficult. This work is one of the earliest attempts to try to relate clumped isotope paleotemperatures to ore genesis. However, what emerges is a cautionary tale, calcite at Tara Deep does not preserve the primary depositional temperature and have undergone significant alteration because the region has been exposed to P-T conditions (>150°C) that have subsequently resulted in C–O bond alteration in calcite. Several lines of evidence agree with this, detailed petrography of textures suggest that it is highly unlikely for early diagenetic cements to record apparent temperature of 93 to 147 °C. In addition, there

are also no correlations between the Δ47 and bulk isotopic compositions globally or among the different sample types present. However, because re-equilibration during exhumation and cooling will draw the TΔ47 towards lower values, the temperatures recorded in our samples place a lower bound on the peak paleotemperatures at 175°C. Finally, dolomites within our field area record a lower apparent temperature to the re-ordered calcites, suggesting that the Δ47 of our dolomite samples were not completely reset during the geological history of those rocks. Overall, clumped isotope palaeothermometers of calcite at Tara Deep should not be considered as primary depositional temperatures and related to ore deposition but they do provide constraints on the subsequent thermal history.

A3.9 References

Anderson, I.K., 1990. Ore depositional processes in the formation of the Navan zinc-lead deposit, Co. Meath, Ireland. Unpublished PhD thesis, University of Strathclyde, p.290.

Anderson, I.K., Ashton, J.H., Boyce, A.J., Fallick, A.E. and Russell, M.J., 1998, Ore Depositional processes in the Navan Zn-Pb deposit, Ireland. Economic Geology 93, p. 535-563.

Anderson, N.T., Kelson, J.R., Kele, S., Daëron, M., Bonifacie, M., Horita, J., Mackey, T.J., John, C.M., Kluge, T., Petschnig, P. and Jost, A.B., 2021. A Unified Clumped Isotope Thermometer Calibration (0.5–1,100° C) Using Carbonate-Based Standardization. *Geophysical Research Letters*, *48*(7).

Anderson, T.F., 1969. Self-diffusion of carbon and oxygen in calcite by isotope exchange with carbon dioxide. *Journal of Geophysical Research*, *74*(15), p.3918-3932.

Andrew C.J., (1986) The tectono-stratigraphic controls to mineralization in the Silvermines area, County Tipperary, Ireland. In: Andrew CJ, Crowe RWA, Finlay S, Pennell WM, and Pyne J (eds.) Geology and Genesis of Mineral Deposits in Ireland, pp. 377–417. Dublin: Irish Association for Economic Geology.

Andrew C.J., (1993) Mineralization in the Irish Midlands. In: Pattrick RAD and Polya DA (eds.) Mineralization in the British Isles. London: Chapman and Hall. p. 208–269.

Ashton, J.H., Beach, A., Blakeman, R.J., Coller, D., Henry, P., Lee, R., Hitzman, M., Hope, C., Huleatt-James, S., O'donovan, B., Philcox, M.E., 2018. Discovery Of The Tara Deep Zn-Pb Mineralisation At The Boliden Tara Mine, Navan, Ireland: Success With Modern Seismic Surveys. In Seg Special Publications No 21, p. 365-381. Doi:10.5382/Sp.21.16: P. 17.

Ashton, J.H.; Blakeman, R.J.; Geraghty, J.F.; Beach, A.; Coller, D.; Philcox, M.E. 2015 The Giant Navan carbonate-hosted Zn–Pb deposit—A review. In Current Perspectives on Zinc Deposits; Archibald, S.M.,Piercey, S.J., Eds.; Irish Association for Economic Geology: Dublin, Ireland, 2015; p. 85–122.

Ashton, J.H.; Downing, D.T.; Finlay, S. 1986. The geology of the Navan Zn–Pb orebody. In Geology and genesis of mineral deposits in Ireland; Andrew, C.J., Crowe, R.W.A., Finlay, S., Pennell, W.M., Pyne, J.F.,Eds.; Irish Association for Economic Geology: Dublin, Ireland, p. 243–280.

Barrie, C., Boyce, A., Boyle, A., Williams, P., Blake, K., Wilkinson, J., Lowther, M., McDermott, P. and Prior, D. 2009. On the growth of colloform textures: a case study of sphalerite from the Galmoy ore body, Ireland. Journal of the Geological Society, 166(3), p.563-582.

Bergmann, K.D., Finnegan, S., Creel, R., Eiler, J.M., Hughes, N.C., Popov, L.E. and Fischer, W.W., 2018. A paired apatite and calcite clumped isotope thermometry approach to estimating Cambro-Ordovician seawater temperatures and isotopic composition. *Geochimica et Cosmochimica Acta*, *224*, p.18-41.

Bernasconi, S.M., Daëron, M., Bergmann, K.D., Bonifacie, M., Meckler, A.N., Affek, H.P., Anderson, N., Bajnai, D., Barkan, E., Beverly, E. and Blamart, D., 2021. InterCarb: A community effort to improve interlaboratory standardization of the carbonate clumped isotope thermometer using carbonate standards. Geochemistry, Geophysics, Geosystems, 22(5).

Boast, A.M., Coleman, M.L., and Halls, C., 1981, Textural and stable isotope evidence for the genesis of the Tynagh base metal deposit, Ireland: ECONOMIC GEOLOGY, v. 76, p. 27–55.

Boliden Summary Report. 2020 [online] Boliden.com. Available at: <https://www.boliden.com/globalassets/operations/exploration/mineral-resources-and-mineral-reserves-pdf/2020/resources-and-reserves-tara-2020-12-31.pdf> [Accessed 1 July 2021].

Boyce, A, J. Coleman M.D. Russel, M.J.1983b. Formation of fossil hydrothermal chimneys and mounds from Silvermines, Ireland: Nature, 306, p. 545–550.

Boyce, A. J., Anderton, R. and Russell, M.J., 1983a, Rapid subsidence and early Carboniferous base-metal mineralization in Ireland. Trans. Instn Min. Metall. (Sect B: Appl. Earth Sci.), 92, p.55-66.

Boyce, A.J., Barrie, C.D., Samson, I.M. and Williams-Jones, A.E. 2015. Aspects of the geochemistry of zinc – a journey to sphalerite. In, Archibald. S and Piercey, S. (Eds) Current Perspectives on Zinc Deposits, Irish Association for Economic Geology, Dublin, p. 38-56.

Boyce, A.J., Fletcher, T.J., Fallick, A.E., Ashton, J., and Russell, M.J., 1993. Petrographic and $\delta^{34}S$ study of Lower Palaeozoic rocks under the Navan Zn + Pb deposits: A source of hydrothermal sulphur, *in* Fenoll Hach-Ali, P., Torres-Ruiz, J., and Gervilla, F., eds, current research in geology applied to ore deposits: Second Biennial SGA Meeting, Granada, 1993, Departa- mento de Mineralogia y Petrologia, Universidad de Granada, Proceedings, p. 53–56.

Boyce, A.J.; Stephen Little, C.; Russell, M. 2003. A New Fossil Vent Biota in the Ballynoe Barite deposit, Silvermines, Ireland: Evidence for Intracratonic Sea-Floor Hydrothermal Activity About 352 Ma.Econ. Geol., 98, 649–656.

Braithwaite, C.J.R. and Rizzi, G., 1997, The geometry and petrogenesis of hydrothermal dolomites at Navan, Ireland. Sedimentology, 44, p. 421-440.

Brand, W.A., Assonov, S.S. and Coplen, T.B., 2010. Correction for the 17O interference in δ (13C) measurements when analyzing CO2 with stable isotope mass spectrometry (IUPAC Technical Report). *Pure and Applied Chemistry*, *82*(8), p.1719-1733.

Came, R.E., Eiler, J.M., Veizer, J., Azmy, K., Brand, U. and Weidman, C.R., 2007. Coupling of surface temperatures and atmospheric CO 2 concentrations during the Palaeozoic era. *Nature*, *449*(7159), p.198-201.

Caulfield, J.B.D., LeHuray, A.P. and Rye, D.M., 1986, A review of lead and sulphur isotopes investigations of Irish sediment-hosted base metal deposits, with new data from Keel, Ballinalack, Moyvoughly and Tatestown deposits. In: Andrew, C.J., Crowe, R.W.A., Finlay, S., Pennell, W.M. and Pyne, J. (Eds). Geology and Genesis of Mineral Deposits in Ireland. IAEG, Dublin, p. 591-616.

Cooke, D., Bull, S., Large, R. and McGoldrick, P., 2000. The Importance of Oxidized Brines for the Formation of Australian Proterozoic Stratiform Sediment-Hosted Pb-Zn (Sedex) Deposits. Economic Geology, 95(1), p.1-18.

Coomer, P.G., and Robinson, B.W., 1976, Sulphur and sulphate-oxygen isotopes and the origin of the Silvermines deposits, Ireland: Mineralium Deposita, 11, p. 155-169.

Dennis, K.J. and Schrag, D.P., 2010. Clumped isotope thermometry of carbonatites as an indicator of diagenetic alteration. *Geochimica et Cosmochimica Acta*, *74*(14), pp.4110-4122.

Derry, D.R., Clark, G.R., and Gillat, N., 1965, The Northgate base-metal deposit at Tynagh, County Galway, Ireland: A preliminary study: Economic Geology, v. 60, p. 1218–1237.

Eiler, J.M., 2011. Paleoclimate reconstruction using carbonate clumped isotope thermometry. *Quaternary Science Reviews*, *30*(25-26), p.3575-3588.

Everett, C. E. and Wilkinson, J., 2001, Fluid Evolution at the Navan Deposit: Preliminary fluid inclusion results. Unpublished Report. p.14.

Everett, C.E., Wilkinson, J.J., and Rye, D.M., 1999. Fracture-controlled fluid flow in the Lower Palaeozoic basement rocks of Ireland: Implica- tions for the genesis of Irish-type Zn-Pb deposits, in McCaffrey, K.J.W., Lonergan, L., and Wilkinson, J.J., eds., Fractures, fluid flow, and min-eralization: Geological Society of London, Special Publications, v. 155, p. 247–276.

Farrelly, I., 1993, The relationships of mineralisation to faulting at Navan Mines, Co Meath, Ireland. Senior Sophistor Project. Trinity College Dublin, p.60.

Farver, J.R., 1994. Oxygen self-diffusion in calcite: Dependence on temperature and water fugacity. *Earth and Planetary Science Letters*, *121*(3-4), p.575-587.

Fernandes, P. and Clayton, G., 2003. Organic Maturation Levels and Thermal History of the Carboniferous Rocks of the Dublin Basin. Proceedings of the XVth International Congress on Carboniferous and Permian Stratigraphy. Utrecht, the Netherlands, 10-16 August.

Finnegan, S., Bergmann, K., Eiler, J.M., Jones, D.S., Fike, D.A., Eisenman, I., Hughes, N.C., Tripati, A.K. and Fischer, W.W., 2011. The magnitude and duration of Late Ordovician–Early Silurian glaciation. *Science*, *331*(6019), p.903-906.

Ford, C.V., 1996, The integration of petrologic and isotopic data from the Boulder Conglomerate to determine the age of the Navan orebody, Ireland. Unpublished PhD Thesis, University of Glasgow, p.176.

Fritschle, T.; Daly, J.S.; McConnell, B.; Whitehouse, M.J.; Menuge, J.F.; Buhre, S.; Mertz-Kraus, R.; Döpke, D.Peri-Gondwanan Ordovician arc magmatism in southeastern Ireland and the Isle of Man: Constraints on the timing of Caledonian deformation in Ganderia. Geol. Soc. Am. Bull. 2018, 130, p.1918–1939.

Ghosh, P., Adkins, J., Affek, H., Balta, B., Guo, W., Schauble, E.A., Schrag, D. and Eiler, J.M., 2006. ^{13}C–^{18}O bonds in carbonate minerals: a new kind of paleothermometer. *Geochimica et Cosmochimica Acta*, *70*(6), p.1439-1456.

Hemingway, J.D. and Henkes, G.A., 2021. A disordered kinetic model for clumped isotope bond reordering in carbonates. *Earth and Planetary Science Letters*, *566*, p.116962.

Henkes, G.A., Passey, B.H., Grossman, E.L., Shenton, B.J., Pérez-Huerta, A. and Yancey, T.E., 2014. Temperature limits for preservation of primary calcite clumped isotope paleotemperatures. *Geochimica et cosmochimica acta*, *139*, p.362-382.

John, C.M. and Bowen, D., 2016. Community software for challenging isotope analysis: First applications of 'Easotope'to clumped isotopes. *Rapid Communications in Mass Spectrometry*, *30*(21), p.2285-2300.

Jones, G. 1992, Irish Carboniferous conodonts record maturation levels and the influence of tectonism, igneous activity and mineralisation. Terra Nova, 4, p. 238-244.

Keating-Bitonti, C.R., Ivany, L.C., Affek, H.P., Douglas, P. and Samson, S.D., 2011. Warm, not super-hot, temperatures in the early Eocene subtropics. *Geology*, *39*(8), p.771-774.

Keith, M. and Weber, J., 1964. Carbon and oxygen isotopic composition of selected limestones and fossils. Geochimica et Cosmochimica Acta, 28(10-11), p.1787-1816.

Kim, S.T., Mucci, A. and Taylor, B.E., 2007. Phosphoric acid fractionation factors for calcite and aragonite between 25 and 75 C: revisited. *Chemical Geology*, *246*(3-4), p.135-146.

Knight, H., 2012, Seeking The deep fluid feeder zone of the Navan Zn-Pb deposit, Republic of Ireland. Unpublished MSc thesis, Imperial College, 44 p.

Kronenberg, A.K., Yund, R.A. and Giletti, B.J., 1984. Carbon and oxygen diffusion in calcite: effects of Mn content and PH 2 O. *Physics and chemistry of minerals*, *11*(3), p.101-112.

Lloyd, M.K., Ryb, U. and Eiler, J.M., 2018. Experimental calibration of clumped isotope reordering in dolomite. *Geochimica et Cosmochimica Acta*, *242*, p.1-20.

McNestry A., Rees J. G. 1992. Environmental and palynofacies analysis of a Dinantian (Carboniferous) littoral sequence: the basal part of the Navan Group, Navan, County Meath, Ireland. Palaeogeography, Palaeoclimatology, Palaeoecology 96: p.175–193

Mering, J., Barker, S., Huntington, K., Simmons, S., Dipple, G., Andrew, B. and Schauer, A., 2018. Taking the Temperature of Hydrothermal Ore Deposits Using Clumped Isotope Thermometry. Economic Geology, 113(8), p.1671-1678.

Mii, H., Grossman, E.L., And Yancey, T.E., 1999, Carboniferous Isotope Stratigraphies Of North America: Implications For Carboniferous Paleoceanography And Mississippian Glaciation: Geological Society Of America, Bulletin, V. 111, p. 960–973.

Mills, H., Halliday, A.N., Ashton, J.H., Anderson, I.K., Russell, M.J., 1987, Origin of a giant orebody at Navan, Ireland. Nature, 327, p. 223-226.

Murphy, F.C., Anderson, T.B., Daly, J.S., Gallagher, V., Graham, J.R., Haroer, D.A.T., Johnston, J.D., Kennan, P.S., Kennedy, M.J., Long, C.B., Morris, J.H., O'Keefe, W.G., Parkes, M., Ryan, P.D., Sloan, R.J., Stillman, C.J., Tietzch-Tyler, D., Todd, S.P., Wrafter, J.P., 1991. An appraisal of Caledonian suspect terranes in Ireland. Irish Journal of Earth Sciences, 11, p.11-41.

Nolan, S.C., 1989, The style and timing of Dinantian synsedimentary tectonics in the eastern part of the Dublin Basin, Ireland. In: Arthurton, R.S., Gutteridge, P. and Nolan,S. C. (Eds). The role of tectonics in Devonian and Carboniferous sedimentation in the British Isles. Yorkshire Geological Society, Occasional Publication 6, p. 83-97.

O'Keeffe, W.G., 1986, Age and postulated source rocks for mineralization in central Ireland, as indicated by lead isotopes. In: Andrew, C.J., et al. (Eds). Geology and Genesis of Mineral Deposits in Ireland. IAEG, Dublin, p.617–624.

Passey, B.H. and Henkes, G.A., 2012. Carbonate clumped isotope bond reordering and geospeedometry. *Earth and Planetary Science Letters*, *351*, p.223-236.

Peace, W.M., 1999, Carbonate-hosted Zn-Pb mineralisation within the Upper Pale Beds at Navan, Ireland: Unpub. Ph.D. thesis, Univ. Melbourne, p.284.

Peace, W.M., Wallace, W.M., Holdstock, M.P. and Ashton, J.H., 2003, Ore textures within the U lens of the Navan Zn-Pb deposit, Ireland. Mineralium Deposita. 38, p. 568–584.

Petersen, S.V., Defliese, W.F., Saenger, C., Daëron, M., Huntington, K.W., John, C.M., Kelson, J.R., Bernasconi, S.M., Colman, A.S., Kluge, T. and Olack, G.A., 2019. Effects of improved 17O correction on interlaboratory agreement in clumped isotope calibrations, estimates of mineral-specific offsets, and temperature dependence of acid digestion fractionation. *Geochemistry, Geophysics, Geosystems*, *20*(7), p.3495-3519.

Philcox, M.E., 1989, The Mid-Dinantian Unconformity At Navan, Ireland. In: Arthurton R.S., Gutteridge, P. And Nolan,S. C. (Eds). The Role Of Tectonics In Devonian And Carboniferous Sedimentation In The British Isles. Yorkshire Geological Society, Occasional Publication, 6, p. 67-81.

Price, G.D. and Passey, B.H., 2013. Dynamic polar climates in a greenhouse world: Evidence from clumped isotope thermometry of Early Cretaceous belemnites. Geology, 41(8), p.923-926.

Raiswell, R., Bottrell, S., Dean, S., Marshall, J., Carr, A. and Hatfield, D., 2002. Isotopic constraints on growth conditions of multiphase calcite-pyrite-barite concretions in Carboniferous mudstones. Sedimentology, 49(2), p.237-254.

Redmond, P.B., 1991, The production of a complete NW strike section across the Navan orebody with a study of the stratigraphy, mineralization and diagenetic history across the section, accompanied by a study of mineralization in underground exposure. Unpublished BSc Thesis, Trinity College Dublin, p.111.

Rizzi, G. and Braithwaite, C.J.R., 1996, Cyclic emersion surfaces and channels within Dinantian limestones hosting the giant Navan Zn-Pb deposit, Ireland. In: Strogen P.,

Somerville, I.D. & Jones, G.Ll. (eds), Recent Advances in Lower Carboniferous Geology, Geological Society Special Publication No. 107, p. 207-219.

Rizzi, G. And Braithwaite, C.J.R., 1997. Sedimentary cycles and selective dolomitization in limestones hosting the giant Navan zinc-lead ore deposit, Ireland. Exploration and Mining Geology, v. 6, p. 63-77.

Rizzi, G., 1992, The sedimentology and petrography of Lower Carboniferous limestones and dolomites; host rocks to the Navan zinc-lead deposit, Ireland. Unpublished PhD thesis, University of Glasgow, p.369.

Romano, M., 1980. The stratigraphy of the Ordovician rocks between Slane (County Meath) and Collon (County Louth), Eastern Ireland. J Earth Sci. Dubl. Soc. 3. p53-79.

Rosenbaum, J. and Sheppard, S.M.F., 1986. An isotopic study of siderites, dolomites and ankerites at high temperatures. Geochimica et cosmochimica acta, 50(6), p.1147-1150.

Russell, M.J., 1975, Lithogeochemical environment of the Tynagh base-metal deposit, Ireland, and its bearing on ore deposition: Transactions of the Institution of Mining and Metallurgy, v. 84B, p. 128–133.

Ryb, U. and Eiler, J.M., 2018. Oxygen isotope composition of the Phanerozoic ocean and a possible solution to the dolomite problem. *Proceedings of the National Academy of Sciences*, *115*(26), p.6602-6607.

Ryb, U., Lloyd, M.K. and Eiler, J.M., 2021. Carbonate clumped isotope constraints on burial, uplift and exhumation histories of the Colorado Plateau. *Earth and Planetary Science Letters*, *566*, p.116964.

Shelton, K., Hendry, J., Gregg, J., Truesdale, J. and Somerville, I., 2019. Fluid Circulation and Fault- and Fracture-related Diagenesis in Mississippian Syn-rift Carbonate Rocks On the Northeast

Margin of the Metalliferous Dublin Basin, Ireland. Journal of Sedimentary Research, 89(6), p.508-536.

Stolper, D.A. and Eiler, J.M., 2015. The kinetics of solid-state isotope-exchange reactions for clumped isotopes: A study of inorganic calcites and apatites from natural and experimental samples. American Journal of Science, 315(5), p.363-411.

Stolper, D.A., Eiler, J.M. and Higgins, J.A., 2018. Modeling the effects of diagenesis on carbonate clumped-isotope values in deep-and shallow-water settings. *Geochimica et Cosmochimica Acta*, *227*, p.264-291.

Strogen, P., Jones, G. And Somerville, I., 1990. Stratigraphy And Sedimentology Of Lower Carboniferous (Dinantian) Boreholes From West Co. Meath, Ireland. Geological Journal, 25(2), p.103-137.

Taylor S (1984) Structural and paleotopographic controls of leadzinc mineralization in the Silvermines orebodies, Republic of Ireland. Econ Geol 79: p.529–548

Taylor, S and Andrew, C.J., 1978, Silvermines orebodies, Co. Tipperary, Ireland: Transactions of the Institution of Mining and Metallurgy, v. 87B, p. 111–124.

Thorpe, T.M., 2001, A Petrographic and Cathodoluminescence Study of Part of the Navan Zn-Pb Deposit, County Meath, Ireland. Unpublished MSci Research Project. Imperial College, p.73.

Vaughan, A. and Johnston, J. D., 1992, Structural constraints on closure geometr across the Iaepetus suture in eastern Ireland. Journal of the Geological Society of London, 149, p. 65-74

Wilkinson, J.J., 2010, A Review of Fluid Inclusion Constraints on Mineralization in the Irish Orefield and Implications for the Genesis of Sediment-Hosted Zn-Pb deposits. Economic Geology, 105, p. 417-442.

Wilkinson, J.J., Boyce, A.J., Everett, C.E., Lee, M.J., 2003, Timing and depth of mineralization in the Irish Zn–Pb orefield. In: Kelly, J.G., Andrew, C.J., Ashton, J.H., Boland, M.B., Earls, G., Fusciardi, L., Stanley, G. (Eds.), Europe's Major Base Metal Deposits. Irish Assoc. Econ. Geol., Dublin, p. p.483- 497.

Wilkinson, J.J., Eyre, S.L. and Boyce, A.J., 2005, Ore-forming processes in Irish-type carbonate-hosted Zn-Pb deposits: Evidence from mineralogy, chemistry and isotopic composition of sulfides at the Lisheen Mine. Economic Geology, 100, p. 63-86.

Wilkinson, J.J.; Hitzman, M.W. The Irish Zn–Pb Orefield: The View from 2014. In Current Perspectives on Zinc Deposits; Archibald, S.M., Piercey, S.J., Eds.; Irish Association for Economic Geology: Dublin, Ireland, 2015; p. 59–72.

Table A3.1 Clumped Isotope Analyses

Sample Name	Category	Sample Type	Replicates	$\delta^{13}C$ VPDB (‰)	$\delta^{18}O$ VSMOW (‰)	Δ47 (‰)	Temperature (°C; Anderson calibration)	T+DT	T-DT	Temperatures (°C) Calculated assuming equilibrium with Mississippian Seawater (See Chapter 4; 4.7.3)
N02417/01 K04	Calcite Veining (Associated with Mineralization)	Calcite	3	-0.09	21.55	0.351	173	185	162	N.a.
N02454/03 L48	Calcite Veining (Associated with Mineralization)	Calcite	3	0.38	22.53	0.396	129	137	122	N.a.
N02416/04 Concretion	Concretion	Calcite	3	-14.23	29.21	0.399	126	133	119	20-30
N2454/13 FE RICH DOL INFILL	D2 Fe-rich dolomite infill	Dolomite	1	1.65	23.29	0.422	109	120	99	~80
N02445/06 5LENS DOL	Dolomite (D1 and D2 Bulk)	Dolomite	3	2.27	24.63	0.424	108	121	96	~80
N02505/15 5LENS DOL	Dolomite (D1 and D2 Bulk)	Dolomite	3	1.76	23.12	0.392	133	140	125	~80
N02505/18 HOST ROCK DOLOMITE	Dolomite (D1 and D2 Bulk)	Dolomite	3	1.68	23.00	0.377	146	156	137	~80
N02454/13 MICRITE HOST ROCK	Micrite Unit Host Rock	Calcite	3	1.76	25.02	0.412	116	125	108	30 to 40
N02505/04 oolite	Pale Beds	Calcite	3	1.91	24.88	0.376	147	155	139	30 to 40
N02416/10A D3	Pale Beds (HC)	Calcite	3	2.26	26.34	0.388	136	149	124	~40
N02445/02 HOST ROCK	Pale Beds (HC)	Calcite	2	2.14	25.74	0.370	152	163	142	~40
N02508/01 HOST ROCK CAL	Pale Beds (HC)	Calcite	3	2.65	26.96	0.375	147	156	139	~40
N02416/10A D2	Pressure Solution	Dolomite	2	2.52	23.70	0.388	136	145	127	~85
N02445/02 FISSURE FILL DOL	Pressure Solution	Dolomite	2	2.31	24.51	0.416	113	132	97	~85
N02508/01 DISSOLUTION	Pressure Solution	Dolomite	1	1.14	23.91	0.464	82	91	74	~85
N02505/04 RED ALTERATION	Red Alteration	Calcite	3	1.95	25.21	0.349	175	192	160	N.a.
N02416/04 HOST ROCK	TBU Host Rock	Calcite	1	2.89	25.71	0.446	93	103	84	30-40

Appendix 4: ADDITIONAL PUBLICATIONS

Drummond, D, A., Cloutier, J., Boyce, A, J., Prave, A. 2020. Petrogenesis and geochemical halos of the amphibolite facies, Lower Proterozoic, Kerry Road volcanogenic massive sulfide deposit, Loch Maree Group, Gairloch, NW Scotland. *Ore Geology Reviews*, 124.

Yesares L., **Drummond D., A.**, Hollis S., Doran A., Menuge JF., Boyce AJ., Blakeman RJ., Ashton JH. 2019. Coupling mineralogy, textures, stable and radiogenic isotopes in identifying ore-forming processes and geochemical vectoring possibilities in Irish-type carbonate hosted Zn-Pb deposits. Minerals.

Yesares, L., Menuge, J., Blakeman, R, J., Ashton, J, H., Boyce, A, J., Coller, D., **Drummond, D, A.,** Farrelly, I. 2021. Pyritic Mineralization Halo Above The Tara Deep Zn-Pb Deposit, Navan, Ireland: Evidence For Sub-Seafloor Exhalative Hydrothermal Processes? [Accepted by Ore Geology Reviews July 2021]